The Role of Molecular Packing in Singlet Fission

by

Eric A. Buchanan

B.A., University of Texas, 2008

M.S., University of Colorado, 2015

A thesis submitted to the

Faculty of the Graduate School of the

University of Colorado in partial fulfillment

of the requirement for the degree of

Doctor of Philosophy

Department of Chemistry

2019

This thesis entitled:

The Role of Molecular Packing in Singlet Fission

written by Eric A. Buchanan

has been approved for the Department of Chemistry

_____

Josef Michl

_____

Justin Johnson

Date _____

The final copy of this thesis has been examined by the signatories, and we

Find that both the content and the form meet acceptable presentation standards

of scholarly work in the above mentioned discipline.

Buchanan, Eric A. (Ph.D., Chemistry)

The Role of Molecular Packing in Singlet Fission

Thesis directed by Professor Josef Michl

Abstract

Over a decade ago, the process of singlet fission (SF) was shown to be able to increase the efficiency of solar cells. In that time, much work has been done in the field, yet there are still few known materials which undergo fast SF and are also suitable for use in a photovoltaic device. In addition, there is little guidance as to how the material should be arranged in the solid. This thesis investigates how molecular packing affects SF. It begins with a review of the work that has been done in the field on this subject. A simple frontier orbital model for SF is then described which is has been incorporated into a program, SIMPLE, which first searches the 6-dimensional space of possible arrangements of a pair of chromophores to identify all significant, physically accessible local maxima of the square of the electronic matrix coupling element for SF ($|T^*|$) on a grid of 10^8 to 10^9 pair geometries. The effects of intermolecular interaction on the energy balance of SF and therefore the rate constant of SF are approximated by Marcus theory and disqualify many of the maxima. The program then optimizes the selected pair geometries for maximum rate of singlet fission. The model and program are first applied to the pair geometry optimization of the common SF chromophore tetracene followed by optimization of a 1,3-diphenylisobenzofuran pair. Next, in a different application, two crystal polymorphs of 1,3-diphenylisobenzofuran and crystals structures of 11 fluorinated derivatives are analyzed with the model to explain why some perform fast SF while others do not. Finally, possible methods for expanding the simple model are explored.

I dedicate this work to my son Jett.

Acknowledgments

I would like to offer my thanks to my advisor, Professor Josef Michl, for expanding my research interests from only high-level methods and computation to include qualitative models and approaches which offer less accuracy but often provide deeper understanding. More importantly, I will forever be grateful to Josef for his kindness and understanding. In particular, I will never forget his support and all he did for me when my son was in the hospital.

Additionally, I would like to thank all the many members of the Michl group who have helped me throughout my time in the lab: Akin Akdag, Zdeněk Havlas, Jirka Kaleta, Lukáš Kobr, Chris Pochas, and the many more. I would especially like to thank Matthew MacLeod for helping me to get started in theoretical chemistry in the group and preparing me to be the systems administrator and IT help.

I have to give special thanks to the good friends I've made in my time here: Ethan Miller, Andrew Chomas, Alex Gilligan, and Jacek Pecyna. I couldn't imagine reaching this point without them.

The never failing support of my family has been invaluable during my time at the University of Colorado. Without it, I would certainly not have made it to this point.

Most importantly and above all else, I thank my son Jett for being the greatest thing to ever exist. Whenever all felt lost and hopeless, you were what kept me going.

Lastly, I thank science for bringing me together with all of these people.

CONTENTS

TABLES

Table

FIGURES

"We are the Priests of the Temples of Syrinx
Our great computers fill the hallowed halls.
We are the Priests of the Temples of Syrinx
All the gifts of life are held within our walls"
-Neil Peart

Chapter I

Introduction

1.1. Motivation

The Shockley-Queisser thermodynamic efficiency limit for single-junction organic solar cells is about 32%.[1] This assumes that when a photon with energy greater than the bandgap is absorbed, excess energy quickly dissipates as heat to the bottom of the band and a single electron-hole pair is created. When the proper conditions are met, a singlet exciton in a chromophore may split into a pair of triplet excitons through the process of singlet fission. While doubling the number of excitons doubles the current, the voltage is cut in half. This may not seem useful, but if a solar cell contains a layer capable of singlet fission for harvesting higher energy photons and an ordinary sensitizer layer for harvesting lower energy photons, analysis shows the maximum theoretical efficiency is increased to around 45% for organic solar cells.[2] Increasing the efficiency of solar cells with minimal increase in cost is vitally important for solar energy to become economically competitive enough to fully replace fossil fuels.

Designing singlet fission materials for solar cells has many challenges though. Few solids, for example crystals of tetracene and 1,3-diphenylisobenzofuran, are known to exhibit singlet fission with a triplet quantum yield near 200%. Therefore, the identification of chromophores capable of undergoing singlet fission is important. In addition to this, small changes in the relative orientations of chromophores in the solid phase can have large effects on the efficiency of singlet fission. Maximizing the rate of singlet fission by identifying optimal geometrical arrangements of chromophores is then another important requirement for the design

of singlet fission materials. Calculating the rate of singlet fission for all possible orientations of two molecules for many chromophores is computationally cost prohibitive unless a simple model is used. To this end, our lab has developed a program SIMPLE using an algebraically simple model for the rate of singlet fission which depends only on the relative orientation of two partners and properties of the chromophore.

Building on previous work from our lab, the focus of this thesis work is to extend the simple model for singlet fission to account for the effects of molecule pair orientation on intermolecular interactions, energetics, and ultimately the rate of singlet fission. This thesis will begin with a review of studies on the effect of molecular packing on singlet fission followed by a detailed overview of the theoretical model. The model is then used to optimize the pair structures of two chromophore pair systems: tetracene and 1,3-diphenylisobenzofurn. Finally, the model is used to analyze singlet fission in crystals of 1,3-diphenylisobenzofuran and eleven of its fluorinated derivatives.

1.2. Singlet Fission: The Role of Molecular Packing[3]

1.2.1. Introduction

Singlet fission (SF) is a photophysical process in a molecular solid in which a singlet exciton and a ground-state molecule are converted into two independent triplet excitons (Figure 1). SF is spin-allowed because the two triplet excitons are initially coupled into an overall singlet. The SF process is over when the two triplet excitons lose electronic coherence and hop apart. All spin coherence between them is usually lost by spin-lattice relaxation much later, over a period of tens of nanoseconds.

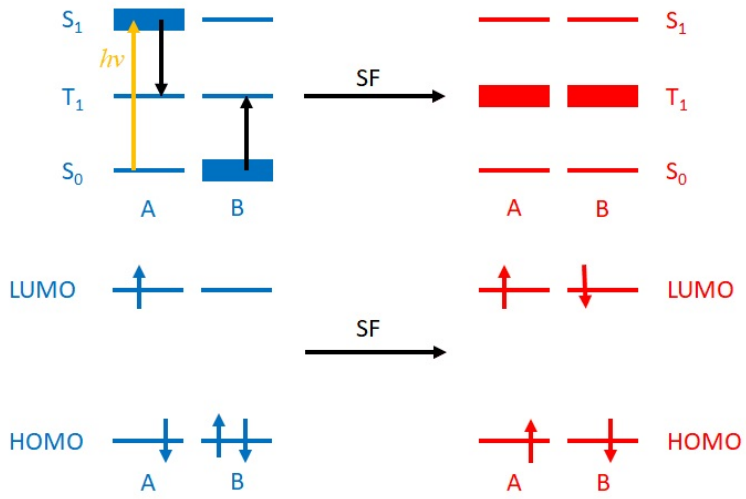

Figure 1. Above: Evolution of electronic states of partners A and B in the SF process. Below: Evolution of the most significant orbital configuration to the wavefunctions of the partners. Reproduced from Ref. 10 with permission from Elsevier.

Electronic excitation in a singlet exciton could in principle be located on a single molecule but is commonly delocalized over a group of molecules that are in close contact. Singlet excitons are quite mobile and short-lived. Even if they decayed by no other processes, fluorescence would usually limit their lifetime to nanoseconds. In a triplet exciton, the electronic excitation is normally located on a single molecule and moves within the solid more slowly, by hopping from molecule to molecule. It usually has a much longer lifetime, often tens or even hundreds of microseconds.

SF has been known for half a century[4] but emerged from obscurity only when it was realized early in this millennium[2] that a combination of an SF-capable absorption layer for high-energy solar photons followed by a layer of ordinary solar cell material for absorption of low-

energy photons does not require expensive current matching and yet allows an increase in maximum theoretical efficiency to nearly 1/2, well above the Shockley-Queisser limit[1] of 1/3. An earlier suggestion in this direction[5] was published at a time when there was limited interest in solar energy and was largely ignored.

Hundreds of studies of SF have been published in the last ten years. They have been primarily driven by an as yet unfulfilled desire to identify an SF-capable solid that not only yields two triplet excitons for every photon absorbed, but also meets all the usual requirements imposed on solar cell materials, especially light fastness. It would be quite hopeless to attempt a comprehensive review of the current state of SF research in a chapter; it now calls for a book. For the time being, the reader is referred to existing review articles.[6-14] Here, we shall survey an aspect of SF that does not appear to have been reviewed recently: studies of the effect of molecular packing in the solid on the SF rate.

The SF process is now known to be rather complex (Figures 2 and 3). The initial event is the conversion of a singlet exciton into a singlet biexciton, a molecular pair in which each partner is in its triplet state and the two triplets are coupled into an overall singlet. It is usually formed in a single step, although in rare cases it is known to proceed in two steps:[15] first, a transition to an observable charge-separated state in which one partner has transferred an electron to the other, and second, a transition from the charge-separated state to the biexciton (the charge-separated state may also form a single triplet by rapid intersystem crossing and the two mechanisms of triplet formation may be difficult to distinguish[16]). The much more usual single-step conversion proceeds at a rate that can be described as a sum of two contributions. The first "superexchange" contribution is usually completely dominant. It is mediated by virtual states of charge-separated

character that are too high in energy to be actually populated. The second "direct" contribution usually is of negligible importance and is provided by the two-electron part of the interaction Hamiltonian.

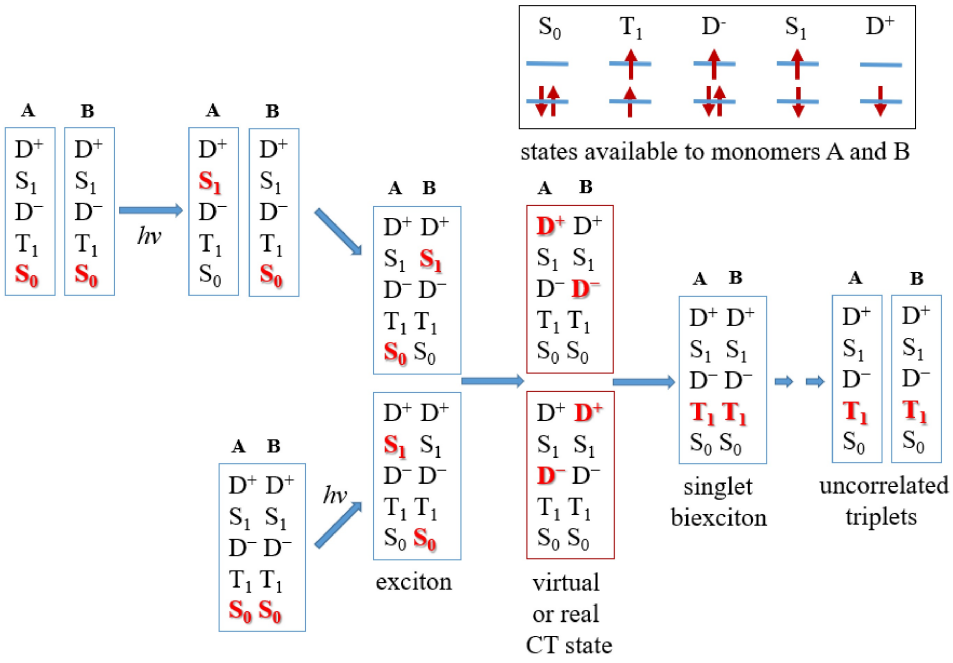

Figure 2. Top right: symbolic representation of electronic states of partners A and B in SF. Center: Sequence of events (competing decay paths not shown). Possible (black) and actually occupied (red) electronic states in frames (blue, real species; red, a species that can be virtual or real). Narrow frames: separated partners, wide frames: partners in contact. Top path: SF in solution; bottom path: SF in crystal, aggregate, or dimer (in covalent dimers, the last step on the right is absent). All steps are reversible. Reproduced by permission from ref. 10.

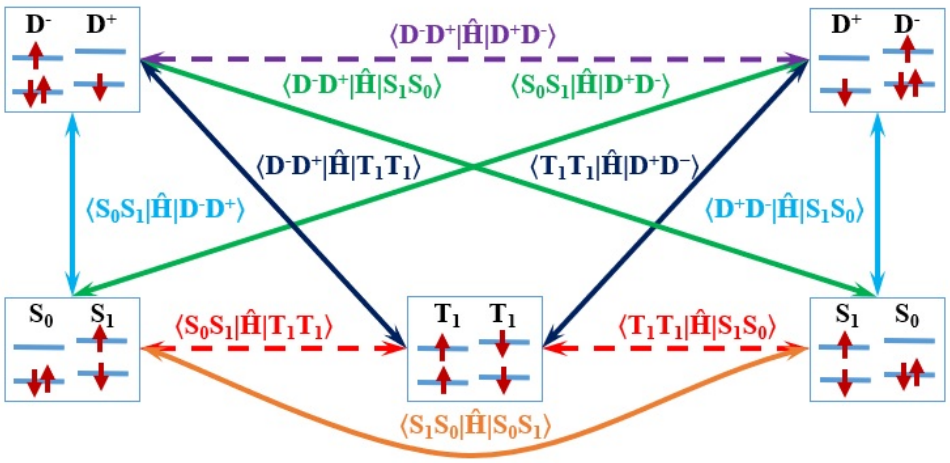

Figure 3. Electron configurations of a molecular pair important for SF and interactions between them. Solid lines: potentially strong interactions; broken lines: weak interactions.

After this initial biexciton forming event, which may be reversible,[17] the two triplet excitations need to overcome their mutual binding energy and move apart before SF is complete. Little is known about this process. Small terms in the interaction Hamiltonian that are familiar from EPR spectroscopy of triplets, and also Zeeman interactions with any magnetic field imposed from the outside, cause a conversion of the biexciton from its initial singlet state into a quintet state and then probably its triplet state before the two triplet excitations spatially separate by a hop of one of them to a neighboring molecule.[6,18-20]

SF has also been observed in concentrated solutions in which the formation of an encounter complex of a singlet excited and a ground state molecule permits the formation of two triplet excited molecules which then overcome their binding energy and diffuse apart. Often, the term SF is applied also to events that occur in solutions of pairs of chromophores attached to each other by covalent bonds. Under these circumstances, a singlet biexciton can form and

subsequently change its spin state in various ways, but the two triplet excitations cannot separate and SF thus cannot really be completed.

When the interaction between the two covalently connected chromophores is strong, especially when the bridging unit or units are capable of π conjugation, it becomes difficult and ultimately even impossible to distinguish the now intramolecular singlet biexciton state from other intramolecular singlet excited states and the use of the term SF is then questionable. It would be unusual to refer to the internal conversion of the optically allowed B_u state of 1,3-butadiene into its "double triplet" A_g state as SF, although their wave functions suggest it. It is not obvious just where to draw the line.

It is generally difficult to extrapolate results obtained for covalently bound chromophore pairs to solids containing monomers of the same chromophores. Not only are the two triplet excited moieties in the covalent pair unable to separate, but the additional chromophores present in the solid environment and absent in the molecular pair also may affect differentially both the energies and the mutual coupling of the various electronic states involved.

1.2.2. Optimization of Triplet Exciton Yields

If a SF material is to be practically useful, it is absolutely essential for its triplet exciton yield to be very close to 200%. Unfortunately, only a handful of such organic solids are known, and they do not meet other essential requirements, such as long-term stability in sunlight in the presence of traces of air. It is therefore not surprising that much effort is being invested in efforts to find additional candidates and to formulate general rules for optimal material structures.

The optimization of triplet exciton yield requires a maximization of the rate of SF and

minimization of the rates of all competing processes. This needs to be done under the constraint of avoiding losses of electronic excitation energy by making SF too exothermic and thus converting electronic to vibrational energy and ultimately, heat. Ideally, all the other requirements typical of SF solar cell materials are also considered at the same time. Examples are (i) keeping the first triplet and singlet excitation energies at their optimal values of about 1.1 and 2.2 eV, respectively, (ii) assuring high absorption coefficients everywhere above 2.2 eV, (iii) testing that the triplets are long-lived, (iv) securing suitable transport properties for charges and/or triplet excitons, (v) choosing redox properties appropriate for the intended junction, (vi) guaranteeing long-term stability, (vii) making sure that the cost is acceptable, and (ix) checking environmental friendliness.

The maximization of the SF rate can be subdivided into a search for the best chromophore and a search for the best packing of the chromophore in the solid. An obvious and very severe constraint on both the chromophore choice and its packing is the requirement that the SF process must be fast and therefore cannot be strongly endoergic. Singlet fission is isoergic when the singlet exciton contains twice the excitation energy of the triplet exciton. When isoergic, or even better, slightly exoergic, it can occur on the time scale of tens of femtoseconds, similarly as other spin-allowed internal conversion or short-range energy transfer processes.

Typically, molecular properties of a chromophore under consideration are examined first, usually in dilute solution. Only the relatively rare compounds for which the singlet excitation energy $E(S_1)$ is approximately twice the triplet excitation energy $E(T_1)$ come under further consideration. For those in which $E(S_1)$ is significantly less than twice $E(T_1)$, there is not much hope that the singlet exciton will have more than twice the excitation energy of the triplet

exciton, whereas for those in which $E(S_1)$ is significantly more than twice $E(T_1)$ SF may be fast but they are poor prospects because SF will incur losses by converting too much of the excitation energy of the singlet exciton into heat. Two classes of π-electron chromophores were identified early on as likely candidates for meeting the condition $E(S_1) = 2E(T_1)$, large alternant hydrocarbons and biradicaloids.[21] There may be others.

Packing in the solid state needs to be considered as well, because intermolecular interactions have the potential for making the energies of the singlet and triplet excitons, respectively, quite different from the $E(S_1)$ and $E(T_1)$ energies observed in isolated molecules (Davydov splitting). Most frequently, they stabilize the first excited singlet considerably more than the first excited triplet and thus convert situations that looked quite hopeful in the isolated molecule, $E(S_1) = 2E(T_1)$, into cases of endoergic SF.

A second and equally important reason for optimizing packing in the solid state follows from the application of the Fermi Golden rule to the rate of SF. In the diabatic basis, this yields for the rate W of the initial step of SF, in which the lower energy exciton state S* and a ground state molecule are converted to the singlet biexciton ^{1}TT*:

$$W(S^*) = 2\pi\hbar^{-1}|\langle S^*|H_{int}|{}^1TT^*\rangle|^2\rho(E), \quad (1)$$

and similarly for the upper exciton state S**, which may also be populated. H_{int} is the interaction Hamiltonian for A and B (the part of the electrostatic Hamiltonian that is absent if A and B are infinitely far apart) and $\rho(E)$ is the density of states at the energy of the ^{1}TT* state. The electronic matrix element whose square appears in the expression is a sensitive function of

molecular packing and can range from zero, imposed by symmetry, to large values. Both aspects of the role that molecular packing plays in the optimization of SF rate, will be considered in the next section.

If the maximization of the rate of SF looked difficult, the minimization of the rates of all competing processes is harder. It, too, can be subdivided into a search for the best chromophore and a search for the best packing of the chromophore in the solid. Once again, molecular properties of the chromophore in dilute solution are examined first. Recognizing that fluorescence is an unavoidable and ever-threatening decay channel, we need to reduce the rate constants of other competing processes below the rate constant of fluorescence. Since we wish to have a strongly absorbing first transition to S_1, a typical fluorescence rate constant will be 0.1 - 1 ns^{-1}. The most common competitors are intersystem crossing to the triplet manifold, internal conversion to S_0, and photochemical reactions. A high fluorescence quantum yield is a good but insufficient indicator that a chromophore is a likely candidate.

Intermolecular interactions present considerably more difficulty. The most likely intermolecular mechanisms for decay of a singlet exciton are the formation of an excimer and the formation of a charge-separated species, both of which are apt to decay to the ground state, but in some cases bimolecular photochemical reactions may interfere as well. Equilibrium geometry in the excimer state of a molecular pair generally corresponds to perfect stacking of the two parallel planar partners at an interplanar distance that is significantly reduced relative to the ground state van der Waals contact distance. Slipping one of the partners relative to the other does not increase the potential energy much. The formation of an excimer is favored by crystal structures in which the two partners are already appropriately pre-positioned and merely need to approach

each other more closely, especially when the excimer binding energy is large. It has been known for a long time that under such circumstances an excimer can form in times as short as hundreds of femtoseconds.[22] It can be conjectured that excimer formation is also facilitated at grain boundaries and in amorphous domains, where increased molecular mobility is likely. However, it has also been pointed out that grain boundaries[23] and other defects[24] may also increase the square of the matrix element for SF and that their presence is not necessarily detrimental. Specific guidelines for preventing excimer formation do not seem to have been formulated, but it appears prudent to avoid crystal structures in which the chromophores are obviously pre-positioned for excimer formation and excimer binding energies are high. Most simply stated, it is desirable to avoid structures with large Davydov splitting.

Even less seems to be known about avoiding the generation of charge-separated species. These structures can be viewed as a limiting case of excimers. While it is often estimated that the wave function of excimers contains roughly comparable amounts of the two locally excited and the two charge-separated electron configurations, in the charge-separated species the energies of the charge-separated configurations are sufficiently lower than those of the locally excited configurations to make mixing with the latter negligible. Such a situation is most likely to occur when the ionization potential of the chromophore is low, its electron affinity high, the energy lowering due to the electrostatic attraction of the two charged partners is substantial, and the crystal environment is highly polarizable.

The mutual mixing of the two charge-separated configurations is due to a small matrix element containing only the two-electron part of the Hamiltonian (Figure 3) and is therefore easily prevented by even relatively weak perturbations that make their energies unequal. Then,

one of the charge-separated configurations by itself provides a good description of the wave function. Perturbations that favor one of the charge-separated configurations over the other can be caused by dissymmetry in the arrangement of the two partners, or by lack of symmetry in the environment provided by the crystal. Based on these considerations, it would appear prudent not only to avoid crystal packings that are predisposed to the formation of excimers, but also to avoid chromophores that have very low ionization potentials combined with high electron affinities. Considering that it is desirable for the excitation energy of the chromophore to be low, with a triplet at ~1.1 eV and singlet at ~2.2 eV, this sounds like a contradiction - the HOMO-LUMO gap in the chromophore molecule is to be simultaneously large and small. It actually is not a contradiction, because the electronic excitation energies are not equal to the difference between the energies of the HOMO and the LUMO, but are reduced by a large electron repulsion term. For instance,[25] the white anthracene (**1**) and blue azulene (**2**) have nearly identical ionization potentials and electron affinities (and thus HOMO and LUMO energies), but very different lowest singlet HOMO-LUMO excitation energies (all molecular structures are collected in Figure 4).

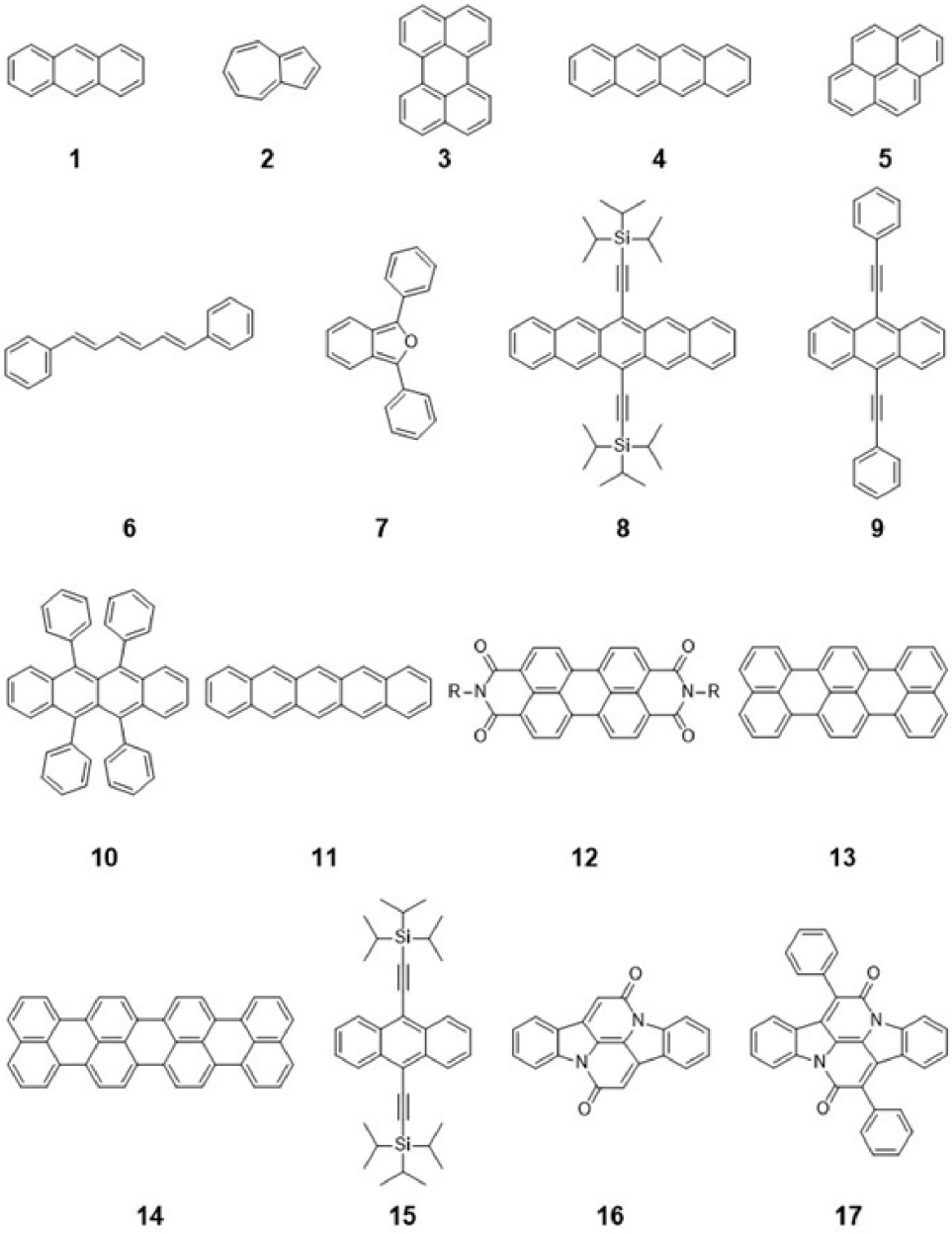

Figure 4. Molecular structures of chromophores.

1.2.3. SF Rates and Molecular Packing in the Solid

We can now examine what is known about the relation of SF rates to molecular packing in the solid. The most convincing experimental evidence for the importance of the crystal packing is provided by observations of the SF process in different crystal modifications of the same compound. The first such observation dates from 1978, when it was noted that the α and β crystal forms of perylene (**3**) differ in their SF properties.[22] The β structure is herringbone, similar to that of anthracene (**1**) and tetracene (**4**), which do not form excimers (Figure 5). The α structure is predisposed to excimer formation and is similar to that of pyrene (**5**), which forms excimers. The vibrationally relaxed singlet exciton in either form of the perylene (**3**) crystal does not have enough energy to perform SF, but when excited with photons of sufficiently higher energy, either crystal form will perform SF in competition with vibrational relaxation and give a small yield of triplets. In the **β3** crystal, the energy threshold at which SF sets in is equal to twice the excitation energy of a triplet exciton. In contrast, in **α3**, the threshold lies 3 500 cm^{-1} higher. The proposed interpretation of this observation is that in **β3** all of the photon energy is available for the competing processes of SF and vibrational equilibration, whereas in **α3** excimer formation occurs at a faster rate than either of these, wasting 3 500 cm^{-1} of electronic excitation energy in the form of phonons and ultimately, heat.

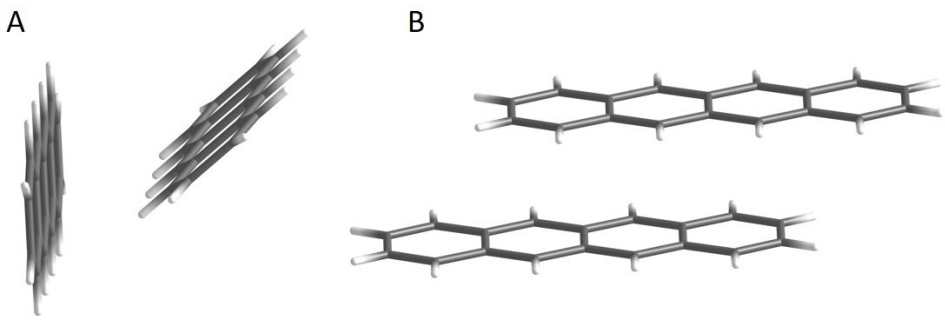

Figure 5. Nearest neighbor molecular pairs of tetracene (**4**). A: herringbone and B: slip-stacked.

It could be argued that this very nice piece of work primarily illustrates the importance of molecular organization in the solid for the rate of excimer formation and not for the SF rate, which might be affected only indirectly. The next example provides clear evidence from ps time-resolved fluorescence that molecular organization in the solid affects the SF rate constant directly.[27] 1,6-Diphenyl-1,3,5-hexatriene (**6**) is available as monoclinic and orthorhombic crystals. Their herringbone structures are quite similar, with neighbors slip-stacked (Figure 6). In the monoclinic form neighbors are somewhat closer together, the dihedral angle of their planes is smaller, and their slip is smaller. Although the $E(S_1)$ and $E(T_1)$ energies measured in solution suggest that SF should be exoergic, the singlet and triplet exciton energies in the solid are such that SF in both actually is slightly endoergic to the same degree. In both crystals, 90% of singlet excitons perform SF, but in the monoclinic form the rate constant for singlet exciton conversion to the biexciton is 1.5 times and that for biexciton dissociation into free triplet excitons is 3.5 times larger. The differences cannot be explained by the slightly different energetics in the two cases.

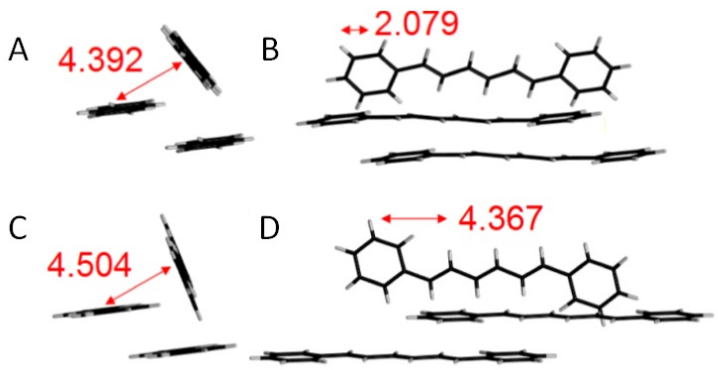

Figure 6. Crystal packing patterns of **mono-6** (A: top-down view and B: side view) and **ortho-6** (C: top-down view and D: side view).[27] The edge-to-face distance and vertical slip distance (in Å) are measured from the long axis of each molecule. Reprinted by permission from ref. 27. Copyright 2014 American Chemical Society.

A very striking example are the α and β crystal forms of 1,3-diphenylisobenzofuran (**7**).[28,29] The α form performs SF efficiently and yields 140% triplet at room temperature (200% at 77 K), whereas the room-temperature triplet yield from the β form is about 10%. The room temperature fluorescence yields are 10% from the α and 60% from the β form. In both cases, the S_1 lifetime equals the rise time of the triplet. The SF rate constants are 56±6 and 10±4 ns^{-1} for α and β crystal form, respectively. Yet, the crystal structures of both forms are nearly identical (Figure 7). The relation of any molecule to all of its nearest neighbors is the same in both within a small fraction of an Å, and only the relation to the next nearest neighbors is different. This cannot be accounted for by theories that only consider two molecules at a time, since the distance between next nearest neighbors is large enough for their direct interaction to effectively vanish, and the interaction must be mediated by a third molecule that is a neighbor to both, and possibly by others as well. A similar conclusion was reached more tentatively by the authors of a study of two crystal forms of **4**, TcI and TcII.[30] They found that films of **4** showed SF lifetimes of 125 ps

in the former and 22 ps in the latter when the crystalline domains were large, but essentially equal values of 32±1 ps when the domains were small, and were unable to account for the results using a standard theory that considers only pairwise intermolecular interactions. The need for going beyond pairwise contributions has also been formulated in purely theoretical papers.[31,32]

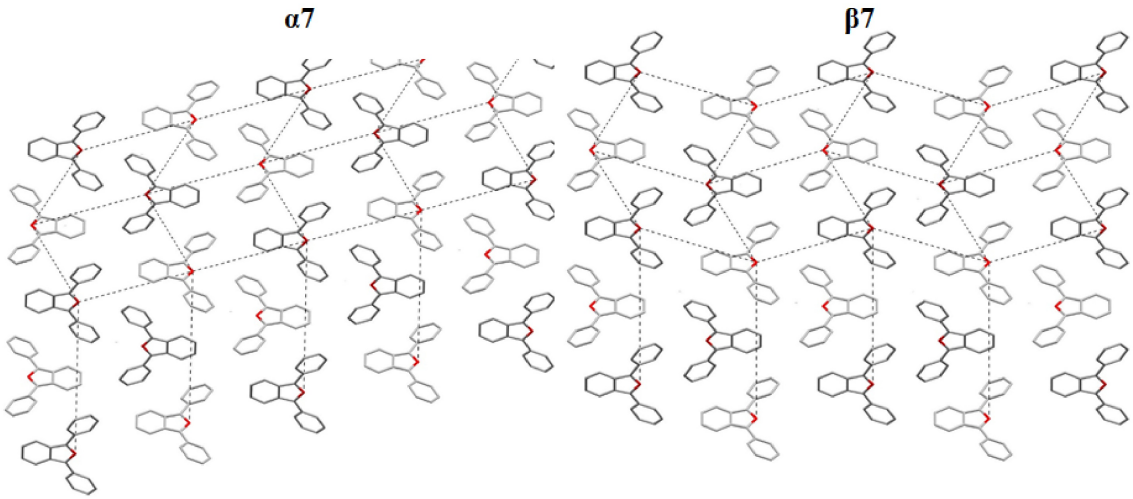

Figure 7. Crystal structures of 1,3-diphenylisobenzofuran: **α7**, *ac* plane, and **β7**, *bc* plane. Reprinted by permission from ref. 29. Copyright 2019 American Chemical Society.

SF formed biexcitons on a sub-100 fs time scale in thin layers of form-I and form-II polymorphs of 6,13-bis(triisopropylethynyl)pentacene (TIPS-pentacene) (**8**),[33] but the authors were able to measure the rate of biexciton dissociation into free triplet excitons and found that it occurred twice faster in form-I. The same ratio of two was found for the rates of triplet diffusion in the two polymorphs and the authors proposed that triplet energy transfer is the limiting factor for biexciton dissociation. The same conclusion has been reached more recently from measurements of the temperature dependence of SF in **8**.[33]

Two types of thin films of 9,10-bis(phenylethynyl)anthracene (**9**) were compared,[34] one containing essentially only the Pbcn polymorph, and the other containing 60% of the C2/c and 40% of the Pbcn polymorph. The former was claimed to produce an 80±20% yield of triplet by SF and a 27±4% yield of fluorescence, whereas in the latter, the numbers were 180±20% and 4±1%. If some fraction of the material in the films was amorphous and remained undetected in

the XRD analysis, the compositions used would be inaccurate, but there is no doubt that the two polymorphs behave differently.

In addition to these comparisons in which the structures of both solids were known from X-ray crystallography, there are others in which the structure of one or both was uncertain, but the two structures were known to be different. A comparison of single-crystalline and polycrystalline **4**,[35] of crystalline and amorphous rubrene (**10**),[36] of nanoparticles of **8** and similar compounds prepared under different conditions,[37-40] and of micelles produced from polymers end-functionalized by click reaction with **8**[41] all showed differences in SF behavior as a function of structure.

In addition, there are studies that found considerable differences in SF behavior within a series of compounds containing the same chromophore modified with very weakly interacting substituents and therefore packing differently in the solid phase.[29,42-45]

Finally, there is a large number of computational studies that examine the dependence of SF rates calculated as a function of molecular packing at various levels of sophistication, mostly within a small subspace within the overall 6-dimensional space of all possible orientations and separations of two chromophores, located close to an experimentally known geometry of a molecular pair. They all find a strong dependence on the packing geometry. Here, we only quote a few: pentacene (**11**),[46] its derivatives,[47] rubrene (**10**),[48,49] perylenedicarboximides (**12**),[50-52] terrylene (**13**) and quaterrylene (**14**),[53] and TIPS-anthracene (**15**).[54] The only instance in which packing geometry does not seem to matter is strongly exothermic SF. For example, **11** seems to undergo SF rapidly regardless of how it is packed. Unfortunately, not only are such chromophores extremely rare, they are also undesirable for high efficiency solar cells, as noted

above.

1.2.4. Optimization of Molecular Packing for High SF Rates

Our laboratory has developed a method for identification of the best packing motifs for high SF rates by prediction from first principles,[55] meant to provide a starting point for searches by more advanced methods. It also offers insight into SF in amorphous materials, aggregates and solutions, as well as guidelines for crystal engineering and for the synthesis of covalently bound molecular pairs. Many such pairs have been investigated already,[16,56-65] but in the absence of packing guidelines the mutual disposition of the two chromophores was more or less random and dictated more by synthetic convenience than by any attempt to optimize conditions for SF. Now that our geometry optimization computer code for SF rates is readily available as freeware on the internet,[55] structural targets for any π-electron chromophore pair can be easily identified.

Ideally, a code of this type should be applicable to crystalline solids as well, but in this regard the current version has two serious limitations: (i) it identifies molecular pair geometries that maximize the rate of SF but does not evaluate the rates of competing decay processes, such as excimer formation, charge-separated state formation, and photochemical reactions, and therefore is unable to optimize SF triplet yields; (ii) since it only considers two chromophore molecules at a time, it misses possibly present many-body effects. As noted above, there is experimental[29] and theoretical[23,31] evidence that at least in some cases such effects are important.

The identification of molecular pair geometries that optimize the SF rate requires a search for all local maxima of a function that decribes the dependence of the SF rate constant k_{SF} on the six variables needed to describe all possible geometries of a pair of rigid bodies under the

constraint that they do not interpenetrate. The variables were chosen to be the three translations and three rotations needed to bring the two partners into superimposition and the impenetrability constraint was imposed in the hard sphere approximation.

The expression for k_{SF} was derived from the Fermi golden rule, eq. (1). The code first locates all local maxima of $|\langle S_1S_0^*|H_{int}|^1TT^*\rangle|^2$ in the six-dimensional space of pair geometries. Here, $S_1S_0^*$ stands for a wave function containing a configuration in which one of the partners has been excited and an admixture of charge-transfer configurations. It then evaluates the effects of intermolecular interaction on the SF energy balance at these geometries. The geometries are further optimized to find the maxima of the relative SF rate constants k_{SF}, using Marcus theory and allowing the populations in both exciton states, S* and S**, to contribute. Finally, the biexciton binding energies at the final optimized geometries are evaluated. Since the number of geometries at which k_{SF} needs to be calculated is in the billions, it was necessary to introduce physically motivated neglects and approximations. This was justified by the limited goals of the procedure: it does not attempt to compute absolute values of k_{SF}, only to identify geometries at which k_{SF} has significant local maxima. The validity of the approximate results for this limited purpose was checked by comparison with the results of high-level ab initio calculations of the SF matrix elements and in many cases, also Davydov splittings, at nearly a hundred pair geometries.[55,66] The theory and approximations of the model are detailed in the following chapter.

1.3. References

1. Shockley, W.; Queisser, H. J. *J. Appl. Phys*. **1961**, *32*, 510.

2. Hanna, M. C.; Nozik, A. J. *J. Appl. Phys.* **2006**, *100*, 074510/1.

3. Adapted from Buchanan, E.; Michl, J. Singlet Fission: The Role of Molecular Packing, Specialist Periodical Reports, in press, with permission from The Royal Society of Chemistry.

4. Singh, S.; Jones, W. J.; Siebrand, W.; Stoicheff B. P.; Schneider, W. G. *J. Chem. Phys.* **1965**, *42*, 330.

5. Dexter, D. L. *J. Luminescence* **1979**, *18*, 779.

6. Smith, M. B.; Michl, J. *Chem. Rev.* **2010**, *110*, 6891.

7. Smith, M. B.; Michl, J. *Annu. Rev. Phys. Chem.* **2013**, *64*, 361.

8. Monahan, N.; Zhu, X.-Y. *Annu. Rev. Phys. Chem.* **2015**, *66*, 601.

9. Berkelbach, T. C. *Adv. Chem. Phys.* **2017**, *162*, 1.

10. Buchanan, E. A.; Havlas, Z. ; Michl, J. in *Advances in Quantum Chemistry: Ratner Volume, Volume 75*, eds. Sabin, J. R.; Brändas, E. J. Elsevier, Cambridge, MA, **2017**, p. 175. Erratum: In the last paragraph of section 2.5 (p. 205), delete $(h_A h_A|h_B h_B) + (h_A h_A|l_B l_B) + (l_A l_A|h_B h_B) + (l_A l_A|l_B l_B)$ in the expression for $|E(^1\mathrm{TT}) - E(\mathrm{T+T})|$.

11. Casanova, D. *Chem. Rev.* **2018**, *118*, 7164.

12. Krishnapriya, K. C.; Musser, A. J.; Patil, S. *ACS Energy Lett.* **2019**, *4*, 192.

13. Rao, A.; Friend, R. H. *Nat. Rev. Mater.* **2017**, *2*, 17063.

14. Miyata, K.; Conrad-Burton, F. S.; Geyer, F. L.; Zhu, X.-Y. *Chem. Rev.* **2019**, *119*, 4261.

15. Margulies, E. A.; Logsdon, J. L.; Miller, C. E.; Ma, L.; Simonoff, E.; Young, R. M.; Schatz, G. C.; Wasielewski, M. R. *J. Am. Chem. Soc.* **2017**, *139*, 663.

16. Johnson, J. C.; Akdag, A.; Zamadar, M.; Chen, X.; Schwerin, A. F.; Paci, I.; Smith, M. B.; Havlas, Z.; Miller, J. R.; Ratner, M. A.; Nozik, A. J.; Michl, J. *J. Phys. Chem. B* **2013**, *117*, 4680.

17. Burdett, J. J.; Bardeen, C. J. *J. Am. Chem. Soc.* **2012**, *134*, 8597.

18. Swenberg, C. E. ; Geacintov, N. E. *Org. Mol. Photophysics* **1973**, *18*, 489.

19. Basel, B. S.; Zirzlmeier, J.; Hetzer, C.; Phelan, B. T.; Krzyaniak, M. D.; Reddy, S. R.; Coto, P. B.; Horwitz, N. E.; Young, R. M.; White, F. J.; Hampel, F.; Clark, T.; Thoss, M.; Tykwinski, R. R.; Wasielewski M. R.; Guldi, D. M. *Nat. Comm.* **2017**, *8*, 15171.

20. Weiss, L. R.; Bayliss, S. L.; Kraffert, F.; Thorley, K. J.; Anthony, J. E.; Bittle, R.; Friend, R. H.; Rao, A.; Greenham, N. C. *Nat. Phys.* **2017**, *13*, 176.

21. Paci, I.; Johnson, J. C.; Chen, X.; Rana, G.; Popović, D.; David, D. E.; Nozik A. J.; Ratner, M. A. *J. Am. Chem. Soc.* **2006**, *128*, 16546.

22. Albrecht, W. G.; Michel-Beyerle, M. E.; Yakhot, V. *Chem. Phys.* **1978**, *35*, 193.

23. Petelenz, P.; Snamina, M. *J. Phys. Chem. Lett.* **2016**, *7*, 1913.

24. Snamina, M.; Petelenz, P. *ChemPhysChem* **2017**, *18*, 149.

25. Michl, J.; Thulstrup, E. W. *Tetrahedron* **1976**, *32*, 205.

26. Casanova, D. *J. Chem. Theory and Comp.* **2013**, *10*, 324.

27. Dillon, R. J.; Piland, G. B.; Bardeen, C. J. *J. Am. Chem. Soc.* **2013**, *135*, 17278.

28. Ryerson, J.; Schrauben, J. N.; Ferguson, A. J.; Sahoo, S. C.; Naumov, P.; Havlas, Z.; Michl, J.; Nozik, A. J.; Johnson, J. C. *J. Phys. Chem. C* **2014**, *118*, 12121.

29. Buchanan, E. A.; Kaleta, J.; Wen, J.; Lapidus, S. H.; Císařová, I.; Havlas, Z.; Johnson, J. C.; Michl, J. *J. Phys. Chem. Lett.* **2019**, *10*, 1947.

30. Arias, D. H.; Ryerson, J. L.; Cook, J. D.; Damrauer, N. H.; Johnson, J. C. *Chem. Sci.* **2016**, *7*, 1185.

31. Berkelbach, T. C.; Hybertsen, M. S.; Reichman, D. R. *J. Chem. Phys.* **2014**, *141*, 074705.

32. Petelenz, P.; Snamina, M. *J. Phys. Chem. C* **2015**, *119*, 28570.

33. Grieco, C.; Doucette, G. S.; Munro, J. M.; Kennehan, E. R.; Lee, Y.; Rimshaw, A.; Payne, M. M.; Wonderling, N.; Anthony, J. E.; Dabo, I.; Gomez, E. D.; Asbury, J. B. *Adv. Funct. Mater.* **2017**, *27*, 1703929.

34. Bae, Y. J.; Kang, G.; Malliakas, C. D.; Nelson, J. N.; Zhou, J.; Young, R. M.; Wu, Y.-L.; Van Duyne, R. P.; Schatz, C. G.; Wasielewski, M. R. *J. Am. Chem. Soc.* **2018**, *140*, 15140.

35. Piland, G. B.; Bardeen, C. J. *J. Phys. Chem. Lett.* **2015**, *6*, 1841.

36. Piland, G. B.; Burdett, J. J.; Kurunthu, D.; Bardeen, C. J. *J. Phys. Chem. C* **2013**, *117*, 1224.

37. Tayebjee, M. J. Y.; Schwarz, K. N.; MacQueen, R. W.; Dvořák, M.; Lam, A. W. C.; Ghiggino, K. P.; McCamey, D. R.; Schmidt, T. W.; Conibeer, C. J. *J. Phys. Chem. C* **2016**, *120*, 157.

38. Stuart, A. N.; Tapping, P. C.; Schrefl, E.; Huang, D. M.; Kee, T. W. *J. Phys. Chem. C* **2019**, *123*, 5813.

39. Pensack, R. D.; Tilley, A. J.; Parkin, S. R.; Lee, T. S.; Payne, M. M.; Gao, Jahnke, A.; Oblinsky, D. G.; Li, P.-F.; Anthony, J. E.; Seferos, D. S. *J. Am. Chem. Soc.* **2015**, *137*, 6790.

40. Pensack, R. D.; Tilley, A.; Grieco, C.; Purdum, G.; Ostroumov, E.; Granger, D. B.; D. Oblinsky, D.; Dean, J.; Doucette, G.; Asbury, J.; Loo, Y.-L.; Seferos, D.; Anthony, J. E.; Scholes, G. *Chem. Sci.* **2018**, *9*, 6240.

41. Tilley, A. J.; Pensack, R. D.; Kynaston, E. L.; Scholes, G. D.; Seferos, D. S. *Chem. Mater.* **2018**, *30*, 4409.

42. Hartnett, P. E.; Margulies, E. A.; Mauck, C. M.; Miller, S. A.; Wu, Y.; Wu, Y. L.; Marks, T. J. *J. Phys. Chem. B* **2016**, *120*, 1357.

43. Dron, P. I.; Michl, J.; Johnson, J. C. *J. Phys. Chem. A* **2017**, *121*, 8596.

44. Mauck, C. M.; Hartnet, P. E.; Margulies, E. A.; Ma, L.; Miller, C. E.; Schatz, G. C.; Tobin, J. M.; Wasielewski, M. R. *J. Am. Chem. Soc.* **2016**, 138, 11749.

45. Wu, Y.; Liu, K.; Liu, H.; Zhang, Y.; Zhang, H.; Yao, J.; Fu, H. *J. Phys. Chem. Lett.* **2014**, *5*, 3451.

46. Wang, L.; Olivier, Y.; Prezhdo, O. V.; Beljonne, D. *J. Phys. Chem. Lett.* **2014**, *5*, 3345.

47. Wang, X.; Liu, X.; Tom, R.; Cook, C. *J. Phys. Chem. C* **2019**, *123*, 5890.

48. Wang, X.; Garcia, T.; Monaco, S.; Schatschneider, B.; Marom, N. *CrystEngComm* **2016**, *18*, 7353.

49. Sutton, C.; Tummala, N. R.; Beljonne, D.; Brédas, J.-L. *Chem. Mater.* **2017**, *29*, 2777.

50. Renaud, N.; Sherratt, P. A.; Ratner, M. A. *J. Phys. Chem. Lett.* **2013**, *4*, 1065.

51. Le, A. K.; Benders, J. A.; Arias, D. H.; Cotton, D. E.; Johnson, J. C.; Roberts, S. T. *J. Am. Chem. Soc.* **2018**, *140*, 814.

52. Farag, M. H.; Krylov, A. I. *J. Phys. Chem. C* **2018**, *122*, 25753.

53. Nagami, T.; Ito, S.; Kubo, T.; Nakano, M. *ACS Omega* **2017**, *2*, 5095.

54. Bhattacharyya, K.; Datta, A. *J. Phys. Chem. C* **2017**, *121*, 1412.

55. Zaykov, A.; Felkel, P.; Buchanan, E. A.; Jovanovic, M.; Havenith, R. W. A.; Kathir, R. K.; Broer, R.; Havlas, Z.; Michl, J. "Singlet Fission Rate: Optimized Packing of a Molecular Pair. Ethylene as a Model", submitted for publication.

56. Müller, A. M.; Avlasevich, Y. S.; Schoeller, W. W.; Müllen, K.; Bardeen, C. J. *J. Am. Chem. Soc.* **2007**, *129*, 14240.

57. Sanders, S. N.; Kumarasamy, E.; Pun, A. B.; Trinh, M. T.; Choi, B.; Xia, J.; Taffet, E. J.; Low, J. Z.; Miller, J. R.; Roy, X.; Zhu, X. Y.; Steigerwald, M. L.; Sfeir, M. Y.; Campos, L. M. *J. Am. Chem. Soc.* **2015**, *137*, 8965.

58. Zirzlmeier, J.; Lehnherr, D.; Coto, P. B.; Chernick, E. T.; Casillas, R.; Basel, B. S.; Thoss, M.; Tykwinski, R. R.; Guldi, D. M. *Proc. Natl. Acad. Sci. USA* **2015**, *112*, 5325.

59. Gilligan, A. T.; Miller, E. G.; Sammakia, T.; Damrauer, N. H. *J. Am. Chem. Soc.* **2019**, *141*, 5961.

60. Schrauben, J. N.; Akdag, A.; Wen, J.; Havlas, Z.; Ryerson, J. L.; Smith, M. B.; Michl, J.; Johnson, J. C. *J. Phys. Chem. A* **2016**, *120*, 3473.

61. Margulies, E. A.; Miller, C. E.; Wu, Y.; Ma, L.; Schatz, G. C.; Young, R. M.; Wasielewski, M. R. *Nature Chem.* **2016**, 8, 1120.

62. Korovina, N. V.; Das, S.; Nett, Z.; Feng, X.; Joy, J.; Haiges, R.; Krylov, A. I.; Bradforth, S. E.; Thompson, M. E. *J. Am. Chem. Soc.* **2016**, *138*, 617.

63. Margulies, E. A.; Shoer, L. E.; Eaton, S. W.; Wasielewski, M. R. *Phys. Chem. Chem. Phys.* **2014**, *16*, 23735.

64. Mauck, C. M.; Bae, Y. J.; Chen, M.; Powers-Riggs, N.; Wu, Y.-L.; Wasielewski, M. R. *ChemPhotoChem* **2018**, *2*, 223.

65. Bhattacharyya, K.; Dey, D.; Datta, A. *J. Phys. Chem. C* **2019**, *213*, 4749.

66. Ryerson, J. L.; Zaykov, A.; Aguilar Suarez, L. E.; Havenith, R. W. A.; Stepp, B. R.; Dron, P. I.; Kaleta, J.; Akdag, A.; Teat, S. J.; Magnera, T. F.; Miller, J. R.; Havlas, Z.; Broer, R.; Faraji, S.; Michl, J.; Johnson, J. C. "Structure and Photophysics of Indigoids for Singlet Fission: Cibalackrot", submitted for publication.

Chapter II

Theoretical Model

2.1. Model & Approximations[1]

2.1.1. HOMO/LUMO Model

This work was performed in collaboration with Zdenek Havlas. The HOMO/LUMO model of singlet fission[2,3] treats explicitly only electrons in the frontier orbitals on each partner (HOMO is the highest occupied and LUMO is the lowest unoccupied MO in the ground configuration). It is assumed that the initial singlet state on each partner is well described as a HOMO-LUMO excitation, and that electrons in molecular orbitals of lower energy than the HOMO on each partner can be treated as a rigid core. This assumption is most easily fulfilled when the HOMO to LUMO excited state is S_1, but it could also be met when this state is S_2 (or an even higher excited singlet), if the absorbed photon has sufficient energy and if SF is faster than internal conversion to S_1, as is the case in certain carotenoids.[4] The HOMO/LUMO model has seen much use over the past decades for many purposes.[5,6,7,8,9,10]

Even under the best of circumstances, the description of the S_1 state of a chromophore as a HOMO-LUMO excitation and the limitation of the active space to only two orbitals on each partner are only approximate. Although the HOMO/LUMO model therefore cannot be exactly correct, it is appealing conceptually and it has seen wide use in SF studies. In particular, it was employed very successfully in the first microscopic dynamical calculations of SF in polyacenes.[11,12] It is also supported by the results of a treatment of tetracene and pentacene pairs by active space decomposition,[13] and we believe that it represents a good starting point for even simpler treatments

that are needed if thorough searches of the six-dimensional space of relative geometries of two rigid bodies are to be made, as described below.

It is assumed that the two interacting chromophores A and B have equal excitation energies, but they may differ in their reduction and oxidation potentials. The singlet ground state of the chromophore pair is represented by a Slater determinant constructed from doubly occupied orbitals, $S_0^A S_0^B = S_0 S_0$. In this notation the state of chromophore A is on the left and that of chromophore B is on the right (cf. Figure 2). We consider the ground state S_0, the lowest excited singlet state S_1, and the lowest triplet state T_1 of each partner, and the two lowest-energy charge separated states $^1D^+D^-$ and $^1D^-D^+$, in which an electron is transferred from A to B or from B to A, respectively (Figure 2). The singlet excited states of A and B result from electron promotion from the HOMO h_A or h_B into the LUMO l_A or l_B, respectively. When we need to refer to an unspecified general state of partner A or B, we use U_A and U_B. The α and β symbols refer to spin functions.

The six-dimensional singlet state subspace treated explicitly in the model allows local excitations in either chromophore, a simultaneous triplet excitation in both chromophores, and the charge transfer $^1D^+D^-$ and $^1D^-D^+$ excitations:

$$S_0S_0 = N_{S0S0}\,|h_A\alpha\, h_A\beta\, h_B\alpha\, h_B\beta| \tag{2}$$

$$S_1S_0 = N_{S1S0}\,2^{-1/2}\,(\,|h_A\alpha\, l_A\beta\, h_B\alpha\, h_B\beta| - |h_A\beta\, l_A\alpha\, h_B\alpha\, h_B\beta|\,) \tag{3}$$

$$S_0S_1 = N_{S0S1}\,2^{-1/2}\,(\,|h_A\alpha\, h_A\beta\, h_B\alpha\, l_B\beta| - |h_A\alpha\, h_A\beta\, h_B\beta\, l_B\alpha|\,) \tag{4}$$

$$^1D^+D^- = N_{+-}\,2^{-1/2}\,(\,|h_A\alpha\, l_B\beta\, h_B\alpha\, h_B\beta| - |h_A\beta\, l_B\alpha\, h_B\alpha\, h_B\beta|\,) \tag{5}$$

$$^1D^-D^+ = N_{-+}\,2^{-1/2}\,(\,|h_A\alpha\, h_A\beta\, l_A\alpha\, h_B\beta| - |h_A\alpha\, h_A\beta\, l_A\beta\, h_B\alpha|\,) \tag{6}$$

$$^1T_1T_1 = N_{T1T1}\,3^{-1/2}\,[\,|h_A\alpha\, l_A\alpha\, h_B\beta\, l_B\beta| + |h_A\beta\, l_A\beta\, h_B\alpha\, l_B\alpha| - \tfrac{1}{2}\,(\,|h_A\alpha\, l_A\beta\, h_B\alpha\, l_B\beta| + |h_A\alpha\, l_A\beta\, h_B\beta\, l_B\alpha| + |h_A\beta$$

$l_A\alpha\ h_B\alpha\ l_B\beta| + |h_A\beta\ l_A\alpha\ h_B\beta\ l_B\alpha|\ )]$ (7)

The normalization factor $1/\sqrt{(N!)}$ for a Slater determinant is included implicitly ($N = 4$ is the number of electrons in the active space). In the wave functions (2) - (7), core electrons are not shown.

Because orbitals h_A and l_A are not orthogonal to orbitals h_B and l_B, the normalization factors N_x depend on intermolecular overlap integrals:

$$N_{S0S0} = \{(S_{hAhB} - 1)^2\}^{-½} \quad (8)$$

$$N_{S1S0} = (2\ S_{hAhB2}\ S_{lAhB2} - S_{hAhB2} - S_{lAhB2} + 1)^{-½} \quad (9)$$

$$N_{S0S1} = (2\ S_{hAhB2}\ S_{hA/B2} - S_{hAhB2} - S_{lAhB2} + 1)^{-½} \quad (10)$$

$$N_{+-} = (-S_{hAhB2} + S_{hA/B2} + 1)^{-½} \quad (11)$$

$$N_{-+} = (-S_{hAhB2} + S_{lAhB2} + 1)^{-½} \quad (12)$$

$$N_{TT} = \{(S_{hAhB}\ S_{lA/B} - S_{hA/B}\ S_{lAhB})^2 + ½(S_{hAhB2} + S_{hA/B2} + S_{lAhB2} + S_{lA/B2}) + 1\}^{-½} \quad (13)$$

where $S_{ab} = \int a(r_1)\ b(r_1)\ \mathrm{d}r_1$.

The Hamiltonian matrix is

$$\begin{bmatrix}
\langle S_0S_0|\hat{H}|S_0S_0\rangle & \langle S_0S_0|\hat{H}|S_1S_0\rangle & \langle S_0S_0|\hat{H}|S_0S_1\rangle & \langle S_0S_0|\hat{H}|{}^1D^+D^-\rangle & \langle S_0S_0|\hat{H}|{}^1D^-D^+\rangle & \langle S_0S_0|\hat{H}|{}^1T_1T_1\rangle \\
\langle S_0S_0|\hat{H}|S_1S_0\rangle & \langle S_1S_0|\hat{H}|S_1S_0\rangle & \langle S_1S_0|\hat{H}|S_0S_1\rangle & \langle S_1S_0|\hat{H}|{}^1D^+D^-\rangle & \langle S_1S_0|\hat{H}|{}^1D^-D^+\rangle & \langle S_1S_0|\hat{H}|{}^1T_1T_1\rangle \\
\langle S_0S_0|\hat{H}|S_0S_1\rangle & \langle S_1S_0|\hat{H}|S_0S_1\rangle & \langle S_0S_1|\hat{H}|S_0S_1\rangle & \langle S_0S_1|\hat{H}|{}^1D^+D^-\rangle & \langle S_0S_1|\hat{H}|{}^1D^-D^+\rangle & \langle S_0S_1|\hat{H}|{}^1T_1T_1\rangle \\
\langle S_0S_0|\hat{H}|{}^1D^+D^-\rangle & \langle S_1S_0|\hat{H}|{}^1D^+D^-\rangle & \langle S_0S_1|\hat{H}|{}^1D^+D^-\rangle & \langle {}^1D^+D^-|\hat{H}|{}^1D^+D^-\rangle & \langle {}^1D^+D^-|\hat{H}|{}^1D^-D^+\rangle & \langle {}^1D^+D^-|\hat{H}|{}^1T_1T_1\rangle \\
\langle S_0S_0|\hat{H}|{}^1D^-D^+\rangle & \langle S_1S_0|\hat{H}|{}^1D^-D^+\rangle & \langle S_0S_1|\hat{H}|{}^1D^-D^+\rangle & \langle {}^1D^+D^-|\hat{H}|{}^1D^-D^+\rangle & \langle {}^1D^-D^+|\hat{H}|{}^1D^-D^+\rangle & \langle {}^1D^-D^+|\hat{H}|{}^1T_1T_1\rangle \\
\langle S_0S_0|\hat{H}|{}^1T_1T_1\rangle & \langle S_1S_0|\hat{H}|{}^1T_1T_1\rangle & \langle S_0S_1|\hat{H}|{}^1T_1T_1\rangle & \langle {}^1D^+D^-|\hat{H}|{}^1T_1T_1\rangle & \langle {}^1D^-D^+|\hat{H}|{}^1T_1T_1\rangle & \langle {}^1T_1T_1|\hat{H}|{}^1T_1T_1\rangle
\end{bmatrix} \quad (14)$$

and the model permits an approximate description of processes such as energy transfer (ET), charge transfer (CT), and SF. This requires an evaluation of matrix elements in terms of integrals over the one-electron and two-electron parts of the Hamiltonian and of overlap integrals S_{hAhB}, $S_{lA/B}$, $S_{hA/B}$, and S_{lAhB} (note that $S_{hA/A} = S_{hB/B} = 0$). Those expressions that are needed for a description of SF were published previously.[14]

2.1.2 Expressions for T_{RP}

In the first approximation,[2] the initial state in SF is represented by the configuration S_1S_0 if it is localized, and either $S_1S_0 + S_0S_1$ or $S_1S_0 - S_0S_1$ if it is fully delocalized. The final state is represented by the configuration $^1T_1T_1$. Very similar formulas result in both cases.[2] Here we state results for T_{RP} applicable for a localized initial state. Those for the delocalized initial state are given in section 2.2.2, equations (51).

The matrix element $T_{RP} = H_{RP} - S_{RP}E$ becomes[15] $T_{RP} = T_{S1S0/T1T1} = H_{S1S0/T1T1} - S_{S1S0/T1T1}E_{S1S0}$, where $H_{S1S0/T1T1} = \langle {}^1T_1T_1|\hat{\mathbf{H}}|S_1S_0\rangle$, $S_{S1S0/T1T1} = \langle {}^1T_1T_1|S_1S_0\rangle$, and $E_{S1S0} = \langle S_1S_0|\hat{\mathbf{H}}|S_1S_0\rangle$. The matrix element $T_{S1S0/T1T1}$ that approximates T_{RP} in this treatment is commonly referred to as the "direct" term.

In a better approximation, the initial state is assumed to be a linear combination of S_1S_0 with a small admixture of $^1D^+D^-$ and $^1D^-D^+$, and the final state is a similar linear combination of $^1T_1T_1$ with $^1D^+D^-$ and $^1D^-D^+$. If the initial and final states are degenerate and the $^1D^+D^-$ and $^1D^-D^+$ states are also degenerate and higher in energy by ΔE, and if we use first-order perturbation theory and neglect terms containing products of two small numbers, the matrix element T_{RP} becomes[3,12]

$$T_{RP} = T_{S1S0/T1T1} - (T_{S1S0/+-}T_{+-/T1T1} + T_{S1S0/-+}T_{-+/T1T1})/\Delta E. \quad (15)$$

where the subscript +− stands for $^1D^+D^-$ and the subscript −+ stands for $^1D^-D^+$.

The expression for T_{RP} now consists of the direct term $T_{S1S0/T1T1}$ and a term mediated by the virtual states $^1D^+D^-$ and $^1D^-D^+$, which contains division by the energy difference ΔE. Formula (15) is the standard first-order expression for T_{RP} that is applicable when the energies of the charge separated states $^1D^+D^-$ and $^1D^-D^+$ are the same. It has seen much use and it shall also be used in the following. If the energies of the charge-transfer states $^1D^+D^-$ and $^1D^-D^+$ are different, the result changes to

$$T_{RP} = T_{S1S0/T1T1} - [(T_{S1S0/+-}T_{+-/T1T1}/\Delta E(^1D^+D^-) + T_{S1S0/-+}T_{-+/T1T1})/\Delta E(^1D^-D^+) \quad (16)$$

If the $^1D^+D^-$ and $^1D^-D^+$ states are very close in energy to the S_1S_0 and $^1T_1T_1$ states, the first-order expressions (15) and (16) will overestimate the magnitude of the mediated term. Then, an explicit diagonalization within the three-dimensional [$^1D^+D^-$, $^1D^-D^+$, S_1S_0] and [$^1D^+D^-$, $^1D^-D^+$, $^1T_1T_1$] spaces is necessary and a more complicated formula for T_{RP} results.

Formulas (15) and (16) also assume that the coupling between the initial S_1S_0 and final $^1T_1T_1$ states is weak relative to the effects of the phonon bath and that the initial excitation does not produce their coherent superposition. If this condition is not satisfied, a diagonalization in the full four-dimensional space [$^1D^+D^-$, $^1D^-D^+$, S_1S_0, $^1T_1T_1$] is needed. This appears to be the case for the very fastest SF events, observed in crystalline pentacene.[16]

Only the two-electron part of the Hamiltonian contributes to the direct term $T_{S1S0/T1T1} = \langle ^1T_1T_1|\hat{H}|S_1S_0\rangle$ when inter-chromophore overlap is neglected and it is very small (typically on the order of meV), because the two-electron integrals involved represent electrostatic interactions

between overlap densities at least one of which is very small (it originates in the multiplication of a molecular orbital located on A with a molecular orbital located on B).

It is generally reasonable to state that the rate of singlet fission is primarily determined by interactions of starting and final states mediated by virtual charge-transfer states.[3,11,17] The mediated (indirect) term on the right-hand side of equation (13), $-(T_{S1S0/CA}T_{CA/T1T1} + T_{S1S0/AC}T_{AC/T1T1})/\Delta E$, contains contributions both from the two-electron and the one-electron part of the Hamiltonian. It typically amounts to hundreds of meV at realistic geometries, even though it contains a division by a potentially large energy difference between the initial and the charge-separated states and also sometimes suffers from destructive interference of the two paths mediated by the virtual charge-transfer states (Figure 3). The interference is reflected in the term $\langle S_1S_0|\hat{H}\,|{}^1D^+D^- + {}^1D^-D^+\rangle = \langle S_1S_0|\hat{H}\,|{}^1D^+D^-\rangle + \langle S_1S_0|\hat{H}\,|{}^1D^-D^+\rangle$, where the two matrix elements on the right could be comparable in size and opposite in sign.

Intermolecularly Non-Orthogonal Orbitals. When the four inter-chromophore overlap integrals $S_{h\mathrm{A}h\mathrm{B}}$, $S_{l\mathrm{A}l\mathrm{B}}$, $S_{h\mathrm{A}l\mathrm{B}}$, and $S_{l\mathrm{A}h\mathrm{B}}$ are not neglected, the expressions for the terms that occur in eq. (15) are quite lengthy and complicated. They have been published, partly in Supporting Information.[16] Full results for all elements of the Hamiltonian matrix (14) and the associated overlap integrals permit not only an evaluation of the expression (15) for SF, but also a similar treatment of processes such as energy transfer (ET) and charge transfer (CT). The closest analog are the previously reported[17] expressions for ET matrix elements $\langle S_0S_1|\hat{H}|S_1S_0\rangle$, derived after setting $S_{h\mathrm{A}l\mathrm{B}} = S_{l\mathrm{A}h\mathrm{B}} = 0$. We see no physical justification for such selective neglect of these two of the four overlap integrals.

For realistic pair geometries, the inter-chromophore overlaps are usually smaller than 0.1.

Terms that are higher than first order in overlap can therefore be safely neglected. To first order in overlap, the results are

$$\langle S_1S_0|\hat{H}\ |S_1S_0\rangle = N_{S1S0}{}^2\ \{F_{hAhA} + F_{lAlA} + 2\ F_{hBhB} - (h_Ah_A|h_Ah_A) - (h_Bh_B|h_Bh_B) - 4(h_Ah_A|h_Bh_B) + 2(h_Ah_B|h_Ah_B) + 2(h_Al_A|h_Al_A) - (h_Ah_A|l_Al_A) - 2S_{lAhB}\,[F_{lAhB} - (h_Ah_A|l_Ah_B) + 2\,(h_Al_A|h_Ah_B)] - 2S_{hAhB}\,[F_{hAhB} - (h_Ah_A|h_Ah_B) + (h_Ah_B|l_Al_A) + (h_Al_A|l_Ah_B)]\} \quad (17)$$

$$\langle S_1S_0|\hat{H}\ |{}^1D^+D^-\rangle = N_{S1S0}\ N_{+-}\ \{F_{lAlB} - (h_Ah_A|l_Al_B) + 2\ (h_Al_A|h_Al_B) + S_{hAlB}\,[F_{hAlA} - (h_Ah_A|h_Al_A)] + S_{lAlB}\,[F_{hAhA} + 2\ F_{hBhB} - (h_Ah_A|h_Ah_A) - 4(h_Ah_A|h_Bh_B) + 2(h_Ah_B|h_Ah_B) - (h_Bh_B|h_Bh_B)] - S_{lAhB}\,[F_{hBlB} + 2(h_Ah_B|h_Al_B) - (h_Ah_A|h_Bl_B)] - S_{hAhB}\,[2(h_Ah_B|l_Al_B) + (h_Al_A|h_Bl_B) + (h_Al_B|l_Ah_B)]\} \quad (18)$$

$$\langle S_1S_0|\hat{H}\ |{}^1D^-D^+\rangle = N_{S1S0}\ N_{-+}\ \{-F_{hAhB} - (h_Ah_B|l_Al_A) + 2(h_Al_A|l_Ah_B) + 2S_{lAhB}\,[F_{hAlA} - (h_Al_A|h_Bh_B)] - S_{hAhB}\,[F_{hBhB} + F_{lAlA} + F_{hAhA} - 3(h_Ah_A|h_Bh_B) - (h_Ah_A|l_Al_A) - (h_Ah_B|h_Ah_B) + 2(h_Al_A|h_Al_A) - (h_Bh_B|h_Bh_B) + 2(l_Ah_B|l_Ah_B) - (l_Al_A|h_Bh_B) - (h_Ah_A|h_Ah_A)]\} \quad (19)$$

$$\langle S_1S_0|\hat{H}\ |{}^1T_1T_1\rangle = N_{S1S0}\ N_{T1T1}\ (3/2)^{1/2}\ \{\ (l_Ah_B|l_Al_B) - (h_Ah_B|h_Al_B) + S_{lAlB}\,[F_{lAhB} - (h_Ah_A|l_Ah_B)] - S_{hAlB}\,[F_{hAhB} - (h_Ah_A|h_Ah_B) + (h_Ah_B|l_Al_A) - (h_Al_A|l_Ah_B)] + S_{lAhB}\,[F_{lAlB} - (h_Ah_A|l_Al_B) + 2(h_Al_A|h_Al_B) - (l_Ah_B|h_Bl_B) - (l_Al_B|h_Bh_B)]\ - S_{hAhB}\,[F_{hAlB} - (h_Ah_B|h_Bl_B) + (h_Al_A|l_Al_B) - (h_Ah_B|h_Bh_B) + (h_Al_B|l_Al_A) - (h_Ah_A|h_Al_B)]\} \quad (20)$$

$$\langle {}^1D^+D^-|\hat{H}\ |{}^1T_1T_1\rangle = N_{+-}\ N_{T1T1}\ (3/2)^{1/2}\ \{F_{lAhB} - (h_Ah_A|l_Ah_B) + (l_Ah_B|l_Bl_B) - S_{lAlB}\,(h_Ah_B|h_Al_B) + S_{lAhB}\,[F_{hAhA} + F_{hBhB} + F_{lBlB} - (h_Ah_A|h_Ah_A) - 3(h_Ah_A|h_Bh_B) + 2(h_Ah_B|h_Ah_B) - (h_Ah_A|l_Bl_B) + 2(h_Al_B|h_Al_B) - (h_Bh_B|l_Bl_B) - (h_Bh_B|h_Bh_B)] + S_{hAlB}\,[2(h_Al_B|l_Ah_B) - (h_Ah_B|l_Al_B)] - S_{hAhB}\,[F_{hAlA} - (h_Ah_A|l_Al_A) + (h_Ah_B|l_Ah_B) - (h_Al_A|h_Bh_B) + (h_Al_A|l_Bl_B) + (h_Al_B|l_Al_B)]\} \quad (21)$$

$$\langle {}^1D^-D^+|\hat{H}\ |{}^1T_1T_1\rangle = N_{-+}\ N_{T1T1}\ (3/2)^{1/2}\ \{F_{hAlB} - (h_Al_B|h_Bh_B) + (h_Al_B|l_Al_A) - S_{lAlB}\,(h_Ah_B|l_Ah_B) + S_{hAlB}\,[F_{hAhA}$$

$$+ F_{h\mathrm{B}h\mathrm{B}} + F_{l\mathrm{A}l\mathrm{A}} - (h_\mathrm{B}h_\mathrm{B}|h_\mathrm{B}h_\mathrm{B}) - 3(h_\mathrm{A}h_\mathrm{A}|h_\mathrm{B}h_\mathrm{B}) + 2(h_\mathrm{A}h_\mathrm{B}|h_\mathrm{A}h_\mathrm{B}) - (l_\mathrm{A}l_\mathrm{A}|h_\mathrm{B}h_\mathrm{B}) + 2(l_\mathrm{A}h_\mathrm{B}|l_\mathrm{A}h_\mathrm{B}) - (h_\mathrm{A}h_\mathrm{A}|l_\mathrm{A}l_\mathrm{A})$$
$$- (h_\mathrm{A}h_\mathrm{A}|h_\mathrm{A}h_\mathrm{A})] + S_{l\mathrm{A}h\mathrm{B}}[2(h_\mathrm{A}l_\mathrm{B}|l_\mathrm{A}h_\mathrm{B}) - (h_\mathrm{A}h_\mathrm{B}|l_\mathrm{A}l_\mathrm{B})] - S_{h\mathrm{A}h\mathrm{B}}[F_{h\mathrm{B}l\mathrm{B}} - (h_\mathrm{B}h_\mathrm{B}|h_\mathrm{B}l_\mathrm{B}) + (h_\mathrm{A}h_\mathrm{B}|h_\mathrm{A}l_\mathrm{B}) - (h_\mathrm{A}h_\mathrm{A}|h_\mathrm{B}l_\mathrm{B})$$
$$+ (l_\mathrm{A}h_\mathrm{B}|l_\mathrm{A}l_\mathrm{B}) + (l_\mathrm{A}l_\mathrm{A}|h_\mathrm{B}l_\mathrm{B})]\} \tag{22}$$

$$\langle \mathrm{S}_1\mathrm{S}_0|^1\mathrm{D}^+\mathrm{D}^-\rangle = N_{\mathrm{S}1\mathrm{S}0}\, N_{+-}\, (-S_{h\mathrm{A}h\mathrm{B}}{}^2\, S_{l\mathrm{A}l\mathrm{B}} - S_{h\mathrm{A}h\mathrm{B}}\, S_{h\mathrm{A}l\mathrm{B}}\, S_{l\mathrm{A}h\mathrm{B}} + S_{l\mathrm{A}l\mathrm{B}}) \tag{23}$$

$$\langle \mathrm{S}_1\mathrm{S}_0|^1\mathrm{D}^-\mathrm{D}^+\rangle = N_{\mathrm{S}1\mathrm{S}0}\, N_{-+}\, S_{h\mathrm{A}h\mathrm{B}}\, (S_{h\mathrm{A}h\mathrm{B}}{}^2 - S_{l\mathrm{A}h\mathrm{B}}{}^2 - 1) \tag{24}$$

$$\langle \mathrm{S}_1\mathrm{S}_0|^1\mathrm{T}_1\mathrm{T}_1\rangle = N_{\mathrm{S}1\mathrm{S}0}\, N_{\mathrm{TT}}\, (3/2)^{1/2}\, (S_{l\mathrm{A}h\mathrm{B}}\, S_{l\mathrm{A}l\mathrm{B}} - S_{h\mathrm{A}h\mathrm{B}}\, S_{h\mathrm{A}l\mathrm{B}}) \tag{25}$$

$$\langle {}^1\mathrm{D}^+\mathrm{D}^-|^1\mathrm{T}_1\mathrm{T}_1\rangle = N_{+-}\, N_{\mathrm{TT}}\, (3/2)^{1/2}\, (-S_{h\mathrm{A}h\mathrm{B}}\, S_{h\mathrm{A}l\mathrm{B}}\, S_{l\mathrm{A}l\mathrm{B}} + S_{h\mathrm{A}l\mathrm{B}}{}^2\, S_{l\mathrm{A}h\mathrm{B}} + S_{l\mathrm{A}h\mathrm{B}}) \tag{26}$$

$$\langle {}^1\mathrm{D}^-\mathrm{D}^+|^1\mathrm{T}_1\mathrm{T}_1\rangle = N_{-+}\, N_{\mathrm{TT}}\, (3/2)^{1/2}\, (-S_{h\mathrm{A}h\mathrm{B}}\, S_{l\mathrm{A}h\mathrm{B}}\, S_{l\mathrm{A}l\mathrm{B}} + S_{l\mathrm{A}h\mathrm{B}}{}^2\, S_{h\mathrm{A}l\mathrm{B}} + S_{h\mathrm{A}l\mathrm{B}}) \tag{27}$$

where $\hat{F}$ is the Fock operator for the ground state configuration $\mathrm{S}_0\mathrm{S}_0$. This operator includes the mutual interactions of electrons in the active space but also their interaction with those in the inactive core. The symbols $(ab|cd) = \int a(r_1)b(r_1)(1/r_{12})c(r_2)d(r_2)\mathrm{d}r_1\mathrm{d}r_2$ represent the two-electron (electron-electron repulsion energy) integrals in the basis of molecular orbitals of the partners.

Three comments can be made:

(i) The direct term in eq. (15) contains off-diagonal elements of the Fock operator such as $F_{l\mathrm{A}h\mathrm{B}}$ and $F_{h\mathrm{A}h\mathrm{B}}$. They are generally small relative to the diagonal elements such as $F_{h\mathrm{A}h\mathrm{A}}$, because they contain one molecular orbital on each partner. Moreover, they enter multiplied by an overlap integral. Nevertheless, their contribution to the direct term might still exceed the contribution provided by the minute two-electron integrals, and this may lead to situations in which the direct term need not be entirely negligible in eq. (15) relative to the mediated term.

(ii) The mediated term in eq. (15) contains not only these off-diagonal one-electron integrals, but also the much larger diagonal ones, albeit multiplied by overlap integrals. The latter contribution

could be comparable to those provided by off-diagonal one-electron integrals and could have a significant effect on the structural dependence of the mediated term.

(iii) The third comment does not refer to SF itself, but to the possible decay of the real (not virtual) $^1D^+D^-$ or $^1D^-D^+$ intermediate that intervenes when the conversion of the initial S_1S_0 state to the biexciton $^1T_1T_1$ state occurs in two steps. We have noted under (ii) that the presence of overlap influences the mediated term in equation (15) through its effect on the indirect coupling of the S_1S_0 state and the $^1T_1T_1$ state via the virtual $^1D^+D^-$ and $^1D^-D^+$ charge-transfer states. It introduces similar diagonal one-electron integrals into the coupling of the $^1D^+D^-$ and $^1D^-D^+$ states with the S_0S_0 ground state and thus might play a role in expressions for back-electron transfer through which these charge-transfer states are deactivated to the ground state. Because of the potential importance of overlap-containing terms, in exact solutions of the HOMO/LUMO model we do not neglect intermolecular overlap even though it is small. In the development of simple formulas, we neglect it.

The expressions (17) - (27) that include overlap are useful for qualitative considerations such as the above points (i) - (iii), but for actual numerical computations of exact solutions of the HOMO/LUMO model, we prefer to perform a Löwdin orthogonalization of the orbitals located on different partners, and subsequently use the simple formulas for orthogonal orbitals.

Intermolecularly Orthogonalized Orbitals. The neglect of intermolecular overlap in the simplified procedure or the use of intermolecularly Löwdin orthogonalized molecular orbitals in the exact solution of the HOMO/LUMO model simplifies expressions (17) - (27) considerably. The normalization factors N_x in (8) - (13) become equal to unity, the overlap integrals in (23) - (27) vanish, and the expressions (17) - (22) for the Hamiltonian matrix elements simplify to the previously published[2] simple formulas (28) - (32), written in terms of the Fock operator for the

ground state $\hat{F}$, which includes interactions with core electrons:

$$\langle S_1S_0|\hat{H}|{}^1T_1T_1\rangle = (3/2)^{1/2}\,[(l_Ah_B|l_Al_B) - (h_Ah_B|h_Al_B)] \tag{28}$$

$$\langle S_1S_0|\hat{H}|{}^1D^+D^-\rangle = \langle l_A|\hat{F}|l_B\rangle + 2(h_Al_A|h_Al_B) - (h_Ah_A|l_Al_B) \tag{29}$$

$$\langle S_1S_0|\hat{H}|{}^1D^-D^+\rangle = -\langle h_A|\hat{F}|h_B\rangle + 2(h_Al_A|l_Ah_B) - (h_Ah_B|l_Al_A) \tag{30}$$

$$\langle {}^1D^+D^-|\hat{H}|{}^1T_1T_1\rangle = (3/2)^{1/2}\,[\langle l_A|\hat{F}|h_B\rangle + (l_Ah_B|l_Bl_B) - (h_Ah_A|l_Ah_B)] \tag{31}$$

$$\langle {}^1D^-D^+|\hat{H}|{}^1T_1T_1\rangle = (3/2)^{1/2}\,[\langle h_A|\hat{F}|l_B\rangle + (l_Bh_A|l_Al_A) - (h_Al_B|h_Bh_B)] \tag{32}$$

The Fermi golden rule formula for the SF rate then is

$$W(\mathrm{SF}) = (2\pi/\hbar)|\{\langle S_1S_0|\hat{H}|{}^1T_1T_1\rangle - [\langle S_1S_0|\hat{H}|{}^1D^+D^-\rangle\langle {}^1D^+D^-|\hat{H}|{}^1T_1T_1\rangle/\Delta E({}^1D^+D^-) + \langle S_1S_0|\hat{H}|{}^1D^-D^+\rangle\langle {}^1D^-D^+|\hat{H}|{}^1T_1T_1\rangle/\Delta E({}^1D^-D^+)]\}|^2\rho(E) \tag{33}$$

where the matrix elements of the Hamiltonian are given by expressions (28) - (32).

2.1.3. Approximations

For a rapid search for local maxima of $|T_{RP}|$ as a function of the relative disposition of two chromophores, it is desirable to simplify the expressions derived so far. The approximations to be introduced need to be fairly accurate at pair geometries at which the absolute value of T_{RP} is large, but they do not need to be valid at all at geometries at which $|T_{RP}|$ is small. We shall assume the energy differences between the charge separated states and the initial and final states are large enough for the charge separated state to be virtual and not a separate minimum on the S_1 surface and

for permitting the use of the first-order perturbation approximation and equation (15). If needed, first-order perturbation can be replaced by exact diagonalization, which makes the resulting formulas more complicated but does not involve much penalty in computation time.

Starting with the exact solution of the HOMO/LUMO model for a pair of chromophores A and B, the following approximations were introduced:[16]

Neglect of Intermolecular Overlap. This simplifies the expressions for matrix elements that are needed for the rate equation (33) to expressions (28) - (32). As is common in semiempirical theories, atomic orbitals are considered to be intramolecularly Löwdin orthogonalized and yet retain their atomic properties.

Zero Differential Overlap (ZDO). Neglect of all electron repulsion integrals that involve charge densities resulting from products of orbitals located on different partners makes the direct term vanish and simplifies the mediated term greatly. The matrix elements needed for equation (33) now are:

$$\langle S_1S_0|\hat{H}\,|{}^1T_1T_1\rangle = 0 \tag{34}$$

$$\langle S_1S_0|\hat{H}\,|{}^1D^+D^-\rangle = \langle l_A|\hat{F}|l_B\rangle \tag{35}$$

$$\langle S_1S_0|\hat{H}\,|{}^1D^-D^+\rangle = -\langle h_A|\hat{F}|h_B\rangle \tag{36}$$

$$\langle {}^1D^+D^-|\hat{H}\,|{}^1T_1T_1\rangle = (3/2)^{1/2}\,\langle l_A|\hat{F}|h_B\rangle \tag{37}$$

$$\langle {}^1D^-D^+|\hat{H}\,|{}^1T_1T_1\rangle = (3/2)^{1/2}\,\langle h_A|\hat{F}|l_B\rangle \tag{38}$$

The validity of the ZDO approximation has been verified numerically for many different

geometries of a pair of ethylenes[16]. As an example, Figure 8 shows the three contributions to the matrix element $\langle {}^1D^+D^-|\hat{H}|{}^1T_1T_1\rangle$ in eq. (31) for two slip-stacked ethylenes. It demonstrates that in the region of geometries where this matrix element is large, the two contributions neglected in the ZDO approximation, $(l_A h_B|l_B l_B)$ and $(h_A h_A|l_A h_B)$, are indeed negligible relative to the contribution $(3/2)^{1/2}\,\langle l_A|\hat{F}|h_B\rangle$ that is kept in eq. (37).

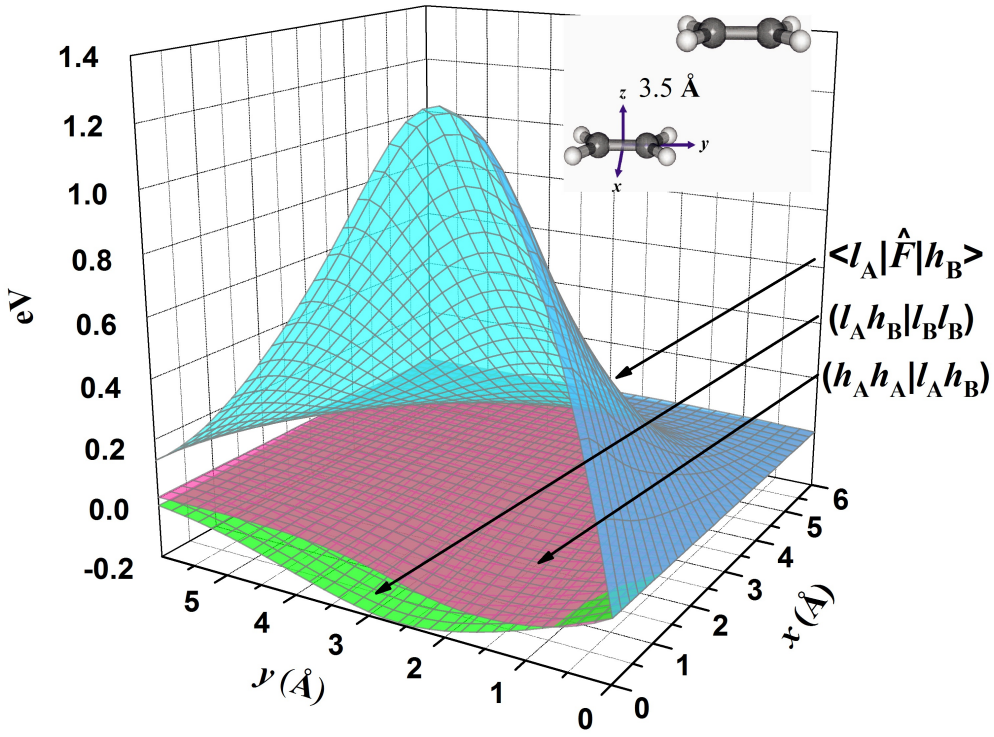

Figure 8. Equation (31): the three contributions to the matrix element $\langle {}^1D^+D^-|\hat{H}|{}^1T_1T_1\rangle$ for two parallel ethylene molecules separated by z = 3.5 Å, as a function of slip along directions x and y. A similar example was published previously.[16]

The formula for the SF rate now simplifies to

$$W(\mathrm{SF}) = (3\pi/\hbar)|\langle l_A|\hat{F}|l_B\rangle\langle l_A|\hat{F}|h_B\rangle/\Delta E(^1\mathrm{D}^+\mathrm{D}^-) - \langle h_A|\hat{F}|h_B\rangle\langle h_A|\hat{F}|l_B\rangle/\Delta E(^1\mathrm{D}^-\mathrm{D}^+)|^2\rho(E) \quad (39)$$

A Minimum Valence Basis Set of NAOs. In the next step, we express the HOMO and LUMO in a minimum basis sets of natural AOs (μ or κ on partner A and ν or λ on partner B). On each partner, this basis set is orthonormal (Löwdin orthogonalized AOs), but the AOs on partner A may have a non-zero overlap with those on partner B. Fock operator ($\hat{F}$) elements between AOs on different partners are equated to resonance (hopping) integrals $\beta_{\mu\nu}$, which are then related to AO overlaps through the Mulliken approximation:[18,19]

$$\langle \mu|\hat{F}|\nu\rangle = \beta_{\mu\nu} = kS_{\mu\nu} \quad (40)$$

where the proportionality constant k is a function of the nature of atoms μ and ν via the Wolfsberg-Helmholtz formula[20] used in Extended Hückel theory (EHT),[21]

$$k = K(H_{\mu\mu} + H_{\nu\nu})/2 \quad (41)$$

and $H_{\mu\mu}$ is the standard EHT parameter describing the electron binding energy of orbital μ. In EHT calculations the value of K is usually set to 1.75 and this works well when the atoms μ and ν are separated by the usual intramolecular bonding distances. However, for distances close to or exceeding the sum of van der Waals radii, the value needs to be reduced. For $(2p\text{-}2p)_\pi$ and $(2p\text{-}2p)_\sigma$ interactions at 3 - 5 Å, the Linderberg formula[20] yields K = ~1.0. We adopt K = 1.03, for which the $|T_{RP}|$ values obtained from the simplified and the exact solution of the HOMO/LUMO model for

ethylene pair at a variety of geometries are nearly identical.

The final expression for the rate of SF now is

$$W(\mathrm{SF}) = (3\pi k^4/\hbar)\rho(E)[(\Sigma_{\mu\nu}c_{l\mu}c_{h\nu}S_{\mu\nu})(\Sigma_{\kappa\lambda}c_{l\kappa}c_{l\lambda}S_{\kappa\lambda})/\Delta E(^1\mathrm{D}^+\mathrm{D}^-) - (\Sigma_{\mu\nu}c_{h\mu}c_{l\nu}S_{\mu\nu})(\Sigma_{\kappa\lambda}c_{h\kappa}c_{h\lambda}S_{\kappa\lambda})/\Delta E(^1\mathrm{D}^-\mathrm{D}^+)]^2 \quad (42)$$

This general result can sometimes be simplified further. For qualitative considerations, it is often possible to neglect the dependence of $\Delta E(^1\mathrm{D}^+\mathrm{D}^-)$ and $\Delta E(^1\mathrm{D}^-\mathrm{D}^+)$ on the geometry of the A,B pair, since A and B need to be in contact. Typical values are 30 - 50 kcal/mol, but values outside this range are easily possible. If charge transfer is equally likely in both directions, for instance if the two partners are symmetry-related identical chromophores, it is possible to assume $\Delta E(^1\mathrm{D}^+\mathrm{D}^-) = \Delta E(^1\mathrm{D}^-\mathrm{D}^+) = \Delta E$, and (42) then simplifies to

$$W(\mathrm{SF}) = (3\pi k^4/\hbar\Delta E^2)\rho(E)[(\Sigma_{\mu\nu}c_{l\mu}c_{h\nu}S_{\mu\nu})(\Sigma_{\kappa\lambda}c_{l\kappa}c_{l\lambda}S_{\kappa\lambda}) - (\Sigma_{\mu\nu}c_{h\mu}c_{l\nu}S_{\mu\nu})(\Sigma_{\kappa\lambda}c_{h\kappa}c_{h\lambda}S_{\kappa\lambda})]^2 \quad (43)$$

If the two partners are different and electron transfer from A to B is much easier than from B to A, $\Delta E = \Delta E(^1\mathrm{D}^+\mathrm{D}^-) << \Delta E(^1\mathrm{D}^-\mathrm{D}^+)$, the second term in the brackets in equation (42) can be neglected and the expression simplifies to

$$W(\mathrm{SF}) = (3\pi k^4/\hbar\Delta E^2)\rho(E)[(\Sigma_{\mu\nu}c_{l\mu}c_{h\nu}S_{\mu\nu})(\Sigma_{\kappa\lambda}c_{l\kappa}c_{l\lambda}S_{\kappa\lambda})]^2 \quad (44)$$

The simple expressions (43) and (44) are easily programmed but in many cases they can be

understood qualitatively upon visual inspection. After all, even for large molecules any one AO on partner A normally overlaps strongly with only very few AOs on partner B (often, none, but sometimes up to three or four), and most of the terms in the sums in equations (42) - (44) are negligible. Although our treatment deals with cases in which the two partner molecules are distinct, it can be used for qualitative insight even if they are covalently bound. E.g., when a donor A and an acceptor B are connected through a single bond that links atom 1 on A with atom 1' on B, the only significant overlap integral is $S_{11'}$ and the brackets in equation (44) equal $S_{11'}{}^2 c_{l1}{}^2 c_{h1'} c_{l1'}$. Then, to maximize $|T_{RP}|$, the LUMO of A should have a large coefficient at its link atom 1, both the LUMO and the HOMO of B should have a large coefficient at its link atom 1', and the linking bond should not be twisted too much.

Our search for a mutual disposition of partners A and B that optimizes the rate of the S_1S_0 to $^1T_1T_1$ conversion might thus appear to have been reduced to the maximization of the square in the brackets of equations (42), (43) or (44), requiring only the knowledge of the expansion coefficients on HOMO and LUMO and of the overlap integrals betweeen AOs on one and the other partner.

However, only half of the work has been done, since the density of states factor $\rho(E)$ in expressions (42) - (44) also depends on the choice of geometrical disposition of the partners. The chief reason for that is that the pair geometry affects the energetics of the SF process by Davydov interaction that frequently stabilizes the lowest excited singlet state and leaves the energy of the lowest triplet nearly intact. Its effect on relative SF rates at various partner dispositions may be unimportant in practice if SF is sufficiently exothermic and rapid at all geometries, but it may be essential if SF is isoergic or endoergic at some of them. The factor $\rho(E)$ has been treated by various authors, for example via microscopic dynamics,[11,12,13] in the Marcus theory approximation,[21] or using

a simple kinetic model.[22]

In the next section, we detail how the local maxima of $|T_{RP}|^2$ are located and address the evaluation of the energetics as a function of geometrical arrangement of the partners in a fashion that resembles our treatment of $|T_{RP}|^2$. We take into account both factors that determine the magnitude of the Davydov splitting of the lowest singlet state, the direct interaction between transition densities and the contribution mediated by virtual charge transfer states.[23,24]

2.2. SIMPLE[25] Algorithms

2.2.1. Local Maxima of $|T_{RP}|^2$ in the 6-D Space of Rigid Pair Geometries

The mutual disposition of two rigid molecules is described by six degrees of freedom, three translations (T_x, T_y, T_z) and three rotations (R_x, R_y, R_z). The value of the T_{RP} matrix element is a function of these six variables, $T_{RP} = T_{RP}$ (T_x, T_y, T_z, R_x, R_y, R_z). Since in the rate expressions T_{RP} appears in the second power, our search for the mutual dispositions of two chromophores that maximize the rate constant of the SF process starts with a search for the largest local maxima of $|T_{RP}|^2$ in the 6-D space. Afterwards, we will discard unphysical maxima and possibly also those for which the $\rho(E)$ term is unfavorable.

Locating the maxima of $|T_{RP}|^2$ is an arduous task that requires a systematic search of that part of the 6-D space in which the partners A and B are close to each other. Techniques such as the genetic algorithm[26] that have been developed for such searches do not guarantee that all the local extrema will be found. Our preferred procedure is to combine preselection of extrema on a 6-D grid with subsequent gradient optimization starting at the preselected points. To create a relatively sparse grid in a 6-D space, with 0.2 Å steps for translations and 15° for rotations, one has to evaluate $|T_{RP}|^2$

at 10^7 - 10^9 points or even more, depending on the size of chromophores. A systematic search for maxima on the $|T_{RP}|^2$ surface is therefore presently limited to the use of simple formulas such as (42) - (44). These do not provide any information about intermolecular repulsions and the energetic accessibility of the geometries at which the maxima of $|T_{RP}|^2$ are located. By itself, the function $|T_{RP}|^2$ typically shows local maxima at geometries at which the HOMO and LUMO overlap strongly but the molecules interpenetrate to a ridiculous extent. This is illustrated in Figure 9, which shows a perspective view of a plot of $|T_{RP}|^2$ as a function of T_x and T_y at T_z = 3 Å, $R_x = R_y = R_z = 0$, and thus displays the results for a two-dimensional subspace of the total six-dimensional space. The values of $|T_{RP}|^2$ are quite large, since at T_z = 3 Å the molecules are pressed closer together than they would ever come under ordinary conditions, making the intermolecular overlap integrals fairly large. The value at the maxima drops as T_z is increased and grows as it is decreased. It reaches a peak at T_z = 0, a completely unphysical situation with the molecules interleaved in the same plane. This unphysical maximum could however be viewed as the parent of the various realizable maxima that can be arrived at by moving the two molecules further apart along one or another direction.

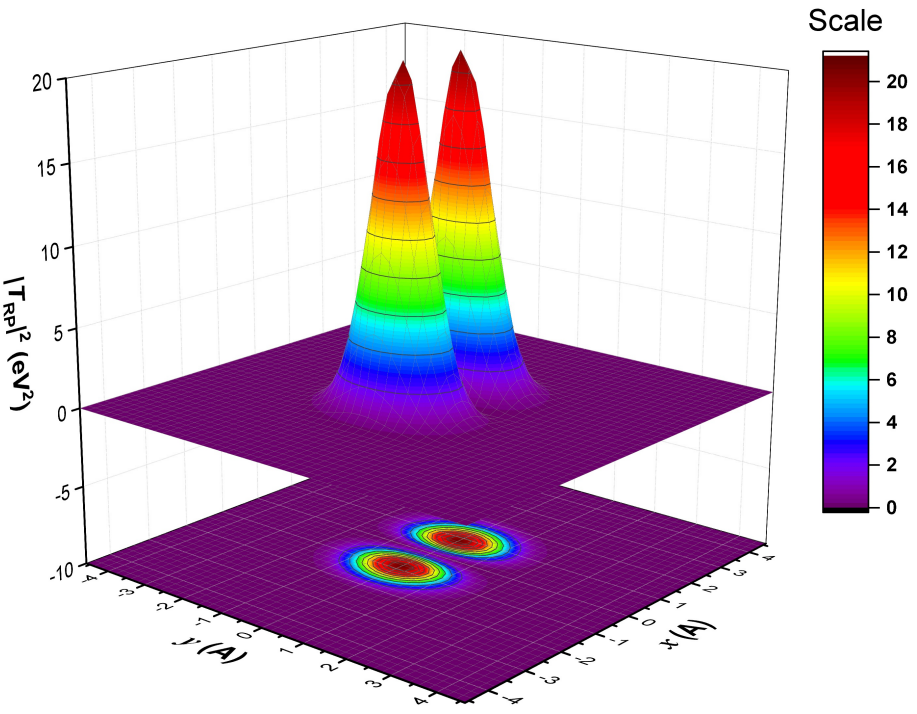

Figure 9. $|T_{RP}|^2$ in units of eV^2 for two parallel ethylene molecules separated by 3.0 Å as a function of slip along in-plane directions x and y. The maxima are located at $x = \pm 1.0$ and $y = 0.0$ Å.

The inaccessible maxima of $|T_{RP}|^2$ thus provide insight into the origin of maxima that can actually be accessed, and our present task is to find the latter. For this purpose, we use a "search function", which combines information about $|T_{RP}|^2$ with information about the part of our 6-D space that is excluded when atoms in the two partner molecules are modeled as hard spheres. The search function is defined as

$$F = \alpha E_{REP}^{\ 2} - |T_{RP}|^2 \tag{45}$$

where E_{REP} is a repulsion term and α is a weighting coefficient. The function F has no real physical significance and only helps us to find structures at which $|T_{RP}|^2$ is large, yet the two partners are not unrealistically close. We have tested the use of several van der Waals potentials for E_{REP} and in the end concluded that for our purpose a hard sphere potential seems to be the best, and use

$$E_{REP}^{\ 2} = 10^{106} \sum_{\mu\nu} \exp[-\varsigma d_{\mu\nu}/(r_{\mu}^{\ vdW} + r_{\nu}^{\ vdW})], \tag{46}$$

where the summation runs over all atoms of molecule A (μ) and molecule B (ν), ς = 244.0, $d_{\mu\nu}$ is the distance between atoms μ and ν, and $r_{\mu}^{\ vdW}$ is the van der Waals radius[27] of atom μ. The results are quite independent of the choice of the weighting coefficient α, and we set α = 1.

Figure 10 shows the value of the search function F in the same two-dimensional subspace T_x,T_y (T_z = 3 Å, $R_x = R_y = R_z = 0$) that was used for Figure 9. Now, the unphysical region of interpenetrated molecules is excluded and the four minima of the search function lie at its circumference. As T_z is increased, the excluded region of the two-dimensional subspace shrinks and ultimately disappears, and the four minima of F coalesce pairwise into two, identical with those of $|T_{RP}|^2$. This is a typical result; the optimal geometries that can be realistically accessed surround a much higher maximum that cannot be accessed because of intermolecular repulsions. Clearly, increased hydrostatic pressure would in general be favorable for reaching higher values of $|T_{RP}|^2$.

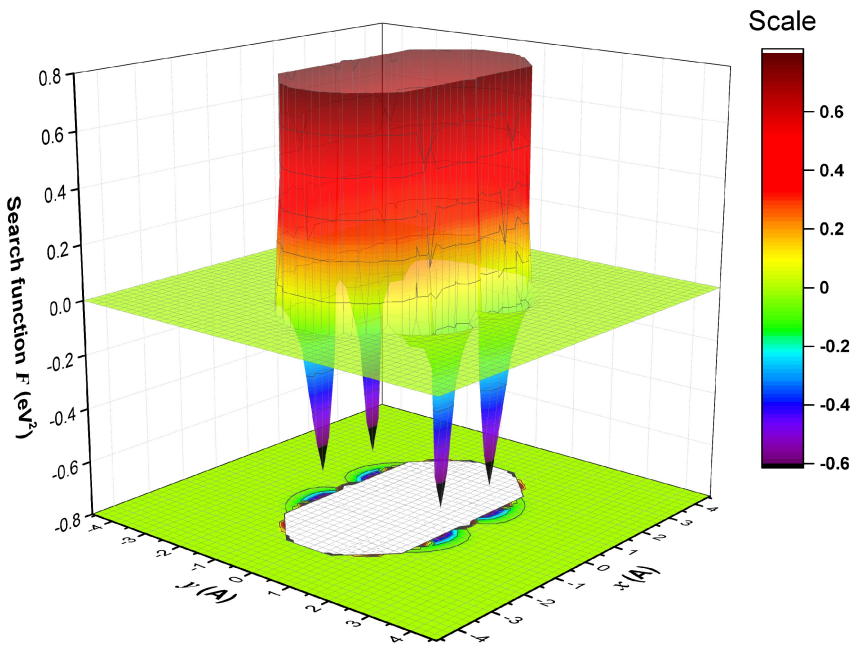

Figure 10. The search function F^2 in units of eV^2 for two parallel ethylene molecules separated by 3.0 Å as a function of slip along in-plane directions x and y.

Using the search function $F(T_x, T_y, T_z, R_x, R_y, R_z)$ and the simple approximation (43) for the evaluation of $|T_{RP}|^2$, numerical determination of the location of minima on a 6-D grid of ~10^9 points takes several hours of CPU time on a modern Intel processor for a small molecule such as ethylene and several days for a large one, such as 1,3-diphenylisobenzofuran. Subsequent refinement of the best pair geometries is performed by an optimization procedure based on numerical evaluation of gradients and the Hessian.

State Energies in the 6-D Space of Rigid Pair Geometries. Up to this point, we have ignored the $\rho(E)$ term in equations (43) and (44). When it is approximated similarly as in Marcus

theory of charge transfer, its effect on the expected rate of SF is reflected in two primary energy-related terms, the reorganization energy λ and the exoergicity of the SF process, ΔE_{SF}. While λ can be reasonably considered independent of the mutual disposition of the partners A and B, the exoergicity ΔE_{SF} cannot. For some chromophores, such as pentacene, the resulting variation of the SF rate may be of little practical consequence since $E(S_1)$ is sufficiently larger than $2E(T_1)$ that SF is exothermic for any realistic mutual disposition of the chromophores A and B and will always prevail over competing decay channels. For chromophores in which $E(S_1)$ and $2E(T_1)$ are less favorable, such as tetracene, the variation of ΔE_{SF} as a function of the mutual chromophore disposition may be critically important for the outcome of the competition between SF and other decay processes.

2.2.2. Delocalization, Couplings, Energies, & Rate

To address the effects of delocalization, intermolecular interactions, and energetics on SF, we shall assume that in the absence of intermolecular interactions, the configurations Φ_A, Φ_B, and Φ_{AB} have the same energy (singlet fission would then be isoergic) and that the configurations Φ_{+-} and Φ_{-+} also have the same energy, which is higher by ΔE. The mixing of these configurations produces the eigenstates of the pair: the two exciton states $S^{\pm}$ and the biexciton state $^1TT^*$ at low energy and the two charge-transfer states $CT^{\pm}$ at higher energy. The initial excitation can be into the S_1 state of a single chromophore if it precedes contact between partners A and B (singlet fission in solution), but normally it is into the allowed S^+ exciton state. If S^- is lower in energy, it is assumed that internal conversion rapidly equilibrates the populations of the two exciton states and will then be the starting state for SF. We will consider both S^+ and S^- in the evaluation of the SF rate using Boltzmann populations. We assume that electronic dephasing by interactions with phonons is fast

enough to decouple excitation from the ground state into $S^{\pm}$ from excitation from the ground state to the biexciton (BE) $^1TT^*$ and that they cannot form a coherent superposition for long.

Many of these assumptions do not need to be made if one does not look for simple algebraic solutions from which not only extremely rapid calculations but also simple qualitative rules and understanding have been shown to follow,[28] but of course no quantitative agreement with experiment. For instance, the Φ_A, Φ_B, and Φ_{AB} configurations do not need to have the same energy, nor do the Φ_{+-} and Φ_{-+} configurations, and one can certainly diagonalize the resulting 5×5 configuration interaction matrix numerically.

The matrix representation of the Hamiltonian in the ZDO approximation, $\hat{H}_{int}$, follows:

$\hat{H}_{int}$	$\|S_1S_0\rangle$	$\|S_0S_1\rangle$	$\|^1D^+D^-\rangle$	$\|^1D^-D^+\rangle$	$\|^1T_1T_1\rangle$
$\langle S_1S_0\|$	$E(S_1S_0)$	$2(h_Al_A\|h_Bl_B)$	$\langle l_A\|\hat{F}\|l_B\rangle$	$-\langle h_A\|\hat{F}\|h_B\rangle$	0
$\langle S_0S_1\|$	$2(h_Al_A\|h_Bl_B)$	$E(S_0S_1)$	$-\langle h_A\|\hat{F}\|h_B\rangle$	$\langle l_A\|\hat{F}\|l_B\rangle$	0
$\langle ^1D^+D^-\|$	$\langle l_A\|\hat{F}\|l_B\rangle$	$-\langle h_A\|\hat{F}\|h_B\rangle$	$E(^1D^+D^-)$	0	$(3/2)^{1/2}\langle l_A\|\hat{F}\|h_B\rangle$
$\langle ^1D^-D^+\|$	$-\langle h_A\|\hat{F}\|h_B\rangle$	$\langle l_A\|\hat{F}\|l_B\rangle$	0	$E(^1D^-D^+)$	$(3/2)^{1/2}\langle h_A\|\hat{F}\|l_B\rangle$
$\langle ^1T_1T_1\|$	0	0	$(3/2)^{1/2}\langle l_A\|\hat{F}\|h_B\rangle$	$(3/2)^{1/2}\langle h_A\|\hat{F}\|l_B\rangle$	$E(^1T_1T_1)$

In a diabatic picture within the ZDO approximation, the BE and LE singlet sub-blocks are not directly coupled, but can couple through interaction with the CT sub-block, the so-called mediated pathway. If Coulomb coupling between sub-blocks is weak, quasi-diabatic states may be obtained through admixture of the two lowest energy CT states into the LE and BE states by perturbation theory. Otherwise, the admixture must be done by diagonalization.

The two diabatic states in the LE sub-block are coupled at most pair geometries through the

Coulomb interaction between their transition densities which allows excitation energy transfer between the two LE states. In a molecule pair where both partners are the same, the two LE states are initially degenerate in the absence of intermolecular interactions and this interaction causes the splitting of the two state energies, known as the Davydov/excitonic splitting. The effect can also be present in pairs where the partners differ. The SF energy balance is important for the efficiency of the process and stabilization of the lower LE state by excitation energy transfer is generally detrimental since it tends to make the SF process too endoergic.

The three quasi-diabatic states required can be generated from the interaction Hamiltonian in a few obvious ways which are implemented in SIMPLE.[27] If we assume that all couplings and therefore admixtures are small, perturbation theory can be used to obtain coefficients $\lambda_{i,j}$ in eqs. (47a-c) from the expression given in eqs. (47d-e). We refer to this method as 'Procedure I.'

$$|S_1S_0^*\rangle = |S_1S_0\rangle + \lambda_{D+D-,S1S0}|^1D^+D^-\rangle + \lambda_{D-D+,S1S0}|^1D^-D^+\rangle \quad (47a)$$

$$|S_0S_1^*\rangle = |S_0S_1\rangle + \lambda_{D+D-,S0S1}|^1D^+D^-\rangle + \lambda_{D-D+,S0S1}|^1D^-D^+\rangle \quad (47b)$$

$$|^1T_1T_1^*\rangle = |^1T_1T_1\rangle + \lambda_{D+D-,T1T1}|^1D^+D^-\rangle + \lambda_{D-D+,T1T1}|^1D^-D^+\rangle \quad (47c)$$

$$|\Phi_{R/P}\rangle \in \{|S_1S_0\rangle, |S_0S_1\rangle, |^1T_1T_1\rangle\}$$

$$\lambda_{D+D-,R/P} = -\langle\Phi_{R/P}|\hat{H}|^1D^+D^-\rangle/[E(^1D^+D^-) - E(\Phi_{R/P})] \quad (47d)$$

$$\lambda_{D-D+,R/P} = -\langle\Phi_{R/P}|\hat{H}|^1D^-D^+\rangle/[E(^1D^-D^+) - E(\Phi_{R/P})] \quad (47e)$$

$$T^A = \langle S_1S_0^*|\hat{H}|^1T_1T_1^*\rangle \quad (47f)$$

$$T^B = \langle S_0S_1^*|\hat{H}|^1T_1T_1^*\rangle \quad (47g)$$

If we assume that couplings may be too strong to treat with perturbation theory we can

proceed by admixing the CT states into the LE and BE states by diagonalization. A method analogous to Procedure I would be to perform three 3×3 diagonalizations to mix the two CT states into the two LE and the BE states separately. We refer to this as 'Procedure II.' If we want to assume excitations are localized (equivalent to setting the integral $(h_A l_A|h_B l_B)$ equal to 0), then both of these methods would produce states in the form of eqs. (47a-c) which would be non-orthogonal due to their CT contributions. The SF couplings for localized singlet excitations on either partner A or B are then defined by eqs. (47f-g). However, the new S_1S_0* and S_0S_1* states are most likely still coupled through the interaction of their transition dipole moments in addition to a mediated coupling through the admixed CT states. To remove this coupling, we can perform a 2×2 diagonalization in the space of the S_1S_0* and S_0S_1* states, resulting in two new excitonic singlet states, $|S'\rangle$ and $|S''\rangle$, with the form of eqs. (48a-b).

We can instead simultaneously address all couplings in the 4×4 sub-block of $\hat{H}_{int}$ which contains the two LE and two CT diabatic states by diagonalization and separately the 3×3 sub-block which contains the two CT and the BE diabatic states and we refer to this as 'Procedure III.' The 4×4 sub-block diagonalization will give four eigenvectors, two of which are our new LE quasi-diabatic states, S' and S''. From the 3×3 sub-block diagonalization, we will obtain the new BE quasi-diabatic state ^{1}TT'. The states $^1T_1T_1$* of eq. (47c) and ^{1}TT' of eq. (48c) are equivalent in form. In general the three new states are defined as in eqs. (48). The S' state is taken as the more stable of the two excitonic singlet states.

$$|S'\rangle = \lambda_{1,1}|S_1S_0\rangle + \lambda_{1,2}|S_0S_1\rangle + \lambda_{1,3}|^1D^+D^-\rangle + \lambda_{1,4}|^1D^-D^+\rangle \quad (48a)$$

$$|S''\rangle = \lambda_{2,1}|S_1S_0\rangle + \lambda_{2,2}|S_0S_1\rangle + \lambda_{2,3}|^1D^+D^-\rangle + \lambda_{2,4}|^1D^-D^+\rangle \quad (48b)$$

$$|^1TT'\rangle = \lambda_{3,3}|^1D^+D^-\rangle + \lambda_{3,4}|^1D^-D^+\rangle + \lambda_{3,5}|^1T_1T_1\rangle \quad (48c)$$

Regardless of which procedure is used to obtain these three states, the ^{1}TT' state is not orthogonal to the excitonic S' and S" states due to contributions from the CT states. Orthogonal states are required which are as similar as possible to the original states but are not biased towards any one state. Symmetric (Löwdin) orthogonalization[29] accomplishes this and we implement it through use of singular value decomposition (SVD). The SVD of a matrix M is defined by $M=U\Sigma V^\dagger$ where U and V are unitary matrices and Σ contains the singular values of M. These are defined by solutions to the following equations:

$$M^\dagger M = V\Sigma^\dagger U^\dagger U\Sigma V^\dagger = V\Sigma^\dagger\Sigma V^\dagger$$

$$MM^\dagger = U\Sigma V^\dagger V\Sigma^\dagger U^\dagger = U\Sigma\Sigma^\dagger U^\dagger$$

If M contains the wavefunction vectors $|\Psi'\rangle = \{|S'\rangle, |S''\rangle, |^1TT'\rangle\}$ stored row-wise then $MM^\dagger$ is equivalent to the overlap matrix, S, and $\Sigma\Sigma^\dagger$ is equivalent to the diagonalized overlap matrix S_d. U and $U^\dagger$ are then the matrices which unitarily diagonalize the overlap matrix. It follows that Σ is the square root of the diagonalized overlap matrix $S_d^{1/2}$. From the definition of the SVD and recognizing that the matrices are all real we have:

$$U\Sigma V^T = \Psi'$$

$$V^T = \Sigma^{-1}U^T\Psi'$$

$$UV^T = U\Sigma^{-1}U^T\Psi' = US_d^{-1/2}U^T\Psi' = \Psi^* \quad (49)$$

The right hand side of eq. (49) is the definition of Löwdin orthogonalization and the symmetrically orthogonalized states $|\Psi^*\rangle = \{|S^*\rangle, |S^{**}\rangle, |^1TT^*\rangle\}$ are the product UV^T obtained by SVD of the non-orthogonal states $|\Psi\rangle$. The three resultant orthonormal states S*, S**, and ^{1}TT* are described by eqs. (50a-c).

The final task is to reconstruct the interaction Hamiltonian in this new basis according to eq. (50d). One will note that orthogonalization will introduce some amount of BE character into the LE states and vise versa.

$|\Psi^*\rangle \in \{|S^*\rangle, |S^{**}\rangle, |^1TT^*\rangle\}$; $|\Phi\rangle \in \{|S_1S_0\rangle, |S_1S_0\rangle, |^1D^+D^-\rangle, |^1D^-D^+\rangle, |^1T_1T_1\rangle\}$

$$|S^*\rangle = \lambda_{1,1}^*|S_1S_0\rangle + \lambda_{1,2}^*|S_0S_1\rangle + \lambda_{1,3}^*|^1D^+D^-\rangle + \lambda_{1,4}^*|^1D^-D^+\rangle + \lambda_{1,5}^*|^1T_1T_1\rangle \quad (50a)$$

$$|S^{**}\rangle = \lambda_{2,1}^*|S_1S_0\rangle + \lambda_{2,2}^*|S_0S_1\rangle + \lambda_{2,3}^*|^1D^+D^-\rangle + \lambda_{2,4}^*|^1D^-D^+\rangle + \lambda_{2,5}^*|^1T_1T_1\rangle \quad (50b)$$

$$|^1TT^*\rangle = \lambda_{3,1}^*|S_1S_0\rangle + \lambda_{3,2}^*|S_0S_1\rangle + \lambda_{3,3}^*|^1D^+D^-\rangle + \lambda_{3,4}^*|^1D^-D^+\rangle + \lambda_{3,5}^*|^1T_1T_1\rangle \quad (50c)$$

$$\langle\Psi_i^*|\hat{H}|\Psi_j^*\rangle = \Sigma_{k=1,5}\Sigma_{l=1,5}\,\lambda_{i,k}^*\lambda_{j,l}^*\langle\Phi_k|\hat{H}_{int}|\Phi_l\rangle \quad (50d)$$

We now have everything required to determine the SF energy balance and the couplings between the excitionic S* and S** states and the biexcitonic ^{1}TT* state in eqs. (51).

$$\Delta E_{DS} = E(S^{**}) - E(S^*) = \langle S^{**}|\hat{H}|S^{**}\rangle - \langle S^*|\hat{H}|S^*\rangle \quad (51a)$$

$$T^* = \langle S^*|\hat{H}|^1TT^*\rangle \quad (51b)$$

$$\Delta E_{SF}(S^*) = E(^1TT^*) - E(S^*) = \langle ^1TT^*|\hat{H}|^1TT^*\rangle - \langle S^*|\hat{H}|S^*\rangle \quad (51c)$$

$$T^{**} = \langle S^{**}|\hat{H}|^1TT^*\rangle \quad (51d)$$

$$\Delta E_{SF}(S^{**}) = E(^1TT^*) - E(S^{**}) = \langle ^1TT^*|\hat{H}|^1TT^*\rangle - \langle S^{**}|\hat{H}|S^{**}\rangle \quad (51e)$$

Optimization of molecule pair structures for maximized squared coupling, $|T^*|^2$, can lead to structures in which the SF process is strongly energetically unfavorable. To incorporate the effects of energetics and reorganization energy λ on the rate of a process, one can use Marcus theory. Marcus theory rates[30,31,32] are obtained using eqs. (52). Marcus rates for the two singlet excimer states are averaged according to two-level Boltzmann statistics[33] at room temperature as in eq. (53).

$$k(\mathrm{S}^*) = (2\pi/\hbar)|T^*|^2(4\pi\lambda k_\mathrm{B}T)^{-1/2}\exp[-(\Delta E_{\mathrm{SF}}(\mathrm{S}^*) + \lambda)^2/4\pi\lambda k_\mathrm{B}T] \tag{52a}$$

$$k(\mathrm{S}^{**}) = (2\pi/\hbar)|T^{**}|^2(4\pi\lambda k_\mathrm{B}T)^{-1/2}\exp[-(\Delta E_{\mathrm{SF}}(\mathrm{S}^{**}) + \lambda)^2/4\pi\lambda k_\mathrm{B}T] \tag{52b}$$

$$k(\mathrm{SF}) = \{1-[\exp(-\Delta E_{\mathrm{DS}}/k_\mathrm{B}T)+1]^{-1}\}k(\mathrm{S}^*) + \{[\exp(-\Delta E_{\mathrm{DS}}/k_\mathrm{B}T)+1]^{-1}\}k(\mathrm{S}^{**}) \tag{53}$$

The BE binding energy is also important to the overall SF process. We define this quantity in eq. (54) as the difference in the energy of the coupled ^{1}TT* state and two non-interacting triplets ($T_1 + T_1$). It is positive when the BE state is stabilized by interactions with the CT states.

$$\Delta E_{\mathrm{BB}} = [\Delta E_{\mathrm{A}}(\mathrm{T}_1) + \Delta E_{\mathrm{B}}(\mathrm{T}_1)] - E(^1\mathrm{TT}^*) \tag{54}$$

2.3. Comparison with *Ab Initio*[34]

We now have a model for predicting the rate constant of SF as a function of molecule pair orientation; however, considering the number of approximations implemented, one must ask if it is accurate enough to provide at least qualitatively correct results. This was examined in work with our European collaborators by Zaykov *et. al.*[27] After optimizing the intermolecular geometry for ethylene pairs, $|T^{\mathrm{A}}|^2$ and ΔE_{DS} were also evaluated by the far more accurate *ab initio* non-orthogonal

configuration interaction (NOCI) method.[35] for many of the pair geometries of local maxima obtained by the simple calculations. To obtain the NOCI results, for each partner A and B, the following calculations were performed: (i) CASSCF(2,2) for the ground state, (ii) ROHF calculation for the S_1 (HOMO to LUMO excitation) state, (iii) ROHF calculation for the T_1 state, (iv) ROHF calculation for the D^+ state (radical cation), and (v) ROHF calculation for the D^- state (radical anion) (6-311G basis set, with GAMESS-UK[36]).

Subsequently, many-electron basis functions (MEBFs, $\Phi_{AB}(IJ) = A[\Psi_A(I)\Psi_B(J)]$) were constructed by forming antisymmetrized product wavefunctions from the monomer wavefunctions $\Psi_A(I)$, describing state I of partner A, and $\Psi_B(J)$, describing state J of partner B. The following six singlet MEBFs were produced: $\Phi_{AB}(S_0S_0)$, $\Phi_{AB}(S_1S_0)$, $\Phi_{AB}(S_0S_1)$, $\Phi_{AB}(^1T_1T_1)$, $\Phi_{AB}(^1D^+D^-)$, and $\Phi_{AB}(^1D^-D^+)$. Both Hamiltonian and overlap matrix elements between the MEBFs were calculated using the GronOR[37] code, which is based on GNOME.[38]

The effective electronic coupling between diabatic states i and j was evaluated according to $t^{eff}_{ij} = H_{ij} - S_{ij}(H_{ii} + H_{jj})/2(1 - S_{ij}^2)$. To allow for delocalization, a NOCI calculation was performed to form the diabatic states $c_1D_{AB}(S_1S_0) + c_2D_{AB}(S_0S_1)$. Similarly, the effect of the charge transfer (CT) configurations was taken into account by performing two NOCI calculations, one in the basis of the MEBFs describing S_1S_0 and/or S_0S_1, $^1D^+D^-$ and $^1D^-D^+$, and one in the basis of the MEBFs describing ($^1T_1T_1$, $^1D^+D^-$ and $^1D^-D^+$). Subsequently, the Hamiltonian and overlap matrices were transformed to the basis of the diabatic states, allowing the evaluation of electronic coupling. Weights of the MEBFs in the final states were assigned according to the Gallup and Norbeck scheme.[39]

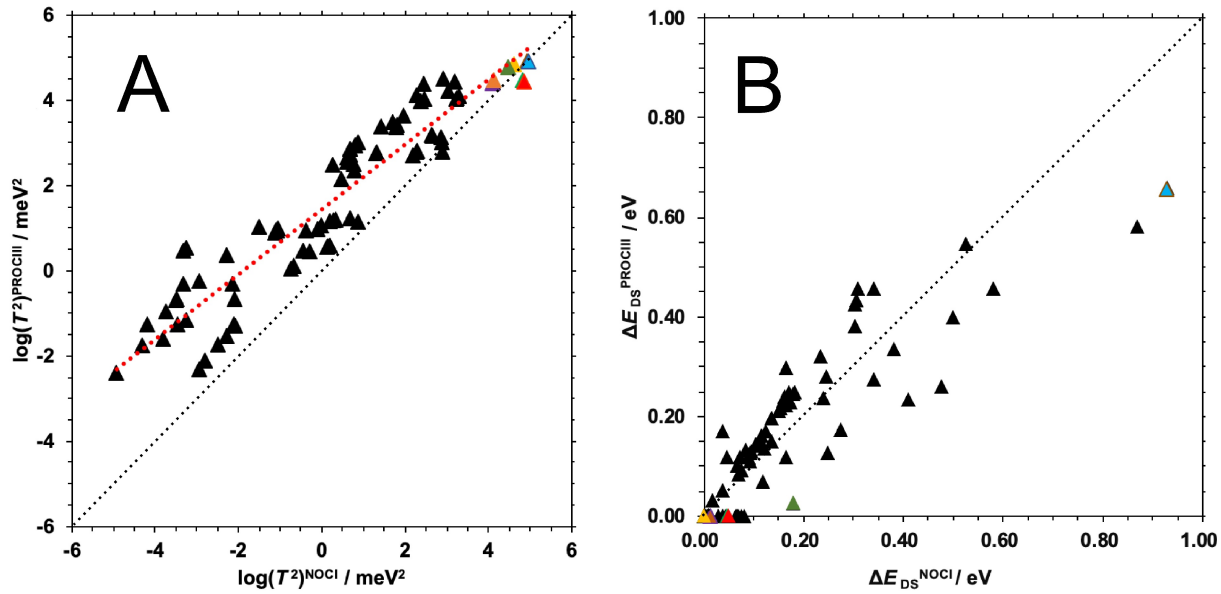

Figure 11. Plot of $\log_{10}(T^2)$ (A) and of Davydov splitting (B) obtained with Procedure III and with *ab initio* nonorthogonal configuration interaction (NOCI). Correlation line (dotted red): $\log_{10}(T^2)^{\text{PROC. III}} = 0.76\ \log_{10}(T^2)^{\text{NOCI}} + 1.44$, $T^2=(T^*)^2 + (T^{**})^2$.

Figure 11 shows the comparison of $|T|^2$ of and ΔE_{SF} calculated by SIMPLE to the much higher level results from NOCI. The agreement of the trends produced by 'Procedure III' with those yielded by the much more elaborate *ab initio* NOCI method suggests that the accuracy is adequate for a rough identification of desirable pair geometries, even though it may not predict relative rates reliably. Figure 11A shows that the accuracy is excellent at those geometries at which T^2 is the largest, as expected from the design of the approximate method. Already at geometries at which T^2 is two orders of magnitude below its maximum, the scatter of points in the log-log plot in Figure 11 is high, and at even smaller values of T^2, it gets much worse still. However, this is of no consequence for our purposes as we are searching for arrangements that produce the larger couplings. This result is reassuring as the exact ranking of the optimized pairs is immaterial as long as the procedure is able to identify all of the largest maxima of $|T|^2$ and discard those which have very

unfavorable energetics.

2.4. Qualitative Design Rules[40]

While computer code now exists to optimize the mutual geometry of a molecule pair for maximized SF rate constant using the diagonalization procedures of Section 2.2.2, a qualitative understanding of what structural factors are important for maximizing the SF rate constant in a pair is lost. It is then desirable to formulate in words a general qualitative guideline for finding pair geometries with a large electronic matrix element $|T|$ for general chromophores. Such a guideline for the maximization of $|T|$ is proposed presently. It only requires the knowledge of the intermolecular overlap of the AOs of the partners and the shape of their frontier orbitals and employs the same approximations detailed in Section 2.1.3.

We define general orbitals r and s on each partner as mixtures of h and l:

$$r = h \cos \alpha + l \sin \alpha \tag{55}$$

$$s = h \sin \alpha - l \cos \alpha \tag{56}$$

where the range of α is 0 [$r \equiv r(0) = h$, $s \equiv s(0) = -l$] to $\pi/2$ [$r \equiv r(\pi/2) = l$, $s \equiv s(\pi/2) = h$]. The evenly mixed orbitals ($\alpha = \pi/4$) are referred to as $p \equiv r(\pi/4) = 2^{-1/2}(h + l)$ and $q \equiv s(\pi/4) = 2^{-1/2}(h - l)$.

The general initial singlets in the SF process in a pair A + B are the excitonic states

$$|S^{+}(\omega)\rangle = |S_1S_0\rangle \cos\omega + |S_0S_1\rangle \sin\omega \tag{57}$$

$$|S^{-}(\omega)\rangle = |S_1S_0\rangle \sin\omega - |S_0S_1\rangle \cos\omega \tag{58}$$

where ω ranges from $-\pi/4$ to $\pi/4$. Often only the lower energy excitonic state will play a significant role, but when the difference $E(\pm)$ of the energies of the $|S^{+}\rangle$ and $|S^{-}\rangle$ states is small, populations in both may contribute to the SF process.

The results of the simple model[49] can be rewritten as equations (59) - (62).

$$\langle S^{+}(\alpha,\omega)|H_{\text{int}}|T_1T_1\rangle \approx T^{+}(\alpha,\omega) = T^{A}(\alpha)\cos\omega + T^{B}(\alpha)\sin\omega \tag{59}$$

$$\langle S^{-}(\alpha,\omega)|H_{\text{int}}|T_1T_1\rangle \approx T^{-}(\alpha,\omega) = T^{A}(\alpha)\sin\omega - T^{B}(\alpha)\cos\omega \tag{60}$$

$$T^{A}(\alpha) = [(3/2)^{1/2}/2\Delta E]\{(\cos 4\alpha)(F_{ss} - F_{rr})(F_{rs} + F_{sr}) +$$
$$[(\sin 4\alpha)/2][(F_{rr} - F_{ss})^2 - (F_{rs} + F_{sr})^2] + (F_{rr} + F_{ss})(F_{sr} - F_{rs})\} \tag{61}$$

$$T^{B}(\alpha) = [(3/2)^{1/2}/2\Delta E]\{(\cos 4\alpha)(F_{ss} - F_{rr})(F_{rs} + F_{sr}) +$$
$$[(\sin 4\alpha)/2][(F_{rr} - F_{ss})^2 - (F_{rs} + F_{sr})^2] - (F_{rr} + F_{ss})(F_{sr} - F_{rs})\} \tag{62}$$

where H_{int} is the interaction Hamiltonian in the diabatic picture, and $\tan 2\omega = 2\langle S_1S_0|H_{\text{int}}|S_0S_1\rangle/[E(S_1S_0) - E(S_0S_1)]$. When $E(\pm) = 0$, the populations of $|S^{+}\rangle$ and $|S^{-}\rangle$ are equal, and ω can be chosen arbitrarily. The sum $|T^{+}(\alpha,\omega)|^2 + |T^{-}(\alpha,\omega)|^2$ is independent of ω and equals $|T^{A}(\alpha)|^2 + |T^{B}(\alpha)|^2$.

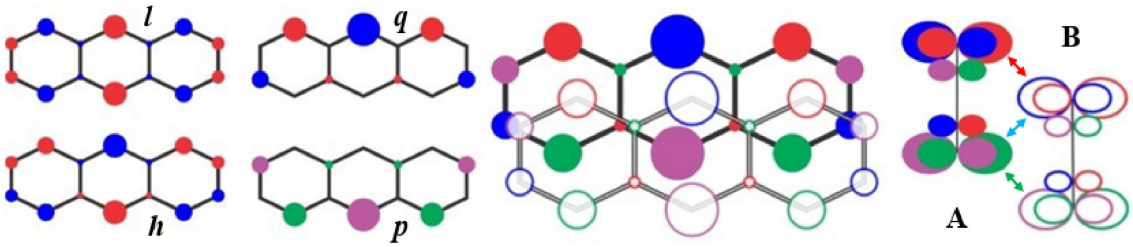

Figure 12. Anthracene as an example. Left: the canonical orbitals *h* and *l* and their sum and difference, *p* and *q*. Right: top and side views of a slip-stacked pair. $|T^{A}|$ is large since both q_A and p_A have significant overlap with q_B (red and blue double-headed arrows), but only p_A overlaps p_B, whereas q_A does not. $|T^{-}|$ is large because p_A has significant overlap with both q_B and p_B (blue and green arrows), but q_A overlaps only q_B (red arrow) and is too far for significant overlap with p_B.

These expressions for the electronic matrix elements *T* simplify when orbitals *r* and *s* are the canonical orbitals *h* and *l* ($\alpha = 0$ or $\pi/2$) or their sum and difference *p* and *q* [$\alpha = \pi/4$, $p = 2^{-1/2}(h + l)$, $q = 2^{-1/2}(h - l)$] (Figure 12), and when the initial excitation is either fully localized on partner A (T^{A}, $\omega = 0$) (or B: T^{B}, $\omega = \pi/2$) or evenly distributed on A and B (T^{+} and T^{-}, $\omega = \pm\pi/4$).

For $\alpha = 0$, the expressions become

$$T^{A} = [(3/2)^{1/2}/\Delta E](F_{hh}F_{hl} - F_{lh}F_{ll}) \quad (63)$$

$$T^{B} = [(3/2)^{1/2}/\Delta E](F_{hh}F_{lh} - F_{hl}F_{ll}) \quad (64)$$

$$T^{+}(0,\pi/4) = T^{+} = [(3)^{1/2}/2\Delta E](F_{hh} - F_{ll})(F_{hl} + F_{lh}) \quad (65)$$

$$T^{-}(\alpha,\pi/4) = T^{-} = [(3)^{1/2}/2\Delta E](F_{hh} + F_{ll})(F_{hl} - F_{lh}) \quad (66)$$

For $\alpha = \pi/4$, the expressions become

$$T^{A} = [(3/2)^{1/2}/\Delta E](F_{pp}F_{qp} - F_{pq}F_{qq}) \quad (67)$$

$$T^{B} = [(3/2)^{1/2}/\Delta E](F_{pp}F_{pq} - F_{qp}F_{qq}) \tag{68}$$

$$T^{+}(\pi/4,\pi/4) = T^{+} = [(3)^{1/2}/2\Delta E](F_{pp} - F_{qq})(F_{pq} + F_{qp}) \tag{69}$$

$$T^{-}(\alpha,\pi/4) = T^{-} = [(3)^{1/2}/2\Delta E](F_{pp} + F_{qq})(F_{qp} - F_{pq}) \tag{70}$$

Note that the expressions for T^{-} have the same form not only for $\alpha = 0$ and $\pm\pi/4$, but for any value of α.

Neglecting the variation of ΔE with geometry, we express $|T|$ in terms of the overlaps between MOs on partner A and those on partner B. The results obtained using the canonical MOs *h* and *l* or the transformed MOs *p* and *q* have the same form:

$$|T^{A}| \approx \text{const}\times|S_{hh}S_{hl} - S_{lh}S_{ll}| = \text{const}\times|S_{pp}S_{qp} - S_{pq}S_{qq}| \tag{71}$$

$$|T^{B}| \approx \text{const}\times|S_{hh}S_{lh} - S_{hl}S_{ll}| = \text{const}\times|S_{pp}S_{pq} - S_{qp}S_{qq}| \tag{72}$$

$$|T^{+}| \approx \text{const}'\times|(S_{hh} - S_{ll})(S_{hl} + S_{lh})| = \text{const}'\times|(S_{pp} - S_{qq})(S_{pq} + S_{qp})| \tag{73}$$

$$|T^{-}| \approx \text{const}'\times|(S_{hh} + S_{ll})(S_{hl} - S_{lh})| = \text{const}'\times|(S_{pp} + S_{qq})(S_{qp} - S_{pq})| \tag{74}$$

Expressions (71) - (74) are simple enough that they permit a formulation of qualitative guidance to optimal pair geometries. For our purposes Hückel MOs are adequate, but MOs obtained by more advanced methods can be used. The choice between MOs *h* and *l* or MOs *p* and *q* is a matter of taste; the same guidelines apply. We find it easier to visualize overlaps of orbitals that are as localized within A and B as possible.

In a molecule that has a plane of symmetry perpendicular to the direction of the $h \rightarrow l$ transition moment and hence MOs not polarized but evenly delocalized along this direction, we

choose to work with p and q, which are partly localized on one and the other side of the symmetry plane. For ethylene, H_2CCH_2, these are the two $2p_z$ AOs, and indeed, equations (71) and (72) revert to those already published.[16] In a polyacene, p is mostly localized along one and q mostly along the other long rim (Figure 12).

In a molecule that has a strong donor character at one end of the $h \rightarrow l$ transition moment direction and strong acceptor character at the other end, and hence has h and l strongly polarized in opposite sense along this direction, we choose to work with orbitals h and l, which are largely localized on the two ends of the molecule. For instance, in aminoborane, H_2BNH_2, in the first approximation h is the $2p_z$ AO on N and l is the $2p_z$ on B. In a polyacene carrying donor moieties along one rim and acceptors along the other, the situation would be similar.

We assume that orbital phases can be chosen in a way that makes products of overlaps such as $S_{pp}S_{qp}$ all positive (suprafacial interaction). When this is not the case (antarafacial interaction), the guidelines for optimizing $|T^A|$ and $|T^B|$ change in an obvious way. Inspection of equations (71) and (72) leads to the conclusion that $|T^A|$ and $|T^B|$ will be large when overlaps are large and the overlap products $S_{pp}S_{qp}$ and $S_{pq}S_{qq}$ (or $S_{pp}S_{pq}$ and $S_{qp}S_{qq}$) have very different magnitudes. *This requires one of the orbitals on partner A, say p_A, to overlap both orbitals p_B and q_B on partner B, and the other orbital on partner A (q_A) to have as little overlap with orbitals on partner B as possible.* Figure 1 provides an illustration (slip-stacked anthracenes).

The rules for optimizing $|T^+|$ or $|T^-|$ are derived similarly from equations (73) and (74). Again assuming that the overlaps are positive, $|T^+|$ will be maximized when the overlaps S_{pq} and S_{qp} are large and either S_{pp} or S_{qq} is large but the other is small, and $|T^-|$ will be maximized when S_{pp} and S_{qq} are large and either S_{pq} or S_{qp} is large, but not both. If the overlaps cannot be all positive, the rule

changes in an obvious fashion (Figure 12).

Polyacene crystals, the champions of singlet fission,[2,3] satisfy the rules for large matrix elements perfectly. The herringbone arrangement of neighbor molecules in their crystals is similar to that in Figure 12, except that in addition to a slip along the short axis, one of the molecules is also tilted relative to the other, and this weakens the overlap indicated by the double-headed green arrow on the right-hand side of Figure 12.

Finally, note that equations (71) - (74) show that if partners A and B both possess a symmetry operation relative to which the $h \rightarrow l$ transition moment is antisymmetric and this operation is preserved at the pair geometry, all four elements T will vanish by symmetry alone (e.g., in a perfectly stacked polyacene, this symmetry element would be reflection in a plane containing the long axes of both partners). This result is valid generally and follows from the antisymmetry of the initial state (one $h \rightarrow l$ excitation) and the symmetry of the final state (two such excitations). The addition of a quantum of an antisymmetric vibration to either the initial electronic state or the final electronic state will remove the forbiddenness. Calculations in which such vibrations were included indeed produced SF rates different from zero even when the equilibrium geometry was perfectly stacked.[41,42]

Simple qualitative expressions can similarly be derived for the Davydov splitting and energy balance of SF. These equations require the evaluation of four Coulomb integrals, but they are all repulsions between localized charge densities and can be estimated visually, similarly as the orbital overlaps. Upon orbital transformation, the two-electron repulsion integral $(h_A l_A | h_B l_B)$ is defined as in eq. (75a). These equations are all derived by first order perturbation theory and the repulsion integrals on the RHS of eqs. (75) are the zeroth order terms while the Fock matrix elements are the first order terms. For the first order perturbation terms, we have assumed that both $[E(^1D^+D^-)$ –

$E(\Phi_{R/P})]$ and $[E(^1D\text{-}D^+) - E(\Phi_{R/P})] = 2$ eV, therefore when estimating various terms in eqs. (75) one must do so on the scale of eV. For tetracene, these terms are all on the order of 10^{-2} to 10^{-1} eV, so when a value is squared it becomes smaller, not larger.

$$(h_A l_A|h_B l_B) = (1/4)\{ (p_A p_A|p_B p_B) - (p_A p_A|q_B q_B) - (q_A q_A|p_B p_B) + (q_A q_A|q_B q_B)\} \quad (75a)$$

$$\Delta E_{DS} = (1/2)[2\{(p_A p_A|p_B p_B) - (p_A p_A|q_B q_B) - (q_A q_A|p_B p_B) + (q_A q_A|q_B q_B)\} + (F_{pp} + F_{qq})^2 - (F_{pq} + F_{qp})^2] \quad (75b)$$

$$\Delta E_{SF}(S^+) = (-1/4)(2\{(p_A p_A|p_B p_B) - (p_A p_A|q_B q_B) - (q_A q_A|p_B p_B) + (q_A q_A|q_B q_B)\} + (1/2)[3\{F_{pp} - F_{qq}\}^2 - \{F_{pq} + F_{qp}\}^2 - 5\{F_{pq} \times F_{qp}\}]) \quad (75c)$$

$$\Delta E_{SF}(S^-) = (1/4)(2\{(p_A p_A|p_B p_B) - (p_A p_A|q_B q_B) - (q_A q_A|p_B p_B) + (q_A q_A|q_B q_B)\} - (1/2)[3\{F_{pq} - F_{qp}\}^2 - \{F_{pp} + F_{qq}\}^2 - 5\{F_{pp} \times F_{qq}\}]) \quad (75d)$$

In the following chapters, the model will be applied to the optimization of pair geometry for tetracene and 1,3-diphenylisobenzofuran. The top pair structures from those optimizations will be analyzed by eqs. (71) - (75) for qualitative insights into what structural factors are either detrimental for maximizing singlet fission rate. Finally, the model will be applied to pairs from the crystal structures of 1,3-diphenylisobenzofuran and 11 of its variously fluorinated derivatives to attempt to explain the results of experimental measurements on their rates of SF.

2.5. References

1. Adapted with permission from Buchanan, E. A.; Havlas, Z.; Michl, J. "Singlet Fission: Optimization of Chromophore Dimer Geometry", in *Advances in Quantum Chemistry: Ratner Volume, Volume 75*; Sabin, J. R.; Brändas, E. J., Eds.; Elsevier: Cambridge, MA, 2017, p. 175. Copyright 2019 Elsevier.

2. Smith, M. B.; Michl, J. Singlet fission. *Chem. Rev.* **2010**, *110*, 6891-6936.

3. Smith, M. B.; Michl, J. *Ann. Rev. Phys. Chem.* **2013**, *64*, 361-386.

4. Wang, C.; Angelella, M.; Kuo, C.-H.; Tauber, M. J. *Proc. SPIE* **2012**, *8459*, 845905-1-845905-13.

5. Dexter, D. L. *J. Chem. Phys.* **1953**, *21*, 836-850.

6. Trlifaj, M. *Czech J. Phys. B* **1972**, *22*, 832-840.

7. Förster, T. In *Modern Quantum Chemistry*; Sinanoglu, O., Ed.; Academic Press: New York, **1965**, Vol. 3.

8. Scholes, G. D.; Harcourt, R. D. *J. Chem. Phys.* **1996**, *104*, 5054-5061.

9. Jortner, J.; Rice, S. A.; Katz, J. L.; Choi, S. I. *J. Chem. Phys.* **1965**, *42*, 309-323.

10. Greyson, E. C.; Vura-Weis, J.; Michl, J.; Ratner, M. A. *J. Phys. Chem. B* **2010**, *114*, 14168.

11. Berkelbach, T. C.; Hybertsen, M. S.; Reichman, D. R. *J. Chem. Phys.* **2013**, *138*, 114103.

12. Busby, E.; Berkelbach, T. C.; Kumar, B.; Chernikov, A.; Zhong, Y.; Hlaing, H.; Zhu, X. Y.; Heinz, T. F.; Hybertsen, M. S.; Sfeir, M. Y.; Reichman, D. R. *J. Am. Chem. Soc.* **2014**, *136*, 10654-10660.

13. Parker, S. M.; Seideman, T.; Ratner, M. A.; Shiozaki, T. *J. Phys. Chem. C* **2014**, *118*, 12700-12705.

14. Havlas, Z.; Michl, J. *Isr. J. Chem.* **2016**, *56*, 96-106.

15. Harcourt, R. D.; Scholes, G. D.; Ghiggino, K. P. *J. Chem. Phys.* **1994**, *101*, 10521-10525.

16. Monahan, N.; Zhu, X.-Y. *Annu. Rev. Phys. Chem.* **2015**, *66*, 601-618.

17. Havenith, R. W. A.; de Gier, H. D.; Broer, R. *Mol. Phys.* **2012**, *110*, 2445-2454.

18. Wolfsberg, M.; Helmholz, L. *J. Chem. Phys.* **1952**, *20*, 837-843.

19. Hoffmann, R. *J. Chem. Phys.* **1963**, *39*, 1397-1412.

20. Linderberg, J. Seamans, L. *Mol. Phys.* **1972**, *24*, 1393-1405.

21. Renaud, N.; Sherratt, P. A.; Ratner, M. A. *J. Phys. Chem. Lett.* **2013**, *4*, 1065-1069.

22. Kolomeisky, A. B.; Feng, Y.; Krylov, A. I. *J. Phys. Chem. C* **2014**, *118*, 5188-5195.

23. Kazmaier, P. M.; Hoffmann, R. *J. Am. Chem. Soc.* **1994**, *116*, 9684-9691.

24. Yamagata, H.; Maxwell, D. S.; Fan, J.; Kittilstved, K. R.; Briseno, A. L.; Barnes, M. D.; Spano, F. C. *J. Phys. Chem. C* **2014**, *118*, 28842-28854.

25. Zaykov, A.; Felkel, P.; Buchanan, E. A.; Jovanovic, M.; Havenith, R. W. A.; Kathir, R. K.; Broer, R.; Havlas, Z.; Michl, J. "Singlet Fission Rate: Optimized Packing of a Molecular Pair. Ethylene as a Model", submitted for publication.

26. Mitchell, M. *An Introduction to Genetic Algorithms*; MIT Press: Cambridge, MA, **1996**.

27. Batsanov, S. S. *Inorg. Mat*. **2001**, *37*, 871-885.

28. Buchanan, E. A.; Michl, J. *J. Am. Chem. Soc.* **2017**, *139*, 15572-15575.

29. Löwdin, P. *Adv. Quant. Chem.* **1970**, *5*, 185-199.

30. Marcus, R. A. *Rev. Mod. Phys.* **1993**, *65*, 599.

31. Marcus, R. A. *J. Chem. Phys.* **1956**, *24*, 966 and 979.

32. Marcus, R. A.; Sutin, N. *Biochim. Biophys. Acta* **1985**, *811*, 265.

33. Harris, S. An Introduction to the Theory of the Boltzmann Equation (Holt, Rinehart and Winston, New York, **1971**).

34. Adapted with permission from Zaykov, A.; Felkel, P.; Buchanan, E. A.; Jovanovic, M.; Havenith, R. W. A.; Kathir, R. K.; Broer, R.; Havlas, Z.; Michl, J. "Singlet Fission Rate: Optimized Packing of a Molecular Pair. Ethylene as a Model", submitted for publication.

35. Havenith, R. W. A.; de Gier, H. D.; Broer, R. *Mol. Phys.* **2012**, *110*, 2445-2454.

36. Guest, M. F.; Bush, I. J.; van Dam, H. J. J.; Sherwood, P.; Thomas, J. M. H.; van Lenthe, J. H.; Havenith, R. W. A.; Kendrick, J. *Mol. Phys.* **2005**, *103*, 719-747.

37. Straatsma, T. P.; Broer, R.; Faraji, S.; Havenith, R. W. A. *Annu. Rep. Comput. Chem.*, **2018**, *14*, 77-91.

38. Broer, R.; Nieuwpoort, W. C. *Theor. Chim. Acta* **1988**, *73*, 405-418.

39. Gallup, G. A.; Norbeck, J. M. *Chem. Phys. Lett.* **1973**, *21*, 495-500.

40. Adapted with permission from Buchanan, E. A.; Michl, J. *J. Am. Chem. Soc.* **2017**, *139*, 15572-15575. Copyright 2017 American Chemical Society.

41 Matsika, S.; Feng, X.; Luzanov, A. V.; Krylov, A. I. *J. Phys. Chem. A* **2014**, *118*, 11943-11955.

42. Tamura, H.; Huix-Rotllant, M.; Burghardt, I.; Olivier, Y.; Beljonne, D. *Phys. Rev. Lett.* **2015**, *115*, 107401.

Chapter III

Optimal Arrangements of Tetracene Molecule Pairs for Fast Singlet Fission

3.1. Introduction

Tetracene is the first compound selected for optimization by the simple model. Tetracene and its simple derivatives are among the best known SF materials. The parent compound crystallizes in a herringbone structure[1] (neighbors are slip-stacked in the direction of the short molecular axis and one is rotated ~51 ° along its long axis), but in certain derivatives such as rubrene[2] neighbors are simply slip-stacked. In the parent, SF is believed to be endoergic by about 0.15 eV, yet it proceeds with a high triplet yield even at very low temperatures.[3] Several explanations of this observation have been proposed.[4,5,6]

Because of its popularity and because its SF is slightly endoergic and thus susceptible to perturbations, tetracene was selected as a suitable candidate for application of our model and program SIMPLE[23] described in the previous chapter. Many calculations for SF in tetracene have been published,[7,8,9,10,11] but to our knowledge ours is the first study whose goal it is not to calculate absolute rates, but to identify all of the favorable geometries of non-covalent tetracene molecule pairs in the full six-dimensional space of possible geometries.

3.2. Methods

Computational Methods. Reorganization energy λ was calculated to be 300 meV from $\lambda = E[T_1,q(S_1)] + E[T_1,q(S_0)] - 2\times E[T_1,q(T_1)]$,[12] where q denotes the equilibrium geometry of the monomer in a particular state. Ground and excited state geometries were optimized in the ORCA[13]

program suite with DFT and TD-DFT (TDA[14]) using the PBE0[15] functional and Def2-TZVP[16] basis set while the Def2-TZVPD[17,17] basis was used for single point energy evaluation. The RIJCOSX[18,19] approximation for Coulomb and exchange integral evaluation, with auxiliary basis sets generated by the AUTOAUX[20] procedure, was employed in all geometry optimizations but not in single point energy evaluations. Singlet excitation energies were calculated via TD-DFT without the TDA. Triplet excitation energies were calculated using the ΔSCF method.[21] Frequency analysis was performed on all optimized geometries to ensure they were true minima. The program SIMPLE[22] was used to calculate all singlet fission couplings, excitonic contributions to energetics, and Marcus theory rates and to optimize the pair structures. For these calculations, a D_{2h} symmetrized geometry of the molecular crystal structure of tetracene[23] was used. The MOs were calculated using the quantum chemistry program ORCA with the RHF[24] method using the 6-311G[25] basis set for all atoms. NAOs were obtained from natural bonding orbital (NBO) analysis performed by the NBO 6.0 program[26] linked to ORCA.

SIMPLE[23] Procedure Details. A "full" scan of the SF coupling squared, $|T^*|^2$, was then performed with SIMPLE[2] using Procedure III in which chromophore B was translated along its internal *x*, *y*, and *z* axes in +0.5 Å increments and rotated about these axes in +15° increments, resulting in 2.8×10^8 geometries. An additional "refined" scan over the most important translational sub-space of the previous scan was performed with translation increments of +0.2 Å in the x and y and +0.1 Å in the z with all rotational increments still +15°, resulting in 2.0×10^8 geometries. Altogether, SF couplings were calculated at ~4.7×10^8 geometries. Due to tetracene's D_{2h} symmetry, the space which needed to be scanned was reduced to just the positive directions of the *x*, *y*, and *z* axes, reducing the required scan space by a factor of 8.

The results of the "full" and "refined" scans were combined, with duplicate geometries removed, and the top 5,000 physically accessible geometries with largest $|T^*|^2$ were selected for optimization of their SF rate constant. The intrinsic endothermicity of SF in the absence of intermolecular interactions was calculated according to the equation $\Delta E_{SF} = 2\Delta E(T_1) - \Delta E(S_1)$ to be ~0 meV. SF in tetracene is known to be endothermic and this value is quite low. A value for ΔE_{SF} of 188 meV[27] was deduced from measurements on crystalline tetracene and as this includes intermolecular effects which stabilize the singlet exciton more than the triplet, it represents an upper bound on the endoergicity of SF in tetracene. They deduced a lower bound of 120 meV, implying an endothermicity of SF in the absence of intermolecular interactions of 154 meV. Using a Bixon-Jortner expression, Yost *et al.*[28] found the reorganization energy of acenoid sysetms to be 130 meV, about half the value we calculated of 300 meV. In our previous work on variously fluorinated crystals of 1,3-diphenylisobenzofuran derivatives,[29] we found variation in the singlet excitation energy of up to 100 meV, in the endothermicity of SF of up to 200 meV, and in the reorganization energy of up to 100 meV. To probe the effects of varying the intrinsic endothermicity of SF and the reorganization energy we performed six optimizations of the top 5,000 structures using the following sets of values in units of meV for these energies respectively: (0, 130), (0, 300), (154, 130), (154, 300), (308, 130), and (308, 300). The diabatic CT states were held at a constant 2 eV above the energy of the LE singlet diabatic states, in line with calculations by Casanova.[8]

3.3. Results

Optimization of the intermolecular geometry for maximum Marcus rate constant of SF of the top 5,000 scanned pair structures with largest $|T^*|^2$ using literature values for the intrinsic

endothermicity and reorganization energy of 154 and 130 meV resulted in 116 optimized pair structures. Table 1 provides energy values and rate constant ratios for the top 21 optimized pairs as well as the herringbone pair found in the crystal and the top pair from optimizations for just the coupling $|T^*|$ or $|T^A|$. Multi-view projections of the optimized pairs are found in Figures 13 and 14. Structure data, energetics, and rate constant ratios for the top 40 optimized pair structures from the (154, 130) optimization as well as the D_{2h} symmetrized crystal herringbone pair are provided in the Appendix. The top 20 pair structures from the five other optimizations with varied parameter sets are also provided. The multi-view projections follow the standard third-angle projection method: the main view of the xy plane is located in the lower right, the top view of the xz plane is above that and is the view if the main view was rotated 90°(about the x axis) out of the plane of the page from the top to bottom, the left side view of the yz plane is to the left and is the view if the main view was rotated 90° (about the y axis) out of the plane of the page from the left to right.

Table 1. Calculated SF Energies and Relative Rates for the Top 21 Tetracene Pairs.[a]

Struct.	$(h_A l_A \vert h_B l_B)$	ΔE_{DS}[b]	$\vert T^* \vert^2$	ΔE_{SF}(S*)[c]	$\vert T^{**} \vert^2$	ΔE_{SF}(S**)[c]	ΔE_{BB}[d]	k/k_0[e]	k/k_1[f]
1	5	16	413	133	0	117	41	564	1.00
2	14	39	238	141	0	103	45	297	0.53
3	6	29	324	151	2	121	27	256	0.45
4	37	119	0	203	779	84	26	90	0.16
5	3	7	0	161	159	154	16	61	0.11
6	7	5	70	151	37	146	24	60	0.11
7	12	38	81	166	29	128	17	50	0.09
8	0	0	50	157	50	157	9	40	0.07
9	0	0	45	158	45	158	8	35	0.06
10	3	32	33	172	60	139	23	33	0.06
11	9	27	43	155	2	128	19	29	0.05
12	4	28	0	175	88	147	19	27	0.05
13	3	31	14	174	64	143	20	25	0.04
14	14	40	43	159	1	120	25	26	0.05
15	8	39	86	177	1	138	7	24	0.04
16	8	36	80	177	6	140	6	23	0.04
17	5	46	0	185	89	139	29	22	0.04
18	0	0	25	155	25	155	7	22	0.04
19	12	19	39	160	6	141	20	22	0.04
20	15	62	95	184	0	122	10	21	0.04
21	4	43	5	181	68	137	28	20	0.04
Crystal[g]	20	63	3	118	2	125	6	1	0.00
1A[h]	116	766	1944	683	0	-83	6	0	0.00
$1B_1$[i]	74	0	1110[j]	154	1110[k]	154	0	1000	1.77
$1B_2$[l]	74	253	0	244	2339	-10	57	15	0.03

[a] Energies in units of meV and couplings in units of meV^2. [b] Davydov splitting $\Delta E_{SF} = E(S^{**}) - E(S^*)$.
[c] Energy balance of SF, $\Delta E_{SF}(S^*) = E(^1TT^*) - E(S^*)$ and $\Delta E_{SF}(S^{**}) = E(^1TT^*) - E(S^{**})$. A positive value represents endoergic SF. A positive value implies exoergic SF. [d] Biexciton binding energy. [e] $k_0 = 1.2\times10^8\ s^{-1}$. [f] $k_1 = 7.0\times10^{10}\ s^{-1}$.
[g] Crystal herringbone pair structure with individual tetracenes adapted to D_{2h} symmetry. [h] Top pair from optimization for $\vert T^* \vert^2$. [i] Top pair from optimization for $\vert T^A \vert^2$. [j] Squared coupling $\vert T^A \vert^2$. [k] Squared coupling $\vert T^B \vert^2$. [l] Pair structure 1B evaluated with procedure III.

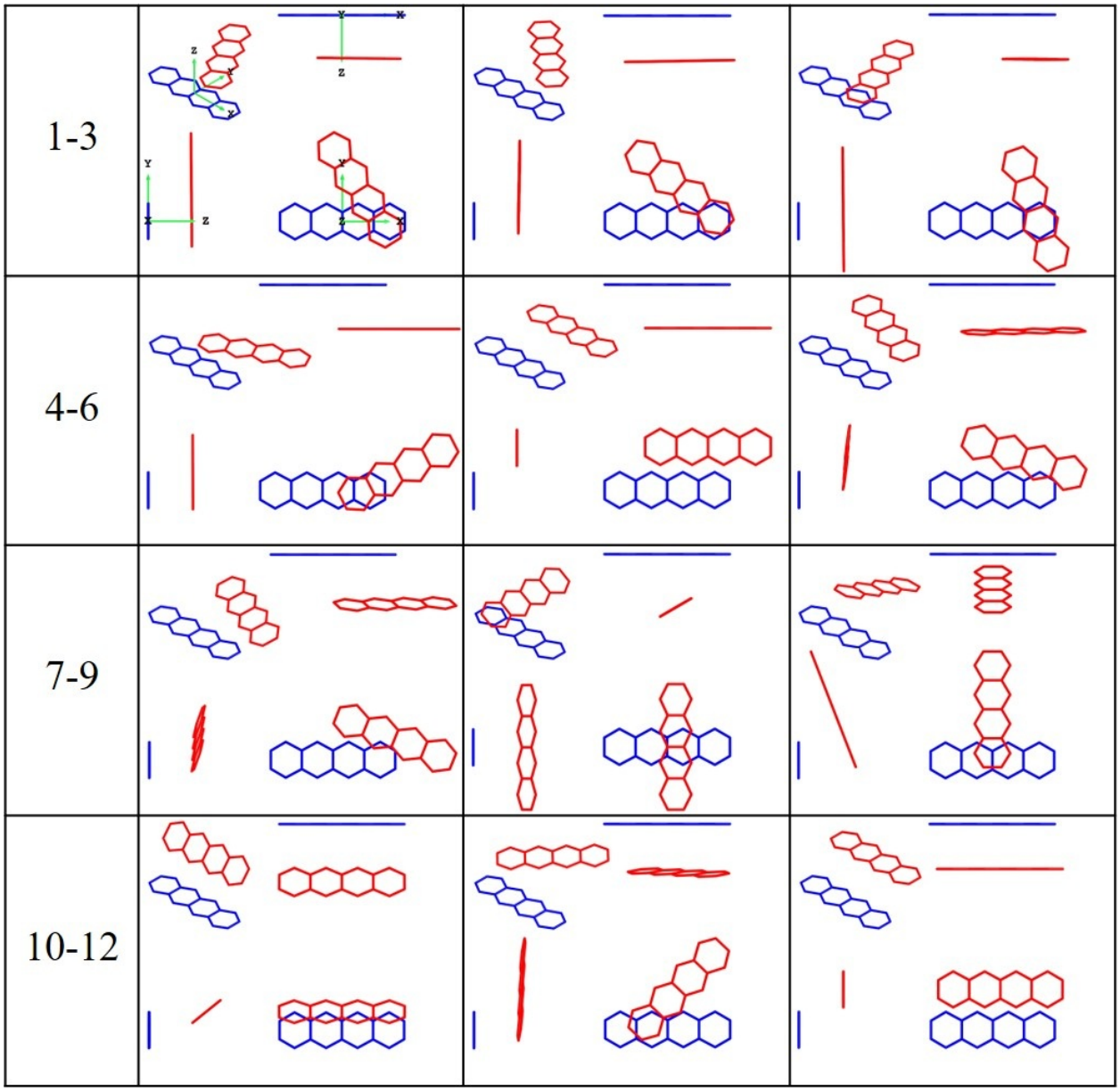

Figure 13. Multi-view projections of the top 12 pair structures.

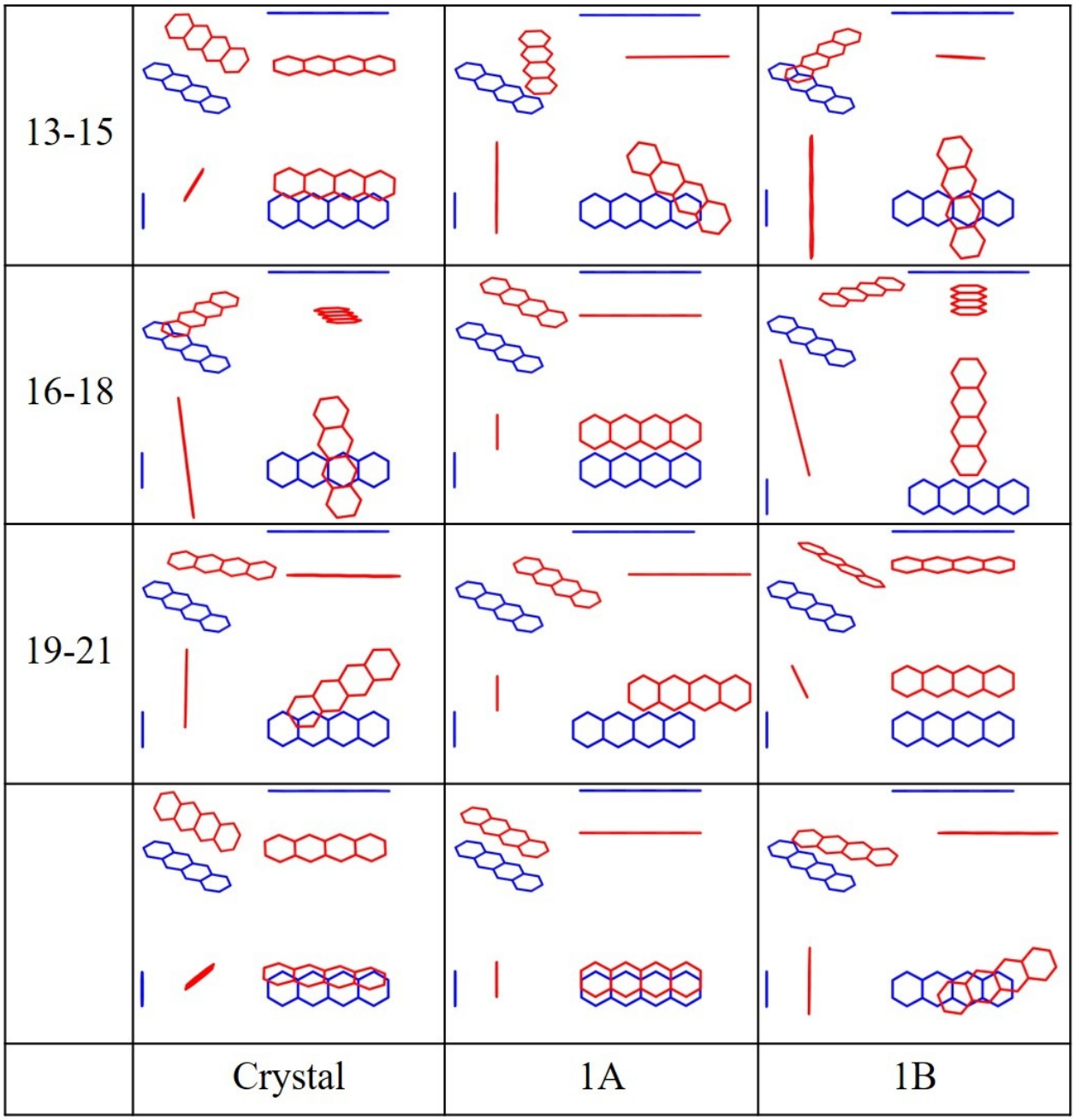

Figure 14. Multi-view projections of the pairs 13-21 as well as 1A, 1B, and the crystal herringbone pair.

Table 2 provides the ranking of the pair structures from Figures 13 and 14 in the six optimizations with different parameter sets. Most of the pair geometries that appear as a result of optimization are the same in all six, just ranked differently. Pairs 1C through 4C are not found among the top 21 pairs from the (154, 130) optimization illustrated in Figures 13 and 14 and are shown in Figure 15.

Table 2. Top 11 Pair Structures from the Six Optimizations with Varied Intrinsic Endothermicity and Reorganization energy.

Optimization [a]	1st	2nd	3rd	4th	5th	6th	7th	8th	9th	10th	11th
(154,130)	1	2	3	4	5	6	7	8	9	10	11
(154,300)	1	3	2	5	6	7	4	1C	8	9	15
(0,130)	1	2	3	5	7	1C	6	15	2C	8	14
(0,300)	1	3	2	1C	5	6	15	2C	8	11	14
(308,130)	1B	1	4	2	3	3C	5	6	11	17	4C
(308,300)	1	2	3	4	5	6	7	8	10	9	1B

[a] Parameter set used for optimization (intrinsic endothermicity of SF, reorganization energy) with energies in units of meV.

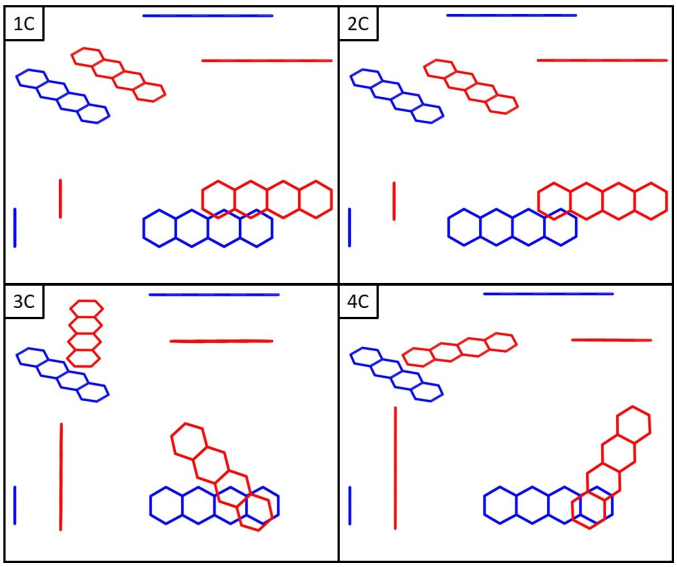

Figure 15. Multi-view projections of pairs 1C-4C.

3.4. Discussion

We will mostly limit the discussion to the top 10 pairs from the (154, 130) optimization, based on published energy values. The 10th best pair structure is very similar to the herringbone pair found in the crystal with a root mean square deviation (RMSD) in the positions of carbon atoms of only ~0.2 Å. It is noteworthy that this structure is so similar to that found in the crystal but is still predicted to have a 33 times higher SF rate constant. This demonstrates the sensitivity of the optimized pair structures. This sensitivity is structure dependent, as pair 17 differs from pair 12 by an additional 0.6 Å slip along the *x* axis which increases the Davydov splitting by 65% and biexciton binding energy by 50% while the couplings and endothermicities remain relatively unchanged, all resulting in a decrease in SF rate constant of only 20%.

One nice result from this exploration of the parameter space is that the top five to eight pairs, particularly the top 3, are rather robust. Even with deviation in the intrinsic endothermicity of SF of ± 100% and more than doubling the reorganization energy, the better pair structures do not really change as seen in Table 2. This is encouraging as the chemical modifications required to produce the various pair geometries will likely change these two values. It is interesting to note that only in the (308, 130) optimization does a new pair geometry show up for the top pair. This pair happens to be the 29th pair in the (154, 130) optimization using literature values and is also the top pair, 1B, from the optimization for $|T^{A}|^2$.

Binding energies of the biexciton calculated for these pairs are mostly predicted to be less than or nearly equal to 25 meV ($k_B T$ at room temperature). Pairs 1 and 2 are noteworthy in that they are calculated to have BE binding energies nearly twice $k_B T$ at room temperature, a possible disadvantage.

Optimized Pair Structures. Pairs 1A and 1B (Fig. 14) are the result of optimizing the pair geometries not for the Marcus rate constant k but for the squared coupling to either the more stable, delocalized excitonic state S* in the case of 1A or the localized state S_1S_0* for 1B. This is equivalent to setting the coupling between singlet configurations S_1S_0 and S_0S_1 to 0 for the optimization resulting in pair 1B. In this optimization, the structure of pair 1A has the second largest value of $|T^{A}|^2$. These two pairs are included to demonstrate the need to account for the energy balance of the SF process and the delocalization of the initial singlet excitation. While the optimization which resulted in 1B may show squared couplings to both the S_1S_0* and S_0S_1* of 1110 meV^2 and a rate constant 1,000 times larger than that of the idealized crystal herringbone pair, once the two singlets are allowed to interact, all of the coupling is to the destabilized excitonic state S**. The coupling

to this state may be incredibly large at 2339 meV^2 relative to 3 meV^2 in the symmetrized crystal, but due to the large Davydov splitting of 253 meV reducing population of the destabilized S** state, the Boltzmann averaged rate constant drops to 15 times that of the crystal pair, making it the 29th best pair in the (154, 130) optimization. Pair 1B demonstrates the need to consider the effect of intermolecular interactions on the initial singlet excitation.

Pair 1A illustrates the need to consider the energy balance of SF in addition to the coupling. This pair has very large coupling to its stabilized excitonic singlet state; however, due to the very strong interaction between diabatic singlet states [$(h_A l_A|h_B l_B)$ = 116 meV], it has a huge Davydov splitting (766 meV) and the more stable singlet exciton is far too stable, making SF endothermic by 683 meV. This large endothermicity results in a severely depressed rate constant that is 16 orders of magnitude smaller than that of the crystal pair despite the extremely strong coupling of 1944 meV^2. Clearly, energetics are as important as coupling to the SF process.

Given that SF is already intrinsically endoergic by 150 meV in tetracene, it is no surprise that the pairs mostly optimized to minimize Davydov splitting and endoergicity at the expense of larger coupling, with the exception of pair 4. There are three general types of pairs with regard to energetics and couplings: those with coupling primarily to the S* state, those with coupling split between the two excitonic singlet states, and those with coupling primarily to the S** state. When coupling is primarily to the more stable singlet state, as in pairs 1, 2, and 3, the magnitude of the Davydov splitting is not a concern for the Boltzmann statistics as there is no coupling to the less stable singlet. Very large Davydov splitting would be beneficial in this regard, so that the less stable singlet state with no coupling to the biexciton would not be populated; however, as SF is already endothermic by 154 meV before the contribution of CT states is even considered, further

stabilization of the S* state is very detrimental. It follows then that these three states have the smallest Davydov splitting. Pairs 6 through 10 are of the second type where in addition to modest coupling to the S* state, there is significant coupling to the less stable excitonic singlet state S** as well as small Davydov splitting, allowing both states to contribute to the Boltzmann averaged SF rate constant. Pairs 8 and 9 achieve these energetics by having the long axes of the two partners perpendicular to each other, removing the coupling between the diabatic S_1S_0 and S_0S_1 configurations. The last type of pair is represented by pairs 4 and 5. In these pairs, there is no coupling to the more stabile singlet state, it is all to the destabilized S** state. In pair 4, the coupling is very large (779 meV^2) but so is the Davydov splitting at 119 meV. The larger splitting reduces the population of the less stabile singlet, but the large coupling ensures that when the state is populated, it undergoes SF quickly. Pair 5 takes the opposite approach with a $|T^{**}|^2$ value of only 159 meV^2 but a Davydov splitting of only 7 meV resulting in more population of the S** state relative to pair 4 but with SF occurring much more slowly from that state. This difference in approach leads to pair 4 having a rate constant 50% larger than that of pair 5; however, in relation to all of the pairs, their rate constants are similar.

A few structural motifs are seen in the optimized in Figures 13 and 14. Most of the top pairs are slip and/or twist-stacked with rotation of partner B primarily about the z-axis (axis pointing out of the page) relative to partner A. Pairs 8, 9, 10, 13, and 21 are exceptions and have significant rotation of partner B (red) about its long or short axis. Pair 10 is very similar to the crystal herringbone structure with a 51° rotation about its long axis as is pair 13, though its rotation about the long axis is only 32°. Also, with a few exceptions, 6 to 7 carbon atoms from each partner overlap each other with some amount of offset. For those pairs where the partners are only slip-

stacked with no rotation, this is accomplished by having part of the lower perimeter of one partner overlap the upper perimeter of the other. In the twist-stacked structures, one ring of one partner tends to overlap a ring of the other. Exceptions are pairs 6 and 7 in which partner B is rotated about its z-axis but only has perimeter overlap with its partner .

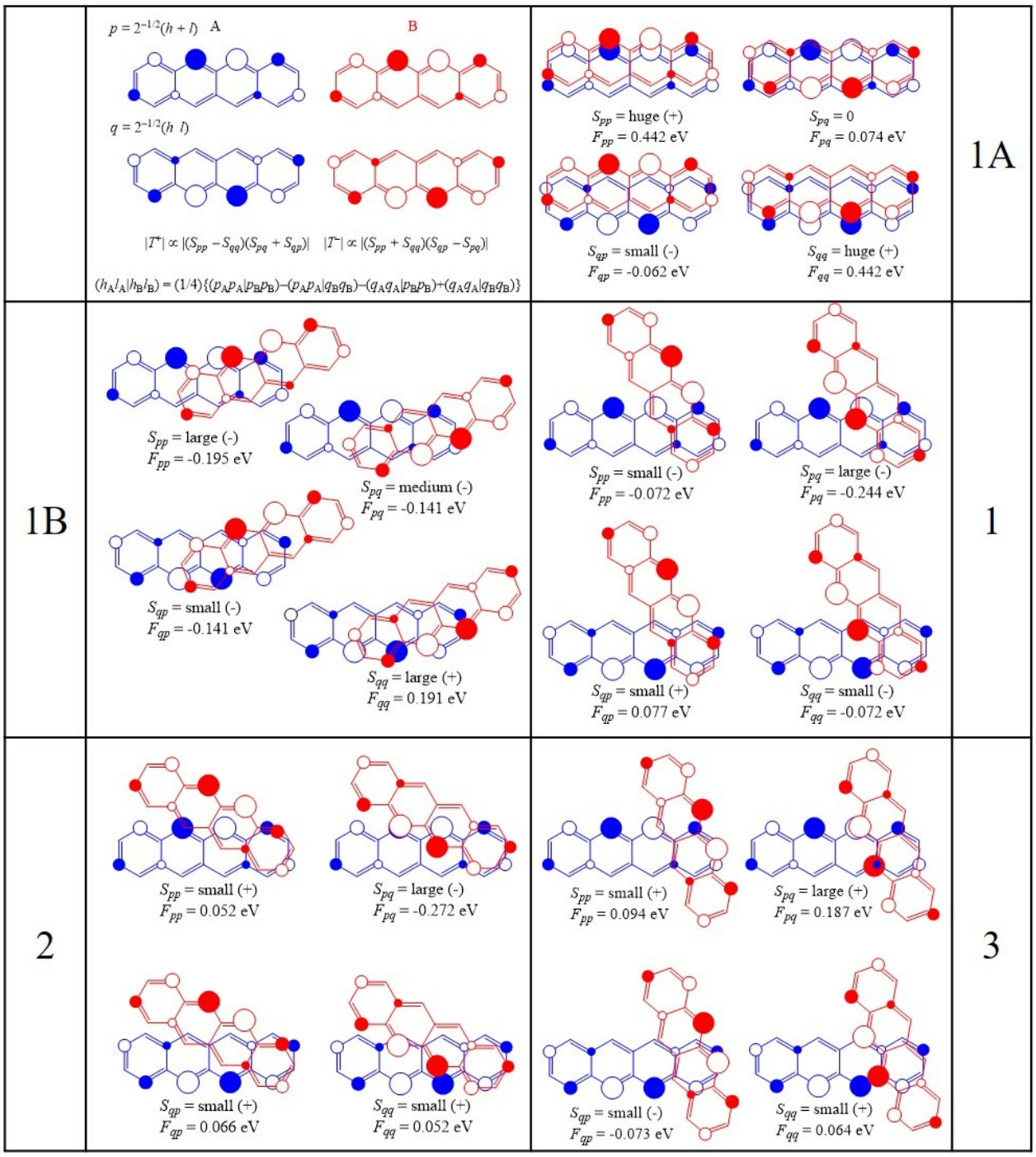

Figure 16. Qualitative analysis of pairs 1 through 3 as well as 1A and 1B. Orbitals *p* and *q* for partners A and B are shown in the upper left corner.

Qualitative Analysis. The particularly large rate constants of pairs 1 through 3 and the poor performance of pairs 1A and 1B can be understood through the use of the simple qualitative rules in eqs. (71) - (75). In this analysis, we will disregard the contribution of the intrinsic endothermicity of SF, though it can simply be included in the estimation of the overall endothermicity of SF by addition. The localized, in- and out-of-phase combinations of the HOMO and LUMO orbitals, p and q, are shown in the top left of Figure 16. We need to visually evaluate the overlaps $S(p_A p_B)$, $S(p_A q_B)$, $S(q_A p_B)$, and $S(q_A q_B)$ to estimate the magnitude of the coupling. To estimate the energy balance we will also need to visually evaluate the four two-electron repulsion integrals $(p_A p_A|p_B p_B)$, $(p_A p_A|q_B q_B)$, $(q_A q_A|p_B p_B)$, and $(q_A q_A|q_B q_B)$. These are all repulsions between semi-localized charge densities and are relatively simple to estimate. In Figure 16, S_{ij} correspond to the authors' visual estimation of the overlap while F_{ij} are the calculated Fock matrix elements. In almost all cases, the visual estimations of the overlaps agree qualitatively with the calculated values of the matrix elements.

From eqs. (71) - (74) for the couplings, it is seen in Figure 16 that for pair 1B the SF couplings to the localized singlets, $|T^A|$ and $|T^B|$, will be very large and equal. As S_{pp} and S_{qq} are both large and of opposing sign, all of the coupling will be to the in-phase excitonic singlet. To check the energy balance of SF from the in-phase excitonic state in pair 1B, eq. (75c) must be evaluated. The repulsion between the electrons in the same type of orbital (p or q) on different partners, $(p_A p_A|p_B p_B)$ and $(q_A q_A|q_B q_B)$, are large while that between electrons in different types of orbitals on different partners, $(p_A p_A|q_B q_B)$ and $(q_A q_A|p_B p_B)$, are smaller. The sum of the repulsion integrals in eq. (75a) will therefore be positive and of moderate magnitude (the calculated value is 74 meV). Substituting the qualitative evaluations into eq. (75c) results in $\Delta E_{SF}(S^+) \approx (-1/4)(2\{(\text{large}) - (\text{small}) - (\text{small}) + (\text{large})\} + (1/2)[3\{\text{large} + \text{large}\}^2 - \{\text{medium} + \text{medium}\}^2 - 5\{\text{medium}\times\text{medium}\}]) \approx$

$(-1/4)(2\{\text{large}\} + [6\{\text{large}\}^2 - 7\{\text{medium}\}^2])$. Here the values of each element are on the order of 10^{-2} to 10^{-1} eV, resulting in squared values becoming smaller, not larger. With that in mind, this will be a value that is medium in magnitude and negative. It is calculated to be −160 meV when the intrinsic endothermicity is not considered. In the same manner, eq. (75b) can be evaluated for the Davydov splitting, i.e., $\Delta E_{DS} \approx (1/2)[2\{(\text{large}) - (\text{small}) - (\text{small}) + (\text{large})\} + (\text{large} - \text{large})^2 - (\text{medium} + \text{medium})^2] \approx (1/2)[2\{\text{large}\} - 4(\text{medium})^2]$. This will be large and positive and is calculated to be 253 meV. With the derived qualitative rules, starting with just knowledge of the HOMO and LUMO, one can simply evaluate the approximate couplings and energy balances. In this case, we can quickly estimate that all the coupling is to the in-phase excitonic state and that SF is moderately exothermic. The large Davydov splitting results in a small contribution from this state to the Boltzmann averaged rate constant and it can be ruled out as a target for improved SF in tetracene. Pair 4 is similar to 1B, but the additional translation along the x and y axes reduces the squared coupling and Davydov splitting by about 50%, resulting in a 6 fold increase in SF rate constant of pair 4 relative to 1B.

Pair 1A is even simpler to evaluate. As the two partners are only slightly slip stacked, the overlap of orbitals of the same type is very large while the overlap of orbitals of different type is very small. This is seen in values of the Fock matrix elements in Figure 16. The same holds true for the repulsion between charge densities. This means that $|T^-|$ will be very large and $|T^+|$ should be 0. By the same measure, $\Delta E_{SF}(S^-)$ and ΔE_{DS} will have large, positive contributions from the zeroth order terms and also the first order terms. These values are calculated to be 529 and 766 meV respectively, deserving of the term "very large" relative to the other pairs. Again it is seen that focusing only on

maximizing coupling at the expense of energy balance leads to disaster: a predicted rate constant 10^{-16} times that of the crystal pair.

Pair 1, when compared to pairs 1A and 1B, demonstrates a better approach to designing SF materials. It has moderately large coupling, particularly relative to 1A and 1B, but has greatly reduced Davydov splitting, minimizing its endothermicity of SF. The result is a Boltzmann averaged rate constant which is 19 orders of magnitude larger than 1A despite having a fifth of the squared coupling.

Figure 16 shows the same qualitative analysis for pairs 1, 2, and 3, which are far and away the best pairs for SF rate. Given the qualitative rules, one can understand why these motifs result in large rate constants. Large overlap of the HOMO and LUMO or their in- and out-of-phase combinations leads to large coupling of the singlet states to the biexciton state. However, large overlap also leads to large coupling of the two localized singlet diabatic states which results in large Davydov splitting and endothermicity for the stabilized state (usually the out-of-phase combination). There are then two obvious approaches to remedy the unfavorable energy balance and improve the rate of SF. Starting from a pair structure like 1A, if one wants to reduce the Coulomb repulsion, partner B can be rotated about one of its benzene rings, reducing the overlaps of all other rings between the partners and greatly reducing the interaction of their transition dipole moments. The overlap which results from having 1-1.5 overlapping benzene rings appears to provide sufficient SF coupling while the rotation moves the charge densities on the two partners far enough away from each other that there is minimal Davydov splitting. Another way to achieve 1-1.5 benzene rings worth of overlap is to not rotate partner B, but displace it so that a section of the two partners' perimeters overlap, as seen in pair 5. These results all point to the conclusion that thinking only of

maximizing SF coupling is insufficient. In the case of alternant hydrocarbons at least, the best approach is to begin with a slight slip-stack along pair structure to maximize overlap and SF coupling and then to displace and rotate one partner as to maintain a fraction of overlap while separating their charge densities.

A pattern which is seen in pairs 1, 2, and 3 is for S_{pp}, S_{pq}, and S_{qq} to all be of the same sign with S_{pq} being large and S_{pp} and S_{qq} being small to medium in magnitude. S_{qp} must then be small and of opposing sign. Pairs with these overlaps will have strong coupling to the biexciton from the out-of-phase singlet ($|T^-|$ will be large) and almost no coupling from the in-phase singlet per eq. (73) and (74). These overlaps are achieved by keeping a section of the partners overlapped while rotating other sections away from each other, so when estimating the exo/endothermicity of SF for the out-of-phase singlet using eq. (75d), the sum of the zeroth order terms (the repulsion integrals) will be small. The first order terms (the Fock matrix elements, here estimated by the overlaps) will partially cancel when summed and should provide a small correction to an already small number. This will make SF from the out-of-phase singlet slightly endothermic and possibly slightly exothermic as seen in pair 1. Energy values for these pairs provided in Table 1 confirm this analysis recalling that $(h_A l_A|h_B l_B) = (1/4)\{ (p_A p_A|p_B p_B) - (p_A p_A|q_B q_B) - (q_A q_A|p_B p_B) + (q_A q_A|q_B q_B)\}$.

3.5. Conclusion

A model for SF in molecule pairs based on frontier orbitals had been described. An algorithm for the optimization of the rate of SF based on Marcus theory has been applied to a pair of D_{2h} symmetrized tetracene molecules and the top 21 pairs have been described. The structural motifs found can inform the design of SF materials and are in agreement with previously published

design rules. The results show the importance of both the energy balance of SF and the coupling to the rate of SF. The top 9 pairs are good targets for synthetic efforts and crystal engineering, particularly the top three pairs which are predicted to enhance the rate of SF 250-550 times relative to the symmetrized crystal herringbone pair. The fact that the 10th pair is predicted to have a 33 fold improvement in SF rate relative to the crystal pair despite being so similar demonstrates that small deviations from the optimized geometries can sometimes significantly reduce the rate of SF.

3.6. References

1. Holmes, D.; Kumaraswamy, S.; Matzger, A. J.; Vollhardt, K. P. C. *Chem. Eur. J.* **1999**, *5*, 3399.

2. Henn, D. E.; Williams, W. G.; Gibbons, D. J. *J. Appl. Cryst.* **1971**, *4*, 256.

3. Wilson, M. W. B.; Rao, A.; Johnson, K.; Gélinas, S.; di Pietro, R.; Clark, J.; Friend, R. H. *J. Am. Chem. Soc.* **2013**, *135*, 16680– 16688.

4. Chan, W. L.; Ligges, M., Zhu, X-Y. *Nat. Chem.* **2012**, *4*, 840-845.

5. Burdett, J. J.; Gosztola, D.; Bardeen, C. J. *J. Chem. Phys.* **2011**, *135*, 214508.

6. Kolomeisky, A. B.; Feng, X.; Krylov, A. I. *J. Phys. Chem. C* **2014**, *118*, 5188-5195.

7. Casanova, D. *J. Chem. Theory Comput.* **2014**, *10*, 324-334.

8. Havenith, R. W. A.; de Gier, H. D.; Broer, R. *Mol. Phys.* **2012**, *109*, 2445-2454.

9. Morrison, A. F.; Herbert, J. M. *J. Phys. Chem. Lett.* **2017**, *8*, 1442-1448.

10. Ito, S.; Nagami, T.; Nakano, M. *J. Phys. Chem. Lett.* **2015**, *6*, 4972-4977.

11. Chan, W-L.; Berkelbach, T. C.; Provorse, M. R.; Monahan, N. R; Tritsch, J. R.; Hyvertsen M. S.; Reichman, D. R.; Gao, J.; Zhu, X-Y. *Acc. Chem. Res.* **2013**, *46*,1321-1329.

12. Subotnik, J. E.; Vura-Weis, J.; Sodt, A. J.; Ratner, M. A. *J. Phys. Chem. A.* **2010,** *114*, 8665–8675.

13. Neese, F. The ORCA program system, *Wiley Interdiscip. Rev.: Comput. Mol. Sci.* **2012**, *2*, 73-78.

14. Hirata, S.; Head-Gordon, M. *Chem. Phys. Lett.* **1999**, *314*, 291– 299.

15. Adamo, C.; Barone, V. *J. Chem. Phys.* **1999**, *110*, 6158.

16. Weigend, F.; Ahlrichs, R. *Phys. Chem. Chem. Phys.* **2005**, *7*, 3297.

17. Rappoport, D.; Furche, F. *J. Chem. Phys.* **2010**, *133*, 134105.

18. Izsak, R.; Neese, F. *J. Chem. Phys.* **2011**, *135*, 144105.

19. Neese, F.; Wennmohs, F.; Hansen, A.; Becker, U. *Chem. Phys.* **2009**, *356*, 98-109.

20. Stoychev, G. L.; Auer, A. A.; Neese, F. Automatic Generation of Auxiliary Basis Sets *J. Chem. Theory Comput.* **2017**, *13*, 554-562.

21. Jones, R. O.; Gunnarsson, O. *Rev. Mod. Phys.* **1989**, *61*, 689– 746.

22. Zaykov, A.; Felkel, P.; Buchanan, E. A.; Jovanovic, M.; Havenith, R. W. A.; Kathir, R. K.; Broer, R.; Havlas, Z.; Michl, J. "Singlet Fission Rate: Optimized Packing of a Molecular Pair. Ethylene as a Model", submitted for publication.

23. Holmes, D.; Kumaraswamy, S.; Matzger, A. J.; Vollhardt, K. P. C. CCDC 114446: Experimental Crystal Structure Determination, **2000**.

24. Roothaan, C. C. J.; Sachs, L. M.; Weiss, A. W. *Rev. Mod. Phys.* **1960**, *32*, 186-194.

25. Krishnan, R.; Binkley, J. S.; Seeger R.; Pople, J. A. *J. Chem. Phys.* **1980**, *72*, 650.

26. Glendening, E.D.; Landis, C.R.; Weinhold, F. *J. Comput. Chem.* **2013**, *34*, 1429-1437.

27. Tomkiewicz, Y.; Groff, R. P.; Avakian, P. *J. Chem. Phys.* **1971**, *54*, 4505-4507.

28. Yost, S. R.; Lee, J.; Wilson, M. W. B.; Wu, T.; McMahon, D. P.; Parkhurst, R. R.; Thompson, N. J.; Congreve, D. N.; Rao, A.; Johnson, K.; Sfeir, M. Y.; Bawendi, M. G.; Swager, T. M.; Friend, R. H.; Baldo, M. A.; Van Voorhis, T. *Nat. Chem.* **2014**, *6*, 492– 497.

29. Buchanan, E. A.; Kaleta, J.; Wen, J.; Lapidus, S. H.; Císařová, I.; Havlas, Z.; Johnson, J. C.; Michl, J. *J. Phys. Chem. Lett.* **2019**, *10*, 1947 – 1953.

Chapter IV

Optimal Arrangements of 1,3-Diphenylisobenzofuran Molecule Pairs for Fast Singlet Fission[1]

4.1. Introduction

The second chromophore selected for optimization is 1,3-diphenylisobenzofuran (**7**),[2,3,4,5,6,7] shown in Figure 17. This is the first successful chromophore theoretically designed to approximately satisfy the requirement for isoergic SF[8] and its α polymorph has a room-temperature triplet yield of 140 ± 25%,[3,6] which increases to 200 ± 30% at 77 K. It thus is an ideal candidate for packing optimization to attempt to push its room-temperature triplet yield closer to 200%. Measurements on three variously fluorinated derivatives of **7** in thin films have indeed shown that crystal packing is decisive.[9] Only about half of the compounds exhibit singlet fission, some faster than others, while the other half only form excimers. These results will be discussed in detail in chapter 5. Up to now, it has however not been clear what packing to aim for to maximize the triplet yield.

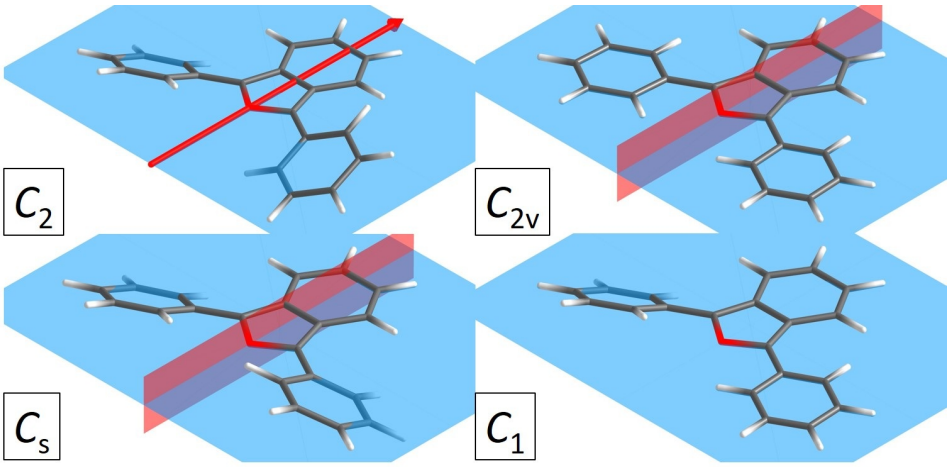

Figure 17. C_2, C_{2v}, C_s, and C_1 rotamers of **7**. The *xy* plane of the isobenzofuran ring is shown in blue, the *y* axis of twofold symmetry in **7**(C_2) and the *yz* plane of symmetry in **7**(C_{2v}) and **7**(C_s) are shown in red.

The crystal structure of **7** contains both herringbone and slip-stacked pair motifs (Figure 18) and attracts attention by its peculiar polymorphism: the α and β forms have an almost identical crystal structure. Despite this similarity, they have different appearances with the α polymorph forming dull yellow-orange blocks and the β forming bright yellow-green needles.[2] All nearest-neighbor molecular pairs are effectively identical in the two forms, and only the relations between next-nearest neighbors are different.[9] Yet, the SF rate constant in the former is about 6 times larger than that in the latter. As a result, a pair model cannot differentiate between the two, but it might still suggest which type of structure to aim for.

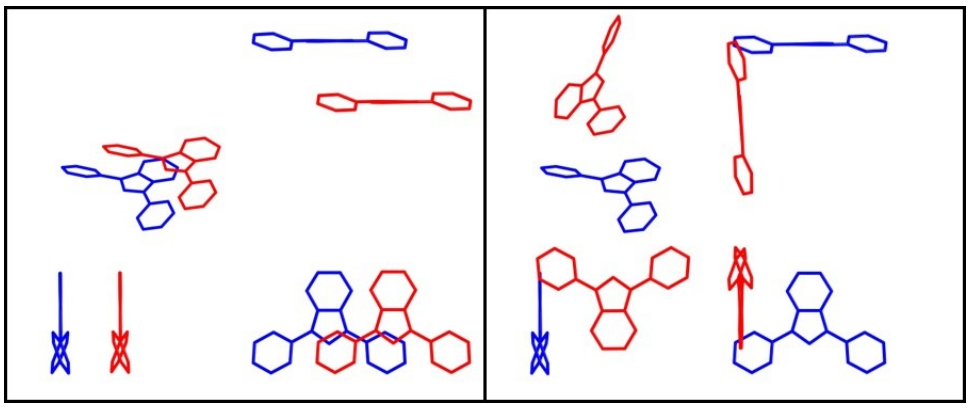

Figure 18. Multi-view projections of pair geometries found in the crystal structure of **7**(C_2). Left, a slip-stacked pair; right, a herringbone pair.

Figure 17 shows the four rotamers of **7** that are investigated in this study. The phenyl groups in the C_2 and C_s rotamers are disrotated and conrotated out of the plane of the isobenzofuran moiety, respectively, whereas in the C_{2v} rotamer both lie in this plane. In the C_1 rotamer one phenyl group is in the plane and the other is rotated. These four rotamers reflect symmetrized chromophore geometries found in crystals of variously fluorinated derivatives of **7**.[9] Presently, the packing structure within pairs of each of the four rotamers will be optimized, keeping the same rigid structure for both partners in a pair.

4.2. Method

Computational Procedures. Geometries used to calculate reorganization energy were optimized in ORCA[10] using DFT for the S_0 and T_1 electronic states and TD-DFT (TDA[11]) for the S_1 electronic state using the PBE0[12] functional with the Def2-TZVP[13] basis set and the RIJCOSX[14,15] approximation for Coulomb and exchange integral evaluation with Def2/JK.[16] The Def2-TZVPD[13,17] basis and auxiliary basis set generated by the AUTOAUX[18] procedure were used for single point

energy evaluations with analytic integral evaluation. Singlet excitation energies were calculated via TD-DFT[19] without the TDA. Triplet energies were calculated using the ΔSCF[20] method. Frequency analysis was performed on all optimized geometries to ensure they were true minima. The SIMPLE program[21,22] was used to calculated all singlet fission couplings, excitonic contributions to energetics, and Marcus theory rates.

SIMPLE[21,22] Procedure Details. The crystal structure of **7** was symmetrized to C_2, C_{2v}, and C_s point symmetry groups, yielding three of the rotamers. The C_1 rotamer geometry was generated from those of the C_{2v} and C_2 rotamers. The quantum chemistry program ORCA[10] version 4.0.1 was used to calculate MOs with the RHF[23] method using the 6-311G[24] basis set. Natural bonding orbital (NBO) analysis was performed by the NBO 6.0 program[25] linked to ORCA to generate NAOs. Since the C_{2v} rotamer has *xy* and *yz* planes of symmetry (Fig. 17), only one quadrant of the translational space is unique. Chromophore B was therefore translated relative to A in 0.5 Å increments along the positive *x* axis for 32 steps, the positive *z* axis for 22 steps, and both the positive and negative *y* axis for 25 steps. It was rotated about its *x*, *y*, and *z* axes for 25 steps of +15° increments, resulting in 5.5×10^8 pair geometries. The C_2 rotamer's reduced symmetry requires additional translational steps along the negative *x* axis while the C_s rotamer's reduced symmetry requires them along the negative *z* axis, resulting in 1.1×10^9 pair geometries each. As the C_1 rotamer does not benefit from any symmetry, it requires translational steps in the positive and negative direction for all three axes, resulting in 2.2×10^9 pair geometries.

The 2,016, 1,276, 2,754, and 4,396 physically accessible geometries with the largest SF coupling squared for the C_2, C_{2v}, C_s, and C_1 rotamers, respectively, were selected for optimization for maximum k_{SF}. The reorganization energy of the C_2 rotamer was calculated to be 400 meV and

was used for rate constant calculations for all rotamers. The optimizations resulted in 142, 67, 214, and 291 unique geometries for the C_2, C_{2v}, C_s, and C_1 rotamers, respectively, which were predicted to be improvements over or equivalent to the C_2 symmetrized crystal slip-stacked pair structure.

When the energy balance without intermolecular interaction was increased from zero to 100 meV and the C_{2v} pair geometries were re-optimized, the structures remained essentially unchanged. The rate constants however were all depressed by about an order of magnitude due to the increased endothermicity and in regions where rate constants of different pair geometries did not differ by much, the order of some pairs exchanged.

4.3. Results

Multi-view projections of the first five optimized pair geometries for the four rotamers of **7** are shown in Figure 19 and the next five are shown in Figure 20. Pairs 11 through 30 for the C_{2v} rotamer are shown in Figure 21. The multi-view projections follow the standard third-angle projection method: the main view of the *xy* plane is located in the lower right, the top view of the *xz* plane is above that and is the view if the main view were rotated 90°about the *x* axis out of the plane of the page from the top to bottom, the left side view of the *yz* plane is to the left and is the view if the main view were rotated 90° about the *y* axis out of the plane of the page from the left to right. Energy values, couplings, and ratios of the predicted SF rate constants to that of the slip-stacked pair in the crystal ($k_0 = 1.05\times 10^8$ s^{-1}) are provided in Tables 3 and 4.

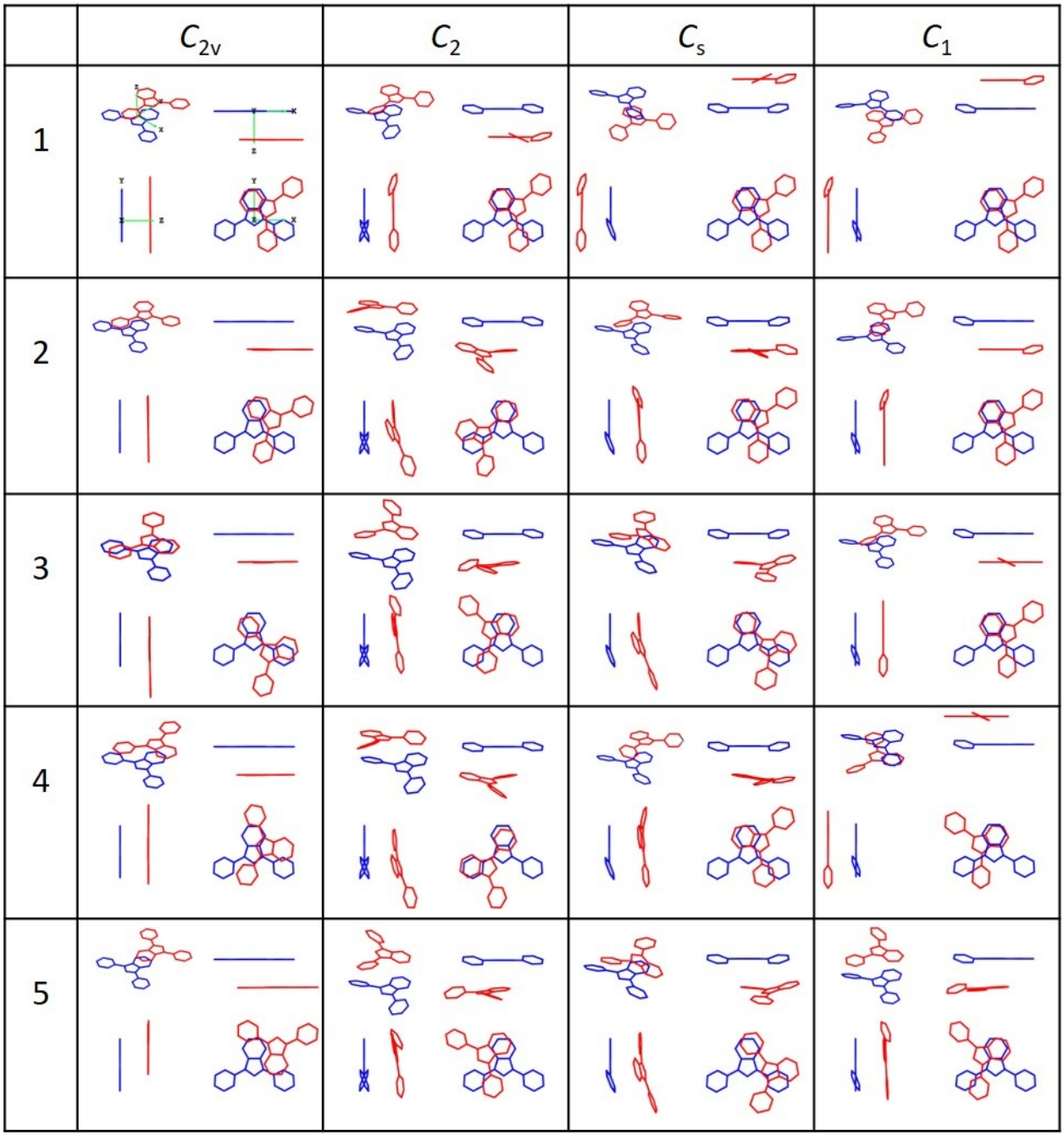

Figure 19. Multi-view projections of optimized pairs 1 through 5 for the four rotamers of **7**.

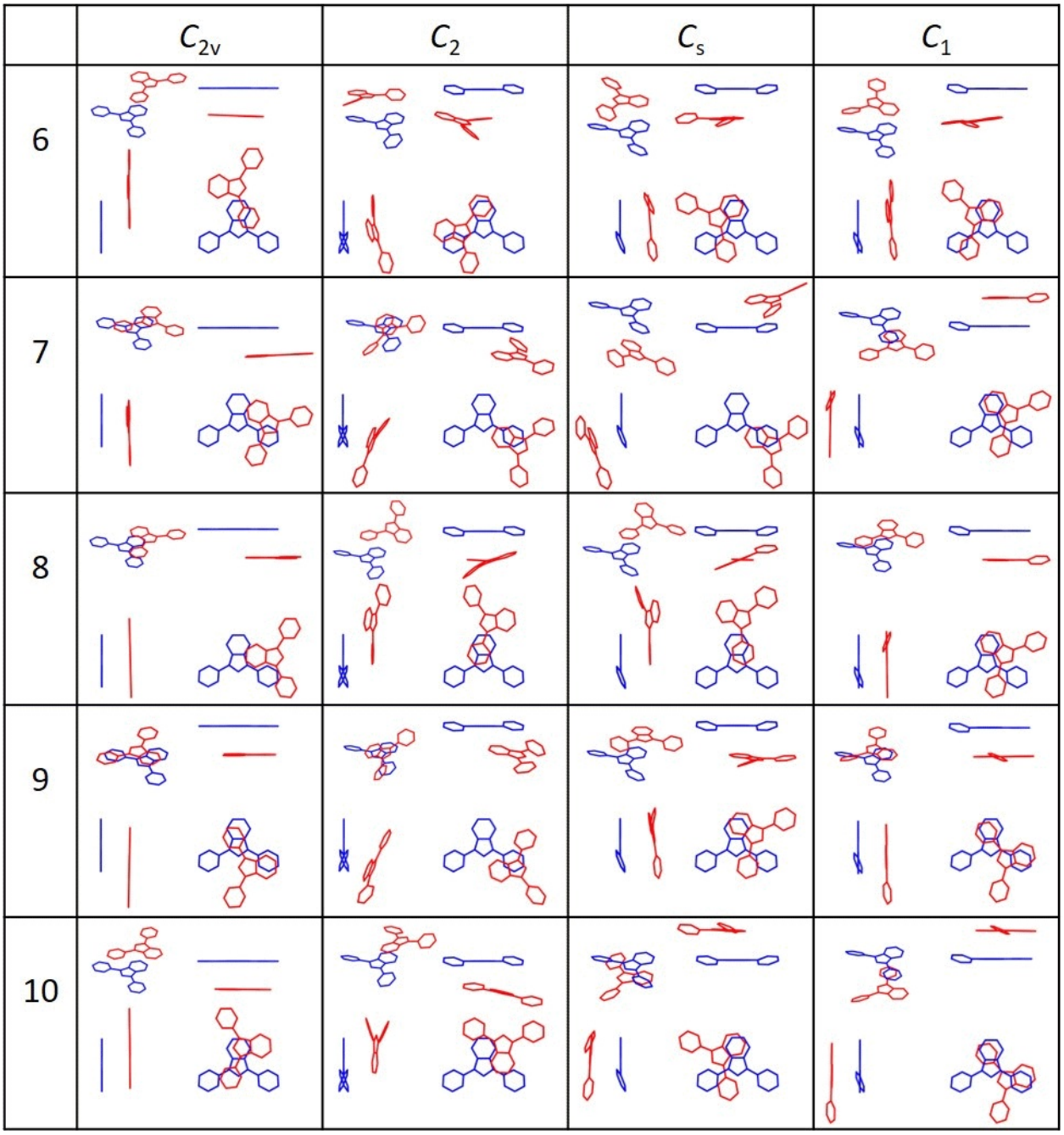

Figure 20. Multi-view projections of optimized pairs 5-10 for the four rotamers of **7**.

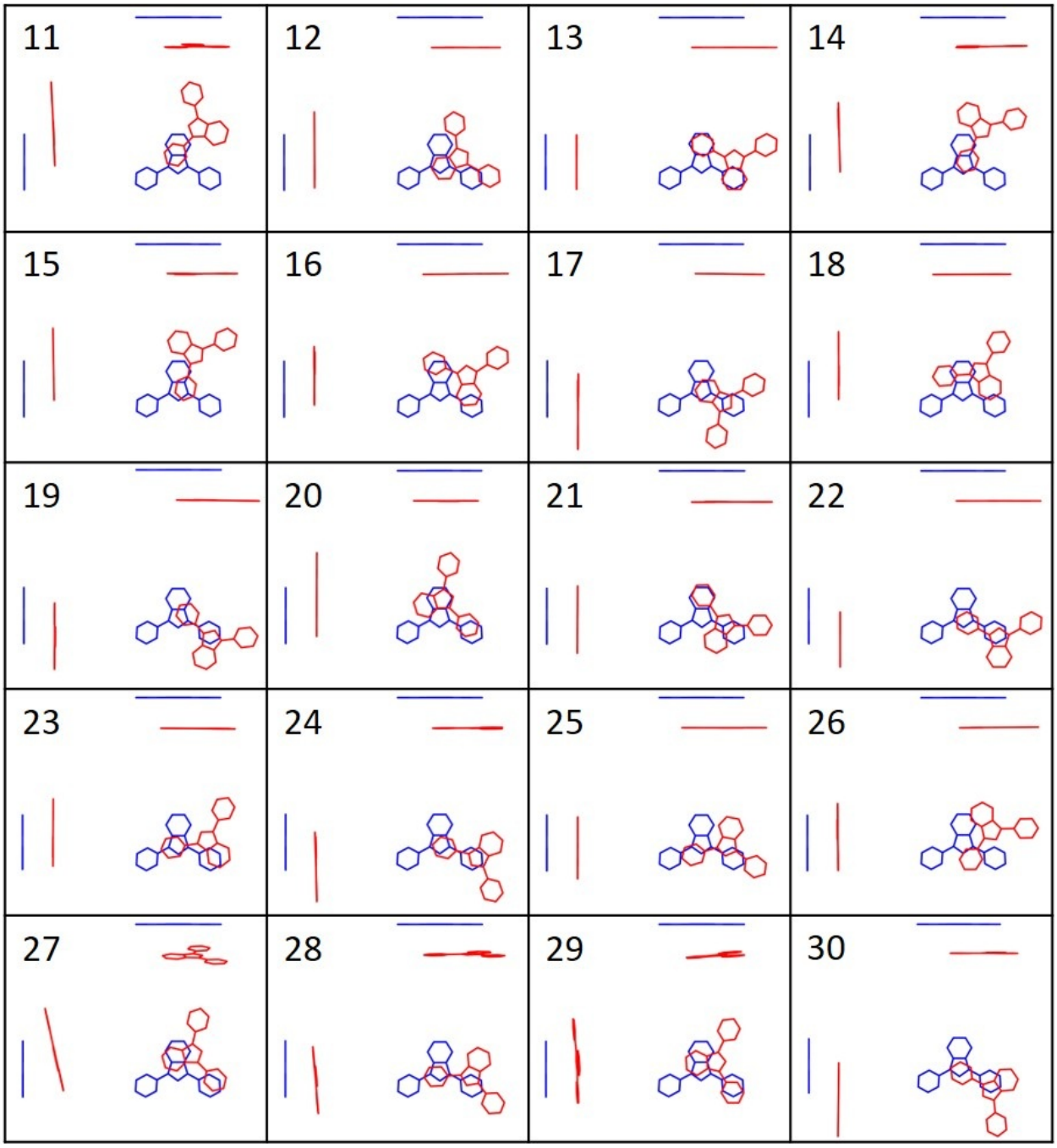

Figure 21. Multi-view projections of optimized pairs 11-30 for the C_{2v} rotamer of **7**.

Table 3. Calculated SF Energetics and Rate Constants for the Top 10 Pairs of **7**(C_2), **7**(C_s), and **7**(C_1).[a]

Struct.	$(h_A l_A \vert h_B l_B)$	ΔE_{DS}[b]	$\vert T^* \vert^2$	ΔE_{SF}(S*)[c]	$\vert T^{**} \vert^2$	ΔE_{SF}(S**)[c]	ΔE_{BB}[d]	k/k_0[e]
C_2								
1	5.8	51.3	1161.7	10.3	0.0	-41.0	34.7	4306
2	14.4	42.5	931.6	15.8	0.0	-26.6	37.6	2944
3	1.1	27.4	625.5	3.1	0.0	-24.4	24.6	2261
4	0.8	25.4	207.3	-5.9	8.7	-31.1	30.1	896
5	11.7	51.4	214.7	4.6	0.0	-46.8	26.8	892
6	5.2	4.3	141.3	-9.8	106.6	-14.1	29.0	806
7	1.6	5.4	149.9	-10.6	61.5	-16.1	23.6	717
8	0.5	9.3	132.5	-8.1	25.4	-17.4	20.8	546
9	1.7	3.4	123.8	-9.4	41.7	-12.8	20.3	536
10	34.2	334.9	334.9	58.7	3.3	-85.2	23.9	504
C_s								
1	11.4	70.5	1489.7	9.4	0.0	-61.1	45.9	5998
2	19.8	93.6	899.7	13.4	8.0	-80.2	46.2	3473
3	13.6	44.8	1022.2	18.2	0.0	-26.7	36.8	3126
4	2.9	32.2	511.5	6.6	0.5	-25.7	22.3	1805
5	1.9	15.3	179.8	-7.1	77.0	-22.4	29.5	901
6	16.1	63.4	185.6	4.7	2.9	-58.7	33.2	808
7	1.8	4.4	162.7	-10.1	68.5	-14.5	23.2	766
8	0.4	14.3	158.4	-5.9	51.3	-20.2	23.2	724
9	12.8	54.2	171.1	6.6	0.0	-47.6	25.6	691
10	19.6	80.7	167.6	15.1	0.0	-65.6	29.8	614
C_1								
1	12.9	76.1	3122.6	-19.7	0.0	-95.8	83.0	22252
2	14.6	83.0	2984.0	-15.9	0.0	-98.8	81.6	20037
3	15.3	87.1	2697.5	-9.4	0.3	-96.5	75.6	16130
4	18.1	99.5	2495.8	-1.7	0.0	-101.2	72.4	13025
5	3.6	49.3	1960.1	-2.6	0.0	-51.9	49.4	9267
6	2.5	42.0	1108.7	5.6	0.3	-36.4	33.1	4286
7	19.2	69.5	498.0	-14.0	0.0	-83.5	60.7	3148
8	21.9	78.3	486.3	-8.6	0.0	-86.9	60.4	2824
9	12.2	10.9	953.6	4.5	0.0	-6.4	42.5	2724
10	13.7	11.7	850.1	3.5	0.0	-8.2	43.5	2506

[a] Energies in units of meV and couplings in units of meV^2. [b] Davydov splitting $\Delta E_{SF} = E(S^{**}) - E(S^*)$.
[c] Endoergicity of SF, $\Delta E_{SF}(S^*) = E(^1TT^*) - E(S^*)$ and $\Delta E_{SF}(S^{**}) = E(^1TT^*) - E(S^{**})$.
[d] Biexciton binding energy. [e] $k_0 = 1.05 \times 10^8$ s^{-1}.

Table 4. Calculated SF Energetics and Rate Constants for the Top 30 Pairs of **7**(C_{2v}).[a]

Struct.	$(h_A l_A \vert h_B l_B)$	ΔE_{DS}[b]	$\vert T^* \vert^2$	ΔE_{SF}(S*)[c]	$\vert T^{**} \vert^2$	ΔE_{SF}(S**)[c]	ΔE_{BB}[d]	k/k_0[e]
1	14.0	78.7	2628.9	-12.4	0.0	-91.1	75.3	16422
2	19.7	69.3	407.3	-7.5	0.0	-76.7	54.4	2273
3	10.0	8.2	742.3	7.1	0.0	-1.1	34.4	1927
4	3.4	16.1	386.0	-2.9	98.3	-19.0	27.8	1625
5	36.6	147.6	846.8	50.2	1.5	-97.4	42.7	1539
6	5.2	35.3	345.6	1.2	40.3	-34.1	28.0	1469
7	3.8	10.8	401.7	-6.2	3.4	-17.0	25.0	1419
8	22.7	96.2	376.5	33.1	49.9	-63.1	28.3	988
9	9.6	67.1	236.9	20.8	26.6	-46.2	28.3	772
10	6.7	34.3	168.8	-0.4	9.5	-34.6	23.1	714
11	10.2	34.7	130.6	9.9	93.3	-24.7	19.9	598
12	47.3	208.2	576.9	83.5	0.0	-124.7	30.2	494
13	14.5	79.8	237.5	45.4	0.0	-34.4	9.2	461
14	9.6	20.5	3.8	9.4	195.0	-11.1	11.8	398
15	2.5	5.4	136.8	1.8	1.9	-3.6	9.7	380
16	26.7	109.4	176.3	42.3	0.8	-67.1	19.9	377
17	41.9	176.8	251.9	64.8	0.0	-112.0	28.1	332
18	43.2	172.1	272.6	80.3	2.8	-91.9	19.9	252
19	3.0	12.4	47.9	4.3	44.7	-8.1	10.6	243
20	44.9	181.4	250.2	79.1	48.6	-102.2	23.7	238
21	44.3	157.8	218.7	74.0	58.1	-83.7	24.3	236
22	14.9	65.4	98.8	39.3	0.0	-26.2	6.3	212
23	19.5	77.5	80.1	32.0	11.2	-45.5	13.6	212
24	2.9	7.8	93.9	16.4	0.0	8.6	3.6	201
25	48.1	153.5	238.3	84.6	0.0	-68.9	22.4	198
26	6.4	18.1	0.1	2.8	84.1	-15.3	10.6	193
27	31.9	108.0	61.3	57.7	200.2	-50.4	14.6	132
28	25.1	100.1	62.2	47.7	0.0	-52.3	9.2	117
29	23.6	76.1	60.8	50.4	19.9	-25.7	6.8	113
30	5.6	24.2	22.1	14.5	29.6	-9.7	6.2	113

[a] Energies in units of meV and couplings in units of meV^2. [b] Davydov splitting $\Delta E_{SF} = E(S^{**}) - E(S^*)$.
[c] Endoergicity of SF, $\Delta E_{SF}(S^*) = E(^1TT^*) - E(S^*)$ and $\Delta E_{SF}(S^{**}) = E(^1TT^*) - E(S^{**})$.
[d] Biexciton binding energy. [e] $k_0 = 1.05 \times 10^8$ s^{-1}.

It is evident from Figures 19 and 20 that the pair structures found for the C_2, C_s, and C_1 rotamers are all variations of pair structures found for the C_{2v} rotamer perturbed to accommodate the twisted phenyls. C_2 pair 1 and 3, C_s pairs 1 and 2, and C_1 pairs 1 through 6 are all of the same type as C_{2v} pair 1. As a result of the symmetry breaking due to the twisted phenyl rotamers, for every pair structure in the C_{2v} optimization there are multiple pairs in the C_2, C_s, and C_1 optimizations, where the arrangement of the isobenzofurans of partners A and B is very similar but the relative rotations of their phenyl groups differ. We will therefore primarily focus on results of the C_{2v} rotamer optimization for simplicity. Structures, energetics, and rate constant ratios for the top 67 optimized pair structures for each of the four rotamers are provided in the Appendix.

Multi-view projections of the slip-stacked crystal pair of **7** and the optimized pair structures which are most similar to it for each rotamer are shown in Figure 22 and energetics, couplings, and the SF rate constant ratios for these pairs are provided in Table 5.

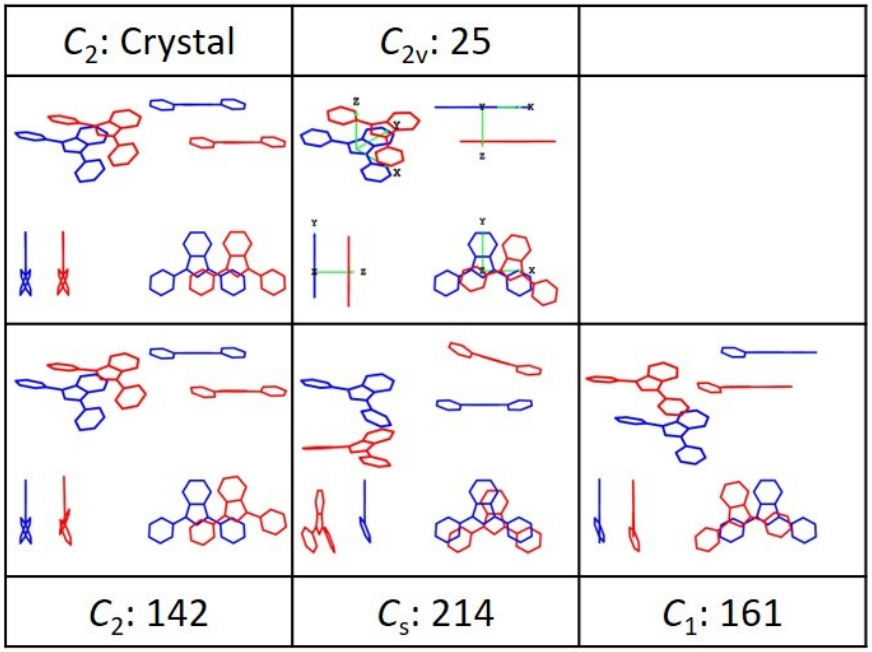

Figure 22. Multi-view projections of crystal pair and most similar optimized pairs for each rotamer.

Table 5. Calculated SF Energetics and Rate Constants for Crystal and Similar Pairs of **7**.[a]

Struct.	$(h_A l_A \vert h_B l_B)$	ΔE_{DS}[b]	$\vert T^* \vert^2$	$\Delta E_{SF}(S^*)$[c]	$\vert T^{**} \vert^2$	$\Delta E_{SF}(S^{**})$[c]	ΔE_{BB}[d]	k/k_0[e]
Crystal[f]	19.0	72.7	0.4	36.2	0.0	-36.5	2.0	1.0
C_2:142	19.5	77.8	0.4	38.0	0.0	-39.8	1.2	0.9
C_{2v}:25	48.1	153.5	238.3	84.6	0.0	-68.9	22.4	198
C_s:214	78.7	319.9	7.78	159.7	0.5	-160.3	3.1	1.0
C_1:161	45.3	139.3	178.9	77.9	22.1	-61.3	21.3	175

[a] Energies in units of meV and couplings in units of meV^2. [b] Davydov splitting $\Delta E_{SF} = E(S^{**}) - E(S^*)$.
[c] Endoergicity of SF, $\Delta E_{SF}(S^*) = E(^1TT^*) - E(S^*)$ and $\Delta E_{SF}(S^{**}) = E(^1TT^*) - E(S^{**})$.
[d] Biexciton binding energy. [e] $k_0 = 1.05 \times 10^8$ s^{-1}.
[f] Crystal slip-stacked pair structure in the α form; the structure is nearly identical in the β form.

Of the 144 optimized pair structures of the C_2 rotamer, the pair which most resembles the slip-stacked pair in the crystal is the 142nd. The primary differences between this structure and that in the crystal are an 8.3° rotation about the *z* axis and an additional 0.3 Å slip along the *y* axis for partner B. These modifications offer no improvement in SF rate constant. Of the optimized C_{2v} rotamer pairs, the most similar pair is 25. This pair's predicted rate constant is 198 times larger than that of the crystal pair. Pair 161 of the 291 C_1 rotamer pairs is very similar to pair 25 for the C_{2v} rotamer (they both have 11° rotation about the *z* axis and very similar translations) and consequently has a rate constant 175 times larger than that of the crystal pair. For the C_s rotamer, it is number 214 of 215 and it offers no improvement in SF rate constant. Despite a 20-fold increase in squared coupling over the crystal, this pair suffers from a large Davydov splitting of 320 meV and consequent endothermicity of SF of 160 meV from its S* state.

The biexciton binding energy is an important factor in the evolution of the electronically and spin coupled ^{1}TT* state to the spatially separated ^{1}(T...T) state that has lost electronic but not spin coherence. These values are reported in column 8 of Tables 3, 4, and 5, and most are below $k_B T$ at

room temperature, ~26 meV. C_{2v} pairs 1, 2, and 5 have relatively large binding energies of 75, 54, and 42 meV respectively, which may be cause for concern for these otherwise promising structures.

4.4. Discussion

As stated above, we will mostly limit the discussion to C_{2v} optimized pairs but will note the strong effect that differences in the relative rotations of phenyl groups have on the predicted relative rates of SF. While pair 1 for each of the four rotamers is nearly identical in the arrangement of isobenzofurans, their different phenyl rotations result in 22 252 and 16 422 fold improvement of the SF rate constant for the C_1 and C_{2v} rotamers but only 4 306 and 5 998 fold improvement for the C_2 and C_s rotamers. The results make it clear that the two effects of intermolecular interactions, one on the coupling constant $|T|$ and the other on the SF energy balance, are of comparable importance. At least in the case of **7**, the effect of intermolecular interactions on the biexciton binding energy is rarely significant.

C_{2v} pairs 1 and 2 demonstrate the effect on the relative SF rate by small deviations from the optimized structure geometry. Partner B (in red in Figure 19) in pair 2 differs from its position in pair 1 by additional 0.09 and 0.56 Å slips along the x and y axes and is rotated 16° less about the z axis. These slight changes result in a relative rate of SF for pair 2 that is reduced by a staggering 73%. While the energetics remain similar, the squared coupling is reduced by 85%.

The SF energy balance is intimately tied to the magnitude of the Davydov splitting between the S* and S** states, which is mostly due to the interaction of the transition densities of partners A and B and only in part to the admixture of the CT configurations, as is clear from the comparison of numbers in columns 2 and 3. Boltzmann statistics favor SF from S* and a large Davydov splitting

makes SF too endoergic, Indeed, the Davydov splitting for the top pair geometries is mostly below 100 meV. Favorable pair geometries also tend to have a large SF coupling to the S* state and little or none to the S** state when the Davydov splitting is significant e.g. pairs 1 through 3, 5, and 7. When the Davydov splitting is small, as in pairs 4, 6, and 11, the SF coupling tends to benefit from both S* and S**. Rarely is the coupling primarily to a slightly exothermic S** state as found in pairs 14 and 26, and this only happens when the Davydov splitting is small and allows significant thermal population in S**.

As also recognized by others,[26] a delicate compromise between the SF energy balance and the SF electronic matrix element thus must be struck in the optimization of pair geometries to maximize the predicted SF rate constant. Within the simplified model, one or both of the sums and differences of the overlaps in the pairs ($S_{hh} - S_{ll}$) and ($S_{hl} + S_{lh}$) or ($S_{hh} + S_{ll}$) and ($S_{hl} - S_{lh}$) must be large for large SF coupling (eqs. 73 and 74); however, at the same time the interaction of the transition densities on partners A and B must not be excessive. This is achieved for **7** in two general classes of structures into which the majority of the optimized pair geometries fall.

One class comprises stacked pair structures with overlapping aromatic rings such as pairs 1, 2, 3, 9, and 13. These pairs can overlap their benzene units (pairs 1 and 2) and then rotate partner B to reduce excitonic splitting and achieve a very large SF coupling. Pair 1 has a squared coupling and improved rate which dwarf all others at 2 629 meV^2 and 16 422 fold, respectively, while a very slight translation and rotation results in pair 2 having about one sixth the coupling squared and one seventh the rate improvement. This massive increase in SF rate constant requires at least one phenyl in plane with the isobenzofuran and is accordingly only present in the top C_{2v} and C_1 structures. Pairs 3, 9, and 13 are examples where the benzene unit of partner A overlaps a phenyl of B and the

benzene unit of B overlaps a phenyl of A. About half of each molecule has overlap with its partner but the other half does not. The result of these structures are 1 927, 722, and 461 fold rate improvements of for pairs 3, 9, and 13.

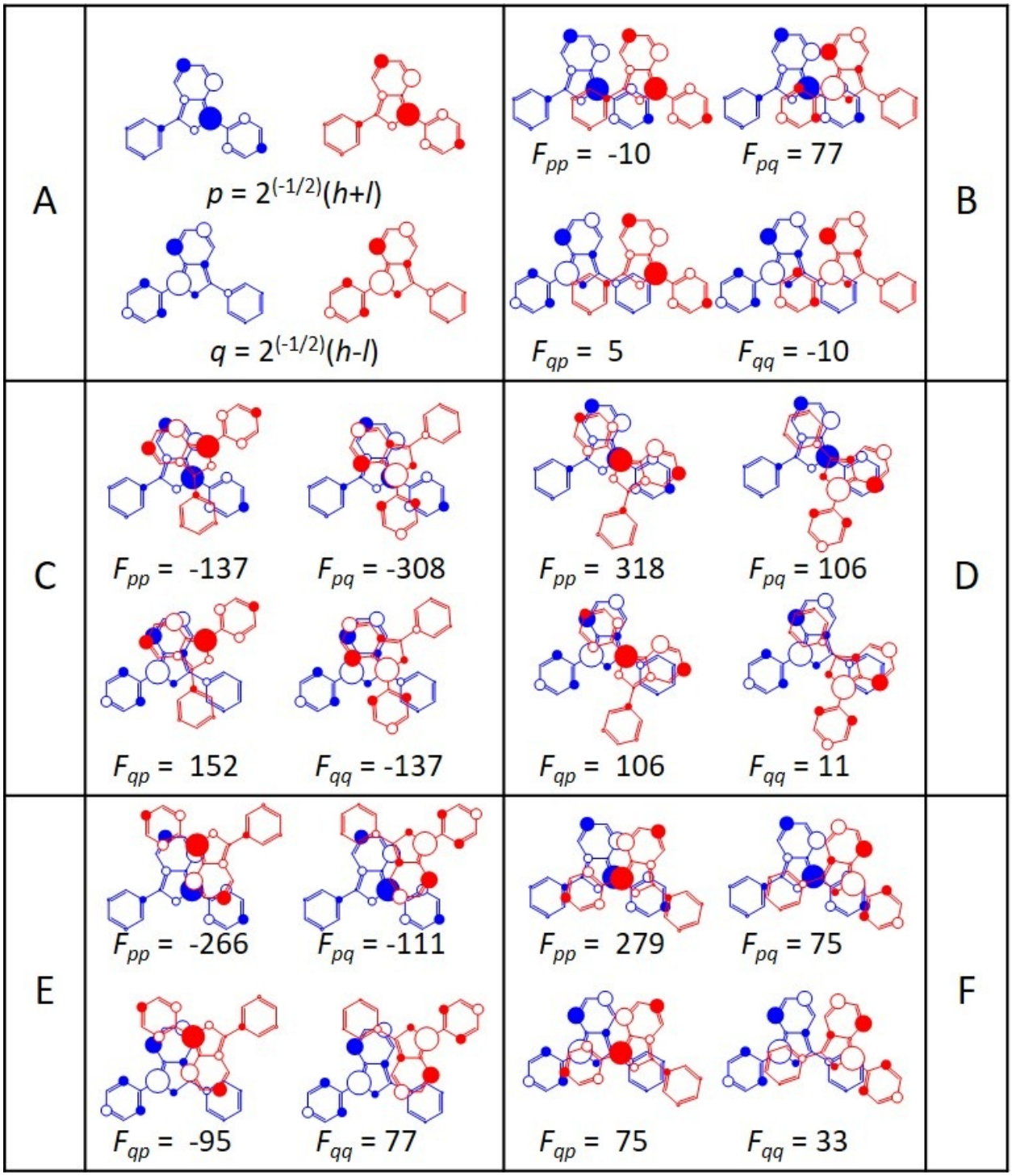

Figure 23. a) Semi-localized orbitals *p* and *q* for the qualitative analysis of b) slip-stacked crystal pair and C_{2v} optimized pairs C: 1, D: 3, E: 5, and F: 25. Approximate values of the Fock matrix elements between semi-localized orbitals are provided.

Figure 23 shows the semi-localized orbitals $p = 2^{-1/2}(h + l)$ and $q = 2^{-1/2}(h - l)$ where h and l are the HOMO and LUMO. The SF matrix element is related to the overlaps S_{pp}, S_{pa}, S_{qp}, and S_{qq}. The overlaps and the SF matrix elements can be visually estimated in panels B through F of Figure 23. For pair 1, one can easily see the large negative values for the overlaps S_{pp} and S_{pq} and the large positive value for S_{qp}. The value of S_{qq} is small and negative, resulting in a very large value for $|T^{-}|$ and zero for $|T^{+}|$. Pair 3 has a large positive value for S_{pp} and a small positive value for S_{pq}, but moderate values for S_{qp} and S_{qq} with the opposite sign, again resulting in a large value for $|T^{-}|$ and zero for $|T^{+}|$

The other major class of optimized pairs comprises those with overlapping perimeters. Some examples are pairs 4, 5, 6, 8, and 25. Pair 5 has double the squared coupling of pairs 4 and 6, but is much more endothermic, reducing its potential enhancement of the SF rate constant. These five pairs have rate constants enhanced 1 625, 1 539, 1 469, 988, and 198 fold. Looking at the semi-localized orbital overlaps in Figure 23 it is easy to understand why these structures are favorable. For pair 6, there is very large negative orbital overlap between p_A and p_B. The orbitals q_A and p_B have large negative overlap while p_A and q_B have medium negative overlap. The overlap of q_A and q_B is small and positive, resulting in a large coupling $|T^{-}|$. Overlapping the perimeters allows pair 6 to have a good SF coupling of 345 meV^2 and minimal excitonic stabilization, with SF being only 1.2 meV endothermic. This is because overlapping just the perimeter allows the majority of the singlet transition charge densities on partners A and B to be far away from each other, greatly reducing their interaction (eqs. 75).

The qualitative rules and semi-local orbitals also explain why pair 25 is predicted to have a SF rate constant 198 times larger than that of the crystal pair though they are similar. In the slip-

stacked crystal pair, partner B is rotated and translated towards A such that the large orbital coefficient on the carbon in the furan ring to which one phenyl is attached has very large overlap with the same atomic orbital on its partner. The decreased separation between the partners in 25 has the effect of doubling the Davydov splitting and endoergicity; however this is more than compensated by the 600-fold increase in coupling squared. This again demonstrates the importance of balancing SF coupling and energetics.

4.5. Conclusion

The results of the optimizations of pairs of four rotamers of 1,3-diphenylisobenzofuran with C_2, C_{2v}, C_s, and C_1 symmetry resulted in 142, 67, 214, and 291 pair structures with singlet fission rate constants predicted to be larger than that found in its regular crystal form. While the simple nature of the model limits its accuracy, certainly many of the top structures predicted are good targets for synthetic efforts and promise large increases in the rates of singlet fission. Structural motifs which overlap sections of the two partners or their perimeters appear to be ideal. None of these structures seem to have been reported in the literature but their synthesis appears feasible, either by crystal engineering or by preparation of covalent dimers. The predicted SF rate constants are sensitive to relatively small deviations in the relative orientations of the optimized pairs, demonstrated by pairs 1 and 2 for the C_{2v} rotamer, likely making the synthesis all the more challenging.

4.6. References

1. Adapted with permission from Buchanan, E. A.; Michl, J. "Optimal Arrangements of 1,3-Diphenylisobenzofuran Molecule Pairs for Fast Singlet Fission" *Photochem. Photobiol. Sci.*, in press, with permission from the European Society for Photobiology, the European Photochemistry Association, and the Royal Society of Chemistry.

2. Ryerson, J. L.; Schrauben, J. N.; Ferguson, A. J.; Sahoo, S. C.; Naumov, P.; Havlas, Z.; Michl, J.; Nozik, A. J.; Johnson, J. C. *J. Phys. Chem. C* **2014**, *118*, 12121.

3. Johnson, J. C.; Nozik, A. J.; Michl, J. *J. Am. Chem. Soc.* **2010**, *132*, 16302.

4. Johnson, J. C.; Michl, J., *Top. Curr. Chem.* **2017**, *375*, 80.

5. Johnson, J. C.; Michl, J. in *Advanced Concepts in Photovoltaics*, eds. Nozik, A. J.; Conibeer, G.; Beard, M. C. Royal Society of Chemistry, Oxfordshire, UK, **2014**, p. 324.

6. Schrauben, J.; Ryerson, J.; Michl, J.; Johnson, J. C. *J. Am. Chem. Soc.* **2014**, *136*, 7363.

7. Schwerin, A. F. ;Johnson, J. C.; Smith, M. B.; Sreearunothai, P.; Popović, D.; Černý, J.; Havlas, Z. ; Paci, I.; Akdag, A.; MacLeod, M. K.; Chen, X.; David, D. E.; Ratner, M. A.; Miller, J. R. ; Nozik, A. J.; Michl, J. *J. Phys. Chem. A* **2010**, *114*, 1457.

8. Paci, I. ;Johnson, J. C.; Chen, X.; Rana, G.; Popović, D.; David, D. E.; Nozik, A. J.; Ratner, M. A.; Michl, J. *J. Am. Chem. Soc.* **2006**, *128*, 16546.

9. Buchanan, E. A.; Kaleta, J.; Wen, J.; Lapidus, S. H.; Císařová, I.; Havlas, Z.; Johnson, J. C.; Michl, J. *J. Phys. Chem. Lett.* **2019**, *10*, 1947.

10. Neese, F. *Wiley Interdiscip. Rev.: Comput. Mol. Sci.* **2012**, *2*, 73.

11. Hirata, S.; Head-Gordon, M. *Chem. Phys. Lett.* **1999**, *314*, 291.

12. Adamo, C.; Barone, V. *J. Chem. Phys.* **1999**, *110*, 6158.

13. Weigend, F.; Ahlrichs, R. *Phys. Chem. Chem. Phys.* **2005**, *7*, 3297.

14. Izsak, R.; Neese, F. *J. Chem. Phys.* **2011**, *135*, 144105.

15. Neese, F.; Wennmohs, F.; Hansen, A.; Becker, U. *Chem. Phys.* **2009**, *356*, 98.

16. Weigend, F. *J. Comput. Chem.* **2008**, *29*, 167.

17. Rappoport, D.; Furche, F. *J. Chem. Phys.* **2010**, *133*, 134105.

18. Stoychev, G. L.; Auer, A. A.; Neese, F. *J. Chem. Theory Comput.* **2017**, *13*, 554.

19. Gross, E. K. U.; Kohn, W. *Adv. Quantum Chem.* **1990**, *21*, 255.

20. Jones, R. O.; Gunnarsson, O. *Rev. Mod. Phys.* **1989**, *61*, 689.

21. Zaykov, A.; Felkel, P.; Buchanan, E. A.; Jovanovic, M.; Havenith, R. W. A.; Kathir, R. K.; Broer, R.; Havlas, Z.; Michl, J. "Singlet Fission Rate: Optimized Packing of a Molecular Pair. Ethylene as a Model", submitted for publication.

22. Buchanan, E. A.; Havlas, Z.; Michl, J. "Optimal Arrangements of Tetracene Molecule Pairs for Fast Singlet Fission", submitted.

23. Roothaan, C. C. J.; Sachs, L. M.; Weiss, A. W. *Rev. Mod. Phys.* **1960**, *32*, 186.

24. Krishnan, R.; Binkley, J. S.; Seeger, R.; Pople, J. A. *J. Chem. Phys.* **1980**, *72*, 650.

25. Glendening, E. D.; Landis, C. R.; Weinhold, F. *J. Comput. Chem.* **2013**, *34*, 1429.

26. Le, A. K.; Bender, J. A.; Arias, D. H.; Cotton, D. E.; Johnson, J. C.; Roberts, S. T. *J. Am. Chem. Soc.* **2018**, *140*, 814.

Chapter V

Analysis of Fluorinated 1,3-Diphenylisobenzofuran Crystals

5.1. Introduction

The SIMPLE model and program were originally intended to be used for the optimization of molecule pair structures; however, we have expanded its use to attempting to analyze differences in rates of singlet fission among molecular crystals. This work was performed in cooperation with many collaborators who were responsible for all experimental and synthetic work: J. Kaleta, S. H. Lapidus, I. Císařová, and J. C. Johnson.[1,2] As singlet fission only proceeds efficiently in a handful of mostly impractical materials, better ones are needed urgently. Both the nature of the chromophores and their packing[3,4,5,6,7,8,9,10,11,12] are crucial. Experimental information on desirable packing consists of observations on covalent dimers[13,14,15,16,17,18,19,20] and materials available as multiple polymorphs.[3,4,5,6,12] Future design of efficient SF materials by crystal engineering or by synthesis of covalent dimers could benefit from comparison of derivatives of a chromophore[9,21,22] that attempt to leave the molecular photophysics unchanged but affect packing. In an effort to test this notion we use fluorine substitution, uncommon in SF studies,[23] and compare 1,3-diphenylisobenzofuran (**7**)[24,25,26] with 11 fluorinated derivatives shown in Figure 24. The polymorphs[5] **7α** and **7β** differ strongly in SF properties, promising sensitivity to packing.

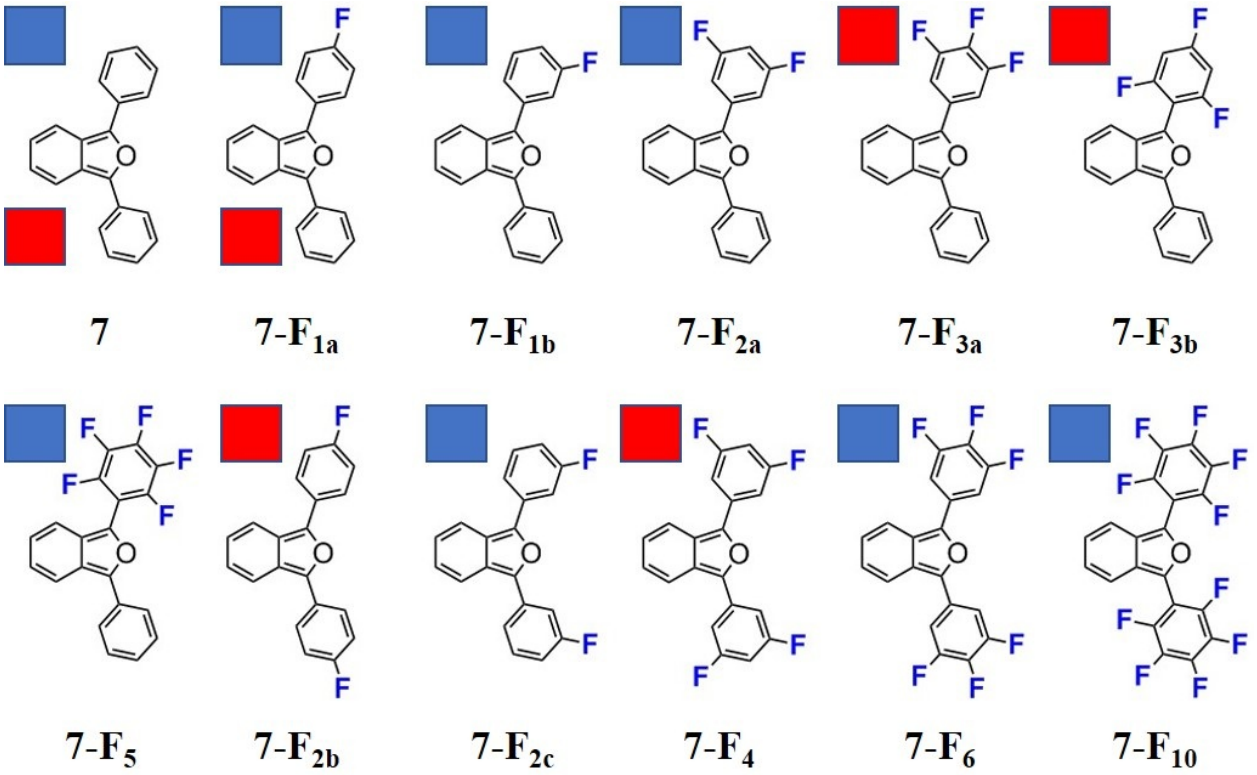

Figure 24. Structures of the parent 1,3-diphenylisobenzofuran (**7**) and 11 derivatives. Compounds marked with a blue square undergo SF while those marked with red form excimers. **7** and **7-F$_{1a}$** undergo SF in their α polymorph and form excimers in their β polymorph.

5.2. Method

Reorganization energies λ were calculated according to the equation $[E(T_1,q(S_1)) + E(T_1,q(S_0)) - 2E(T_1,q(T_1))]$,[27] where q denotes the equilibrium geometry of the monomer in a particular state. Ground and excited state geometries were optimized in the ORCA[28] program suite with density functional theory (DFT) and time-dependent DFT (TD-DFT) with the TDA[29] using two different functionals for comparison. The B3LYP[30,31] functional was used with the Def2-TZVPP[32] basis set and Grimme's DFT-D3[33] dispersion correction. The RIJCOSX[34,35] approximation for Coulomb and exchange integral evaluation, with the Def2/J[36] and Def2-TZVPP/C[37] auxiliary basis

sets, was employed in all geometry optimizations but not in single point evaluations. The PBE0[38] functional was also used with the Def2-TZVP[39] basis set and the RIJCOSX approximation for Coulomb and exchange integral evaluation with the Def2/JK[40] auxiliary basis. The Def2-TZVPD[39,41] basis was used for single point energy evaluations with analytic integral evaluation. Triplet excitation energies were calculated using the ΔSCF[42] method. Singlet excitation energies are calculated by TD-DFT without the TDA. Frequency analysis was performed on all optimized geometries to ensure they were true minima. SIMPLE[43] was used to calculated all singlet fission couplings, energetics, and Marcus rates.

5.3. Results

In the following, the intersection of normalized absorption and fluorescence spectra is used for the S_0-S_1 energy difference. One could also choose the maximum of the absorption or emission peak. This increases the uncertainty in the determination of the intrinsic endothermicity of SF. The S_0-T_1 energy difference is known only for **7**, with almost identical values from bracketing sensitization in solution and electron energy loss spectroscopy on the solid[44] (we use the latter). For the 11 derivatives, the value for **7** is shifted by the difference in DFT calculated triplet excitation energies between the derivative and parent. DFT is also used to calculate the reorganization energy λ for SF. These values and the intrinsic endothermicity of singlet fission [$\Delta E^0(\mathrm{SF}) = 2\Delta E(\mathrm{T_1}) - \Delta E(\mathrm{S_1})$] are reported in Table 6.

Table 6. Calculated and Experimental Energetics (energy units: eV).

Cmpd.	$\Delta E(S_1)$ B3LYP	$\Delta E(S_1)$ PBE0	$\Delta E(S_1)$ Exp.[a]	$\Delta E(T_1)$ B3LYP	$\Delta E(T_1)$ PBE0	$\Delta E(T_1)$ Adj.[b] B3LYP	$\Delta E(T_1)$ Adj.[b] PBE0	$\Delta E^0(SF)$[c] B3LYP	$\Delta E^0(SF)$[c] PBE0	λ[d] B3LYP	λ[d] PBE0
7	2.883	2.681	2.821	1.396	1.411	1.413	1.413	0.006	0.006	0.387	0.407
7-F$_{1a}$	2.871	2.671	2.826	1.393	1.390	1.408	1.393	-0.005	-0.041	0.414	0.441
7-F$_{1b}$	2.909	2.675	2.765	1.405	1.389	1.407	1.392	0.080	0.020	0.386	0.441
7-F$_{2a}$	2.926	2.676	2.755	1.409	1.386	1.403	1.388	0.098	0.022	0.369	0.361
7-F$_{2b}$	2.870	2.636	2.958	1.400	1.399	1.416	1.402	-0.123	-0.155	0.384	0.354
7-F$_{2c}$	2.916	2.687	2.777	1.395	1.376	1.393	1.379	0.048	-0.020	0.388	0.442
7-F$_{3a}$	2.913	2.687	2.767	1.403	1.386	1.403	1.388	0.074	0.009	0.385	0.379
7-F$_{3b}$	3.036	2.803	2.829	1.523	1.513	1.531	1.516	0.251	0.203	0.369	0.350
7-F$_4$	2.951	2.693	2.790	1.402	1.370	1.388	1.373	0.050	-0.044	0.361	0.487
7-F$_5$	3.021	2.813	2.951	1.495	1.498	1.516	1.501	0.074	0.051	0.402	0.427
7-F$_6$	2.928	2.670	2.798	1.389	1.370	1.388	1.373	0.016	-0.052	0.369	0.419
7-F$_{10}$	3.150	2.950	3.100	1.603	1.607	1.625	1.610	0.141	0.120	0.432	0.460

[a] Intersection of absorption and emission curves in toluene. [b] Calculated triplet excitation energy shifted relative to **7**. [c] SF endoergicity expected in the absence of intermolecular interactions (S_1 excitation energy from the intersection of absorption and emission curves). [d] Reorganization energy for SF.

The calculated singlet excitation energies are not used in any further calculations in this work and are provided for comparison to the experimentally determined values. It is seen that PBE0/def2-TZVPD//PBE0/def2-TZVP underestimates these values while B3LYP/def2-TZVPP tends to overestimate them. PBE0 has slightly better agreement with the experimental triplet excitation energy, but as there is only an experimental value for the parent, not much of a comparison can be made. The intrinsic endothermicity of SF (Table 6: columns 9 and 10) and reorganization energies (Table 6: columns 11 and 12) are similar between the two methods [both use the same measured value for $\Delta E(S_1)$], but as the B3LYP calculated triplet excitation energies are generally larger than those resulting from PBE0, the B3LYP method leads to SF being more endoergic and therefore slower. PBE0 tended to produce larger reorganization energies than B3LYP; however, the larger endothermicity from B3LYP tended to decrease the predicted rate constant of SF more than the larger reorganization energies from the PBE0 method. PBE0 has been shown to produce more

accurate optimized geometries than B3LYP for a subset of SF chromophores.[45] For the most part, results from both methods are reported to demonstrate the strong effects energetics and properties of the individual chomophores have on the SF rate constant predicted for the pair.

Figures 25 through 28 show multi-view projections of all neighboring pairs with non-negligible predicted rate constants of SF that can be excised from the crystal lattices of **7** and its 11 derivatives. Each crystal also contains dimers which are reflections of those reported here. These dimers are not reported as the results do not differ significantly. The multi-view projections follow the standard third-angle projection method: the main view of the *xy* plane is located in the lower right, the top view of the *xz* plane is above that and is the view if the main view were rotated 90°about the *x* axis out of the plane of the page from the top to bottom, the left side view of the *yz* plane is to the left and is the view if the main view were rotated 90° about the *y* axis out of the plane of the page from the left to right.

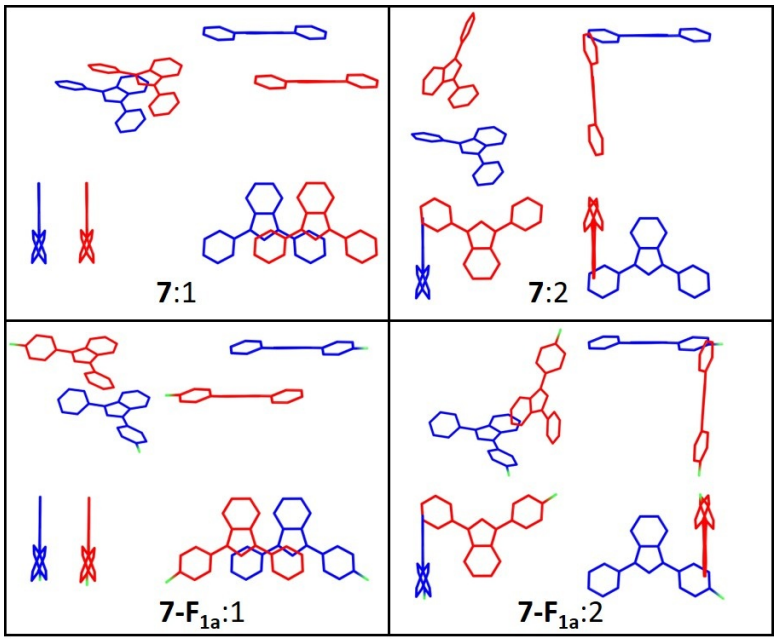

Figure 25. Multi-view projections of SF pairs in **7** and **7-F$_{1a}$**. 1 and 2 refer to different pairs found for the same compound.

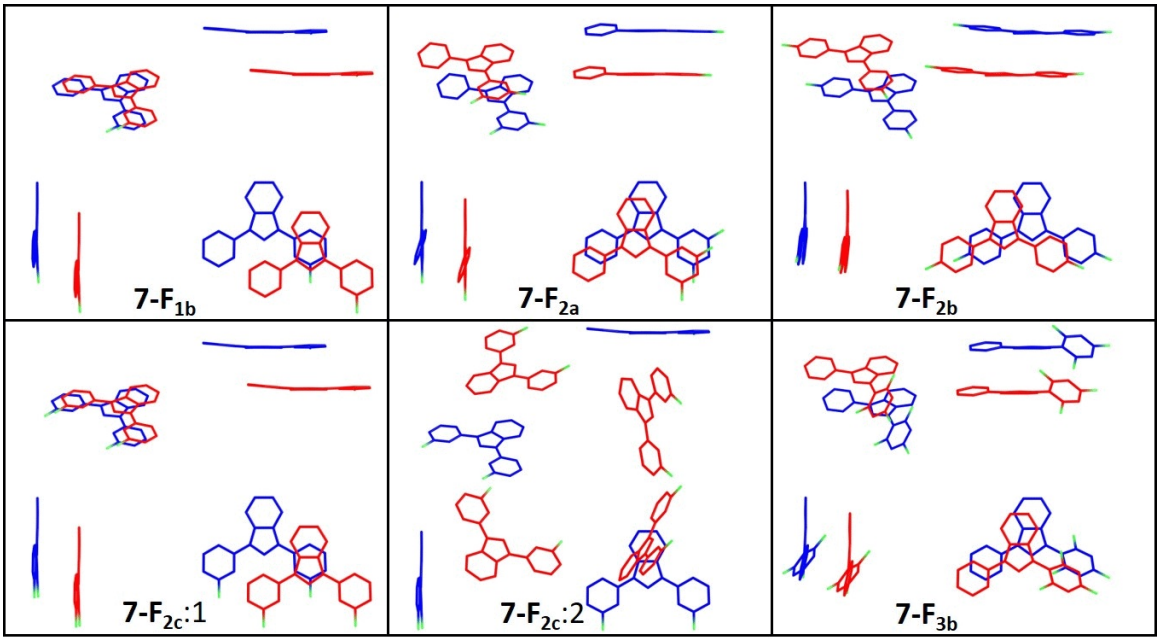

Figure 26. Multi-view projections of SF pairs in **7-F$_{1b}$**, **7-F$_{2a}$**, **7-F$_{2b}$**, and **7-F$_{3b}$**. 1 and 2 refer to different pairs found for the same compound.

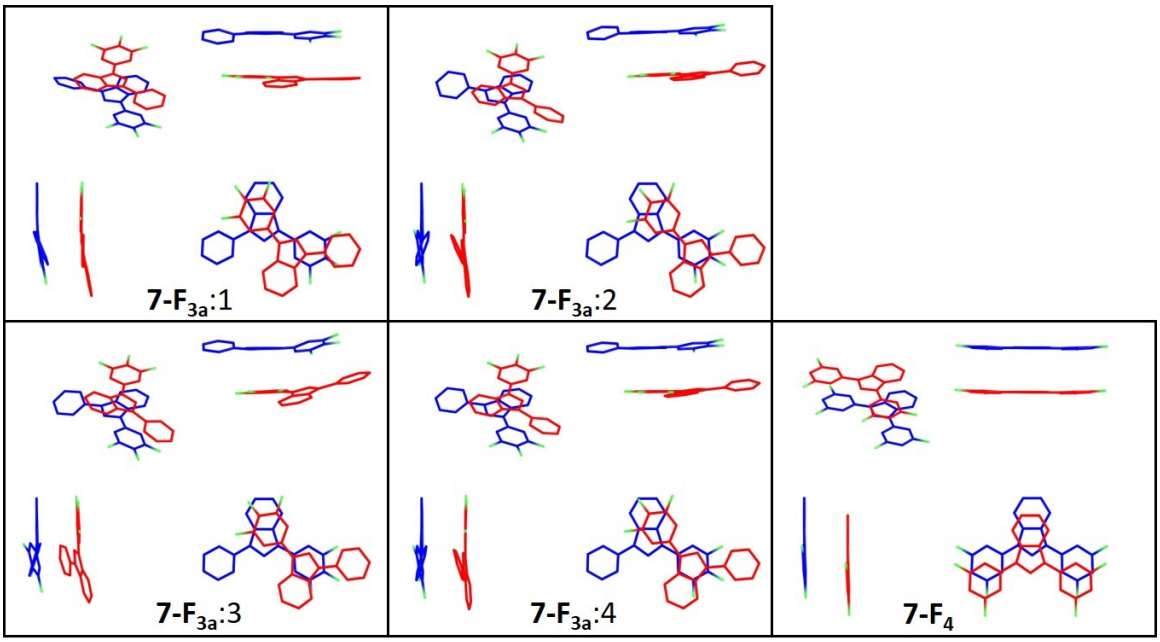

Figure 27. Multi-view projections of SF pairs in **7-F$_{3a}$** and **7-F$_{4}$**. 1 through 4 refer to different pairs found for the same compound.

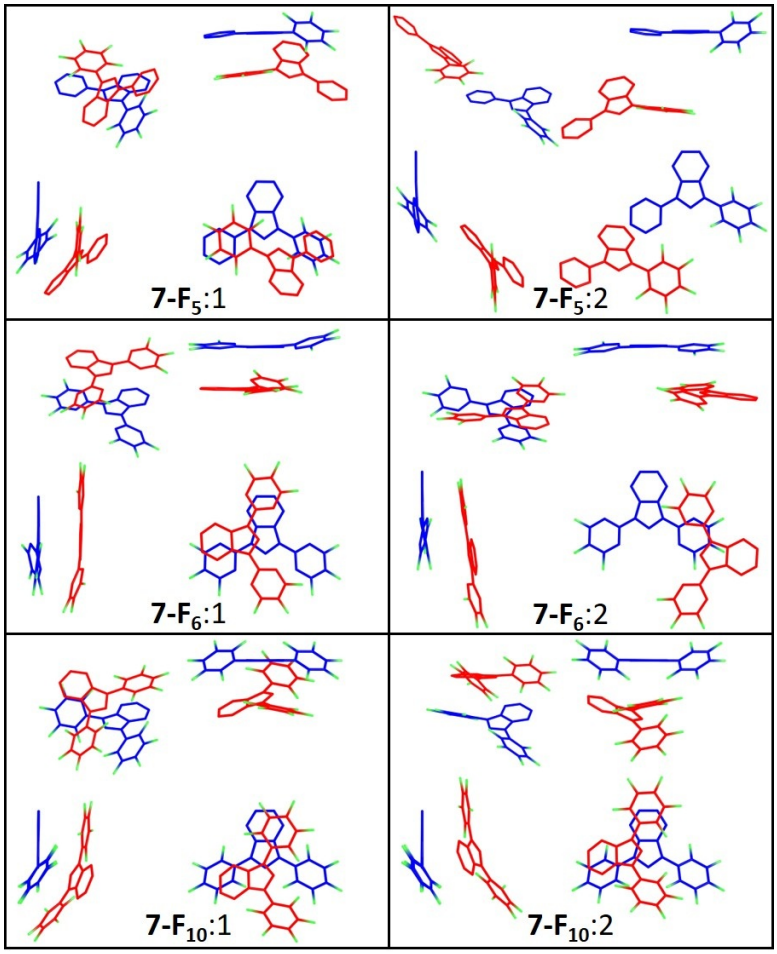

Figure 28. Multi-view projections of SF pairs in **7-F$_5$**, **7-F$_6$**, and **7-F$_{10}$**. 1 and 2 refer to different pairs found for the same compound.

Table 7 provides the energy values and SF couplings for the excised pairs calculated with the PBE0 method. The coupling and Davydov splitting values are nearly identical to those obtained with the B3LYP method, while the endoergicities of SF from the S* and S** states differ due to the different intrinsic endothermicity ΔE^0(SF) calculated by the two methods. This results in predicted SF rate constants that differ by up to an order of magnitude between the two methods. Ratios of the predicted SF rate constant for each pair in each crystal to that of the slip-stacked pair in the crystal

(PBE0: $k_0 = 1.89\times10^7$ s^{-1}; B3LYP: $k_0 = 4.84\times10^7$ s^{-1}) are provided in columns 8 and 9. Columns 10 and 11 provide the ratio K/K_0 of the Boltzmann average of the predicted SF rate constants for both excitonic S* and S** states in all pairs excised from a compound's crystal structure to that of the parent crystal **7** (PBE0: $K_0 = 7.67\times10^6$ s^{-1}; B3LYP: $K_0 = 9.51\times10^6$ s^{-1}). This is only meaningful for compounds with crystal structures that contain multiple unique pairs. The measured rates k_{SF} in column 13 are believed to be good approximations to the true rates of SF.[1] The fact that the simple model predicts the same SF rate constant for **7α** and **7β** while the measured rate of **7β** is only 18% that of **7α** is discussed below.

Table 7. PBE0/Def2-TZVPD//PBE0/Def2-TZVP SF Energetics and Rate Constant Ratios.[a]

Cmpd.	ΔE_{DS}[b]	$\|T^*\|^2$	$\Delta E_{SF}(S^*)$[c]	$\|T^{**}\|^2$	$\Delta E_{SF}(S^{**})$[c]	ΔE_{BB}[d]	k/k_0[e] PBE0	k/k_0[f] B3LYP	K/K_0[g] PBE0	K/K_0[h] B3LYP	k_{SF}/k_0[i] Exp.	k_{SF}/ns^{-1}[j] Exp.
7α									1.0	1.0	1.0	56
1	72	0.2	41	0.0	-31	2.1	1.0	1.0				
2	176	0.0	92	1.4	-83	1.8	0.08	0.08				
7β									0.93	0.93	0.18	10
1	71	0.2	40	0.0	-31	2.0	1.0	1.0				
2	179	0.0	94	1.4	-85	2.1	0.08	0.08				
7-F$_{1a}$									3.6	4.6	0.98	55
1	77	0.2	-1.9	0.0	-79	2.1	2.1	1.2				
2	175	0.0	47	1.3	-128	1.9	0.11	0.07				
7-F$_{1b}$	122	16	81	33	-41	9.0	30	10	30	10	1.36	76
7-F$_{2a}$	495	53	264	7.3	-231	10	1.0	0.05	1.0	0.05	0.89	50
7-F$_{2b}$	376	0.1	71	172	-305	3.1	0.68	0.21	0.68	0.21	0.00	N/A[k]
7-F$_{2c}$									284	89	0.75	42
1	141	20	54	35	-87	8.6	62	19				
2	11	0.5	-13	0.0	-24	0.6	3.9	1.4				
7-F$_{3a}$									0.21	0.02	0.00	N/A
1	709	0.1	364	0.3	-345	0.6	0.00	0.00				
2	369	6.0	185	14	-184	13	1.2	0.13				
3	283	96	256	135	-27	42	2.2	1.2				
4	421	27	215	5.4	-206	8.5	2.2	0.22				
7-F$_{3b}$	423	85	403	0.2	-20	15	0.009	0.001	0.009	0.001	0.00	N/A
7-F$_4$	536	1.8	240	5.0	-296	0.4	0.03	0.002	0.03	0.002	0.00	N/A
7-F$_5$									22	11	0.86	48
1	286	44	195	0.5	-91	4.9	4.3	2.2				
2	4	0.0	53	0.0	49	0.0	0.08	0.05				

[a] Energies in units of meV and couplings in units of meV^2. [b] Davydov splitting $\Delta E_{SF} = E(S^{**}) - E(S^*)$. [c] Endoergicity of SF, $\Delta E_{SF}(S^*) = E(^1TT^*) - E(S^*)$ and $\Delta E_{SF}(S^{**}) = E(^1TT^*) - E(S^{**})$. [d] Biexciton binding energy. [e] $k_0 = 1.89\times10^7$ s^{-1}. [f] $k_0 = 4.84\times10^7$ s^{-1}. [g] $K_0 = 7.67\times10^6$ s^{-1}. [h] $K_0 = 9.51\times10^6$ s^{-1}. [i] Ratio of measured rate constants of SF: $k_0 = 56$ ns^{-1}. [j] Mean values were obtained from measurement on several films (on each film, five measurements on different spots). Decay time of S_1 is equal to the rise time of triplet. Assuming SF is the dominant process, its rate constant is the inverse of the decay time. [k] Excimer formed, no SF.

Table 7 (Cont.). PBE0/Def2-TZVPD//PBE0/Def2-TZVP SF Energetics and Rate Constant Ratios.[a]

Cmpd.	ΔE_{DS} [b]	$\|T^*\|^2$	$\Delta E_{SF}(S^*)$ [c]	$\|T^{**}\|^2$	$\Delta E_{SF}(S^{**})$ [c]	ΔE_{BB} [d]	k/k_0 [e] PBE0	k/k_0 [f] B3LYP	K/K_0 [g] PBE0	K/K_0 [h] B3LYP	k_{SF}/k_0 [i] Exp.	k_{SF}/ns^{-1} [j] Exp.
7-F_6									47	19	1.05	59
1	29	0.1	-47	12	-76	11	132	58				
2	180	0.6	37	1.7	-143	2.2	3.3	1.0				
7-F_{10}									13	8.3	1.63	91
1	2.5	0.6	117	20	114	8.3	5.8	3.8				
2	22	0.0	132	0.0	110	0.1	0.008	0.005				

[a] Energies in units of meV and couplings in units of meV^2. [b] Davydov splitting $\Delta E_{SF} = E(S^{**}) - E(S^*)$. [c] Endoergicity of SF, $\Delta E_{SF}(S^*) = E(^1TT^*) - E(S^*)$ and $\Delta E_{SF}(S^{**}) = E(^1TT^*) - E(S^{**})$. [d] Biexciton binding energy. [e] $k_0 = 1.89\times10^7\ s^{-1}$. [f] $k_0 = 4.84\times10^7\ s^{-1}$. [g] $K_0 = 7.67\times10^6\ s^{-1}$. [h] $K_0 = 9.51\times10^6\ s^{-1}$. [i] Ratio of measured rate constants of SF: $k_0 = 56\ ns^{-1}$. [j] Mean values were obtained from measurement on several films (on each film, five measurements on different spots). Decay time of S_1 is equal to the rise time of triplet. Assuming SF is the dominant process, its rate constant is the inverse of the decay time. [k] Excimer formed, no SF.

5.4. Discussion[46]

Both the measured and calculated SF rate constants differ significantly among nearest neighbor pairs in the same crystal and among pairs in different crystals. Evaluation of the SF electronic matrix element T^2 and the SF energy balance for all nearest neighbors identifies the most strongly interacting pairs to be considered (Figures 25 through 28). Using only these pairs and the calculated values of λ and of state energy shifts due to intermolecular interaction (Table 6), Marcus theory yields SF rate constants that are three orders of magnitude too small.

The parent **7** undergoes SF, so taking its predicted rate as K_0 and the rate predicted for pair 1 as k_0, any compound with a rate constant ratio close to 1 or larger should perform SF as fast as or faster than **7**. SF in any crystal with a predicted ratio less than 0.25 will then likely be too slow for the process to compete successfully. Inspecting the predicted relative rates Boltzmann averaged over all pairs in the crystal K/K_0 (Table 7: columns 10 and 11) for the 11 derivatives and comparing them to the designations in Figure 24 as to whether they undergo SF or form excimers, there is excellent agreement for all but possibly two of the 11 derivatives studied. It is quite an achievement for the simple model to be able to correctly identify the derivatives of a known compound that will also exhibit SF will also perform SF, knowing only their crystal structure, something that the model and the program were not designed for. That the model can do this despite a large uncertainty in the T_1 excitation energies is even more encouraging.

In **7-F$_{3a}$**, both methods predict at least one of the four distinct slip-stacked pairs found in the crystal to undergo SF at least as fast as **7**, but SF is not seen experimentally. It is entirely possible that pair 3 in **7-F$_{3a}$** and possibly pairs 2 and 4 do undergo SF as quickly as the slip-stacked pair 1 in **7**, but pair 1 in **7-F$_{3a}$** has such large excitonic stabilization (ΔE_{DS} = 709 meV) of its S* state that it

functions as an exciton trap in that crystal and there is no population of the less stable S* states in pairs 2, 3, or 4 that could undergo SF rapidly. In fact, when the Boltzmann average of the SF rate constant is over all pairs in the crystal, a rate constant ratio K/K_0 of 0.2 or 0.02 is found depending on the method used. This is in perfect agreement with the experimental observation.

Even in the two derivatives where the agreement is not good, it is unclear whether the model is wrong. For **7-F$_{2a}$** and **7-F$_{2b}$**, the PBE0 and B3LYP methods disagree, with the former predicting SF and the latter predicting excimer formation. In reality, **7-F$_{2a}$** performs SF and **7-F$_{2b}$** forms excimers. This discrepancy is due entirely to the different predicted intrinsic endothermicity of SF between the two methods.

Comparing the predicted ratio of SF rate constants by either method (Table 7: columns 10 and 11) to the ratios of measured values (column 13) shows that the trend in rate constants is not reproduced well by the simple model. The variation in the SF rate constant that is predicted is much larger than the variation observed, and the predicted ratios are off by up to two orders of magnitude. Comparing the results from the PBE0 and B3LYP methods, it is obvious that the predicted SF rate constants are very sensitive to the intrinsic endothermicity of SF, ΔE^0(SF). Having accurate S_1 and T_1 excitations energies appears to be vital in predicting rates of SF. This is particularly challenging for T_1 excitation energies. The ambiguity in assigning the S_1 and T_1 excitation energies and in the resulting intrinsic endothermicity of SF can easily account for the discrepancies between the predicted and experimental results.

As predicted by the optimization of **7** in the previous chapter, the pair structures which are best for SF in each crystal are slip or twist-stacked. The primary pairs found in the parent **7** are the slip-stacked pair 1 and herringbone pair 2, and **7-F$_{1a}$** is nearly identical (Figure 25). The primary SF

pair in **7-F$_{1b}$** is also slip-stacked but partner B is slipped parallel to the twofold axis *y* of the isobenzofuran core of partner A (in blue) as well as its other in-plane axis *x* (Figure 26). **7-F$_{2a}$**, **7-F$_{2b}$**, **7-F$_{2c}$**, and **7-F$_{3b}$** (Figure 26) all contain SF pairs which are also slip-stacked. **7-F$_{3a}$** has a less regular crystal packing, containing the four similar yet distinct twist-stacked pairs found in Figure 27. The four pairs have similar structures to the 19th ranked **7**(C_{2v}) pair from Figure 21 in the previous chapter and pairs 2, 3, and 4 are very similar to each other yet their predicted energetics and rate constants in Table 7 are distinct. Interestingly, the SF pair in **7-F$_4$** is slipped almost exclusively along the *y* axis of partner A, with only a very slight slip along *x*.

The SF pair in **7-F$_5$** has an interesting structure where one partner's fluorinated phenyl ring overlaps the non-fluorinated ring of the other, causing the isobenzofuran cores to avoid each other and not overlap. The structure of pair 1 in **7-F$_6$** is similar to the 4th ranked optimized **7**(C_{2v}) pair from Figure 19 in Chapter 4 except that the red partner is slipped further along the *y* axis of the isobenzofuran core of the blue partner in the **7-F$_6$** pair. Being similar to the 4th best optimized pair, it is not too surprising that this pair structure has the largest predicted rate constant ratio. The last and most fluorinated derivative **7-F$_{10}$** has two primary pairs in its crystal and they have structures that are somewhat similar to the 3rd and 5th best optimized pairs for **7**(C_s) from Figure 19 of Chapter 4.

Next, we turn to the so far unexplained at least fivefold difference in the SF rate constants for **7α** and **7β**. Figure 29 illustrates the differences between the two polymorphs. Vertical columns are all virtually equivalent both within the same form and between the two forms. In both **7α** and **7β**, each next column to the right is offset from the previous column to the left by 10.1 Å. The difference between the two forms results from the angle of the offset. In **7α**, each next column is offset from the previous column at an angle of 16.19°, whereas in **7β**, the offset angle alternates

between +16.35° and −16.35°. The result of this symmetry is that all possible nearest-neighbor dimers in **7β** are also found in **7α** form (cf. Table 8) and only the relation to next nearest neighbors is different. However, we find that the latter are too far apart for any possible chromophore pair to play a significant role in the calculation of T^2 values, energetics, and thus the SF rate constants, at least using the simple model. This equivalence is why the simple model predicts basically identical values for the energies, couplings, and rates of **7α** and **7β**. For the same reasons, we expect any model that considers only two molecules at a time to yield imperceptible differences between **7α** and **7β**, because it ignores interactions between distant molecules that are mediated by an interposed third molecule. Clearly, experimental evidence demands that a general model consider at least three molecules simultaneously. Such calculations have been recently reported[47] for another chromophore and application of many-body theory has also been attempted.[48] However, while complete searches for local maxima in the six-dimensional space of all pair geometries have been performed, the search space for trimer geometries is 12-dimensional and will pose an interesting challenge.

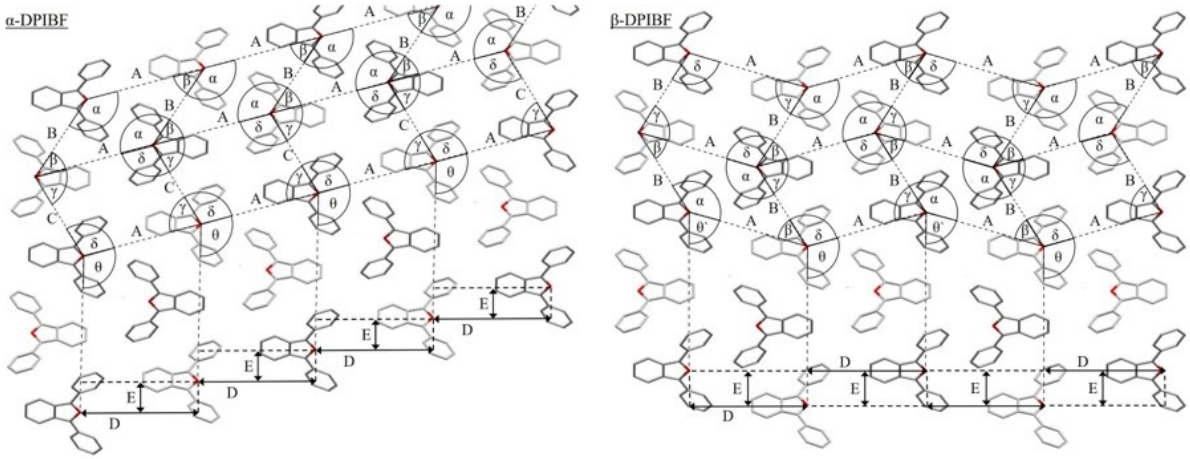

Figure 29. Crystal structures of **7α**, *ac* plane, and **7β**, *bc* plane. Reprinted by permission from ref. 1. Copyright 2019 American Chemical Society.

Table 8. Parameters for Figure 29.[a]

Polymorph of **1**	α	β	γ	δ	θ	θ`	A	B	C	D	E
α	138.70	41.30	73.63	106.37	106.19	N/A	10.153	7.176	7.174	9.750	2.831
β	138.77	41.23	73.91	106.09	106.35	73.65	10.121	7.703	N/A	9.712	2.849

[a] Angles in degrees and lengths in Å.

When in the Marcus equation the solution S_1 excitation energy is used only for **7α** and the difference between the solid S_1 excitation energies of **7α** and **7β** is added to the solution excitation energy to obtain an S_1 excitation energy for **7β**, the resulting SF rate constants of **7β** are a sensitive function of the value chosen for the difference (Table 9, columns 4 - 6). It is not easy to determine the singlet excitation energies and Davydov splittings from the spectra of **7α** and **7β** solids. The S_1 excitation energy of **7α** is clearly higher than that of **7β**, but the difference could be as little as 200 and as much as 900 cm^{-1} depending on how it is evaluated; 600 cm^{-1} was considered to be the most likely value.[5] According to Table 9, the SF rate should then be about five times slower in **7β**, just

about what is actually observed. It thus appears likely that the different SF rates in **7α** and **7β** are not due to a diffrence in the SF matrix element *T*, but to a difference in excitonic interactions.

The difference cannot be accounted for by the simple model, in which the Davydov splitting is evaluated separately for each molecular pair and the results are added: the Davydov splitting ΔE_{DS} calculated in this way for the two polymorphs, summing dozens of neighbor interactions, are essentially the same. This makes sense as their geometries are nearly identical. This is evidence that many-body effects are required for a proper description of Davydov splitting and therefore, of the SF rate.

Table 9. Experimental and Calculated SF Rate Constant Ratios for **7β** Relative to **7α**.

Cmpd.	Exp.	Calcd.	200 cm^{-1} [a]	500 cm^{-1} [b]	900 cm^{-1} [c]
7β	0.18	0.99	0.58	0.25	0.07

[a] Calculated with SF 200 cm^{-1} more endoergic in **7β** than **7α**. [b] Calculated with SF 500 cm^{-1} more endoergic in **7β** than **7α**. [c] Calculated with SF 900 cm^{-1} more endoergic in **7β** than **7α**.

5.5. Conclusion

The results of this work show that the simple model is relatively accurate at comparing the rates of SF between pair structures of the same compound. It is able to identify which pair in a compound's crystal structure is responsible for SF. It is also reasonably accurate when predicting which compounds' crystals will perform singlet fission and which will form excimers. This is quite an achievement for the simple model. However, it clearly lacks the accuracy to predict relative SF rates among different compounds, even when they are derivatives of the same parent. Three factors are likely to be the primary causes for this lack of agreement. As discussed, many-body effects must be important in explaining the differences between the α and β polymorphs and it is likely they are

important in the other crystals as well. Another omission from the simple model is the neglect of competing processes, like excimer formation. And finally, without accurate energy values, a quality comparison of different compounds is infeasible; however, the comparison of different pair geometries of the same compound does not suffer from this issue and is appropriate for the simple model in its current form.

5.6. REFERENCES

1. Buchanan, E. A.; Kaleta, J.; Wen, J.; Lapidus, S. H.; Císařová, I.; Havlas, Z.; Johnson, J. C.; Michl, J. *J. Phys. Chem. Lett.* **2019**, *10*, 1947 – 1953.

2. Unpublished results.

3. Albrecht, W. G.; Michel-Beyerle, M. E.; Yakhot, V. *Chem. Phys.* **1978**, *35*, 193-200.

4. Dillon, R. J.; Piland, G. B.; Bardeen, C. J. *J. Am. Chem. Soc.* **2013**, *135*, 17278-17281.

5. Ryerson, J. L.; Schrauben, J. N.; Ferguson, A. J.; Sahoo, S. C.; Naumov, P.; Havlas, Z.; Michl, J.; Nozik, A. J.; Johnson, J. C. *J. Phys. Chem. C* **2014**, *118*, 12121-12132.

6. Arias, D. H.; Ryerson, J. L.; Cook, J. D.; Damrauer, N. H.; Johnson, J. C. *Chem. Sci.* **2016**, *7.2*, 1185-1191.

7. Roberts, S. T.; McAnally, R. E.; Mastron, J. N.; Webber, D. H.; Whited, M. T.; Brutchey, R. L.; Thompson, M. E.; Bradforth, S. E. *J. Am. Chem. Soc*. **2012**, *134*, 6388-6400.

8. Dron, P. I.; Michl, J.; Johnson, J. C. *J. Phys. Chem. A* **2017**, *121*, 8596-8603.

9. Yost, S. R.; Lee, J.; Wilson, M. W. B.; Wu, T.; McMahon, D. P.; Parkhurst, R. R.; Thompson, N. J.; Congreve, D. N.; Rao, A.; Johnson, K.; Sfeir, M. Y. *Nat. Chem.* **2014**, *6*, 492-497.

10. Eaton, S. W.; Miller, S. A.; Margulies, E. A.; Shoer, L. E.; Schaller, R. D.; Wasielewski, M. R. *J. Phys. Chem. A* **2015**, *119*, 4151-4161.

11. Johnson, J. C.; Nozik, A. J., Michl, J. *Acc. Chem. Res.* **2013**, *46*, 1290-1299.

12. Bae, Y. J.; Kang, G.; Malliakas, C. D.; Nelson, J. N.; Zhou, J.; Young, R. M.; Wu, Y.-L.; Van Duyne, R. P.; Schatz, G. C.; Wasielewski, M. R. *J. Am. Chem. Soc*. **2018**, *140*, 15140-15144.

13. Müller, A. M.; Avlasevich, Y. S.; Schoeller, W. W.; Müllen, K.; Bardeen, C. J. *J. Am. Chem. Soc.* **2007**, *129*, 14240-14250.

14. Johnson, J. C.; Akdag, A.; Zamadar, M.; Chen, X. D.; Schwerin, A. F.; Paci, I.; Smith, M. B.; Havlas, Z.; Miller, J. R.; Ratner, M. A.; Nozik, A. J.; Michl, J. *J. Phys. Chem. B* **2013**, *117*, 4680-4695.

15. Sanders, S. N.; Kumarasamy, E.; Pun, A. B.; Trinh, M. T.; Choi, B.; Xia, J.; Taffet, E. J.; Low, J. Z.; Miller, J. R.; Roy, X.; Zhu, X. Y.; Steigerwald, M. L.; Sfeir, M. Y.; Campos, L. M. *J. Am. Chem. Soc.* **2015**, *137*, 8965-8972.

16. Zirzlmeier, J.; Lehnherr, D.; Coto, P. B.; Chernick, E. T.; Casillas, R.; Basel, B. S.; Thoss, M.; Tykwinski, R. R.; Guldi, D. M. *Proc. Natl. Acad. Sci. USA* **2015**, *112*, 5325-5330.

17. Cook, J. D.; Carey, T. J.; Damrauer, N. H. *J. Phys. Chem. A* **2016**, *120*, 4473-4481.

18. Schrauben, J. N.; Akdag, A.; Wen, J.; Havlas, Z.; Ryerson, J. L.; Smith, M. B.; Michl, J.; Johnson, J. C. *J. Phys. Chem. A* **2016**, *120*, 3473-3483.

19. Margulies, E. A.; Miller, C. E.; Wu, Y.; Ma, L.; Schatz, G. C.; Young, R. M.; Wasielewski, M. R. *Nature Chem.* **2016**, *8*, 1120-1125.

20. Korovina, N. V.; Das, S.; Nett, Z.; Feng, X.; Joy, J.; Haiges, R.; Krylov, A. I.; Bradforth, S. E.; Thompson, M. E. *J. Am. Chem. Soc.* **2016**, *138*, 617-627.

21. Margulies, E. A.; Logsdon, J. L.; Miller, C. E.; Ma, L.; Simonoff, E.; Young, R. M.; Schatz, G. C.; Wasielewski, M. R. *J. Am. Chem. Soc.* **2017**, *139*, 663-671.

22. Margulies, E. A.; Kerisit, N.; Gawel, P.; Mauck, c. M.; Ma, L.; Miller, C. E.; Young, R. M.; Trapp, N.; Wu, Y.-L.; Diederich, F.; Wasielewski, M. R. *J. Phys. Chem. C* **2017**, *121*, 21262-21271.

23. Kolata, K.; Breuer, T.; Witte, G.; Chatterjee, S. *ACS Nano* **2014**, *8*, 7377-7383.

24. Johnson, J. C.; Michl, J. Singlet Fission and 1,3-Diphenylisobenzofuran as a Model Chromophore. In *Advanced Concepts in Photovoltaics*, Nozik, A. J., Conibeer, G., Beard, M. C., Eds.; Royal Society of Chemistry: Oxfordshire, UK, **2014**, pp. 324-344.

25. Schrauben, J.; Ryerson, J.; Michl, J.; Johnson, J. *J. Am. Chem. Soc.* **2014**, *136*, 7363-7373.

26. Johnson, J. C.; Michl, J. *Top. Curr. Chem.* **2017**, *375*, 80.

27. Subotnik, J. E.; Vura-Weis, J.; Sodt, A. J.; Ratner, M. A. Predicting Accurate Electronic Excitation Transfer Rates via Marcus Theory with Boys or Edmiston-Ruedenberg Localized Diabatization *J. Phys. Chem. A.* **2010,** *114*, 8665–8675.

28. Neese, F. The ORCA program system, *Wiley Interdiscip. Rev.: Comput. Mol. Sci.* **2012**, *2*, 73-78.

29. Hirata, S.; Head-Gordon, M. Time-dependent density functional theory within the Tamm-Dancoff approximation *Chem. Phys. Lett.* **1999**, *314*, 291– 299.

30. Becke, A. D. Density functional thermochemistry. III. The role of exact exchange. *J. Chem. Phys.* **1993**, *98*, 5648-5652.

31. Stephens, P. J.; Devlin, F. J.; Chabalowski, C. F.; Frisch, M. J. Ab Initio Calculations of Vibrational Absorption and Circular Dichroism Spectra Using Density Functional Force Fields. *J. Phys. Chem.* **1994**, *98*, 11623-11627.

32. Weigend, F.; Ahlrichs, R. Balanced basis sets of split valence, triple zeta valence and quadruple zeta valence quality for H to Rn: Design and assessment of accuracy *Phys. Chem. Chem. Phys.* **2005**, *7*, 3297.

33. Grimme, S.; Anthony, J.; Ehrlich, S.; Krieg, H. A consistent and accurate ab initio parametrization of density functional dispersion correction (DFT-D) for the 94 elements H-Pu. *J. Chem. Phys.* **2010**, *132*, 154104.

34. Izsak, R.; Neese, F. An Overlap fitted chain of spheres exchange method *J. Chem. Phys.* **2011**, *135*, 144105.

35. Neese, F.; Wennmohs, F.; Hansen, A.; Becker, U. Efficient, approximate and parallel Hartree–Fock and hybrid DFT calculations. A 'chain-of-spheres' algorithm for the Hartree–Fock exchange *Chem. Phys.* **2009**, *356*, 98-109.

36. Weigend, F. Accurate Coulomb-fitting basis sets for H to Rn *Phys. Chem. Chem. Phys.* **2006**, *8*, 1057.

37. Hellweg, A.; Hattig, C.; Hofener, S.; Klopper, W. Optimized accurate auxiliary basis sets for RI-MP2 and RI-CC2 calculations for the atoms Rb to Rn *Theor. Chem. Acc.* **2007**, *117*, 587.

38. Adamo, C.; Barone, V. *J. Chem. Phys.* **1999**, *110*, 6158.

39. Weigend, F.; Ahlrichs, R. *Phys. Chem. Chem. Phys.* **2005**, *7*, 3297.

40. Weigend, F. *J. Comput. Chem.* **2008**, *29*, 167.

41. Rappoport, D.; Furche, F. *J. Chem. Phys.* **2010**, *133*, 134105.

42. Jones, R. O.; Gunnarsson, O. The density functional formalism, its applications and prospects *Rev. Mod. Phys.* **1989**, *61*, 689– 746.

43. Buchanan, E. A.; Havlas, Z.; Michl, J. Singlet Fission: Optimization of Chromophore Dimer Geometry. In Advances in Quantum Chemistry: Ratner Volume, *75*; Sabin, J. R.; Brändas, E. J., Eds.; Elsevier: Cambridge, MA, **2017**, 175-227.

44. Schwerin, A. F.; Johnson, J. C.; Smith, M. B.; Sreearunothai, P.; Popović, D.; Černý, J.; Havlas, Z.; Paci, I.; Akdag, A.; MacLeod, M. K.; Chen, X.; David, D. E.; Ratner, M. A.; Miller, J. R.; Nozik, A. J.; Michl, J. Toward Designed Singlet Fission: Electronic States and Photophysics of 1,3-Diphenylisobenzofuran. *J. Phys. Chem. A* **2010**, *114*, 1457-1473.

45. Grotjahn, R.; Maier, T. M.; Michl, J.; Kaupp, M. *J. Chem. Theory Comput.* **2017**, *13*, 494-4996.

46. Adapted with permission from Buchanan, E. A.; Kaleta, J.; Wen, J.; Lapidus, S. H.; Císařová, I.; Havlas, Z.; Johnson, J. C.; Michl, J. *J. Phys. Chem. Lett.* **2019**, *10*, 1947 – 1953. Copyright 2019 American Chemical Society.

47. Nakano, M.; Nagami, T; Tonami, T.; Okada, K.; Ito, S.; Kishi, R.; Kitagawa, Y.; Kubo, T. *J. Comp. Chem.*, **2019**, *40*, 89-104.

48. Refaely-Abramson, S.; da Jornada, F. H.; Louie, S. G.; Neaton, J. B. *Phys. Rev. Lett.* **2017**, *119*, 267401.

Chapter VI

Conclusions

6.1. Summary

The need for a complete transition to renewable energy presents interesting problems for synthetic, experimental, and theoretical chemists. Towards this end, singlet fission promises to increase the efficiency of solar energy conversion in solar cells if the challenges in material design can be overcome. Two primary challenges are finding chromophores which meet the energetic requirements of SF [$E(S_1) > 2\Delta E(T_1)$] while also being stable and environmentally friendly and their optimal arrangements to maximize triplet yield. The work in this dissertation addressed the latter.

The initial part of this study was the further development of the SIMPLE code and model in our research group to include the effects of molecular packing on delocalization and energetics in SF molecule pairs. The model was expanded to determine admixture of charge-transfer configurations into the singlet and biexciton through diagonalization and to allow the interaction of singlet configurations to form the excitonic S* and S** states. This allowed the model to appropriately treat large couplings and include the effects energetic stabilization of excimer formation on the SF process. The transition to optimizing pair geometries for maximum SF rate constant instead of coupling $|T|^2$ allowed the model to discard pair geometries in which excitonic stabilization of the initial singlet resulted in SF being too endoergic, depressing the rate constant. These expansions to the model beyond the initial use of perturbation theory and neglect of energetics resulted in typical increases in computation time of only 5% or less.

With the improved model and SIMPLE code in hand, the first application was to a pair of D_{2h} symmetrized tetracene molecules. The 21 pairs with largest SF rate constant were reported and the top nine were identified as good targets for synthetic efforts with the top three predicted to be far superior to the rest with rate constants 250-550 times that of the symmetrized crystal herringbone pair. The parameter space of intrinsic endoergicity of SF and reorganization energy was explored and showed that the top pairs found are robust in this space. Even doubling these parameters relative to their literature value did not change the pair structures or their rankings substantially. This is promising for synthetic efforts as chemical modification required to achieve these pair geometries can have a strong effect on these energetics. Unfortunately, the results also showed that the specificity of the pair geometry can be very high. The 10th pair is incredibly similar to the crystal herringbone pair, yet it is predicted to undergo SF 33 times faster. Small deviations can have a dramatic effect on the predicted SF rate.

The next application of the model was to pairs of four rotamers of 1,3-diphenylisobenzofuran with C_2, C_{2v}, C_s, and C_1 symmetry. Similar to the tetracene study, the top three pairs offered significant improvement over the slip-stacked crystal pair. Both of these studies reenforce the notion that energetics are as important to the rate of singlet fission as coupling is. Pair structures in which there is only a slight slip-stacking result in too much interaction of the localized singlet configurations leading to large excitonic stabilization, preventing SF from occurring despite these structures often having incredibly large SF coupling. The results of optimization of both these chromophores pointed towards similar qualitative design rules. Structural motifs which overlap only sections of the two partners or their perimeters appear to be ideal. Twist-stacked structures which overlap one or two aromatic rings from the two partners while rotating the rest of the partners away

from each other lead to enough coupling for fast SF while reducing the interaction of the singlet transition densities to minimize Davydov splitting and the endothermicity of the SF process. The same result can be obtained by overlapping a section of the perimeters of the two partners, usually six to eight carbons, which greatly reduces the interactions that lead to Davydov splitting. These structural motifs likely apply to other chromophores as well.

The final application of the simple model was to the analysis of SF in crystals of 1,3-diphenylisobenzofuran and 11 of its fluorinated derivatives. This allowed for comparison of the predictions of the simple model with experimental measurements of the rates of SF. This study demonstrated the shortcomings of the pair model as the α and β polymorphs have drastically different measured rates of SF yet the simple model predicts they should be equivalent. As the polymorphs contain identical molecule pair structures and only differ when considering three or more bodies. It may be expected then that the model could not accurately reproduce the qualitative ratios of measured SF rate constants for the 12 compounds. However, the model was able to explain why the compounds which did not perform singlet fission instead formed excimers. This is relatively good agreement considering the approximations and known shortcomings of the model in addition to the fact that the model was not conceived to have the accuracy required to reproduce experimental results in this manner. Its intended purpose was to provided guidance for how to optimally arrange molecules in the solid to maximize the rate of SF and it accomplishes that with reasonable accuracy.

6.2. Future Outlook

There are three primary shortcomings of the current simple model that are prime targets for improvement. One is the limitation of only considering pairs of molecules when experimental evidence shows that three or more body effects are important. Addressing this will likely require a large increase in complexity. One possibility is, similarly to what is done now for two chromophores, the full set of six translation and rotation parameters could be scanned for the orientation of the third molecule relative to the second. This would turn a six-dimensional scan into a twelve-dimensional scan. If the same 'brute force' method of search employed now were used, this would be unfeasible. The time required to perform a six-dimensional scan would be multiplied by the number of points to be scanned in the additional six-dimensions typically 10^9 points for each resulting in 10^{18} total geometries. If a scan of 10^9 geometries requires typically six days on average, this method would require roughly 6×10^9 days. Some much more sophisticated method for probing large and most likely sparse spaces would be required. Another option is to treat the environment the pair of molecules is imbedded in classically with some QM/MM approach. This would require some informed prediction of what the crystal structure would be given knowledge of only the pair's structure, which could be very challenging. Again, 1,3-diphenylisobenzofuran shows that for a given molecule pair structure two different crystal forms can still exist which undergo SF at drastically different rates.

Another limitation is the simplicity of the model. This simplicity is required for the six-dimensional scan, but an improved model with greater accuracy could be applied after the initial scan in two obvious ways. The optimization step after the initial scan could be performed with an expanded model on the top few thousand geometries or a 'pre-optimization' could be performed with

the current simple model and the top dozen or so pairs could be re-optimized with a more accurate model. The more accurate model could include many-body effects in was just described by treating the surrounding molecules either explicitly or semi-classically. Couplings and energetics could be calculated with higher level, *ab initio* methods such as RAS-SF, CASSCF, CASPT2, DMRG, MRMP, or other such methods and rates could be calculated via some dynamical model like MC-TDHF. Instead of calculating only the rate of SF, the rates of all reasonable competing decay processes could be calculated as well so that triplet yield could be predicted. These extensions to the model are too computationally expensive to perform at 10^9 geometries, but would be feasible for a half dozen or so.

The main shortcoming of the model is the lack of experimental evidence either confirming or denying the SF properties of the predicted pair structures. The optimization process is not complete until there is feedback on the predicted structures. The author hopes that the results of this work will inspire synthetic chemists to try and make some of the targeted optimized structures from this work either as covalent dimers or through chemical modification and crystal engineering. The success and applicability of the simple model will remain largely unknown until the results are confirmed through experiment.

Bibliography

1. Adamo, C.; Barone, V. *J. Chem. Phys.* **1999**, *110*, 6158.

2. Albrecht, W. G.; Michel-Beyerle, M. E.; Yakhot, V. *Chem. Phys.* **1978**, *35*, 193.

3. Arias, D. H.; Ryerson, J. L.; Cook, J. D.; Damrauer, N. H.; Johnson, J. C. *Chem. Sci.* **2016**, *7*, 1185.

4. Bae, Y. J.; Kang, G.; Malliakas, C. D.; Nelson, J. N.; Zhou, J.; Young, R. M.; Wu, Y.-L.; Van Duyne, R. P.; Schatz, C. G.; Wasielewski, M. R. *J. Am. Chem. Soc*. **2018**, *140*, 15140.

5. Basel, B. S.; Zirzlmeier, J.; Hetzer, C.; Phelan, B. T.; Krzyaniak, M. D.; Reddy, S. R.; Coto, P. B.; Horwitz, N. E.; Young, R. M.; White, F. J.; Hampel, F.; Clark, T.; Thoss, M.; Tykwinski, R. R.; Wasielewski M. R.; Guldi, D. M. *Nat. Comm.* **2017**, *8*, 15171.

6. Batsanov, S. S. *Inorg. Mat*. **2001**, *37*, 871-885.

7. Becke, A. D. *J. Chem. Phys.* **1993**, *98*, 5648-5652.

8. Berkelbach, T. C. *Adv. Chem. Phys.* **2017**, *162*, 1.

9. Berkelbach, T. C.; Hybertsen, M. S.; Reichman, D. R. *J. Chem. Phys.* **2013**, *138*, 114103.

10. Berkelbach, T. C.; Hybertsen, M. S.; Reichman, D. R. *J. Chem. Phys.* **2014**, *141*, 074705.

11. Bhattacharyya, K.; Datta, A. *J. Phys. Chem. C* **2017**, *121*, 1412.

12. Bhattacharyya, K.; Dey, D.; Datta, A. *J. Phys. Chem. C* **2019**, *213*, 4749.

13. Broer, R.; Nieuwpoort, W. C. *Theor. Chim. Acta* **1988**, *73*, 405-418.

14. Buchanan, E. A.; Havlas, Z. ; Michl, J. in *Advances in Quantum Chemistry: Ratner Volume, Volume 75*, eds. Sabin, J. R.; Brändas, E. J. Elsevier, Cambridge, MA, **2017**, p. 175. Erratum: In the last paragraph of section 2.5 (p. 205), delete $(h_A h_A|h_B h_B) + (h_A h_A|l_B l_B) + (l_A l_A|h_B h_B) + (l_A l_A|l_B l_B)$ in the expression for $|E(^1\mathrm{TT}) - E(\mathrm{T+T})|$.

15. Buchanan, E. A.; Kaleta, J.; Wen, J.; Lapidus, S. H.; Císařová, I.; Havlas, Z.; Johnson, J. C.; Michl, J. *J. Phys. Chem. Lett.* **2019**, *10*, 1947.

16. Buchanan, E. A.; Michl, J. *J. Am. Chem. Soc.* **2017**, *139*, 15572-15575.
17. Burdett, J. J.; Bardeen, C. J. *J. Am. Chem. Soc.* **2012**, *134*, 8597.

18. Burdett, J. J.; Gosztola, D.; Bardeen, C. J. *J. Chem. Phys.* **2011**, *135*, 214508.

19. Busby, E.; Berkelbach, T. C.; Kumar, B.; Chernikov, A.; Zhong, Y.; Hlaing, H.; Zhu, X. Y.; Heinz, T. F.; Hybertsen, M. S.; Sfeir, M. Y.; Reichman, D. R. *J. Am. Chem. Soc.* **2014**, *136*, 10654-10660.

20. Casanova, D. *J. Chem. Theory and Comp.* **2013**, *10*, 324.

21. Casanova, D. *J. Chem. Theory Comput.* **2014**, *10*, 324-334.

22. Casanova, D. *Chem. Rev.* **2018**, *118*, 7164.

23. Chan, W-L.; Berkelbach, T. C.; Provorse, M. R.; Monahan, N. R; Tritsch, J. R.; Hyvertsen M. S.; Reichman, D. R.; Gao, J.; Zhu, X-Y. *Acc. Chem. Res.* **2013**, *46*,1321-1329.

24. Chan, W. L.; Ligges, M., Zhu, X-Y. *Nat. Chem.* **2012**, *4*, 840-845.

25. Cook, J. D.; Carey, T. J.; Damrauer, N. H. *J. Phys. Chem. A* **2016**, *120*, 4473-4481.

26. Dexter, D. L. *J. Chem. Phys.* **1953**, *21*, 836-850.

27. Dexter, D. L. *J. Luminescence* **1979**, *18*, 779.

28. Dillon, R. J.; Piland, G. B.; Bardeen, C. J. *J. Am. Chem. Soc.* **2013**, *135*, 17278.

29. Dron, P. I.; Michl, J.; Johnson, J. C. *J. Phys. Chem. A* **2017**, *121*, 8596.

30. Eaton, S. W.; Miller, S. A.; Margulies, E. A.; Shoer, L. E.; Schaller, R. D.; Wasielewski, M. R. *J. Phys. Chem. A* **2015**, *119*, 4151-4161.

31. Farag, M. H.; Krylov, A. I. *J. Phys. Chem. C* **2018**, *122*, 25753.

32. Förster, T. In *Modern Quantum Chemistry*; Sinanoglu, O., Ed.; Academic Press: New York, **1965**, Vol. 3.

33. Gallup, G. A.; Norbeck, J. M. *Chem. Phys. Lett.* **1973**, *21*, 495-500.

34. Gilligan, A. T.; Miller, E. G.; Damrauer, N. H. *J. Am. Chem. Soc.* **2019**, *141*, 5961.

35. Glendening, E.D.; Landis, C.R.; Weinhold, F. *J. Comput. Chem.* **2013**, *34*, 1429-1437.

36. Greyson, E. C.; Vura-Weis, J.; Michl, J.; Ratner, M. A. *J. Phys. Chem. B* **2010**, *114*, 14168.

37. Grieco, C.; Doucette, G. S.; Munro, J. M.; Kennehan, E. R.; Lee, Y.; Rimshaw, A.; Payne, M. M.; Wonderling, N.; Anthony, J. E.; Dabo, I.; Gomez, E. D.; Asbury, J. B. *Adv. Funct. Mater.* **2017**, *27*, 1703929.

38. Grimme, S.; Anthony, J.; Ehrlich, S.; Krieg, H. *J. Chem. Phys.* **2010**, *132*, 154104.

39. Gross, E. K. U.; Kohn, W. *Adv. Quantum Chem.* **1990**, *21*, 255.

40. Grotjahn, R.; Maier, T. M.; Michl, J.; Kaupp, M. *J. Chem. Theory Comput.* **2017**, *13*, 494-4996.

41. Guest, M. F.; Bush, I. J.; van Dam, H. J. J.; Sherwood, P.; Thomas, J. M. H.; van Lenthe, J. H.; Havenith, R. W. A.; Kendrick, J. *Mol. Phys.* **2005**, *103*, 719-747.

42. Harcourt, R. D.; Scholes, G. D.; Ghiggino, K. P. *J. Chem. Phys.* **1994**, *101*, 10521-10525.

43. Hartnett, P. E.; Margulies, E. A.; Mauck, C. M.; Miller, S. A.; Wu, Y.; Wu, Y. L.; Marks, T. J. *J. Phys. Chem. B* **2016**, *120*, 1357.

44. Hanna, M. C.; Nozik, A. J. *J. Appl. Phys.* **2006**, *100*, 074510/1.

45. Harris, S. An Introduction to the Theory of the Boltzmann Equation (Holt, Rinehart and Winston, New York, **1971**).

46. Havenith, R. W. A.; de Gier, H. D.; Broer, R. *Mol. Phys.* **2012**, *110*, 2445-2454.

47. Havlas, Z.; Michl, J. *Isr. J. Chem.* **2016**, *56*, 96-106.

48. Hellweg, A.; Hattig, C.; Hofener, S.; Klopper, W. *Theor. Chem. Acc.* **2007**, *117*, 587.

49. Henn, D. E.; Williams, W. G.; Gibbons, D. J. *J. Appl. Cryst.* **1971**, *4*, 256.

50. Hirata, S.; Head-Gordon, M. *Chem. Phys. Lett.* **1999**, *314*, 291– 299.

51. Hoffmann, R. *J. Chem. Phys.* **1963**, *39*, 1397-1412.

52. Holmes, D.; Kumaraswamy, S.; Matzger, A. J.; Vollhardt, K. P. C. *Chem. Eur. J.* **1999**, *5*, 3399.

53. Ito, S.; Nagami, T.; Nakano, M. *J. Phys. Chem. Lett.* **2015**, *6*, 4972-4977.

54. Izsak, R.; Neese, F. *J. Chem. Phys.* **2011**, *135*, 144105.

55. Johnson, J. C.; Akdag, A.; Zamadar, M.; Chen, X.; Schwerin, A. F.; Paci, I.; Smith, M. B.; Havlas, Z.; Miller, J. R.; Ratner, M. A.; Nozik, A. J.; Michl, J. *J. Phys. Chem. B* **2013**, *117*, 4680.

56. Johnson, J. C.; Michl, J. Singlet Fission and 1,3-Diphenylisobenzofuran as a Model Chromophore. In *Advanced Concepts in Photovoltaics*, Nozik, A. J., Conibeer, G., Beard, M. C., Eds.; Royal Society of Chemistry: Oxfordshire, UK, **2014**, pp. 324-344.

57. Johnson, J. C.; Michl, J., *Top. Curr. Chem.* **2017**, *375*, 80.

58. Johnson, J. C.; Nozik, A. J.; Michl, J. *J. Am. Chem. Soc.* **2010**, *132*, 16302.

59. Jones, R. O.; Gunnarsson, O. *Rev. Mod. Phys.* **1989**, *61*, 689– 746.

60. Jortner, J.; Rice, S. A.; Katz, J. L.; Choi, S. I. *J. Chem. Phys.* **1965**, *42*, 309-323.

61. Kazmaier, P. M.; Hoffmann, R. *J. Am. Chem. Soc.* **1994**, *116*, 9684-9691.

62. Kolata, K.; Breuer, T.; Witte, G.; Chatterjee, S. *ACS Nano* **2014**, *8*, 7377-7383.

63. Kolomeisky, A. B.; Feng, Y.; Krylov, A. I. *J. Phys. Chem. C* **2014**, *118*, 5188-5195.

64. Korovina, N. V.; Das, S.; Nett, Z.; Feng, X.; Joy, J.; Haiges, R.; Krylov, A. I.; Bradforth, S. E.; Thompson, M. E. *J. Am. Chem. Soc.* **2016**, *138*, 617.

65. Krishnan, R.; Binkley, J. S.; Seeger R.; Pople, J. A. *J. Chem. Phys.* **1980**, *72*, 650.

66. Krishnapriya, K. C.; Musser, A. J.; Patil, S. *ACS Energy Lett.* **2019**, *4*, 192.

67. Le, A. K.; Benders, J. A.; Arias, D. H.; Cotton, D. E.; Johnson, J. C.; Roberts, S. T. *J. Am. Chem. Soc.* **2018**, *140*, 814.

68. Linderberg, J. Seamans, L. *Mol. Phys.* **1972**, *24*, 1393-1405.

69. Löwdin, P. *Adv. Quant. Chem.* **1970**, *5*, 185-199.

70. Maple 17. Maplesoft, a division of Waterloo Maple Inc., Waterloo, Ontario.

71. Marcus, R. A. *J. Chem. Phys.* **1956**, *24*, 966 and 979.

72. Marcus, R. A. *Rev. Mod. Phys.* **1993**, *65*, 599.

73. Marcus, R. A.; Sutin, N. *Biochim. Biophys. Acta* **1985**, *811*, 265.

74. Margulies, E. A.; Kerisit, N.; Gawel, P.; Mauck, c. M.; Ma, L.; Miller, C. E.; Young, R. M.; Trapp, N.; Wu, Y.-L.; Diederich, F.; Wasielewski, M. R. *J. Phys. Chem. C* **2017**, *121*, 21262-21271.

75. Margulies, E. A.; Logsdon, J. L.; Miller, C. E.; Ma, L.; Simonoff, E.; Young, R. M.; Schatz, G. C.; Wasielewski, M. R. *J. Am. Chem. Soc.* **2017**, *139*, 663.

76. Margulies, E. A.; Miller, C. E.; Wu, Y.; Ma, L.; Schatz, G. C.; Young, R. M.; Wasielewski, M. R. *Nature Chem.* **2016**, 8, 1120.

77. Margulies, E. A.; Shoer, L. E.; Eaton, S. W.; Wasielewski, M. R. *Phys. Chem. Chem. Phys.* **2014**, *16*, 23735.

78. Matsika, S.; Feng, X.; Luzanov, A. V.; Krylov, A. I. *J. Phys. Chem. A* **2014**, *118*, 11943-11955.

79. Mauck, C. M.; Bae, Y. J.; Chen, M.; Powers-Riggs, N.; Wu, Y.-L.; Wasielewski, M. R. *ChemPhotoChem* **2018**, *2*, 223.

80. Mauck, C. M.; Hartnet, P. E.; Margulies, E. A.; Ma, L.; Miller, C. E.; Schatz, G. C.; Tobin, J. M.; Wasielewski, M. R. *J. Am. Chem. Soc.* **2016**, 138, 11749.

81. Michl, J.; Thulstrup, E. W. *Tetrahedron* **1976**, *32*, 205.

82. Mitchell, M. *An Introduction to Genetic Algorithms*; MIT Press: Cambridge, MA, **1996**.

83. Miyata, K.; Conrad-Burton, F. S.; Geyer, F. L.; Zhu, X.-Y. *Chem. Rev.* **2019**, *119*, 4261.

84. Monahan, N.; Zhu, X.-Y. *Annu. Rev. Phys. Chem.* **2015**, *66*, 601.

85. Morrison, A. F.; Herbert, J. M. *J. Phys. Chem. Lett.* **2017**, *8*, 1442-1448.

86. Müller, A. M.; Avlasevich, Y. S.; Schoeller, W. W.; Müllen, K.; Bardeen, C. J. *J. Am. Chem. Soc.* **2007**, *129*, 14240.

87. Nagami, T.; Ito, S.; Kubo, T.; Nakano, M. *ACS Omega* **2017**, *2*, 5095.

88. Nakano, M.; Nagami, T; Tonami, T.; Okada, K.; Ito, S.; Kishi, R.; Kitagawa, Y.; Kubo, T. *J. Comp. Chem.*, **2019**, *40*, 89-104.

89. Neese, F. The ORCA program system, *Wiley Interdiscip. Rev.: Comput. Mol. Sci.* **2012**, *2*, 73-78.

90. Neese, F. *Wiley Interdiscip. Rev.: Comput. Mol. Sci.* **2012**, *2*, 73.

91. Neese, F.; Wennmohs, F.; Hansen, A.; Becker, U. *Chem. Phys.* **2009**, *356*, 98-109.

92. Paci, I.; Johnson, J. C.; Chen, X.; Rana, G.; Popović, D.; David, D. E.; Nozik A. J.; Ratner, M. A. *J. Am. Chem. Soc.* **2006**, *128*, 16546.

93. Parker, S. M.; Seideman, T.; Ratner, M. A.; Shiozaki, T. *J. Phys. Chem. C* **2014**, *118*, 12700-12705.

94. Pensack, R. D.; Tilley, A.; Grieco, C.; Purdum, G.; Ostroumov, E.; Granger, D. B.; D. Oblinsky, D.; Dean, J.; Doucette, G.; Asbury, J.; Loo, Y.-L.; Seferos, D.; Anthony, J. E.; Scholes, G. *Chem. Sci.* **2018**, *9*, 6240.

95. Pensack, R. D.; Tilley, A. J.; Parkin, S. R.; Lee, T. S.; Payne, M. M.; Gao, Jahnke, A.; Oblinsky, D. G.; Li, P.-F.; Anthony, J. E.; Seferos, D. S. *J. Am. Chem. Soc.* **2015**, *137*, 6790.

96. Petelenz, P.; Snamina, M. *J. Phys. Chem. C* **2015**, *119*, 28570.

97. Petelenz, P.; Snamina, M. *J. Phys. Chem. Lett.* **2016**, *7*, 1913.

98. Piland, G. B.; Bardeen, C. J. *J. Phys. Chem. Lett.* **2015**, *6*, 1841.

99. Piland, G. B.; Burdett, J. J.; Kurunthu, D.; Bardeen, C. J. *J. Phys. Chem. C* **2013**, *117*, 1224.

100. Rao, A.; Friend, R. H. *Nat. Rev. Mater.* **2017**, *2*, 17063.

101. Rappoport, D.; Furche, F. *J. Chem. Phys.* **2010**, *133*, 134105.

102. Refaely-Abramson, S.; da Jornada, F. H.; Louie, S. G.; Neaton, J. B. *Phys. Rev. Lett.* **2017**, *119*, 267401.

103. Renaud, N.; Sherratt, P. A.; Ratner, M. A. *J. Phys. Chem. Lett.* **2013**, *4*, 1065-1069.

104. Roberts, S. T.; McAnally, R. E.; Mastron, J. N.; Webber, D. H.; Whited, M. T.; Brutchey, R. L.; Thompson, M. E.; Bradforth, S. E. *J. Am. Chem. Soc*. **2012**, *134*, 6388-6400.

105. Roothaan, C. C. J.; Sachs, L. M.; Weiss, A. W. *Rev. Mod. Phys.* **1960**, *32*, 186-194.

106. Ryerson, J.; Schrauben, J. N.; Ferguson, A. J.; Sahoo, S. C.; Naumov, P.; Havlas, Z.; Michl, J.; Nozik, A. J.; Johnson, J. C. *J. Phys. Chem. C* **2014**, *118*, 12121.

107. Sanders, S. N.; Kumarasamy, E.; Pun, A. B.; Trinh, M. T.; Choi, B.; Xia, J.; Taffet, E. J.; Low, J. Z.; Miller, J. R.; Roy, X.; Zhu, X. Y.; Steigerwald, M. L.; Sfeir, M. Y.; Campos, L. M. *J. Am. Chem. Soc.* **2015**, *137*, 8965.

108. Scholes, G. D.; Harcourt, R. D. *J. Chem. Phys.* **1996**, *104*, 5054-5061.

109. Schrauben, J. N.; Akdag, A.; Wen, J.; Havlas, Z.; Ryerson, J. L.; Smith, M. B.; Michl, J.; Johnson, J. C. *J. Phys. Chem. A* **2016**, *120*, 3473.

110. Schrauben, J.; Ryerson, J.; Michl, J.; Johnson, J. C. *J. Am. Chem. Soc.* **2014**, *136*, 7363.

111. Schwerin, A. F. ;Johnson, J. C.; Smith, M. B.; Sreearunothai, P.; Popović, D.; Černý, J.; Havlas, Z. ; Paci, I.; Akdag, A.; MacLeod, M. K.; Chen, X.; David, D. E.; Ratner, M. A.; Miller, J. R. ; Nozik, A. J.; Michl, J. *J. Phys. Chem. A* **2010**, *114*, 1457.

112. Shockley, W.; Queisser, H. J. *J. Appl. Phys*. **1961**, *32*, 510.

113. Singh, S.; Jones, W. J.; Siebrand, W.; Stoicheff B. P.; Schneider, W. G. *J. Chem. Phys.* **1965**, *42*, 330.

114. Smith, M. B.; Michl, J. *Chem. Rev.* **2010**, *110*, 6891.

115. Smith, M. B.; Michl, J. *Annu. Rev. Phys. Chem.* **2013**, *64*, 361.

116. Snamina, M.; Petelenz, P. *ChemPhysChem* **2017**, *18*, 149.

117. Stephens, P. J.; Devlin, F. J.; Chabalowski, C. F.; Frisch, M. J. *J. Phys. Chem.* **1994**, *98*, 11623-11627.

118. Stoychev, G. L.; Auer, A. A.; Neese, F. *J. Chem. Theory Comput.* **2017**, *13*, 554-562.

119. Straatsma, T. P.; Broer, R.; Faraji, S.; Havenith, R. W. A. *Annu. Rep. Comput. Chem.*, **2018**, *14*, 77-91.

120. Stuart, A. N.; Tapping, P. C.; Schrefl, E.; Huang, D. M.; Kee, T. W. *J. Phys. Chem. C* **2019**, *123*, 5813.

121. Subotnik, J. E.; Vura-Weis, J.; Sodt, A. J.; Ratner, M. A. *J. Phys. Chem. A.* **2010,** *114*, 8665–8675.

122. Sutton, C.; Tummala, N. R.; Beljonne, D.; Brédas, J.-L. *Chem. Mater.* **2017**, *29*, 2777.

123. Swenberg, C. E. ; Geacintov, N. E. *Org. Mol. Photophysics* **1973**, *18*, 489.

124. Tamura, H.; Huix-Rotllant, M.; Burghardt, I.; Olivier, Y.; Beljonne, D. *Phys. Rev. Lett.* **2015**, *115*, 107401.

125. Tayebjee, M. J. Y.; Schwarz, K. N.; MacQueen, R. W.; Dvořák, M.; Lam, A. W. C.; Ghiggino, K. P.; McCamey, D. R.; Schmidt, T. W.; Conibeer, C. J. *J. Phys. Chem. C* **2016**, *120*, 157.

126. Tilley, A. J.; Pensack, R. D.; Kynaston, E. L.; Scholes, G. D.; Seferos, D. S. *Chem. Mater.* **2018**, *30*, 4409.

127. Tomkiewicz, Y.; Groff, R. P.; Avakian, P. *J. Chem. Phys.* **1971**, *54*, 4505-4507.

128. Trlifaj, M. *Czech J. Phys. B* **1972**, *22*, 832-840.

129. Wang, C.; Angelella, M.; Kuo, C.-H.; Tauber, M. J. *Proc. SPIE* **2012**, *8459*, 845905-1-845905-13.

130. Wang, X.; Garcia, T.; Monaco, S.; Schatschneider, B.; Marom, N. *CrystEngComm* **2016**, *18*, 7353.

131. Wang, X.; Liu, X.; Tom, R.; Cook, C. *J. Phys. Chem. C* **2019**, *123*, 5890.

132. Wang, L.; Olivier, Y.; Prezhdo, O. V.; Beljonne, D. *J. Phys. Chem. Lett.* **2014**, *5*, 3345.

133. Weigend, F. *J. Comput. Chem.* **2008**, *29*, 167.

134. Weigend, F.; Ahlrichs, R. *Phys. Chem. Chem. Phys.* **2005**, *7*, 3297.

135. Weiss, L. R.; Bayliss, S. L.; Kraffert, F.; Thorley, K. J.; Anthony, J. E.; Bittle, R.; Friend, R. H.; Rao, A.; Greenham, N. C. *Nat. Phys.* **2017**, *13*, 176.

136. Wilson, M. W. B.; Rao, A.; Johnson, K.; Gélinas, S.; di Pietro, R.; Clark, J.; Friend, R. H. *J. Am. Chem. Soc.* **2013**, *135*, 16680– 16688.

137. Wolfsberg, M.; Helmholz, L. *J. Chem. Phys.* **1952**, *20*, 837-843.

138. Wu, Y.; Liu, K.; Liu, H.; Zhang, Y.; Zhang, H.; Yao, J.; Fu, H. *J. Phys. Chem. Lett.* **2014**, *5*, 3451.

139. Yamagata, H.; Maxwell, D. S.; Fan, J.; Kittilstved, K. R.; Briseno, A. L.; Barnes, M. D.; Spano, F. C. *J. Phys. Chem. C* **2014**, *118*, 28842-28854.

140. Yost, S. R.; Lee, J.; Wilson, M. W. B.; Wu, T.; McMahon, D. P.; Parkhurst, R. R.; Thompson, N. J.; Congreve, D. N.; Rao, A.; Johnson, K.; Sfeir, M. Y.; Bawendi, M. G.; Swager, T. M.; Friend, R. H.; Baldo, M. A.; Van Voorhis, T. *Nat. Chem.* **2014**, *6*, 492– 497.

141. Zaykov, A.; Felkel, P.; Buchanan, E. A.; Jovanovic, M.; Havenith, R. W. A.; Kathir, R. K.; Broer, R.; Havlas, Z.; Michl, J. "Singlet Fission Rate: Optimized Packing of a Molecular Pair. Ethylene as a Model", submitted for publication.

142. Ryerson, J. L.; Zaykov, A.; Aguilar Suarez, L. E.; Havenith, R. W. A.; Stepp, B. R.; Dron, P. I.; Kaleta, J.; Akdag, A.; Teat, S. J.; Magnera, T. F.; Miller, J. R.; Havlas, Z.; Broer, R.; Faraji, S.; Michl, J.; Johnson, J. C. "Structure and Photophysics of Indigoids for Singlet Fission: Cibalackrot", submitted for publication.

143. Zirzlmeier, J.; Lehnherr, D.; Coto, P. B.; Chernick, E. T.; Casillas, R.; Basel, B. S.; Thoss, M.; Tykwinski, R. R.; Guldi, D. M. *Proc. Natl. Acad. Sci. USA* **2015**, *112*, 5325.

Appendix

for

The Role of Molecular Packing in Singlet Fission

Thesis written by Eric A. Buchanan and directed by Professor Josef Michl

Table of Contents

Tables

1. D_{2h} Symmetrized Tetracene Ground State Geometry

Table A1. *XYZ* Coordinates for Tetracene in Units of Ångstrøms.

30

C	-1.230581	1.397494	0.000000
C	-2.448286	0.727475	0.000000
C	-3.705482	1.400851	0.000000
C	-4.876831	0.714583	0.000000
C	-4.876831	-0.714583	0.000000
C	-3.705482	-1.400851	0.000000
C	-2.448286	-0.727475	0.000000
C	-1.230581	-1.397494	0.000000
C	0.000000	0.728577	0.000000
H	-1.224952	2.347042	0.000000
H	-3.724223	2.350677	0.000000
H	-5.700773	1.187157	0.000000
H	-5.700773	-1.187157	0.000000
H	-3.724223	-2.350677	0.000000
H	-1.224952	-2.347042	0.000000
C	0.000000	-0.728577	0.000000
C	1.230581	-1.397494	0.000000
C	2.448286	-0.727475	0.000000
C	3.705482	-1.400851	0.000000
C	4.876831	-0.714583	0.000000
C	4.876831	0.714583	0.000000
C	3.705482	1.400851	0.000000
C	2.448286	0.727475	0.000000
C	1.230581	1.397494	0.000000
H	1.224952	2.347042	0.000000
H	3.724223	2.350677	0.000000
H	5.700773	1.187157	0.000000
H	5.700773	-1.187157	0.000000
H	3.724223	-2.350677	0.000000
H	1.224952	-2.347042	0.000000

2. Generation of Pair Coordinates from Structure Parameters

The method of generation of the *XYZ* coordinates of each pair is described by the following. Partner A is always the same and its coordinates are obtained from Tables A1 or A11-A14. Partner B's coordinates are obtained by rotation then translation of the coordinates of partner A according to eqs. (A1 - A4). The *XYZ* coordinates are stored row-wise as in eq. (A1). The total rotation matrix is the product of the three rotations about the *x*, *y*, and *z* axes ($R_{tot} = R_z \cdot R_y \cdot R_x$) and it is determined by the three parameters R_x, R_y, and R_z as defined in eq. (A2). The translation matrix T is determined by the three parameters T_x, T_y, and T_z and its form is provided in eq. (A3). The *XYZ* coordinates of partner B stored row-wise are obtained by matrix multiplication of A with the transpose of the total rotation matrix R_{tot} followed by addition of the translation matrix T as shown in eq. (A4). There are as many rows in A, B, and T as there are atoms in the chromophore, 30 in the case of tetracene.

$$A = \begin{pmatrix} x_{1A} & y_{1A} & z_{1A} \\ x_{2A} & y_{2A} & z_{2A} \\ \vdots & \vdots & \vdots \end{pmatrix} \qquad B = \begin{pmatrix} x_{1B} & y_{1B} & z_{1B} \\ x_{2B} & y_{2B} & z_{2B} \\ \vdots & \vdots & \vdots \end{pmatrix} \tag{A1}$$

$$R_{tot} = \begin{pmatrix} \cos R_y \cos R_z & -\cos R_x \sin R_z \sin R_y - \cos R_z \sin R_x & -\cos R_x \cos R_z \sin R_y + \sin R_x \sin R_z \\ \cos R_y \sin R_z & \cos R_x \cos R_z - \sin R_x \sin R_y \sin R_z & -\cos R_z \sin R_x - \cos R_x \sin R_y \sin R_z \\ \sin R_y & \cos R_y \sin R_x & \cos R_x \cos R_y \end{pmatrix} \tag{A2}$$

$$\mathrm{T} = \begin{pmatrix} T_x & T_y & T_z \\ T_x & T_y & T_z \\ \vdots & \vdots & \vdots \end{pmatrix} \tag{A3}$$

$$B = A \cdot R_{tot}^{T} + T \tag{A4}$$

3. Optimized Pair Structure Parameters for Tetracene

Table A2. Pair Structure Parameters for Tetracene Pairs 1-35 for (154, 130) Optimization and for 1A and 1B D_{2h} Symmetrized Crystal Pairs.[a]

Pair	T_z	T_y	T_x	R_z	R_y	R_x	ΔE_{DS}[b]	ΔE_{BB}[c]	k/k_0[d]	k/k_1
1	3.40	2.48	1.35	122.28	-0.46	-0.25	16	41	564	1.00
2	3.51	2.66	0.97	140.64	0.67	0.24	39	45	297	0.53
3	3.48	0.92	3.37	109.46	-0.50	0.53	29	27	256	0.45
4	3.47	1.43	5.91	27.08	-0.03	-0.12	119	26	90	0.16
5	3.40	3.36	3.17	0.00	0.00	0.00	7	16	61	0.11
6	3.64	2.54	2.45	-18.85	-1.17	7.44	5	24	60	0.11
7	3.86	1.68	4.84	-21.53	-1.08	18.60	38	17	50	0.09
8	4.15	0.00	0.67	90.00	0.00	30.25	0	9	40	0.07
9	2.74	4.02	0.00	90.00	158.80	0.00	0	8	35	0.06
10	4.52	1.45	0.00	0.00	0.00	51.30	32	23	33	0.06
11	3.73	3.18	0.86	45.88	1.73	7.79	27	19	29	0.05
12	3.45	3.17	0.59	0.00	0.00	0.00	28	19	27	0.05
13	4.21	2.14	0.51	-1.73	-0.26	31.98	31	20	25	0.04
14	3.49	1.86	3.10	-40.56	-0.25	-0.64	40	25	26	0.05
15	3.57	0.88	0.65	98.34	-0.30	-3.82	39	7	24	0.04
16	3.53	1.03	0.75	97.98	172.99	-2.04	36	6	23	0.04
17	3.51	3.14	0.00	0.00	0.00	180.00	46	29	22	0.04
18	2.28	6.51	0.00	90.00	-13.98	180.00	0	7	22	0.04
19	3.55	3.34	1.23	31.30	0.64	1.47	19	20	22	0.04
20	3.49	2.95	4.52	0.00	0.00	0.00	62	10	21	0.04
21	2.68	3.90	0.00	0.00	0.00	153.84	43	28	20	0.04
22	3.45	3.04	1.82	0.00	0.00	0.00	22	14	21	0.04
23	3.96	2.44	1.44	36.90	-0.22	22.08	53	13	19	0.03
24	3.27	2.49	2.60	145.16	166.98	162.35	53	13	19	0.03
25	3.97	0.00	3.13	90.00	0.00	21.80	0	5	17	0.03
26	3.44	2.12	6.98	0.00	0.00	0.00	85	9	16	0.03
27	3.52	1.42	0.91	106.46	-2.07	-3.13	50	9	17	0.03
28	3.42	2.30	1.14	117.76	154.77	166.85	51	9	15	0.03
29	3.50	-0.68	3.69	-22.30	0.29	-1.45	250	56	15	0.03
30	3.62	2.91	1.37	154.33	1.49	-5.43	19	8	14	0.03
31	3.50	2.17	1.34	134.00	0.08	178.36	62	42	15	0.03
32	3.34	3.50	5.82	180.00	0.00	0.00	29	6	14	0.03
33	3.76	1.32	0.50	109.44	-0.29	168.01	53	9	14	0.02
34	3.59	3.41	2.30	38.06	-7.45	14.67	14	11	13	0.02
35	0.00	5.03	0.00	180.00	180.00	90.00	0	5	12	0.02
Crystal[e]	4.66	1.01	0.32	2.72	0.45	51.37	63	6	1	0.00
1A[f]	3.41	0.74	0.00	0.00	0.00	0.00	766	6	0	0.00
1B[g]	3.47	0.66	3.63	21.74	0.22	1.11	253	57	15	0.03

[a] Translations in units of Å, rotations in units of degrees, and energies in units of meV. [b] Davydov splitting $\Delta E_{DS} = E(S^{**}) - E(S^{*})$. [c] Biexciton binding energy. [d] $k_0 = 1.2\times 10^8\ s^{-1}$. [e] Top pair from optimization with procedure III. [f] Top pair from optimization with procedure I, evaluated with procedure III. [g] Crystal herringbone pair structure with individual tetracenes adapted to D_{2h} symmetry.

Table A3. Pair Structure Parameters for Tetracene Pairs 1-20 for (154, 300) Optimizations.[a]

Pair	T_x	T_y	T_z	R_x	R_y	R_z	ΔE_{DS}[b]	ΔE_{BB}[c]	k/k_0[d]	k/k_1
1	3.41	2.46	1.37	121.34	-0.23	-0.13	19	37	350	1.00
2	3.49	0.82	3.31	109.63	-0.22	0.70	42	26	206	0.59
3	3.47	2.45	0.80	143.31	-0.28	-0.09	69	50	209	0.60
4	3.41	3.26	3.21	0.00	0.00	0.00	7	14	53	0.15
5	3.64	2.59	2.48	-19.71	-1.09	7.00	10	23	46	0.13
6	2.93	4.07	3.91	19.08	-3.56	-13.92	53	17	44	0.12
7	3.49	1.28	6.02	24.07	0.03	0.13	111	21	36	0.10
8	3.45	2.27	4.48	0.00	0.00	0.00	125	16	33	0.10
9	3.93	1.41	0.00	90.00	151.47	0.00	0	8	33	0.10
10	3.96	0.00	2.82	90.00	0.00	161.16	0	7	30	0.09
11	3.55	0.83	0.63	100.11	-0.15	-2.37	59	7	29	0.08
12	4.52	1.45	0.00	0.00	0.00	51.15	30	22	26	0.08
13	3.44	2.10	6.94	0.00	0.00	0.00	87	9	25	0.07
14	3.75	2.88	1.16	39.83	1.53	8.96	60	18	25	0.07
15	3.50	1.82	2.91	146.83	0.71	0.02	68	25	25	0.07
16	3.81	0.53	-0.17	81.58	0.80	13.04	38	7	24	0.07
17	3.46	3.08	0.63	0.00	0.00	0.00	11	17	21	0.06
18	3.46	2.87	1.82	180.00	180.00	180.00	46	14	21	0.06
19	3.51	1.38	0.90	109.22	-1.83	-1.30	75	10	20	0.06
20	2.48	4.01	0.41	1.71	-0.71	148.71	24	19	20	0.06

[a] Translations in units of Å, rotations in units of degrees, and energies in units of meV. [b] Davydov splitting $\Delta E_{DS} = E(S^{**}) - E(S^{*})$. [c] Biexciton binding energy. [d] $k_0 = 5.0\times 10^7\ s^{-1}$.

Table A4. Pair Structure Parameters for Tetracene Pairs 1-20 for (0, 130) Optimizations.[a]

Pair	T_x	T_y	T_z	R_x	R_y	R_z	ΔE_{DS}[b]	ΔE_{BB}[c]	k/k_0[d]	k/k_1
1	3.38	2.42	1.36	121.28	-0.11	-0.06	23	38	338	1.00
2	3.44	2.33	0.75	144.63	0.13	0.04	94	54	262	0.77
3	3.45	0.75	3.26	110.08	-0.03	0.79	54	27	254	0.75
4	3.38	3.17	3.23	0.00	0.00	0.00	15	13	64	0.19
5	3.17	3.42	4.12	14.37	-1.04	-9.74	84	19	60	0.18
6	3.40	2.23	4.49	180.00	180.00	180.00	130	18	57	0.17
7	3.59	2.62	2.49	-20.32	-1.03	6.53	19	23	49	0.14
8	3.50	0.83	0.63	101.09	-0.26	-1.73	71	8	43	0.13
9	3.41	2.03	6.90	0.00	0.00	0.00	91	10	39	0.12
10	3.89	1.32	0.00	90.00	152.52	0.00	0	9	39	0.11
11	3.46	1.76	2.83	148.73	0.65	-0.13	80	26	38	0.11
12	3.63	2.66	1.41	35.50	0.77	7.40	96	23	36	0.11
13	3.89	0.00	2.84	90.00	0.00	162.22	0	8	35	0.10
14	3.82	0.45	-0.05	81.99	0.35	14.76	38	7	31	0.09
15	3.47	1.34	0.87	110.53	-1.46	-1.01	89	11	30	0.09
16	3.42	2.72	1.84	0.00	0.00	0.00	63	15	30	0.09
17	3.49	2.05	2.45	160.25	0.09	177.90	74	23	28	0.08
18	4.48	1.44	0.00	0.00	0.00	51.01	35	23	27	0.08
19	3.42	2.99	0.69	0.00	0.00	0.00	1	14	23	0.07
20	3.45	1.02	6.20	18.95	0.06	180.39	94	15	23	0.07

[a] Translations in units of Å, rotations in units of degrees, and energies in units of meV. [b] Davydov splitting $\Delta E_{DS} = E(S^{**}) - E(S^{*})$. [c] Biexciton binding energy. [d] $k_0 = 1.8\times 10^{10}$ s^{-1}.

Table A5. Pair Structure Parameters for Tetracene Pairs 1-20 for (0, 300) Optimizations.[a]

Pair	T_x	T_y	T_z	R_x	R_y	R_z	ΔE_{DS}[b]	ΔE_{BB}[c]	k/k_0[d]	k/k_1
1	3.39	2.43	1.36	121.20	-0.12	-0.07	22	36	291	1.00
2	3.46	0.73	3.25	110.01	0.03	0.83	56	25	222	0.76
3	3.46	2.31	0.74	144.88	0.18	0.06	98	51	220	0.76
4	3.41	2.19	4.49	0.00	0.00	0.00	134	17	61	0.21
5	3.39	3.17	3.23	0.00	0.00	0.00	17	13	57	0.20
6	3.60	2.63	2.49	-20.59	-1.00	6.61	19	22	42	0.15
7	3.51	0.81	0.62	101.76	-0.19	-1.19	78	8	42	0.14
8	3.42	2.01	6.88	0.00	0.00	0.00	91	10	37	0.13
9	3.90	1.31	0.00	90.00	152.92	0.00	0	8	34	0.12
10	3.60	2.55	1.49	33.78	0.36	7.02	114	23	34	0.12
11	3.47	1.76	2.80	149.59	0.59	-0.05	86	25	34	0.12
12	3.54	2.77	1.50	32.21	0.30	182.89	101	24	33	0.11
13	2.87	3.88	0.00	270.00	17.37	0.00	0	7	31	0.11
14	3.49	1.32	0.84	111.63	-1.15	-0.78	99	11	29	0.10
15	3.85	0.41	-0.01	82.10	0.18	15.21	38	7	28	0.10
16	3.44	2.65	1.85	180.00	180.00	180.00	75	15	28	0.09
17	3.51	2.04	2.40	161.41	0.08	-2.36	82	21	26	0.09
18	4.50	1.45	0.00	0.00	0.00	51.11	33	22	24	0.08
19	3.43	3.00	0.68	0.00	0.00	0.00	0	14	21	0.07
20	3.46	1.08	6.16	20.08	0.06	180.35	98	15	21	0.07

[a] Translations in units of Å, rotations in units of degrees, and energies in units of meV. [b] Davydov splitting $\Delta E_{DS} = E(S^{**}) - E(S^{*})$. [c] Biexciton binding energy. [d] $k_0 = 2.4\times 10^9\ s^{-1}$.

Table A6. Pair Structure Parameters for Tetracene Pairs 1-20 for (308, 130) Optimizations.[a]

Pair	T_x	T_y	T_z	R_x	R_y	R_z	ΔE_{DS}[b]	ΔE_{BB}[c]	k/k_0[d]	k/k_1
1	3.50	0.86	3.56	28.11	0.20	0.81	263	76	801	1.00
2	3.46	2.53	1.34	123.09	-0.66	-0.36	13	39	487	0.61
3	3.49	-1.72	5.65	146.57	0.25	-0.83	139	32	369	0.46
4	3.58	2.89	-1.15	42.36	0.94	-0.37	9	38	221	0.28
5	3.56	3.56	0.17	71.61	0.10	0.93	14	24	162	0.20
6	3.54	2.17	0.57	132.78	0.13	-1.16	104	40	53	0.07
7	3.42	3.57	3.13	0.00	0.00	0.00	26	17	44	0.05
8	3.72	2.51	2.45	161.46	1.21	-8.26	3	22	41	0.05
9	3.52	1.30	2.41	136.86	-1.45	0.62	134	25	32	0.04
10	3.51	3.45	0.00	0.00	0.00	0.00	72	31	31	0.04
11	3.52	2.88	4.78	62.34	0.09	0.15	149	20	30	0.04
12	3.94	1.66	4.88	-22.12	-1.21	19.38	37	16	29	0.04
13	2.67	4.52	3.81	21.33	-6.12	161.53	37	16	29	0.04
14	4.59	1.48	0.00	0.00	0.00	51.75	31	21	25	0.03
15	4.46	1.97	0.20	-0.92	-0.14	41.26	48	23	23	0.03
16	4.23	0.00	-0.68	90.00	0.00	-31.12	0	8	22	0.03
17	3.53	1.61	1.13	34.03	-0.54	-0.08	279	49	21	0.03
18	3.56	0.79	1.89	145.32	-0.27	-0.35	260	40	21	0.03
19	3.51	1.19	0.24	56.89	-0.08	0.84	210	35	21	0.03
20	4.10	0.00	2.73	90.00	0.00	-22.60	0	7	19	0.02

[a] Translations in units of Å, rotations in units of degrees, and energies in units of meV. [b] Davydov splitting $\Delta E_{DS} = E(S^{**}) - E(S^{*})$. [c] Biexciton binding energy. [d] $k_0 = 4.1\times 10^4\ s^{-1}$.

Table A7. Pair Structure Parameters for Tetracene Pairs 1-20 for (308, 300) Optimizations.[a]

Pair	T_x	T_y	T_z	R_x	R_y	R_z	ΔE_{DS}[b]	ΔE_{BB}[c]	k/k_0[d]	k/k_1
1	3.45	2.48	1.37	121.78	-0.37	-0.21	17	37	363	1.00
2	3.56	2.66	0.97	140.91	0.68	0.24	42	42	186	0.51
3	3.53	0.88	3.35	109.19	-0.42	0.62	32	25	176	0.49
4	3.51	1.47	5.87	28.02	179.95	0.22	124	26	62	0.17
5	3.44	3.36	3.18	0.00	0.00	0.00	2	15	46	0.13
6	3.69	2.57	2.47	-19.43	-1.11	7.50	4	22	44	0.12
7	2.76	4.36	3.84	20.33	-5.29	-17.08	42	16	35	0.10
8	4.18	0.00	-0.65	90.00	0.00	-29.31	0	8	29	0.08
9	4.56	1.45	0.00	0.00	0.00	51.45	27	21	26	0.07
10	2.84	3.99	0.00	270.00	19.71	0.00	0	7	26	0.07
11	3.52	-0.83	3.58	-27.08	0.23	-0.97	260	71	25	0.07
12	3.51	3.17	0.53	0.00	0.00	0.00	24	20	22	0.06
13	4.26	2.14	0.49	-2.10	-0.32	32.45	27	20	20	0.06
14	3.60	0.84	0.63	98.83	-0.07	-3.25	45	6	20	0.05
15	3.55	3.16	0.00	0.00	0.00	0.00	38	28	19	0.05
16	3.43	2.10	2.95	135.71	-4.66	7.28	34	17	19	0.05
17	3.70	0.69	-0.41	81.59	1.48	7.91	41	6	19	0.05
18	3.53	2.67	4.49	0.00	0.00	0.00	86	11	18	0.05
19	4.22	2.25	0.00	0.00	0.00	28.75	36	26	17	0.05
20	3.57	3.32	1.26	36.18	0.77	-0.07	46	23	18	0.05

[a] Translations in units of Å, rotations in units of degrees, and energies in units of meV. [b] Davydov splitting $\Delta E_{DS} = E(S^{**}) - E(S^{*})$. [c] Biexciton binding energy. [d] $k_0 = 2.5\times 10^5\ s^{-1}$.

4. Optimized Tetracene Geometries for Energy Calculations

Table A8. *XYZ* Coordinates for Optimized S_0 State of Tetracene in Units of Ångstrøms.

30

C 1.227549 -1.397860 0.000005
C 2.434183 -0.720448 0.000011
C 3.687370 -1.400806 0.000079
C 4.857122 -0.711536 0.000074
C 4.857115 0.711508 -0.000025
C 3.687374 1.400804 -0.000072
C 2.434175 0.720446 -0.000044
C 1.227552 1.397870 -0.000053
C 0.000003 -0.720605 -0.000027
H 1.227922 -2.483802 0.000035
H 3.685623 -2.485842 0.000150
H 5.802330 -1.242279 0.000132
H 5.802312 1.242272 -0.000041
H 3.685638 2.485841 -0.000149
H 1.227929 2.483810 -0.000081
C 0.000002 0.720616 -0.000026
C -1.227548 1.397865 0.000006
C -2.434184 0.720453 0.000015
C -3.687379 1.400804 0.000083
C -4.857125 0.711524 0.000073
C -4.857116 -0.711521 -0.000025
C -3.687368 -1.400805 -0.000069
C -2.434174 -0.720441 -0.000042
C -1.227547 -1.397856 -0.000055
H -1.227921 -2.483797 -0.000078
H -3.685623 -2.485843 -0.000145
H -5.802312 -1.242288 -0.000045
H -5.802334 1.242267 0.000121
H -3.685645 2.485840 0.000154
H -1.227924 2.483807 0.000040

Table A9. *XYZ* Coordinates for Optimized S_1 State of Tetracene in Units of Ångstrøms.
30

C -0.000332 -0.000014 1.855990
C 1.384845 -0.000077 2.163026
C 1.858536 -0.000107 3.478832
C 3.219420 -0.000170 3.749028
C 4.136186 -0.000210 2.704385
C 3.691245 -0.000180 1.390158
C 2.324995 -0.000117 1.091658
C 1.840159 -0.000083 -0.241904
C -0.477012 0.000014 0.543624
H -0.713916 0.000013 2.674236
H 1.142956 -0.000078 4.294611
H 3.565960 -0.000193 4.775932
H 5.199412 -0.000257 2.914566
H 4.406971 -0.000209 0.574544
H 2.558493 -0.000104 -1.055974
C 0.477017 -0.000019 -0.543632
C 0.000333 0.000014 -1.855997
C -1.384845 0.000079 -2.163032
C -1.858543 0.000114 -3.478836
C -3.219428 0.000176 -3.749021
C -4.136190 0.000200 -2.704374
C -3.691243 0.000166 -1.390151
C -2.324991 0.000108 -1.091659
C -1.840155 0.000075 0.241902
H -2.558487 0.000100 1.055972
H -4.406960 0.000184 -0.574528
H -5.199418 0.000248 -2.914549
H -3.565973 0.000199 -4.775925
H -1.142967 0.000093 -4.294618
H 0.713915 -0.000010 -2.674246

Table A10. *XYZ* Coordinates for Optimized T_1 State of Tetracene in Units of Ångstrøms.

30

C	1.855901	0.003275	-0.000002
C	2.164918	-1.386599	-0.000003
C	3.478887	-1.857494	-0.000004
C	3.750835	-3.218758	0.000003
C	2.708055	-4.135461	0.000001
C	1.393366	-3.690402	0.000003
C	1.095731	-2.326442	-0.000002
C	-0.242400	-1.840656	-0.000002
C	0.545263	0.479265	-0.000000
H	2.674378	0.716577	-0.000002
H	4.294079	-1.141193	-0.000007
H	4.778136	-3.564120	0.000000
H	2.918280	-5.198685	0.000008
H	0.578018	-4.406452	0.000005
H	-1.055402	-2.560175	-0.000000
C	-0.545266	-0.479267	-0.000001
C	-1.855903	-0.003276	-0.000002
C	-2.164923	1.386597	-0.000003
C	-3.478890	1.857496	-0.000003
C	-3.750832	3.218761	0.000002
C	-2.708049	4.135463	0.000002
C	-1.393363	3.690400	0.000002
C	-1.095734	2.326438	-0.000000
C	0.242397	1.840653	0.000001
H	1.055397	2.560174	0.000004
H	-0.578010	4.406445	0.000004
H	-2.918271	5.198688	0.000004
H	-4.778133	3.564126	0.000000
H	-4.294085	1.141198	-0.000003
H	-2.674380	-0.716577	-0.000003

5. Symmetrized 1,3-Diphenylisobenzofuran Rotamer Geometries

Table A11. *XYZ* Coordinates for **7**(C_2) in Units of Ångstrøm.

35

O	0.0000000	-0.6883432	0.0000000
C	-3.7022031	-2.5379216	0.5387490
C	3.7022031	-2.5379216	-0.5387490
C	-4.8406069	-1.9068328	0.0953780
C	0.7100903	3.8076831	-0.0000001
C	-4.7672583	-0.6295796	-0.4042319
C	-0.7100903	3.8076831	0.0000001
C	4.7672583	-0.6295796	0.4042319
C	-2.4848470	-1.8865396	0.5039176
C	4.8406069	-1.9068328	-0.0953780
C	-1.4240502	2.6580631	0.0000002
C	2.4848470	-1.8865396	-0.5039176
C	1.4240502	2.6580631	-0.0000002
C	0.7188995	1.4214726	-0.0000001
C	-3.5518787	0.0253856	-0.4579342
C	-2.3927734	-0.5930411	0.0000004
C	3.5518787	0.0253856	0.4579342
C	-1.1155413	0.1026812	0.0000002
C	2.3927734	-0.5930411	-0.0000004
C	-0.7188995	1.4214726	0.0000001
C	1.1155413	0.1026812	-0.0000002
H	-3.7565185	-3.5463635	0.9279490
H	3.7565185	-3.5463635	-0.9279490
H	-5.7935982	-2.4199217	0.1331728
H	1.2264639	4.7591286	-0.0000002
H	-5.6579643	-0.1352807	-0.7706559
H	-1.2264639	4.7591286	0.0000002
H	5.6579643	-0.1352807	0.7706559
H	-1.5942178	-2.3790651	0.8674921
H	5.7935982	-2.4199217	-0.1331728
H	-2.5036057	2.6774204	0.0000004
H	1.5942178	-2.3790651	-0.8674921
H	2.5036057	2.6774204	-0.0000004
H	-3.4997328	1.0128702	-0.8924179
H	3.4997328	1.0128702	0.8924179

Table A12. *XYZ* Coordinates for **7**(C_{2v}) in Units of Ångstrøm.

35

O	0.0000000	-0.6883431	0.0000000
C	-3.6971879	-2.5379211	0.0000000
C	3.6971879	-2.5379211	0.0000000
C	-4.8395476	-1.9068321	0.0000000
C	0.7100611	3.8076829	0.0000000
C	-4.7707134	-0.6295791	0.0000000
C	-0.7100611	3.8076829	0.0000000
C	4.7707134	-0.6295791	0.0000000
C	-2.4801950	-1.8865391	0.0000000
C	4.8395476	-1.9068321	0.0000000
C	-1.4239920	2.6580629	0.0000000
C	2.4801950	-1.8865391	0.0000000
C	1.4239920	2.6580629	0.0000000
C	0.7188697	1.4214719	0.0000000
C	-3.5558678	0.0253849	0.0000000
C	-2.3926755	-0.5930411	0.0000000
C	3.5558678	0.0253849	0.0000000
C	-1.1154955	0.1026809	0.0000000
C	2.3926755	-0.5930411	0.0000000
C	-0.7188697	1.4214719	0.0000000
C	1.1154955	0.1026809	0.0000000
H	-3.7479867	-3.5463631	0.0000000
H	3.7479867	-3.5463631	0.0000000
H	-5.7921595	-2.4199211	0.0000000
H	1.2264130	4.7591279	0.0000000
H	-5.6646914	-0.1352801	0.0000000
H	-1.2264130	4.7591279	0.0000000
H	5.6646914	-0.1352801	0.0000000
H	-1.5863197	-2.3790651	0.0000000
H	5.7921595	-2.4199211	0.0000000
H	-2.5035030	2.6774199	0.0000000
H	1.5863197	-2.3790651	0.0000000
H	2.5035030	2.6774199	0.0000000
H	-3.5076467	1.0128699	0.0000000
H	3.5076467	1.0128699	0.0000000

Table A13. *XYZ* Coordinates for **7**(C_s) in Units of Ångstrøm.

35

O	0.0000000	-0.6883430	0.0000000
C	-3.7022030	-2.5379210	0.5387490
C	3.7022030	-2.5379210	0.5387490
C	-4.8406060	-1.9068320	0.0953770
C	0.7100900	3.8076830	0.0000000
C	-4.7672580	-0.6295790	-0.4042310
C	-0.7100900	3.8076830	0.0000000
C	4.7672580	-0.6295790	-0.4042310
C	-2.4848460	-1.8865390	0.5039170
C	4.8406060	-1.9068320	0.0953770
C	-1.4240500	2.6580630	0.0000000
C	2.4848460	-1.8865390	0.5039170
C	1.4240500	2.6580630	0.0000000
C	0.7188990	1.4214720	0.0000000
C	-3.5518780	0.0253850	-0.4579340
C	-2.3927730	-0.5930410	0.0000000
C	3.5518780	0.0253850	-0.4579340
C	-1.1155410	0.1026810	0.0000000
C	2.3927730	-0.5930410	0.0000000
C	-0.7188990	1.4214720	0.0000000
C	1.1155410	0.1026810	0.0000000
H	-3.7565180	-3.5463630	0.9279490
H	3.7565180	-3.5463630	0.9279490
H	-5.7935980	-2.4199210	0.1331720
H	1.2264630	4.7591280	0.0000000
H	-5.6579640	-0.1352800	-0.7706550
H	-1.2264630	4.7591280	0.0000000
H	5.6579640	-0.1352800	-0.7706550
H	-1.5942170	-2.3790650	0.8674920
H	5.7935980	-2.4199210	0.1331720
H	-2.5036050	2.6774200	0.0000000
H	1.5942170	-2.3790650	0.8674920
H	2.5036050	2.6774200	0.0000000
H	-3.4997320	1.0128700	-0.8924170
H	3.4997320	1.0128700	-0.8924170

Table A14. *XYZ* Coordinates for **7**(C_1) in Units of Ångstrøm.

35

O	0.0000000	-0.6883400	0.0000000
C	-3.7450000	-2.4501400	0.4546400
C	3.6971900	-2.5379200	0.0000000
C	-4.8388100	-1.9081900	-0.0070400
C	0.7100600	3.8076800	0.0000000
C	-4.7219400	-0.7191100	-0.4637000
C	-0.7100600	3.8076800	0.0000000
C	4.7707100	-0.6295800	0.0000000
C	-2.5284600	-1.7979400	0.4589000
C	4.8395500	-1.9068300	0.0000000
C	-1.4239900	2.6580600	0.0000000
C	2.4801900	-1.8865400	0.0000000
C	1.4239900	2.6580600	0.0000000
C	0.7188700	1.4214700	0.0000000
C	-3.5073600	-0.0636600	-0.4611900
C	-2.3926800	-0.5930400	0.0000000
C	3.5558700	0.0253800	0.0000000
C	-1.1155000	0.1026800	0.0000000
C	2.3926800	-0.5930400	0.0000000
C	-0.7188700	1.4214700	0.0000000
C	1.1155000	0.1026800	0.0000000
H	-3.8338000	-3.3888300	0.8159000
H	3.7479900	-3.5463600	0.0000000
H	-5.7911900	-2.4216900	-0.0091800
H	1.2264100	4.7591300	0.0000000
H	-5.5779100	-0.2946000	-0.8251500
H	-1.2264100	4.7591300	0.0000000
H	5.6646900	-0.1352800	0.0000000
H	-1.6725300	-2.2208100	0.8196700
H	5.7921600	-2.4199200	0.0000000
H	-2.5035000	2.6774200	0.0000000
H	1.5863200	-2.3790700	0.0000000
H	2.5035000	2.6774200	0.0000000
H	-3.4219000	0.8554600	-0.8152500
H	3.5076500	1.0128700	0.0000000

6. Top 67 Pair Structures for 4 Rotamers of 1,3-Diphenylisobenzofuran

Table A15. Pair Structure Parameters for **7**(C_2) Pairs 1-34.[a]

Pair	T_z	T_Y	T_x	R_z	R_y	R_x	ΔE_{DS}[b]	ΔE_{BB}[c]	k/k_0[d]
1	3.49	1.45	2.11	68.08	179.60	0.58	51.3	34.7	4306
2	4.00	-0.39	-2.00	248.95	193.73	160.11	42.5	37.6	2944
3	3.93	1.77	-1.89	107.84	174.72	172.76	27.4	24.6	2261
4	4.28	-1.27	-1.42	81.89	165.69	13.89	25.4	30.1	896
5	4.00	1.65	-2.57	127.80	-4.37	188.90	51.4	26.8	892
6	3.98	-0.09	-2.25	79.24	168.15	17.30	4.3	29.0	806
7	3.40	-2.59	4.71	63.41	202.54	0.07	5.4	23.6	717
8	3.80	5.27	0.17	96.43	9.33	197.91	9.3	20.8	546
9	3.55	-2.17	4.46	101.22	199.87	14.64	3.4	20.3	536
10	3.94	3.51	2.33	-2.45	193.37	176.54	143.9	23.9	504
11	3.72	5.46	0.29	102.04	10.42	201.27	27.4	22.6	499
12	3.03	-0.23	-5.84	101.40	-22.06	174.04	18.7	22.3	494
13	3.70	1.35	2.50	50.42	178.00	4.24	90.7	27.2	441
14	3.27	4.94	1.52	78.06	169.03	2.29	60.0	16.0	418
15	3.08	5.82	0.13	88.62	168.62	-2.85	34.5	13.5	354
16	3.40	1.43	-4.86	89.72	-0.80	179.33	125.5	20.2	338
17	3.09	5.79	0.32	263.76	191.48	187.52	32.8	12.9	336
18	3.11	-2.75	3.35	121.96	192.22	201.84	54.1	6.3	316
19	3.39	4.64	-1.98	128.21	-5.17	186.26	3.4	12.0	304
20	3.60	3.22	0.21	95.68	171.33	176.50	22.2	14.4	259
21	3.71	2.98	-0.61	117.31	176.13	10.27	129.0	12.6	250
22	3.92	0.15	-4.49	108.85	-0.07	187.25	55.7	11.5	238
23	3.95	-0.05	3.76	43.51	186.18	7.09	2.2	12.2	239
24	4.21	0.33	-3.92	131.36	1.67	191.97	22.0	9.6	226
25	2.91	3.26	-3.60	146.67	338.63	181.52	0.7	9.8	204
26	4.43	-0.40	-3.57	141.15	192.58	166.69	3.6	9.6	201
27	3.74	1.98	-1.33	103.40	170.46	13.60	29.3	10.0	187
28	3.10	2.53	-3.56	12.82	191.75	193.27	152.4	16.9	182
29	2.96	1.76	-3.65	168.68	165.20	-13.35	134.9	7.8	174
30	4.18	-0.05	4.28	19.72	11.87	192.64	18.9	6.9	168
31	4.31	-0.06	4.23	20.86	15.07	196.68	14.6	5.8	163
32	4.30	-0.06	4.24	20.76	14.65	196.14	15.2	5.9	163
33	3.78	0.06	2.78	269.66	180.29	174.91	4.3	12.6	138
34	4.41	-2.42	-2.24	261.87	195.38	167.53	69.6	10.8	133

[a] Translations in units of Ångstrøm, rotations in units of degree, and energies in units of meV. [b] Davydov splitting $\Delta E_{DS} = E(S^{**}) - E(S^{*})$. [c] Biexciton binding energy. [d] $k_0 = 1.05\times 10^8\ s^{-1}$.

Table A16. Pair Structure Parameters for **7**(C_2) Pairs 35-67.[a]

Pair	T_Z	T_y	T_x	R_z	R_y	R_x	ΔE_{DS}[b]	ΔE_{BB}[c]	k/k_0[d]
35	3.95	-0.98	-2.60	126.74	179.26	172.16	143.7	16.8	132
36	2.95	2.05	-4.56	2.22	14.85	167.49	55.0	9.8	126
37	2.56	-3.66	2.48	108.36	21.51	164.67	6.0	8.4	125
38	3.74	-0.16	2.67	125.01	-0.93	-0.42	118.8	8.3	121
39	3.34	-0.41	-4.62	1.99	8.64	158.98	52.8	8.7	114
40	2.69	-3.49	2.63	110.91	199.42	198.29	8.3	7.2	113
41	4.34	0.86	3.42	-6.25	194.89	166.03	73.9	7.8	110
42	3.60	1.79	2.27	276.56	187.26	179.25	74.3	10.0	109
43	4.06	2.47	0.96	284.59	181.04	167.16	108.5	13.1	104
44	3.97	2.51	1.02	103.85	358.96	-11.17	109.2	13.1	103
45	3.33	-2.36	3.75	167.99	176.37	23.25	90.8	3.9	101
46	3.16	4.72	-2.79	16.97	192.14	182.81	172.9	8.8	97
47	4.24	-0.54	4.23	141.59	5.92	335.42	51.4	7.1	96
48	3.60	5.26	0.55	30.96	188.18	180.40	153.9	11.1	95
49	3.72	-0.79	3.03	58.57	193.24	2.00	53.5	9.1	94
50	4.38	-0.76	-2.08	87.43	-16.82	-17.58	61.8	18.2	92
51	3.61	5.26	0.56	25.20	190.05	180.89	161.2	10.0	93
52	3.26	3.88	-3.88	36.32	185.06	182.56	146.0	11.7	93
53	3.49	3.03	-0.96	64.96	179.99	181.83	229.5	20.0	91
54	4.08	-0.64	-1.68	72.83	-3.20	188.71	82.3	6.4	84
55	4.00	-0.75	-1.98	68.19	178.19	170.26	97.4	4.3	82
56	3.85	0.93	2.57	263.45	180.84	173.98	24.5	4.9	76
57	3.64	2.22	-4.16	150.87	-7.58	189.38	17.5	4.2	76
58	3.46	-0.32	-3.91	201.90	177.26	164.61	103.1	4.5	75
59	4.51	1.01	1.84	84.91	2.71	343.28	11.5	4.5	72
60	4.23	-2.07	-3.70	192.41	174.20	155.49	98.5	7.2	71
61	4.20	2.35	1.34	274.50	191.66	169.21	34.8	3.1	70
62	4.14	2.43	1.18	274.72	189.80	169.08	38.8	3.3	69
63	4.29	6.14	3.04	52.02	199.77	151.00	12.2	4.7	63
64	3.73	-0.67	1.95	108.60	183.77	201.42	98.5	8.7	60
65	3.10	7.34	-2.33	1.89	6.57	176.58	84.2	3.9	59
66	4.58	-0.84	1.17	120.84	-14.53	-6.31	97.6	9.9	58
67	3.50	2.98	1.48	251.52	188.47	184.04	14.1	4.7	57

[a] Translations in units of Ångstrøm, rotations in units of degree, and energies in units of meV. [b] Davydov splitting $\Delta E_{DS} = E(S^{**}) - E(S^{*})$. [c] Biexciton binding energy. [d] $k_0 = 1.05\times 10^8\ s^{-1}$.

Table A17. Pair Structure Parameters for **7**(C_{2v}) Pairs 1-34.[a]

Pair	T_z	T_y	T_x	R_z	R_y	R_x	ΔE_{DS}[b]	ΔE_{BB}[c]	k/k_0[d]
1	3.46	1.28	2.00	64.92	-0.17	-0.26	78.7	75.3	16422
2	3.49	1.19	2.56	48.77	-0.42	-0.93	69.3	54.4	2273
3	3.50	-1.10	1.48	104.39	-0.69	180.89	8.2	34.4	1927
4	3.48	1.35	0.94	82.36	0.09	180.44	16.1	27.8	1625
5	3.46	3.33	2.78	-2.83	-0.33	180.15	147.6	42.7	1539
6	3.38	5.42	0.20	86.56	-0.20	-2.13	35.3	28.0	1469
7	3.36	-0.28	4.12	40.40	-2.50	0.71	10.8	25.0	1419
8	3.44	1.10	4.81	86.41	-1.38	-0.02	96.2	28.3	988
9	3.43	-2.05	0.71	90.83	1.08	180.13	67.1	28.3	772
10	3.45	2.79	0.06	93.81	-0.56	179.63	34.3	23.1	714
11	3.33	4.65	1.88	74.78	-2.40	178.71	34.7	19.9	598
12	3.48	1.35	2.63	123.30	-0.19	0.25	208.2	30.2	494
13	3.47	1.25	3.75	0.00	0.00	180.00	79.8	9.2	461
14	3.38	4.17	2.40	41.27	-1.31	-0.80	20.5	11.8	398
15	3.41	4.30	2.17	50.44	359.31	-0.68	5.4	9.7	380
16	3.44	2.67	3.09	4.88	-0.50	180.10	109.4	19.9	377
17	3.49	-1.17	2.84	54.45	0.39	-0.47	176.8	28.1	332
18	3.44	3.04	1.69	32.35	-0.24	180.14	172.1	19.9	252
19	3.48	-1.66	4.00	158.61	-0.63	-0.64	12.4	10.6	243
20	3.49	2.62	0.89	107.35	0.11	-0.19	181.4	23.7	238
21	3.48	0.11	2.80	152.45	0.09	-0.33	157.8	24.3	236
22	3.47	-1.44	4.08	0.00	0.00	180.00	65.4	6.3	212
23	3.49	1.28	3.02	37.09	0.40	179.96	77.5	13.6	212
24	3.48	-1.51	4.06	137.76	-0.60	181.55	7.8	3.6	201
25	3.46	-0.28	2.88	168.99	0.01	179.93	153.5	22.4	198
26	3.43	1.50	3.43	29.34	-0.53	-0.09	18.1	10.6	193
27	3.63	2.48	2.07	106.00	167.76	-2.43	108.0	14.6	132
28	3.50	-0.59	3.36	154.93	-1.12	185.05	100.1	9.2	117
29	3.51	1.48	2.13	273.30	3.10	175.34	76.1	6.8	113
30	3.48	-2.59	3.34	124.49	0.49	179.40	24.2	6.2	113
31	3.86	3.11	1.30	87.66	158.33	-0.94	11.4	6.5	111
32	3.23	4.63	2.73	-18.19	-9.59	177.66	193.2	9.7	107
33	3.46	-1.54	3.03	85.96	0.52	178.87	114.0	11.9	106
34	4.46	1.82	1.22	97.57	180.20	17.96	56.9	7.4	102

[a] Translations in units of Ångstrøm, rotations in units of degree, and energies in units of meV. [b] Davydov splitting $\Delta E_{DS} = E(S^{**}) - E(S^{*})$. [c] Biexciton binding energy. [d] $k_0 = 1.05\times 10^8\ s^{-1}$.

Table A18. Pair Structure Parameters for **7**(C_{2v}) Pairs 35-67.[a]

Pair	T_z	T_y	T_x	R_z	R_y	R_x	ΔE_{DS}[b]	ΔE_{BB}[c]	k/k_0[d]
35	4.30	2.63	1.29	98.46	165.87	12.20	42.6	4.4	101
36	3.08	7.25	2.67	173.24	8.19	3.28	88.6	5.6	95
37	3.44	7.25	2.01	0.00	0.00	180.00	89.8	5.2	94
38	3.60	7.27	1.68	3.10	4.21	181.52	89.5	5.3	94
39	3.90	0.46	2.63	77.13	180.30	6.51	16.2	5.1	88
40	4.58	6.87	2.85	144.65	-0.32	-17.44	86.9	5.9	66
41	3.54	-2.95	2.05	153.30	-0.88	181.79	173.1	9.4	62
42	2.63	3.99	5.58	85.81	-10.77	8.91	157.4	7.3	60
43	3.36	8.37	-0.75	180.06	180.01	0.05	76.1	4.0	60
44	4.23	1.52	4.21	136.45	176.24	11.84	52.7	6.2	59
45	3.77	5.91	3.63	99.69	1.16	-6.03	131.9	6.9	56
46	4.61	-2.34	0.10	61.60	-19.25	-14.82	151.6	7.0	50
47	3.98	-2.62	0.61	77.21	-8.75	-6.88	124.3	5.7	48
48	3.21	6.53	3.61	0.00	0.00	180.00	66.0	1.8	35
49	2.85	7.02	2.34	152.90	-0.20	8.97	102.6	9.2	32
50	4.27	6.21	3.09	56.37	13.24	189.08	26.0	3.4	32
51	4.29	-2.50	0.80	134.09	168.22	169.22	174.8	5.3	32
52	3.49	0.48	4.46	149.54	0.10	-0.67	0.4	4.2	31
53	2.58	7.11	2.41	98.83	158.78	0.55	82.1	4.6	28
54	3.84	-3.74	1.19	121.40	174.62	174.50	85.8	6.3	27
55	3.99	3.55	4.27	46.86	172.74	15.27	54.1	3.7	25
56	3.47	0.73	3.68	123.49	-0.43	183.17	97.8	2.8	24
57	3.61	3.97	0.54	38.31	-4.45	184.90	193.5	8.8	20
58	3.27	3.04	2.80	144.74	2.99	191.60	226.8	7.4	16
59	3.90	-3.65	1.49	163.01	-5.83	186.27	197.2	6.5	12
60	3.48	-1.26	2.72	40.94	0.02	179.85	218.9	5.5	9
61	4.24	1.75	3.61	54.04	179.84	11.97	20.6	1.6	7
62	3.54	-3.64	2.58	43.28	-1.16	-0.78	225.7	8.6	4
63	3.15	4.89	1.88	59.03	151.61	166.60	18.8	1.0	4
64	3.50	3.44	0.54	0.00	0.00	180.00	296.0	1.9	2
65	4.92	-1.16	0.93	156.54	22.18	202.06	253.2	2.7	1
66	4.67	-0.16	0.41	152.39	17.10	197.31	288.8	9.8	7
67	3.50	-0.39	0.83	16.63	-0.69	177.48	473.3	9.2	1

[a] Translations in units of Ångstrøm, rotations in units of degree, and energies in units of meV. [b] Davydov splitting $\Delta E_{DS} = E(S^{**}) - E(S^{*})$. [c] Biexciton binding energy. [d] $k_0 = 1.05 \times 10^8$ s^{-1}.

Table A19. Pair Structure Parameters for **7**(C_s) Pairs 1-34.[a]

Pair	T_Z	T_Y	T_X	R_Z	R_Y	R_X	ΔE_{DS}[b]	ΔE_{BB}[c]	k/k_0[d]
1	-3.46	1.30	1.93	66.79	180.40	-0.61	70.5	45.9	5998
2	3.53	1.55	1.73	242.59	183.68	179.27	93.6	46.2	3473
3	4.00	-0.39	1.98	290.89	193.66	19.73	44.8	36.8	3126
4	4.02	1.71	1.82	71.41	177.99	9.33	32.2	22.3	1805
5	3.97	-0.11	2.31	279.25	191.79	16.73	15.3	29.5	901
6	3.60	1.45	-2.58	-50.37	3.23	-2.59	63.4	33.2	808
7	-3.38	-2.61	4.69	63.24	157.38	0.08	4.4	23.2	766
8	3.20	5.46	1.03	247.35	190.03	199.86	14.3	23.2	724
9	4.00	1.66	2.58	52.28	175.63	8.89	54.2	25.6	691
10	-3.63	1.31	-2.50	129.39	1.53	176.77	80.7	29.8	614
11	3.44	3.79	2.73	0.00	0.00	180.00	141.5	25.3	580
12	3.22	4.75	1.91	73.79	169.29	202.84	0.2	19.6	542
13	3.06	0.08	5.62	261.46	198.25	186.61	4.8	20.8	533
14	3.60	1.96	1.44	79.09	-4.39	191.52	19.2	11.3	523
15	3.80	5.28	0.15	96.15	9.29	197.67	13.0	20.3	514
16	-3.58	-2.06	4.39	287.04	18.88	163.29	0.2	19.6	513
17	3.53	2.24	1.79	69.62	-3.07	188.99	48.6	11.5	493
18	3.11	3.80	3.04	1.64	166.47	182.99	145.8	23.5	490
19	-3.75	5.35	-0.19	76.47	-10.48	20.36	30.0	22.6	470
20	-3.76	5.33	-0.18	257.01	190.30	199.99	25.9	22.4	469
21	3.71	5.49	-0.28	77.65	190.42	21.51	27.4	22.4	459
22	3.73	5.44	0.27	100.71	370.09	200.66	17.0	22.0	451
23	3.07	5.84	-0.15	91.43	168.66	184.34	39.1	14.7	440
24	3.11	5.78	0.29	266.35	190.91	187.92	43.0	14.8	433
25	-4.17	0.62	4.43	258.10	-0.01	168.81	62.5	16.0	419
26	3.27	4.95	1.53	256.32	191.05	177.42	57.1	15.4	416
27	3.21	3.13	3.20	223.95	190.67	180.21	19.2	15.9	414
28	-3.27	-1.26	1.69	98.35	169.38	1.06	26.0	13.7	370
29	-4.16	-0.24	5.09	268.48	3.31	168.72	35.5	13.5	362
30	-3.46	0.98	-0.07	87.96	174.54	11.11	8.3	17.8	353
31	-4.11	-0.83	5.04	84.18	171.57	-10.83	33.4	12.7	349
32	3.41	1.43	4.86	90.20	179.20	-0.63	124.8	19.6	316
33	-2.93	-2.03	0.90	278.11	199.53	11.77	17.3	16.6	315
34	2.90	0.47	5.38	291.12	15.54	166.12	23.9	16.1	307

[a] Translations in units of Ångstrøm, rotations in units of degree, and energies in units of meV. [b] Davydov splitting $\Delta E_{DS} = E(S^{**}) - E(S^{*})$. [c] Biexciton binding energy. [d] $k_0 = 1.05\times 10^8$ s^{-1}.

Table A20. Pair Structure Parameters for **7**(C_s) Pairs 35-67.[a]

Pair	T_z	T_y	T_x	R_z	R_y	R_x	ΔE_{DS}[b]	ΔE_{BB}[c]	k/k_0[d]
35	-3.30	-1.15	0.73	275.61	188.26	9.10	8.2	19.1	285
36	-3.12	-2.72	3.45	124.23	-12.07	202.59	49.8	6.4	284
37	3.56	1.49	1.55	98.12	-0.33	193.66	128.8	24.5	273
38	-3.04	-1.50	0.07	89.41	167.50	10.08	6.7	14.3	271
39	3.36	4.65	1.86	57.63	173.78	4.43	12.3	10.8	267
40	3.47	1.22	2.88	114.16	174.33	-2.63	144.2	17.0	259
41	3.92	-0.07	2.71	86.54	172.27	5.95	32.6	11.2	260
42	-3.94	-0.07	3.74	223.22	6.24	172.99	0.7	11.5	240
43	3.50	1.96	2.33	111.63	178.16	0.44	207.6	27.5	231
44	-3.59	3.09	0.06	97.40	187.06	182.56	30.0	11.6	230
45	3.93	0.11	4.48	70.51	180.01	7.40	51.2	11.1	225
46	4.21	0.34	3.95	49.03	181.57	11.91	19.9	9.9	225
47	3.51	2.90	0.03	94.88	175.27	184.43	19.4	16.4	225
48	2.89	3.29	3.63	33.59	158.18	1.40	4.6	10.1	200
49	3.60	3.16	1.00	56.90	173.88	170.84	133.9	10.8	197
50	-4.15	-0.10	4.26	22.52	168.35	192.30	18.0	8.4	197
51	4.45	-0.43	3.57	38.74	193.12	13.42	0.7	9.8	198
52	4.61	1.61	3.56	0.51	15.34	187.17	62.2	7.4	195
53	3.57	3.04	0.44	79.52	-3.23	186.61	58.4	11.4	189
54	2.95	1.76	3.22	17.98	163.39	193.11	168.9	12.6	185
55	3.30	3.24	1.70	60.86	-8.24	9.63	28.3	13.8	184
56	-3.22	-2.63	0.31	80.82	163.21	182.02	74.1	14.4	184
57	2.95	1.77	3.66	11.47	165.00	193.41	135.4	7.9	180
58	4.23	-0.22	2.32	98.76	174.64	162.08	17.0	10.4	173
59	-3.93	1.58	1.25	76.81	181.24	180.50	57.1	7.2	171
60	3.87	-1.26	4.51	219.23	186.83	171.71	47.6	12.4	169
61	3.86	-1.08	1.16	98.56	182.06	201.14	45.2	8.7	162
62	3.11	2.52	3.55	167.54	11.46	13.12	154.5	16.0	162
63	-3.67	-0.29	2.61	267.64	3.17	176.29	4.9	10.6	158
64	3.86	-0.90	1.18	98.04	181.66	195.69	39.8	9.5	157
65	3.76	2.61	1.11	90.81	4.34	198.15	77.5	7.1	156
66	3.98	1.84	4.02	0.00	0.00	180.00	70.6	5.9	155
67	-2.53	-2.76	0.22	83.85	336.55	186.79	67.4	9.4	154

[a] Translations in units of Ångstrøm, rotations in units of degree, and energies in units of meV. [b] Davydov splitting $\Delta E_{DS} = E(S^{**}) - E(S^{*})$. [c] Biexciton binding energy. [d] $k_0 = 1.05\times 10^8$ s^{-1}.

Table A21. Pair Structure Parameters for **7**(C_1) Pairs 1-34.[a]

Pair	T_z	T_y	T_x	R_z	R_y	R_x	ΔE_{DS}[b]	ΔE_{BB}[c]	k/k_0[d]
1	-3.44	1.27	1.98	64.80	180.20	-0.31	76.1	83.0	22252
2	3.45	1.25	2.00	63.74	179.86	0.22	83.0	81.6	20037
3	3.44	1.28	2.04	64.45	-0.08	-0.10	87.1	75.6	16130
4	-3.45	1.28	-2.02	115.52	0.09	179.85	99.5	72.4	13025
5	3.67	1.65	-2.05	109.51	178.55	176.21	49.3	49.4	9267
6	3.94	1.85	-2.01	106.24	-1.80	188.05	42.0	33.1	4286
7	-3.47	1.20	2.55	49.08	180.48	-1.04	69.5	60.7	3148
8	3.47	1.16	2.53	48.00	179.58	0.94	78.3	60.4	2824
9	3.48	-1.10	1.44	102.58	-0.88	181.10	10.9	42.5	2724
10	-3.48	-1.11	1.45	102.66	0.90	178.87	11.7	43.5	2506
11	-3.51	1.20	-2.47	130.70	0.78	178.31	93.1	55.5	2284
12	3.68	1.36	-2.46	130.21	177.46	175.70	85.1	53.1	2196
13	-3.50	1.33	-2.60	-51.65	-0.44	1.57	57.1	51.2	2049
14	-3.39	0.00	5.40	86.64	182.09	-0.30	33.5	31.1	1891
15	3.35	-0.30	4.11	40.27	177.67	-0.62	9.8	28.4	1855
16	-3.45	1.37	0.79	80.62	-0.32	179.51	0.5	32.5	1852
17	3.37	5.42	0.20	86.65	179.82	2.17	34.7	30.7	1818
18	3.36	5.43	-0.18	92.91	179.81	177.60	46.5	31.4	1801
19	3.78	-0.39	-2.11	60.73	168.29	19.85	8.0	26.6	1778
20	-3.52	2.82	2.81	40.83	177.39	-1.19	13.2	26.6	1673
21	3.45	3.43	2.68	1.49	180.17	180.07	161.0	47.5	1658
22	-3.35	5.44	-0.29	98.55	180.99	182.25	33.1	29.1	1496
23	-3.58	1.30	1.18	77.39	174.72	180.94	27.8	24.1	1433
24	3.94	1.66	-2.60	127.14	-4.13	188.29	62.1	34.7	1434
25	-3.42	1.08	4.83	86.39	181.58	0.02	94.0	32.7	1334
26	3.43	1.08	4.83	86.30	178.42	-0.01	93.5	31.9	1265
27	3.38	3.88	-2.58	170.99	179.02	-0.61	128.1	33.8	1291
28	3.53	3.73	2.63	2.05	2.47	181.11	131.0	33.2	1291
29	3.53	3.66	2.74	-0.77	2.29	181.17	131.1	33.1	1287
30	-3.43	1.08	4.86	86.58	1.81	0.01	99.4	31.3	1174
31	-3.41	-2.00	0.75	89.97	-1.12	179.96	55.8	34.7	1066
32	3.47	-0.66	2.12	92.21	-0.48	179.48	36.0	27.8	982
33	3.43	-0.59	3.84	215.46	181.37	179.53	21.2	23.6	968
34	3.88	-0.47	1.69	96.50	166.68	2.33	14.5	22.7	903

[a] Translations in units of Ångstrøm, rotations in units of degree, and energies in units of meV. [b] Davydov splitting $\Delta E_{DS} = E(S^{**}) - E(S^{*})$. [c] Biexciton binding energy. [d] $k_0 = 1.05\times 10^8$ s^{-1}.

Table A22. Pair Structure Parameters for **7**(C_1) Pai rs 35-67.[a]

Pair	T_z	T_y	T_x	R_z	R_y	R_x	ΔE_{DS}[b]	ΔE_{BB}[c]	k/k_0[d]
35	-3.69	-0.32	3.96	220.32	180.31	184.24	6.8	19.7	832
36	-3.38	1.66	1.79	55.79	3.27	180.45	100.2	25.6	832
37	-3.50	-0.60	-2.14	57.52	1.18	177.52	96.0	24.2	826
38	-3.31	4.66	1.84	75.89	182.40	178.82	27.8	21.9	795
39	-4.00	3.42	-2.33	2.47	194.96	184.77	103.5	27.7	823
40	3.31	4.66	-1.87	105.03	177.57	-1.26	34.8	21.7	787
41	-4.00	-0.84	1.54	109.23	190.55	190.80	19.2	20.0	778
42	3.53	1.76	1.39	76.82	177.01	177.22	28.3	17.6	767
43	3.31	4.64	1.91	73.95	177.53	181.37	24.1	21.6	758
44	-3.53	4.75	-1.18	95.80	181.58	184.60	74.7	23.9	753
45	-3.32	4.64	-1.89	105.80	182.43	1.28	34.3	21.9	722
46	3.88	-0.36	-1.35	264.65	187.29	5.38	17.0	22.2	712
47	-3.56	-1.23	-1.05	79.10	-0.85	-6.12	5.4	20.9	646
48	-3.68	-2.07	-4.89	109.03	159.68	184.49	9.0	20.8	647
49	3.44	2.82	-0.07	86.23	179.64	-0.16	22.1	24.7	641
50	3.36	4.11	-2.47	143.23	178.90	178.81	22.1	15.6	637
51	3.27	4.92	1.52	257.98	190.88	177.41	43.1	18.7	625
52	-3.53	-2.50	-4.69	112.75	337.52	176.73	2.7	21.7	621
53	3.58	1.90	-1.51	108.26	182.68	2.24	44.0	12.3	616
54	3.53	-0.67	2.31	106.29	178.18	-3.05	42.4	11.6	610
55	-3.27	4.92	-1.51	102.17	10.86	177.34	50.7	18.7	587
56	-3.53	4.65	-1.23	98.43	6.31	173.07	43.5	17.9	581
57	-4.03	0.88	-4.38	99.74	3.59	171.11	47.8	18.2	578
58	3.45	1.20	-4.78	92.83	-1.29	180.29	85.6	21.4	586
59	-3.98	-0.19	-3.75	138.15	171.41	187.35	12.4	18.9	566
60	-3.53	-0.44	2.69	85.49	177.12	-1.76	20.9	23.8	552
61	-3.44	2.80	0.05	95.72	180.49	179.95	47.1	20.6	549
62	-3.27	5.52	0.96	66.46	8.88	173.20	32.1	15.3	545
63	-3.36	4.11	-2.46	142.70	181.18	181.14	24.0	15.0	547
64	3.27	5.52	-0.92	293.43	188.91	173.56	22.5	14.9	534
65	3.37	0.59	2.94	104.91	177.59	-2.20	94.4	20.3	551
66	-3.47	-1.32	4.54	45.08	179.37	-1.14	10.5	12.4	532
67	-3.46	-1.07	4.63	229.92	0.29	179.17	3.1	11.4	527

[a] Translations in units of Ångstrøm, rotations in units of degree, and energies in units of meV. [b] Davydov splitting $\Delta E_{DS} = E(S^{**}) - E(S^{*})$. [c] Biexciton binding energy. [d] $k_0 = 1.05\times 10^8\ s^{-1}$.

7. Optimized 1,3-Diphenylisobenzofuran Geometries for Energy Calculations

Table A23. *XYZ* Coordinates for Optimized S_0 State of **7** in Units of Ångstrøm.

35

O	0.0297399	0.0100260	-0.0302392
C	-0.3181500	-4.1172971	-0.4161545
C	3.8798596	2.4230274	0.0355755
C	0.7299928	-4.9369186	-0.0197967
C	3.6485269	0.0053403	-0.0246503
C	4.4380495	1.1147193	-0.0093507
C	-0.1745180	-2.7419799	-0.4109166
C	1.9236312	-4.3620133	0.3933202
C	2.5329507	2.6217906	0.0250725
C	2.0721871	-2.9863464	0.4075434
C	1.6762903	1.4932971	-0.0203652
C	1.1705131	-0.7118144	-0.0029452
C	2.2403393	0.1685874	-0.0048747
C	1.0280344	-2.1503645	-0.0037252
C	0.3004609	1.3322136	-0.0450977
C	-1.7881501	4.4174047	-0.4416432
C	-3.0342330	3.9627609	-0.0341553
C	-3.1819333	2.6372899	0.3521195
C	-2.0975424	1.7791392	0.3467747
C	-0.8326002	2.2295993	-0.0515671
C	-0.7004608	3.5622608	-0.4574416
H	-1.2563005	-4.5546342	-0.7385777
H	4.5472663	3.2761317	0.0756605
H	0.6153761	-6.0144550	-0.0274299
H	4.0947725	-0.9794124	-0.0665383
H	5.5163686	1.0064854	-0.0274290
H	-0.9925480	-2.1102825	-0.7337337
H	2.7441159	-4.9904321	0.7207483
H	2.1306696	3.6252684	0.0683283
H	2.9953040	-2.5558549	0.7724576
H	-1.6633557	5.4455330	-0.7620529
H	-3.8851272	4.6337287	-0.0238665
H	-4.1517323	2.2694063	0.6676577
H	-2.2183748	0.7507262	0.6636005
H	0.2535419	3.9234108	-0.8181068

Table A24. *XYZ* Coordinates for Optimized S_1 State of **7** in Units of Ångstrøm.

35

O	-0.0027080	0.0002502	-0.0298401
C	-0.4094857	-4.0721449	-0.1027314
C	3.9246067	2.4179098	0.0414391
C	0.6919129	-4.9049039	0.0682186
C	3.6553347	0.0030077	-0.0598584
C	4.4667530	1.1393890	-0.0267214
C	-0.2538151	-2.7025815	-0.1288774
C	1.9581250	-4.3460977	0.2199159
C	2.5436027	2.6255009	0.0559483
C	2.1300296	-2.9785733	0.1943771
C	1.7004850	1.4990133	-0.0006172
C	1.1677660	-0.7050179	-0.0171372
C	2.2590013	0.1808273	-0.0219546
C	1.0264961	-2.1194250	0.0123541
C	0.3052574	1.3316577	-0.0276092
C	-1.7604372	4.4335772	-0.2579100
C	-3.0437661	3.9102698	-0.1248456
C	-3.2120517	2.5381787	0.0323193
C	-2.1194638	1.6979724	0.0611498
C	-0.8088463	2.2143744	-0.0599258
C	-0.6577327	3.6067395	-0.2261037
H	-1.3987869	-4.5002995	-0.2181531
H	4.5872227	3.2744924	0.0834781
H	0.5649327	-5.9810367	0.0880325
H	4.1060927	-0.9744598	-0.1384376
H	5.5435483	1.0198594	-0.0539781
H	-1.1126626	-2.0603172	-0.2731001
H	2.8186242	-4.9886831	0.3670197
H	2.1540678	3.6289204	0.1345385
H	3.1154365	-2.5638704	0.3450799
H	-1.6230709	5.5001492	-0.3942936
H	-3.9056628	4.5669117	-0.1485290
H	-4.2085064	2.1231235	0.1330147
H	-2.2561622	0.6326708	0.1926883
H	0.3268279	4.0289574	-0.3607499

Table A25. *XYZ* Coordinates for Optimized T_1 State of **7** in Units of Ångstrøm.
35

O	0.0085100	-0.0076850	-0.2500771
C	-0.4059972	-4.0892663	-0.0291888
C	3.8945546	2.4244312	0.3640092
C	0.7021778	-4.9250794	0.0774295
C	3.5911318	0.0288253	0.4614221
C	4.4109063	1.1601476	0.5559158
C	-0.2538597	-2.7200608	-0.0633736
C	1.9743330	-4.3631311	0.1428855
C	2.5339032	2.6101926	0.0900472
C	2.1433736	-2.9956603	0.1140102
C	1.7060040	1.5011436	0.0054788
C	1.1602668	-0.7247088	-0.0093960
C	2.2455680	0.1941494	0.1706176
C	1.0305187	-2.1304363	0.0166833
C	0.3028927	1.3387381	-0.2403456
C	-1.7428548	4.4424914	-0.5723482
C	-2.9845518	3.9095518	-0.9086134
C	-3.1253341	2.5289456	-1.0172937
C	-2.0521618	1.6932198	-0.7965391
C	-0.7803438	2.2170193	-0.4614428
C	-0.6581379	3.6207015	-0.3536666
H	-1.4011278	-4.5158841	-0.0854063
H	4.5441420	3.2892686	0.4288999
H	0.5774392	-6.0009527	0.1035877
H	4.0214502	-0.9477102	0.6278886
H	5.4635710	1.0346945	0.7800589
H	-1.1220871	-2.0793853	-0.1382142
H	2.8456484	-5.0045184	0.2117453
H	2.1606036	3.6127242	-0.0590382
H	3.1441807	-2.5913011	0.1369811
H	-1.6238508	5.5158026	-0.4762091
H	-3.8319329	4.5624856	-1.0798821
H	-4.0875651	2.1024743	-1.2775155
H	-2.1707004	0.6221906	-0.8893532
H	0.2853168	4.0630330	-0.0708618

8. Optimized 1,3-Diphenylisobenzofuran Derivative Geometries for Energy Calculations

Table A26. *XYZ* Coordinates for Optimized S_0 State of **7-F_{1a}** in Units of Ångstrøm.
35

O	8.24417643046714	8.04673887445180	2.79147546241467
C	5.28331341563621	11.80650923793845	2.85263249544230
C	5.31777092140291	10.37346605173683	0.91029489593251
C	11.12648376020612	5.68143674556390	0.90490721720179
C	6.17757185168844	9.51232231196493	1.56718654650918
C	6.14852254248681	10.94174421574700	3.49789908056544
C	8.75292293460899	7.56056566140825	7.28202270047404
C	10.28232799447842	6.55975207519225	1.55998787471430
C	11.19014177232707	4.28077606031960	2.84838707859982
C	7.73139472291939	8.55298630060157	7.27938652498785
C	7.23714615004290	9.06027100586773	6.11683497650175
C	8.99945740467780	7.23337656508268	3.56254968804162
C	9.24994566150526	7.04815702392229	6.12269092679658
C	10.34122794229579	5.15204330116559	3.50788968449180
C	9.87869845473529	6.31256479082373	2.87776502114200
C	7.49017892245359	8.86135601776136	3.55945849107870
C	6.60296072361926	9.77455163981239	2.87496836969272
C	7.75115620889162	8.57480452086872	4.88792690309732
C	4.87596527770800	11.50621750066519	1.56755847461074
C	8.73900288277319	7.52775261328034	4.89003269717185
C	11.59016140740503	4.53992978560956	1.54504865552016
H	4.93308778566381	12.71407836446062	3.32824672359805
H	4.98050315994484	10.17259852884658	-0.09905993783811
H	11.43052719787555	5.89297258912632	-0.11399680591605
H	6.51877926064543	8.61408589592113	1.06782023089407
H	6.50058137791863	11.19510482808739	4.48922548130840
H	9.13668821670207	7.20685046840410	8.23203896418095
H	9.93584269767804	7.45494967735523	1.05842352598054
H	11.53166507251592	3.38441075694129	3.35354118988419
H	7.34515285804559	8.91029717139058	8.22705590178642
H	6.45486461373435	9.80813521977222	6.13610230050547
H	10.03149094537318	6.29992429399739	6.14677549274240
H	10.00587043363323	4.91347501913406	4.50896700089246
F	4.03570283189708	12.33896017706431	0.94192566352284
H	12.25357025864310	3.85491876941462	1.03034357727118

Table A27. *XYZ* Coordinates for Optimized S_1 State of **7-F_{1a}** in Units of Ångstrøm.
35

O	8.23473104691618	8.04492751708223	2.77426630924493
C	5.10244222384787	11.64928122130935	2.89313736295018
C	5.68912891197830	10.56765070718704	0.80567346452120
C	10.77511191786637	5.50150177899015	0.81282273933888
C	6.50131937768979	9.69157294298239	1.49166682542590
C	5.91158588190801	10.76903133058833	3.57753332216119
C	8.76400766860024	7.58477837556885	7.33333525965455
C	9.97030033165080	6.39269876847025	1.48994876267550
C	11.33848878847537	4.41966091485530	2.88560729882061
C	7.75042121859187	8.53611723499845	7.33543984090971
C	7.21924882542226	9.04136509957352	6.14623270943992
C	9.00010137722708	7.24593321522558	3.57712695502339
C	9.28199330528248	7.07094437408656	6.14184912395347
C	10.54136968378301	5.30676179133464	3.57730098764267
C	9.83868105890866	6.32172450745739	2.89560621585811
C	7.47554878948695	8.84654468257172	3.57971992532838
C	6.62907021067813	9.76249562942709	2.89813714526622
C	7.73985635723038	8.55945073525347	4.92892453969466
C	4.99673526994463	11.53507306707865	1.51549339218794
C	8.74775972290365	7.54313238151826	4.92734032155210
C	11.46621811763331	4.51027665736753	1.50228854701662
H	4.55505580629934	12.42898388567843	3.40814300846555
H	5.58170927146493	10.51474763554324	-0.27076678817641
H	10.86803039273034	5.57646182517509	-0.26471065120794
H	7.04114677138085	8.92580121266919	0.95088384833334
H	6.01729365497708	10.87664740113122	4.64656918513390
H	9.16187872148098	7.23104969998664	8.27735880489076
H	9.44196505247219	7.16703228871071	0.94940641781395
H	11.86390176589088	3.64126753659124	3.42697998062815
H	7.36304169284242	8.89677448422965	8.28122389006020
H	6.41571637195875	9.76121855006929	6.18177698418895
H	10.08599584855243	6.35155804159007	6.17186592558643
H	10.42941465447889	5.20040923818684	4.64606065246638
F	4.20884524496570	12.38453519384447	0.85405177324033
H	12.09673966447986	3.81067807366715	0.96601991991022

Table A28. *XYZ* Coordinates for Optimized T_1 State of **7-F_{1a}** in Units of Ångstrøm.
35

O	8.24150778621324	8.04767198918563	2.75550855291788
C	5.09230978798640	11.66653820105744	2.90577720778521
C	5.64006352474907	10.57605375912937	0.81612119687309
C	10.81218769647371	5.48489477356565	0.81999218978613
C	6.47630258767086	9.71167013057836	1.48838423234160
C	5.92538644465750	10.79940620818539	3.57780938303388
C	8.73358789399678	7.56805239735379	7.33196472142762
C	9.98854129812429	6.36624959999051	1.48645686586208
C	11.36875261753887	4.41387323586870	2.89709503876085
C	7.75906233553145	8.54360670446194	7.33129503244033
C	7.25866655494555	9.05661109346353	6.12802789345311
C	9.00306839144024	7.22248461034084	3.55650317999009
C	9.23236228855052	7.05128541788231	6.12923516006201
C	10.55230808457439	5.29022836271899	3.57910266666297
C	9.84230199280754	6.30091380572501	2.89269623824383
C	7.48268296128083	8.87411842686186	3.55670136167637
C	6.63507883491060	9.78754579334688	2.89289075395024
C	7.75488463922408	8.56818060880994	4.92871001727946
C	4.95217571259513	11.54141411916929	1.53312439091958
C	8.73473496783183	7.53556707455158	4.92930469925542
C	11.51244298239695	4.50293115856828	1.51510850508922
H	4.55201291925016	12.44601080084112	3.42857009888569
H	5.51014784791287	10.51285408278219	-0.25731519389109
H	10.91361227359539	5.56104369489520	-0.25674331779804
H	7.01116175787959	8.94879424778757	0.93928103772368
H	6.05155658380530	10.92552511502856	4.64245122735299
H	9.11989442517554	7.18955373643201	8.27093734116661
H	9.45520823141599	7.13103024666900	0.93811191885533
H	11.89816395249618	3.64401288904597	3.44700350751225
H	7.37353431570993	8.92470448781172	8.26958095366551
H	6.48671456258896	9.81150144524740	6.16038044512760
H	10.00325500777132	6.29550915431886	6.16172356003769
H	10.43666162848261	5.17598010863696	4.64663709745914
F	4.13642096782892	12.38042161823471	0.88525501846079
H	12.15810023518736	3.81184496115348	0.98663009143089

Table A29. *XYZ* Coordinates for Optimized S_0 State of **7-F_{1b}** in Units of Ångstrøm.
35

O	2.73430119020496	6.69921155851899	11.40231469461158
F	-1.55550546424923	4.94570616984443	13.24933252398004
C	-0.69000076827649	5.89171901914746	13.64143045358568
C	-0.85316728228853	6.46987384295485	14.88655725057266
H	-1.65532562675195	6.14261945054802	15.53562320325515
C	0.04443740664412	7.45944629631020	15.26413620095242
H	-0.05434336385709	7.92277414133131	16.23888688412494
C	1.07150924641087	7.85130825492780	14.42240230889796
H	1.79031069321389	8.58734129848618	14.75834564519760
C	1.22445955310476	7.25300108673893	13.16561658606474
C	0.31919703911244	6.25873052027068	12.77850088328375
H	0.39656658978258	5.77803229876575	11.81265831672700
C	3.02013026596882	10.07294761773928	12.68362399908676
H	2.28600219566350	10.32368569044223	13.43893257803047
C	3.06742884835538	8.77505474584325	12.11684512240575
C	2.30639460242962	7.63143583660636	12.28426044807375
C	3.89613506191166	11.01217437033189	12.23083162328441
H	3.86637177607342	12.01393521992417	12.64400338305146
C	4.84610078933990	10.71825357116602	11.20943683335114
H	5.50855115536678	11.50663341749797	10.87055363264773
C	4.91858787221523	9.48530505623056	10.63686699785286
H	5.62219755475163	9.29008331632719	9.83743387963376
C	4.02468544750840	8.47777401544621	11.08428528658050
C	3.77887327795805	7.17283430082157	10.69052045023741
C	4.39368818458303	6.27871707125877	9.73552799844426
C	5.73285407419875	6.45076603984838	9.36916927714974
H	6.31747797314868	7.23388597700611	9.83523541421052
C	6.32983105416633	5.59860238061009	8.45719059499937
H	7.36831544725997	5.75111153544025	8.18571432646941
C	5.61141569457574	4.54942266804651	7.89989111085994
H	6.08334948458708	3.87831170727651	7.19216139618580
C	4.28461695502543	4.36219256889709	8.26511280819481
H	3.71318309829172	3.54760715750039	7.83531366905184
C	3.67908190780607	5.21590457187571	9.17014192511053
H	2.64112881976444	5.06727936001882	9.44188885383426

Table A30. *XYZ* Coordinates for Optimized S_1 State of **7-F_{1b}** in Units of Ångstrøm.
35

O	2.69786755345239	6.71665653528660	11.35375828707922
F	-1.26587751713172	4.63888854968309	13.27022085528545
C	-0.61469013946958	5.77695331438700	13.53820524102785
C	-1.06552152935284	6.56650868234858	14.58386503650015
H	-1.92584477102580	6.25536286945792	15.16281934289642
C	-0.37785942412310	7.74539367710500	14.85615175228965
H	-0.70281488036203	8.37309000958588	15.67754506780638
C	0.71221598364149	8.12416036780203	14.10170327861101
H	1.24494278178256	9.02852403701097	14.35304857648608
C	1.15931256547117	7.31726979054523	13.03449415958814
C	0.46963352974835	6.11374912228751	12.76652206101861
H	0.77396862439788	5.46546001630863	11.95636407730767
C	3.11673496813091	10.06194931924593	12.77270691062022
H	2.32552757653302	10.37083048839782	13.43902338501645
C	3.11840478898517	8.79871139542622	12.15348373025278
C	2.28177677966239	7.67271450899679	12.23825188551282
C	4.16064847031307	10.94234995407451	12.48103799411003
H	4.17470344431916	11.91836110475187	12.95170989959244
C	5.18261858961915	10.59257342083459	11.60473430978495
H	5.98909544918739	11.29285513216058	11.42131032033271
C	5.19239399697983	9.35969329601846	10.95099700366422
H	6.01249944224892	9.10677431536789	10.29619042519802
C	4.13460136702456	8.46482648955642	11.20066177060477
C	3.80932501623484	7.18807189949624	10.71359029834484
C	4.36446387960590	6.31998353464062	9.73402411311957
C	5.40636408625761	6.72976707253325	8.87614148145130
H	5.78285422348960	7.74038906791333	8.93191437185261
C	5.92197659370714	5.86318815489308	7.93636716957649
H	6.71647751852084	6.19943600380800	7.28007684149095
C	5.42715033801716	4.56675799020387	7.81996686722543
H	5.84048560749207	3.89002036959944	7.08119707795094
C	4.39552435412305	4.14785698289132	8.65400909001216
H	4.00359114192821	3.14088876200401	8.56678810312777
C	3.86380032775275	5.00538900624445	9.59332538430736
H	3.06691926283850	4.67163475913289	10.24478383095449

Table A31. *XYZ* Coordinates for Optimized T_1 State of **7-F$_{1b}$** in Units of Ångstrøm.
35

O	2.60231883488890	6.74656178569197	11.29211344771537
F	-1.11719904670130	4.52005497048334	13.49454464146278
C	-0.52709323177431	5.70736090548170	13.69559353698448
C	-0.99276858109561	6.50850922372984	14.72718975762918
H	-1.81771132843861	6.17516304889495	15.34325713400049
C	-0.36099012134093	7.73342912253087	14.92922632389993
H	-0.70296264214025	8.38276266128770	15.72702571441263
C	0.69456463093724	8.13352282166533	14.13748857253532
H	1.17307997715618	9.07797762712640	14.34709657898570
C	1.15690263809123	7.31588435424074	13.07991345024996
C	0.50968379994828	6.07289585004450	12.87435633398778
H	0.82774517140373	5.40539546417885	12.08620374448254
C	3.16713883188553	10.04038797356415	12.78217525347686
H	2.45889944621959	10.31789455199459	13.54936729077319
C	3.11377484010194	8.81174996641233	12.14277890507012
C	2.23510877073629	7.67739143854895	12.24276188302033
C	4.14966422738382	10.96377871311902	12.39743867576360
H	4.19199092895391	11.92754458186355	12.89040103028398
C	5.05432097482892	10.66464806052965	11.39877888419667
H	5.79426451273032	11.39930998041013	11.10266293679954
C	5.01981470569213	9.42721566063288	10.74746366783238
H	5.71608276212451	9.22539630163043	9.94552319223557
C	4.06258856727640	8.49740314267076	11.13023850675045
C	3.74229969110379	7.18777513269558	10.65465714243778
C	4.33356432373364	6.31967612358974	9.70911527639055
C	5.65528273906592	6.52055955127633	9.25435261368886
H	6.24728857678065	7.32616569921477	9.66515519095534
C	6.22335355767196	5.66008656418509	8.33965073123158
H	7.24346305783554	5.82970869370804	8.01437045221003
C	5.50614250516920	4.57536928487969	7.84153369046299
H	5.95968060757254	3.90220887184332	7.12404486443613
C	4.20344496781279	4.35891530526806	8.28367821942375
H	3.63479755021934	3.51953305273985	7.89996414980518
C	3.62487382567297	5.20429695270889	9.20688288662947
H	2.60985992849376	5.03050656115803	9.53998531977948

Table A32. *XYZ* Coordinates for Optimized S_0 State of **7-F_{2a}** in Units of Ångstrøm.
35

O	2.07829504161993	10.95710303659679	6.17437557385028
F	4.66609327288988	10.22080557602508	11.45750993878401
F	1.46167994937584	7.38779933556904	9.59045589105936
C	2.13111126349571	11.86349043713032	5.17645028067707
C	2.71180179296251	13.02273298938206	5.67206423503991
C	2.61381962969461	11.46385962173022	7.30719013795409
C	3.00719510888341	12.76906708486740	7.05719448042816
C	1.68304072240946	11.43354692578290	3.87070561154749
C	2.72296777009489	10.57173779840530	8.43705169211736
C	3.62383178081847	15.22408659247184	5.89161323165972
H	3.90396081915181	16.17960520982125	5.46364712289901
C	2.16296973341023	8.52551078205652	9.54998230082411
C	1.49899296842892	10.07354973312142	3.59189871126168
H	1.66459264552555	9.34491284060448	4.37557404434887
C	3.76710921258450	9.95532397169920	10.50301473132813
C	3.56493993400721	13.79809040228404	7.85702867559372
H	3.74830881241589	13.65104372119124	8.91349894506449
C	3.06810464131199	14.26859016652797	5.09690512369285
H	2.91531621067241	14.46639096711636	4.04493466367339
C	1.45869951627017	12.35571438775249	2.84232697257009
H	1.53860978820207	13.41613834017324	3.03757255924619
C	1.98127793704243	9.38391972927708	8.48680299827149
H	1.27884552848077	9.12842146921110	7.70497629325281
C	3.04846588103038	8.77721239702585	10.58227551115150
H	3.18237934106198	8.08132017074854	11.39902445370848
C	1.13793422701863	9.65378391013401	2.32468622813621
H	1.00437457395349	8.59557987888502	2.12958752276349
C	3.62477813119406	10.85429436333952	9.47008761255716
H	4.25621781014975	11.72970718795063	9.45097090637567
C	0.95954209064007	10.57634073771947	1.30276129152071
H	0.69154702751574	10.24345131155139	0.30703880594104
C	3.84999053313549	14.99697853902899	7.27656851604675
H	4.26612421788747	15.79743735352595	7.87706866433213
C	1.11455464448626	11.92790419876533	1.57273488395613
H	0.95796800817804	12.65890095052792	0.78760222936643

Table A33. *XYZ* Coordinates for Optimized S_1 State of **7-F_{2a}** in Units of Ångstrøm.
35

O	2.22208771009472	10.90781351400548	6.08395436640829
F	4.17390891031323	10.43275067382873	11.69103388324792
F	1.70494638161381	7.28433923373470	9.28990671757851
C	2.23975922974531	11.85631706063351	5.10114840501515
C	2.81696215322434	13.03942055024374	5.59171648787006
C	2.76277830835066	11.45729123242262	7.21414705210699
C	3.12639862346292	12.79205263362036	6.96873571787333
C	1.69691657403779	11.44927730060938	3.85163408002093
C	2.83089788627439	10.59118572857786	8.33846128660140
C	3.67753659697000	15.27424777243539	5.82310962925602
H	3.91342570181312	16.23974871804339	5.39131615358403
C	2.28942414105931	8.48374115789801	9.35844483902861
C	1.34050112758784	10.09596059624950	3.64813806570040
H	1.48929990328297	9.38458239466495	4.44978688225209
C	3.53182698353413	10.07946670863651	10.57421707443436
C	3.67142625659008	13.81309482895212	7.76628788116828
H	3.86437165221252	13.67569180398765	8.81946979415657
C	3.11660477577870	14.28677807684971	5.01328540939322
H	2.94865488892728	14.48623615803309	3.96581854936759
C	1.49624143853184	12.35581798511024	2.78978720187181
H	1.71964297654243	13.40343109610667	2.92595941438297
C	2.22369316529950	9.31677360886109	8.26860522916134
H	1.69765433423663	8.99777325438119	7.38013810965685
C	2.93563380482345	8.82752351943285	10.53497067601188
H	2.97542689193288	8.15358124913830	11.37988429039153
C	0.83399633608201	9.67717425759752	2.43642809870853
H	0.57650218012437	8.63349735080512	2.29641652993467
C	3.49758107754134	10.96312089577266	9.52374752390199
H	4.00995969812270	11.90746376427888	9.61809724829450
C	0.65141212201357	10.58354249851530	1.39695970068246
H	0.25151394691986	10.25043265692018	0.44633217740239
C	3.93672054810402	15.04769927625000	7.17105357986479
H	4.35656665785663	15.84483322636504	7.77304126146968
C	0.98034193125177	11.92345033559496	1.58714013167799
H	0.82718986674389	12.63649889144319	0.78523181952282

Table A34. *XYZ* Coordinates for Optimized T_1 State of **7-F_{2a}** in Units of Ångstrøm.
35

O	1.97698502073115	10.95596368425624	6.14371976166505
F	4.62453485456894	10.29246907559978	11.43965887951689
F	1.45715285928477	7.42000676418757	9.56358849677111
C	2.09788724516266	11.87388439910879	5.11504765695306
C	2.73079457719740	13.05422783654622	5.62331643675812
C	2.61842628097034	11.45245312344972	7.25439733359400
C	3.06607410629267	12.78769257851283	6.97854011931811
C	1.64575463734527	11.46437458763579	3.84415988190172
C	2.73574076694058	10.59492971362153	8.37019117769318
C	3.62215157727523	15.26922621582761	5.86487733140406
H	3.84554165669049	16.23890479703716	5.43569576335172
C	2.15823308373051	8.55769944029641	9.50851735496228
C	0.96045252541009	10.23547559419732	3.69908742750171
H	0.77773310025998	9.63042544204792	4.57659588871283
C	3.74210497679894	10.01524686160468	10.47260570760658
C	3.66015489875404	13.76680593480665	7.75804293597519
H	3.89172743791529	13.60401141463910	8.80111754894117
C	3.00036698418053	14.29837262393334	5.07218678997434
H	2.71204828355170	14.54699835722776	4.06137599912727
C	1.87846027703192	12.22842231263318	2.67811723009140
H	2.44148961905097	13.14757870916548	2.73601991204271
C	2.00430088206415	9.38537995930946	8.42282203367375
H	1.32491956165359	9.11063549361408	7.62838217737478
C	3.02089285658264	8.83380427502139	10.55897156148207
H	3.13523294313138	8.15562969907976	11.39312833653575
C	0.52354300184932	9.81333495201511	2.46298271367657
H	-0.00196278330020	8.86957146992617	2.37740464354774
C	3.61502759887670	10.89983563785337	9.43227676159652
H	4.24058864116711	11.77816477818154	9.42077091491315
C	0.75412835074919	10.58320015346920	1.32664781706306
H	0.41152794073044	10.24138712122343	0.35730825573118
C	3.94417964152999	15.01085604185042	7.18105694532165
H	4.41215790268302	15.78037370845222	7.78303747028255
C	1.43813429363060	11.78987538967196	1.44914991685502
H	1.64235439950859	12.38750185399682	0.56795081808368

Table A35. *XYZ* Coordinates for Optimized S_0 State of **7-F_{2b}** in Units of Ångstrøm.

35

F	-0.81882579269585	15.44815190239010	10.61241407818869
F	5.62072799892291	8.19172496531989	17.51724788481527
C	-0.16268504248650	13.32493241726008	9.85825258141958
C	-0.35437656973294	14.22338850344984	10.88990211390773
C	0.33778365850038	12.06821775205801	10.14902894331459
C	-0.06993111765409	13.89297754027559	12.20108334931982
C	0.63900755914396	11.69517320931748	11.46370754549416
C	0.41975193240449	12.63146159816225	12.48202368418852
C	1.20615755827181	10.40258334405955	11.77459086239809
C	1.32145280918887	9.18745683867780	11.11957639088336
C	2.32808776517674	9.05738241851584	13.14139209553134
C	0.86776892938024	8.68890892326171	9.87283185270849
C	2.06535837624393	8.32206696231980	11.99860945207883
C	3.09362495040539	8.82186394350388	14.34336437676070
C	1.19999879672721	7.41926329470305	9.51053256169863
C	2.42176937769215	7.01978871147965	11.56923396467633
C	3.39304739702074	7.52413134877795	14.77267614478814
C	3.60264562997509	9.89992913564840	15.07840830304229
C	1.99911770341484	6.59144078969820	10.34893029230782
C	4.23448334855279	7.30601693139172	15.84885951818018
C	4.43529518198864	9.69300145808657	16.16177248505742
C	4.76319112092921	8.39702227275616	16.51134529843078
O	1.80886886807932	10.29161026341912	12.97884427073578
H	-0.24191726354689	14.61886212252447	12.98631428945169
H	-0.38838065982086	13.62189777447230	8.84141850756498
H	0.53656726920465	11.38497984194375	9.33421050835274
H	0.64110244326846	12.36092991636029	13.50648999935196
H	0.26193584486899	9.29865161811164	9.21527126915572
H	0.85537872015437	7.02517012490810	8.56163454449388
H	3.03320566772533	6.37851402470689	12.19084112932679
H	2.95177712847011	6.67515125618622	14.26748628488750
H	3.36131243887493	10.90982295359433	14.77279500333597
H	2.27838140338256	5.60445253048620	9.99917367204008
H	4.48727628292676	6.30721657477150	16.18299057662020
H	4.84924128504224	10.52099973740171	16.72370116549193

Table A36. *XYZ* Coordinates for Optimized S_1 State of **7-F_{2b}** in Units of Ångstrøm.
35

F	-0.85758189416563	15.39969583758267	10.64370002829689
F	5.30317820244965	8.21495827810675	17.73833878158044
C	-0.35640636263826	13.22797015168055	9.91731016741114
C	-0.33600138492393	14.20005136116074	10.90516415777470
C	0.17623163573938	11.98661146596528	10.18812307047190
C	0.21497553106038	13.96263084778903	12.15388677837040
C	0.74099726889666	11.69609251838356	11.44758029282533
C	0.75137597028465	12.72207059617080	12.42046713963095
C	1.29357448359058	10.42283081197026	11.75433445169429
C	1.36031417469213	9.18555494279165	11.09208485434152
C	2.43040351610530	9.07531274206146	13.08742328319391
C	0.87477753432851	8.71765613505174	9.85460363929164
C	2.10988395160303	8.31715884907745	11.94858580873853
C	3.16391952592730	8.83164800559368	14.28035662905688
C	1.15932534486890	7.39898316785142	9.49127728495868
C	2.38932518242503	6.99455959804253	11.55036089772915
C	3.64586790378843	7.54981481063598	14.61848590729229
C	3.42866577451088	9.89502332881526	15.17417913989150
C	1.90172187561276	6.56138693287105	10.31482516236674
C	4.36067826812035	7.34225322623677	15.77772377993158
C	4.14652555225572	9.69095057490492	16.33193944889481
C	4.60650988705339	8.41615301188043	16.61887629056710
O	1.93068046765220	10.34121171085931	12.96092315787699
H	0.21412156186527	14.75022462107943	12.89740415903045
H	-0.78579786332272	13.45810205885190	8.95013388541174
H	0.18191049503642	11.23879819071088	9.40999450181693
H	1.17496381315723	12.52121556628961	13.39530909663138
H	0.27580341565506	9.33341355261700	9.20163883057977
H	0.79164164673965	7.02160594866257	8.54420345281243
H	2.98286442864223	6.32526178794518	12.15364831302369
H	3.43435209204519	6.70807100602919	13.97711886429612
H	3.07311888474872	10.88789434706487	14.93374345919437
H	2.10920686898144	5.54794345849451	9.99166499599785
H	4.72898785928605	6.35940043958607	16.04443964201197
H	4.35808538792804	10.50263311718548	17.01710564700592

Table A37. *XYZ* Coordinates for Optimized T_1 State of **7-F_{2b}** in Units of Ångstrøm.
35

F	-0.70680481305493	15.46572687782056	10.57170481442833
F	5.61459571102824	8.23892852032063	17.51827849787716
C	-0.20634273684680	13.28487902854601	9.85952761789556
C	-0.27938755277463	14.23310454332545	10.86771762755301
C	0.24236982571150	12.01739205027051	10.16147083404261
C	0.08817057406755	13.94144226756742	12.17069402737566
C	0.63722231880174	11.67621107008761	11.47419935494199
C	0.54555758368310	12.67725371199034	12.46988275034245
C	1.15782349440049	10.40669952145333	11.80798995805911
C	1.29123076206635	9.15426746182821	11.12669947662242
C	2.29205066062576	9.04476022073522	13.18221619371970
C	0.86104449632326	8.69073097187801	9.89443078657620
C	2.03764919327272	8.30066869810426	11.98776145987684
C	3.05924682906942	8.80599504363355	14.34409435601160
C	1.21161004901105	7.39382665059062	9.49457526507858
C	2.40567960386419	7.03338871405312	11.56466277527329
C	3.49485204435223	7.51244561211978	14.70477394382628
C	3.45026313434150	9.88819263280980	15.16594344399821
C	1.98264409117207	6.58816604206425	10.30578958501460
C	4.33430592327112	7.31990513728196	15.78087040609003
C	4.30069724438705	9.69915275857999	16.23360333038716
C	4.75136357719096	8.41965367455488	16.51325354109224
O	1.73306056664175	10.29785942627738	13.05733893072160
H	0.01102227121042	14.70799134775017	12.93222623748718
H	-0.49267927539304	13.55670521727757	8.85111408456070
H	0.33752372303043	11.29575965186126	9.36273851055702
H	0.83947015553924	12.43843889400094	13.48278727991552
H	0.26046604382337	9.30309492187259	9.23639510963523
H	0.87537272996660	7.02685921365571	8.53230215960675
H	3.02017607362221	6.38831500821304	12.17717439582389
H	3.14350363128396	6.65252090702600	14.15229479643601
H	3.10301994378981	10.88321962297715	14.92273729680268
H	2.27175602735746	5.60018576176115	9.96792154366993
H	4.67666652503033	6.33271508233134	16.06607383917780
H	4.63300057013350	10.52868673538015	16.84571076952261

Table A38. *XYZ* Coordinates for Optimized S_0 State of **7-F_{2c}** in Units of Ångstrøm.
35

F	3.56494086006788	3.34932320126429	8.14198828082576
O	2.71745168713097	6.81851716775588	11.56624664676556
C	4.24285964566060	4.43487246308211	8.53660553638679
C	5.51083391582302	4.65276309141072	8.02892773394396
H	5.93724518199304	3.95563214701351	7.31929242427838
F	-1.54618238253863	5.00421771725620	13.37812572243215
C	6.19982856854306	5.77351083577832	8.47064911224344
H	7.19959455848547	5.96536272021253	8.09958749754237
C	5.63837679684229	6.64006211081147	9.39135940132691
H	6.21634362092668	7.47488961327904	9.76285835965419
C	4.34652046373134	6.41561922827066	9.88066580451508
C	3.64653974487231	5.28801745077156	9.43749784971833
H	2.64731722316830	5.07330335255519	9.79151062478578
C	3.75259543610186	7.30620384520402	10.84915850893835
C	3.99870455419697	8.60664501302583	11.26101166925985
C	4.88597430323490	9.62681293449499	10.82896981344756
H	5.58446516951529	9.45586289704714	10.02029531058413
C	4.81610399234487	10.84655894747671	11.42996565198566
H	5.47543295936227	11.64232761623179	11.10224454825953
C	3.87507052169016	11.11770742863160	12.46491880367532
H	3.84783899542002	12.11029200244395	12.89952129056569
C	3.00541098467228	10.16645414753101	12.90436248255092
H	2.27754497703352	10.39697960826286	13.67196975019208
C	3.05134274243510	8.88198296245610	12.30908583453904
C	2.29475931315020	7.73293998670061	12.46479335291888
C	1.21506194247241	7.33469688131556	13.34082728396006
C	0.31759190923641	6.34149039179109	12.93329220877543
H	0.39939499394730	5.88063524627919	11.95812452826892
C	-0.69018932383899	5.95060230441319	13.78708188512704
C	-0.85895245439241	6.50517825906898	15.04230172861471
H	-1.66001773923193	6.16090057408470	15.68375159473214
C	0.03102322128760	7.49373848345248	15.43993236650407
H	-0.07339788548168	7.93745273128104	16.42314158769340
C	1.05793934137420	7.90755586049379	14.60832051035190
H	1.77204110976330	8.64126622485189	14.95925087663661

Table A39. *XYZ* Coordinates for Optimized S_1 State of **7-F_{2c}** in Units of Ångstrøm.

35

F	3.57545336221128	3.22271880049924	8.39101765622212
O	2.65445664210080	6.82492295105792	11.50700283988696
C	4.20083988425939	4.37537698620932	8.65383639860454
C	5.36381124068595	4.67114335990663	7.96090978646791
H	5.74669643933196	3.97375675413944	7.22659096072340
F	-1.23451927261197	4.66871744976582	13.48556279102514
C	6.00616002450855	5.87265336387072	8.24476622834963
H	6.92066308386104	6.12314573063683	7.72017524885909
C	5.50047748995816	6.74594676730249	9.18407830265090
H	6.03195738295915	7.66031403629904	9.39623493851193
C	4.31314767360447	6.43885272108597	9.88187812324758
C	3.66357230501514	5.21694591934770	9.59565000276416
H	2.75262165481474	4.93604727053603	10.10537405085753
C	3.75772510547113	7.30869532453928	10.85953189686061
C	4.06812627855042	8.59155618455170	11.34283550951482
C	5.07202100245959	9.52963878807884	11.04128384282125
H	5.83366955320231	9.33662861379617	10.30169083888109
C	5.05954414223362	10.75339337557461	11.71107458481405
H	5.82666494360144	11.48521326065697	11.48703163398877
C	4.07849703955281	11.05837202169556	12.64889743792391
H	4.08986474119258	12.02691391359375	13.13468302551178
C	3.07457379703400	10.14582895315853	12.97392646109033
H	2.30672654831998	10.42456261533800	13.67965300343024
C	3.07816807917950	8.89300914960837	12.33472776427822
C	2.25546696855371	7.75749426449134	12.42210171178117
C	1.15674276083979	7.37581442660418	13.23964461263234
C	0.47270348677019	6.17035493928999	12.96615088934408
H	0.76628489255348	5.53595033501324	12.14127590462042
C	-0.58907132199532	5.80807645285193	13.75760682644313
C	-1.02130051765888	6.57403179932858	14.82845608779705
H	-1.86370227527621	6.24317987534585	15.42269525927354
C	-0.33877454484701	7.75462987018460	15.10632772330461
H	-0.64956867342734	8.36332410136421	15.94721512612881
C	0.72860653685841	8.15815171066289	14.33275674425596
H	1.25853254613313	9.06275091361421	14.58873978713287

Table A40. *XYZ* Coordinates for Optimized T_1 State of **7-F_{2c}** in Units of Ångstrøm.
35

F	3.64370071929246	3.17189492499890	8.45283714222066
O	2.66786830321906	6.81079009716895	11.53371291240635
C	4.23412100954617	4.35512659034294	8.67107108312839
C	5.34925349859423	4.68711129360783	7.91609584200580
H	5.72133024883074	4.00069896411985	7.16680711701321
F	-1.16763306123063	4.60736763329980	13.55687475903957
C	5.95993405908487	5.91327268266120	8.16781135473412
H	6.83892346698911	6.19700406258734	7.60118463938576
C	5.47293642070950	6.76925517657052	9.13186042594482
H	5.98875217061716	7.69881901160138	9.31419127379204
C	4.32421431829547	6.43315090016353	9.88458868606237
C	3.71154208575913	5.18216032553250	9.63325925831923
H	2.83478910382168	4.87240029932218	10.18376896811282
C	3.77589586384953	7.28608378090404	10.86666154562741
C	4.08492350202781	8.59669256246547	11.36299667215993
C	5.05105980641150	9.53455419396177	11.02680834385814
H	5.78185403906393	9.35096174791043	10.25297177368868
C	5.07435194424610	10.75684962854698	11.70683730145593
H	5.82386611983700	11.49443902910392	11.44448564736363
C	4.15117454650197	11.03478941501991	12.69479576468021
H	4.18403794186195	11.98701779797786	13.21035866098242
C	3.16963662990623	10.10020471809941	13.04517970748442
H	2.45707901797926	10.35294652157857	13.81671999569422
C	3.12907134945511	8.88506019816963	12.37751326976830
C	2.26466551033751	7.74162873153850	12.46693067700450
C	1.14936712476047	7.38297806632760	13.25640891020965
C	0.50309544140556	6.14539388077108	13.01834803275536
H	0.84601750332104	5.48015545200241	12.23887768632088
C	-0.57546157214623	5.78754384268750	13.78785408839108
C	-1.08100216802035	6.59086893613042	14.79867589222327
H	-1.93880300599988	6.26394657371353	15.37163090173389
C	-0.45055699477303	7.81002298102200	15.03285051159986
H	-0.82549641134463	8.46092378450530	15.81420068805087
C	0.64470892900819	8.20201273914529	14.29262884794413
H	1.11762153878201	9.14398645644144	14.52358561883807

Table A41. *XYZ* Coordinates for Optimized S_0 State of **7-F_{3a}** in Units of Ångstrøm.

35

F	-17.25754796227799	1.88323692382917	36.88321438353411
O	-12.64187576709381	2.25953851377008	35.08032142947689
F	-14.63708677483793	2.40510829619804	40.69973490647362
F	-17.04984183077469	2.00910545989573	39.56279346577813
C	-11.47743497494756	2.13465145276712	33.00885947400679
C	-12.49601908808168	1.34714626387265	32.45634080341475
H	-13.27632007461945	0.96009006774089	33.09924391007586
C	-10.47393013637235	2.61797050261630	32.16095131586655
H	-9.69906088877557	3.26395419677505	32.55102977088777
C	-13.69110066116428	2.45783440274473	37.20473047236845
C	-9.18056048149737	3.30624940893142	35.21627613400791
H	-8.63485021861545	3.16697428678686	34.29264481255105
C	-8.54921721491108	3.80673637061386	36.31377683937293
H	-7.50378008206137	4.08535900786647	36.25085442726613
C	-15.97228013694439	2.15250990141804	38.80544229225649
C	-14.72570722895093	2.36084104310915	39.37276127913724
C	-10.54055014472772	3.62497715352479	37.69306333564946
H	-11.03695344855032	3.78085167576811	38.64096924326926
C	-10.48452506346591	2.31283332651270	30.81093007628443
H	-9.70365944218813	2.70460976486846	30.16926640731491
C	-11.22782198050603	3.07669722663007	36.58101746130182
C	-9.23545757743742	3.98478593251673	37.54668437084870
H	-8.70119726042717	4.41291657782411	38.38687666946917
C	-16.05826651676084	2.09013506747142	37.42290612972147
C	-14.94799490434052	2.24159240895517	36.62251925636374
H	-15.06841385526118	2.19754192108316	35.54811944292574
C	-12.51976687830391	2.61681625415669	36.37659789833940
C	-13.59576029726814	2.50571491713410	38.60031460533314
H	-12.64968976808278	2.62916793914411	39.10649959539801
C	-10.55004998654556	2.95360667062563	35.31676590941225
C	-12.50248823613049	1.05062204584395	31.10509121586940
H	-13.29690394765305	0.43742518238791	30.69539714931787
C	-11.49642994871420	1.52753577572365	30.27575420906397
H	-11.50165067154712	1.28606016684557	29.21913948841551
C	-11.48282655016357	2.45573389404810	34.41900181922702

Table A42. *XYZ* Coordinates for Optimized S_1 State of **7-F_{3a}** in Units of Ångstrøm.
35

F	-17.14190029562646	1.51863630948850	36.81527492098525
O	-12.64980460538388	2.25466146214091	35.06363973305275
F	-14.69402829014884	2.50247055386156	40.66185126149390
F	-17.02217470268293	1.83694879524098	39.48756179631011
C	-11.45220981604061	2.20082887392888	33.03394114250947
C	-12.58438141357453	1.61366844797465	32.42412870456315
H	-13.43714564438073	1.35119353257268	33.03619162130214
C	-10.35137932722335	2.52883940110896	32.21585669700920
H	-9.48829754907251	3.01593998772987	32.64491632671495
C	-13.64213883180240	2.40728819849410	37.19394869956478
C	-9.12313263115278	3.20137674846207	35.26872495079741
H	-8.56169697065057	3.04029474434809	34.36081990871391
C	-8.47736089696696	3.68665391731693	36.40649482573654
H	-7.42083693750352	3.92172891034873	36.35349534667495
C	-15.93953222092873	2.01639460905058	38.75083581630206
C	-14.72829281805993	2.36775461994545	39.34004661039494
C	-10.51453472824498	3.56648503460818	37.72886366501436
H	-11.02047196229323	3.75094222942192	38.66470483182400
C	-10.38337951999843	2.27139911978387	30.86205389112440
H	-9.53103330814477	2.53841037980483	30.24799692176424
C	-11.18287139458556	3.04249783739974	36.60781192692098
C	-9.16033337437796	3.88190128270324	37.60219956895817
H	-8.63047230539359	4.28360021437315	38.45782593143717
C	-15.98190470516051	1.85585954448378	37.37035148410454
C	-14.86615687828190	2.03715963350155	36.59318011020726
H	-14.94450482154418	1.90899990151407	35.52265938711810
C	-12.49368252892893	2.59366960311407	36.37989480666363
C	-13.59468105233766	2.56629674602950	38.59372043096353
H	-12.67756873204019	2.80759018913013	39.10864207991376
C	-10.49666514019139	2.90639432960357	35.35716543077594
C	-12.59871365393911	1.35612344977566	31.06988880342477
H	-13.47298613838102	0.89824223435826	30.62140822299849
C	-11.50058826562976	1.67897973405517	30.27919429527616
H	-11.51632952761078	1.47545287376198	29.21480908537763
C	-11.45443412971733	2.45667417956438	34.43298645300720

Table A43. *XYZ* Coordinates for Optimized T_1 State of **7-F_{3a}** in Units of Ångstrøm.
35

F	-16.99532805172216	1.03992286827565	36.89936511909391
O	-12.61013267112030	2.15139729505410	35.09329898122073
F	-14.92815200253970	3.15366529166556	40.51049824647627
F	-17.08855342722549	1.95123354428105	39.43883867341943
C	-11.44577997826306	2.21722042565612	33.02951210138365
C	-12.58619650636415	1.64129329857430	32.42053745115851
H	-13.42874452636993	1.36395484234743	33.03878003360919
C	-10.36430541989698	2.57141156903519	32.19236163596303
H	-9.48852254903149	3.04608235531660	32.60949984037170
C	-13.62729745739801	2.37703934048109	37.21379265072689
C	-9.13282723123585	3.25776350686361	35.26960070727906
H	-8.60273568561209	3.21349477553634	34.32940345300546
C	-8.44736215941694	3.65879295423067	36.42140689102779
H	-7.40437788533064	3.94237347680730	36.34429773057097
C	-15.98157706008172	2.08610877469838	38.72423239245851
C	-14.85241575829026	2.69630597025261	39.26333407312716
C	-10.42963935258289	3.34230400171250	37.76734163856945
H	-10.89083940081499	3.35780773781275	38.74462473064072
C	-10.42357279811071	2.35350537143313	30.83255638199070
H	-9.58407505330441	2.64409914062946	30.21125584690710
C	-11.12555580614271	2.95274779232187	36.63497705546349
C	-9.08212896887595	3.70291406374355	37.64504849084164
H	-8.53542251753694	4.01476194504491	38.52686495241799
C	-15.91637684331781	1.62815491062535	37.41324023912983
C	-14.78095320379307	1.77385756713323	36.65908924551299
H	-14.77916038283962	1.40832423402446	35.64285008686573
C	-12.47228278544602	2.50861054552882	36.41387879567409
C	-13.69129662038274	2.83865401481541	38.54704131452566
H	-12.86180097917871	3.33861241655916	39.02329221799559
C	-10.47021094984120	2.90377025306895	35.37278990115128
C	-12.62713014187039	1.42496666587365	31.06040989289962
H	-13.50969585462788	0.97678539548855	30.61823672561234
C	-11.54968759015560	1.77472796469634	30.25233707031339
H	-11.58767811943653	1.59819123065075	29.18391106275753
C	-11.43380937984307	2.43050208876115	34.42458005883858

Table A44. *XYZ* Coordinates for Optimized S_0 State of **7-F_{3b}** in Units of Ångstrøm.
35

O	11.82244617455076	2.71296950589780	6.36710196012385
F	10.50489673013943	2.60830261544599	10.19489775025446
F	9.52869068406756	1.52199521706639	5.72659154429598
F	6.22022505585216	1.25913497386486	8.98357519216133
C	13.77921147890114	2.22394788014534	7.29086675477346
C	12.73262002343256	1.89859312578628	8.22215680629617
C	13.15421412049916	2.74049316361676	6.16665836415333
C	13.62162830556725	3.23953261707731	4.89350609021315
C	15.12564090512298	1.91731114239507	7.61483549737869
H	15.92260093532398	2.09323862762407	6.90439179726107
C	10.14636920971878	2.04470247179426	7.93861393865691
C	11.54204349197663	2.21298483771944	7.59044629309166
C	15.39857231075906	1.36906462451878	8.83051191121860
H	16.42112356720313	1.12417689908898	9.09406692054148
C	9.66823648675615	2.18235971177804	9.24597751965620
C	13.05618722560958	1.31979094662504	9.47465432820302
H	12.28134038530430	1.07187802929510	10.18623656493788
C	8.36879238578161	1.91866672116327	9.62598505992016
H	8.06010020004819	2.03292276090892	10.65602653022887
C	14.36373577211237	1.08159950828529	9.76414033959472
H	14.62957406771524	0.64250487442474	10.71836416008345
C	9.17181120301393	1.67470757122173	7.00082745518715
C	14.93584490940690	3.69350422941130	4.74297177831616
H	15.58804852140176	3.74837976124096	5.60492942149744
C	7.85369134353237	1.42507949582730	7.31919991031155
H	7.14945808535317	1.12899178969490	6.55380432009589
C	14.56510809377876	4.10523378270292	2.40313045988881
H	14.93417693142162	4.43489350961044	1.43906125898747
C	15.40210465097818	4.10933375647787	3.50947417257886
H	16.42488585553434	4.45523468673405	3.41420645769476
C	7.48005120081445	1.53269239889925	8.64364048388894
C	12.77814791445508	3.26185612399109	3.77687536224169
H	11.75614021425548	2.91781021339930	3.87807454237450
C	13.24750002877488	3.69309773663684	2.54938290576830
H	12.58045153083704	3.69642568963034	1.69467414812401

Table A45. *XYZ* Coordinates for Optimized S_1 State of **7-F_{3b}** in Units of Ångstrøm.
35

O	11.82824474679672	2.58438785961775	6.31704360319618
F	10.51087688619802	2.53950930205249	10.15640051215201
F	9.60583117255652	1.35967801287398	5.69024840408309
F	6.19336684580169	1.42604240314730	8.84277164386203
C	13.82311355144478	2.21124205097508	7.33475479455046
C	12.77633128522380	1.86591645449240	8.25072490451905
C	13.18871702543820	2.66872510798319	6.16832684941994
C	13.62876091581011	3.17171927803273	4.91567043525217
C	15.16733439124367	2.00697493460256	7.69554819099717
H	15.97881983752063	2.22122317817430	7.01648141662194
C	10.19443888422527	1.93954064133435	7.90335604825352
C	11.57413270169691	2.11983060179803	7.57376736568795
C	15.44175523235046	1.47129705990846	8.95548964674724
H	16.47313452217949	1.30962194423000	9.24634300389077
C	9.68319245895080	2.12031480230677	9.20474450891774
C	13.07953700093136	1.31178254115508	9.50594736358389
H	12.30044594571322	1.03419743360998	10.19977874092313
C	8.36154124529615	1.95049588152136	9.54391283931665
H	8.02683010079704	2.12291956062081	10.55779371648470
C	14.42190687356591	1.12983885021112	9.83865544943070
H	14.67454709492441	0.70808016904026	10.80439871299229
C	9.21988944507586	1.58721819090994	6.94149700218145
C	14.98417654535129	3.47241190982493	4.66217219005462
H	15.71772153662894	3.35342495706458	5.44591229616148
C	7.88679897136713	1.41193278270038	7.23115377127115
H	7.19027540813313	1.11918055178911	6.45727324740862
C	14.44253725761298	4.15268291738663	2.41745560367302
H	14.75940576151424	4.52947376743714	1.45190864817274
C	15.37631313369406	3.95342077586605	3.43187183251565
H	16.42102208294950	4.18415052463539	3.25751755732754
C	7.47867208457774	1.59394141403934	8.54010056427185
C	12.69058129293937	3.39244118543913	3.87940038377082
H	11.64666826389119	3.17005319874449	4.05841220580065
C	13.10025358577927	3.87145860611872	2.65371519187094
H	12.36849591182010	4.02828215035615	1.86930935463687

Table A46. *XYZ* Coordinates for Optimized T_1 State of **7-F_{3b}** in Units of Ångstrøm.
35

O	11.80285977562787	2.67331857521920	6.30974115201508
F	10.48597045539960	2.55088907484730	10.19985091067108
F	9.51253796086454	1.62881544105520	5.67708937527829
F	6.23446720665831	1.15692506924440	8.93606964794367
C	13.80319362959290	2.23122802984872	7.32907125491285
C	12.76358138909439	1.95967824871257	8.26153158022466
C	13.17398472035113	2.72707587664316	6.14319881426198
C	13.63789112326347	3.21176816310221	4.90412800987706
C	15.11687488440757	1.92178802583926	7.64358561292836
H	15.91549500863588	2.05348152522621	6.92659989168570
C	10.16196671281182	2.03706420717647	7.91932182373982
C	11.53115163589936	2.23802367105782	7.58408818031949
C	15.40645219354141	1.39513319880572	8.90972625459239
H	16.43203829058625	1.15565564552360	9.16525926048337
C	9.66898324802875	2.11481353378126	9.23840153018611
C	13.06239720732265	1.42417469253660	9.50341824497596
H	12.28668144840385	1.20192237111892	10.22070998391504
C	8.37789328942224	1.81656284759454	9.60446795428747
H	8.06778349888665	1.89178946325970	10.63788294648235
C	14.40051135285392	1.15923949417919	9.82201016519090
H	14.64018260987429	0.74221287839338	10.79258346365909
C	9.17089985654612	1.71776912674389	6.96023783118849
C	14.99145793636785	3.55476604174885	4.68942148771498
H	15.69312313921188	3.51635444633609	5.51139687981488
C	7.86114815502248	1.43865832655868	7.27518077639936
H	7.15825191112862	1.17461887908252	6.49672794664973
C	14.52618281828498	4.09566770995832	2.39153222862489
H	14.87218918492719	4.43224188336622	1.42169342147425
C	15.42069942805650	3.98358892827357	3.45304697350634
H	16.46228403749865	4.24948602527883	3.31215007664727
C	7.48840675567580	1.46631988645492	8.60641125109639
C	12.73490565459464	3.36724614019709	3.82615126518575
H	11.69196624661641	3.12048096273027	3.97529887389734
C	13.18297025408186	3.79298435930717	2.59497938897095
H	12.47828698046018	3.89166825079815	1.77689354119867

Table A47. *XYZ* Coordinates for Optimized S_0 State of **7-F_4** in Units of Ångstrøm.
35

F	2.59823895348681	1.45825167215593	0.21249681891984
F	-0.93191636423523	0.31830904120625	3.04148455533638
F	1.89064999717836	8.56369118161740	9.24893528810289
F	-0.81316905908990	4.77444213524886	9.56060278643109
O	0.89511719375742	4.68525112174344	4.84405378757642
C	1.10900177274194	5.93937893148174	5.30461347195493
C	1.49468477801538	6.73949050747270	4.24078469395746
C	1.76394418602951	8.12399708783257	4.09419376647262
H	1.71441052783485	8.79863229281479	4.93838732783833
C	2.04557580638492	8.60657798336349	2.85251578681376
H	2.24272240318092	9.66485064350223	2.72392311408668
C	2.07657632348801	7.75949515859734	1.70877085735904
H	2.29142059691979	8.19837357719920	0.74139426807300
C	1.82559710247849	6.42513200105379	1.80739828004719
H	1.82145837705394	5.79542292331753	0.92658038124318
C	1.53155932955187	5.88525215260649	3.08515649432413
C	1.16451656739050	4.62508864077784	3.52190176618100
C	1.03208152558011	3.34260748719521	2.86227033265210
C	1.87379505862901	3.02123869600920	1.79129692716490
H	2.64946842171480	3.69748044337628	1.45807260738987
C	1.75044453668178	1.78531288020499	1.19242426462147
C	0.80855946777308	0.85212799753151	1.58303283222879
H	0.72205184238177	-0.10723579249219	1.09189106466177
C	-0.01021705362415	1.20034897267557	2.64139848134727
C	0.08484088736093	2.40923017759543	3.29789472216379
H	-0.58237730372441	2.62624024363965	4.12078862453524
C	0.91652647785954	6.17741335589090	6.71714803048520
C	1.51429600783797	7.28589033491692	7.33029456270729
H	2.16525140823612	7.95423722975275	6.78619940531878
C	1.30619908186072	7.50664952802091	8.67396709756039
C	0.52573347512158	6.67920344371004	9.45900905675051
H	0.36279052889994	6.87647255030038	10.50973090998384
C	-0.04389436989320	5.58732107540771	8.82898261374323
C	0.13560881995751	5.30977422678294	7.49058665804851
H	-0.33957202382067	4.44218507949023	7.05393983891909

Table A48. *XYZ* Coordinates for Optimized S_1 State of **7-F_4** in Units of Ångstrøm.

35

F	1.22237474334606	1.79944204817592	-0.36250157698834
F	-0.03350652394178	0.05908681150526	3.77997383062417
F	1.23852867462674	8.70983490076357	9.22393375818702
F	-0.74119929765585	4.48821835717915	9.39482170032855
O	0.87309608434023	4.72322315839691	4.81406634906414
C	1.13814605746500	5.98629078859507	5.26654442270433
C	1.67696158718525	6.76064974675770	4.22657917294651
C	2.07436263371102	8.10423300371059	4.12160758168262
H	1.94671280474859	8.80295419540890	4.93480010242788
C	2.61963458855124	8.54274489481737	2.91591273996055
H	2.93146315181359	9.57610027721487	2.82185881894384
C	2.77569103421191	7.68031861370740	1.83460794660437
H	3.22158906043200	8.05027175511159	0.91905473405051
C	2.36733365469670	6.34903582479062	1.90183701186763
H	2.52132986526089	5.70118738731831	1.05195212483153
C	1.78810969996118	5.88606687849190	3.09536109750200
C	1.25609729288910	4.65188128403884	3.50334003738164
C	1.04101565006795	3.39509210208511	2.87488016606299
C	1.25708786357100	3.20728874270153	1.49465031204223
H	1.56674988093514	4.01396125818586	0.84919962644222
C	1.02610992334000	1.96964750340919	0.94683048079782
C	0.59184095372204	0.87954865363006	1.68731235982010
H	0.42165877825681	-0.08526869755110	1.22902216234478
C	0.38453024815649	1.08914051076605	3.04110469871104
C	0.58857308898526	2.30336709534630	3.65027184488342
H	0.41633581726801	2.40591728586696	4.71216503154598
C	0.84656007602968	6.21460091920499	6.63876199329118
C	1.20413991791750	7.41527122380600	7.28532391252715
H	1.74455207145864	8.19850381720683	6.77755750346782
C	0.89039597238159	7.57522288704735	8.61257767960935
C	0.22963250811625	6.61002409305491	9.35908714232174
H	-0.00834562191687	6.76561940804498	10.40264824784225
C	-0.10586147515693	5.43663115350711	8.70300963323655
C	0.18335041097399	5.21030844306963	7.37951338078009
H	-0.11252463974840	4.27925966363429	6.91765098515436

Table A49. *XYZ* Coordinates for Optimized T_1 State of **7-F_4** in Units of Ångstrøm.
35

F	1.65840252811916	1.68555945658470	-0.27734693703126
F	-0.56223592466120	0.21801234374841	3.56307174923264
F	1.04575322192159	8.84590138467065	9.13271816086693
F	-0.48741705353236	4.44622818168142	9.51906371069776
O	0.94511532926122	4.66899619778231	4.85685048978262
C	1.21301614606032	5.93863156531440	5.32274101646037
C	1.71639002872450	6.73169756118200	4.23899758943613
C	2.09382812831837	8.06046385436271	4.13237043991668
H	2.06802533737669	8.73297241765029	4.97652868218083
C	2.50795120448383	8.55072452118380	2.89043967728486
H	2.80999488882267	9.58762471516657	2.80568419229564
C	2.53453505160475	7.73388356363951	1.77892955232368
H	2.85360067224690	8.13383404167649	0.82398005682583
C	2.15375921157657	6.39073291747493	1.86893400330227
H	2.15691904173236	5.78090529464918	0.97729003624092
C	1.75639645201992	5.88711365183705	3.09733616170647
C	1.28578606688942	4.60258911942505	3.52218069322502
C	1.07510592350975	3.36650668085011	2.87570819334344
C	1.51569812049783	3.11884520578160	1.55638716125122
H	2.08781025955514	3.84057621219563	0.99579800783641
C	1.23936690963688	1.90670572790462	0.97389951609475
C	0.53889861898882	0.89669087966271	1.61625559038227
H	0.31791262890952	-0.04251393102056	1.12832430841347
C	0.12865885869422	1.15932981243070	2.91453734591290
C	0.38315731974891	2.34304615112377	3.55893064591801
H	0.02645192900390	2.48953381721603	4.56759881247920
C	0.92833008501167	6.18763553016920	6.68065104750952
C	1.16323970052698	7.44695041718957	7.27746858736553
H	1.60427360934332	8.26821319960915	6.73704743601983
C	0.82985148711852	7.64057304968309	8.59352865210699
C	0.27617737396101	6.65003005678438	9.39100140433750
H	0.01170977040784	6.82926917985638	10.42392141971198
C	0.06026493120471	5.42003975261098	8.78588567792788
C	0.37058105996324	5.15978449583477	7.47516333604924
H	0.17253108295301	4.18097897408841	7.06335158259248

Table A50. *XYZ* Coordinates for Optimized S_0 State of **7-F_5** in Units of Ångstrøm.
35

O	3.88701282953057	6.99287356492313	4.07484241071350
F	2.24773245136256	8.29903284411222	5.80360757708290
C	3.44678944997914	7.67727782314770	2.00824061607128
F	-0.21152837952590	8.19764137310054	6.82952919270269
C	2.90905330376786	8.14387036646860	0.78282149558011
H	1.84362913123090	8.29538397822106	0.66797288960766
F	-2.27044605995506	7.23249906387073	5.35561626865533
C	3.76336535649454	8.38686760155632	-0.24819950044702
H	3.37336536483119	8.74383888118129	-1.19438468589997
F	-1.82591823682713	6.34927275068276	2.83311248770803
C	5.16569358675566	8.17132934779599	-0.12257896287158
H	5.80128885388836	8.35409054947068	-0.98114317687794
F	0.64217394460730	6.36738508776305	1.81226299369640
C	5.71862852680573	7.74048312445080	1.04456940920661
H	6.78499016603541	7.57047158409624	1.11494861329089
C	4.86806081177663	7.50339372537591	2.15324379812719
C	5.07974146544696	7.08356842352833	3.45753794184192
C	6.24312453194580	6.72078674322336	4.23887916337496
C	7.51700520570967	7.18483473943412	3.89752982832849
H	7.63832547924592	7.85984347197595	3.06029651587277
C	8.62246080096678	6.82486772910224	4.64861914770985
H	9.60089964903567	7.20142144566483	4.37312258961387
C	8.48060354166634	6.00192660959132	5.75674497419484
H	9.34739659438447	5.72257514421725	6.34397683243338
C	7.21817408350831	5.54656258021204	6.11247564456332
H	7.09583710291445	4.90626684026000	6.97860742315704
C	6.10981268495942	5.89984739777385	5.36465156564765
H	5.12885141774294	5.53558823465240	5.64322100256385
C	1.54914415049414	7.33078447668875	3.76681106611125
C	1.27751343537505	7.78545668698013	5.06076899052811
C	0.00559222704056	7.75095495925856	5.60158885095246
C	-1.05122962629168	7.26856124847843	4.84616259522839
C	-0.82148765838352	6.82424416370677	3.55440835116323
C	0.46096760532331	6.85231452900580	3.03568545705452
C	2.89441720815764	7.34350991002886	3.22866563331395

Table A51. *XYZ* Coordinates for Optimized S_1 State of **7-F_5** in Units of Ångstrøm.

35

O	3.89491645709986	6.95236702837478	4.10454874068347
F	2.25981402373048	7.84908865394672	5.94657309682677
C	3.45693233799641	7.68072575068797	2.00006661407212
F	-0.21058682303834	7.69723098472855	6.90199308689869
C	2.90988173979339	8.20096809817356	0.81699548237887
H	1.84438947673414	8.33404417007163	0.70307889750477
F	-2.28639312575835	7.08522659539700	5.27150949717983
C	3.77793049933922	8.53954762754310	-0.21951857774014
H	3.37160478539249	8.93698183668108	-1.14189995070799
F	-1.83326119665857	6.54957397571464	2.65390407082057
C	5.15562487111245	8.38230064143586	-0.09052302449295
H	5.80213832477556	8.66022392508156	-0.91451796695922
F	0.63854735381295	6.58600863857135	1.67803596213605
C	5.72609208164686	7.88793041532926	1.08163913937610
H	6.80040353621666	7.81579480449958	1.16215959365585
C	4.87593654137801	7.53162485763625	2.14363344283991
C	5.09404785575114	7.06709173618112	3.45039206636831
C	6.23715027051077	6.71992174289054	4.21820926652855
C	7.52474393057462	6.62878508682675	3.64722975730392
H	7.65806726833837	6.79343204950210	2.58820788436452
C	8.61266778804055	6.29342086589359	4.42310154539281
H	9.59255184346684	6.22098029236413	3.96544974052982
C	8.46167738124076	6.04095471774299	5.78511079521432
H	9.32295378262101	5.77999612470277	6.38902000860333
C	7.19863292164897	6.12105990066619	6.36360123330944
H	7.07498480869334	5.92361012583253	7.42234024083213
C	6.09851163532640	6.44858955274354	5.60047233261354
H	5.11821305731388	6.51255454022037	6.05463881887757
C	1.57323494056460	7.25210723881689	3.75034573328117
C	1.29214688476813	7.49308631812242	5.11377874440273
C	0.01123723707953	7.43580560797699	5.62260227300306
C	-1.05784306104948	7.13465319269386	4.78914794109587
C	-0.82296132931683	6.88005819404296	3.44388215898006
C	0.46169847231128	6.93162653228171	2.94597949109052
C	2.90535442854292	7.30225517662566	3.23302686373561

Table A52. *XYZ* Coordinates for Optimized T_1 State of **7-F_5** in Units of Ångstrøm.
35

O	3.90458775717846	7.13008325089324	4.18220228748983
F	2.15580962171178	8.10741244547120	5.92938952106392
C	3.47012775381238	7.74044036658340	2.01986751225400
F	-0.32484530055791	7.84551526928857	6.84307756945111
C	2.91823786155129	8.20265600766370	0.83681277358247
H	1.84939184554722	8.31791034741623	0.72366675273809
F	-2.30582430524018	6.95414176903602	5.22581539334664
C	3.77464863295066	8.52045665276360	-0.22444831169073
H	3.35450161258387	8.87773827503080	-1.15694657192643
F	-1.75105686246261	6.30027320062158	2.65190564965754
C	5.14129310703178	8.39148827252483	-0.09106074319704
H	5.79031758284194	8.64820628714041	-0.91981385041467
F	0.73189014702018	6.47516199939338	1.72053150396502
C	5.71183814569991	7.94617939510944	1.11015406760943
H	6.78761000483399	7.89557823041445	1.19644136625636
C	4.87928531425432	7.61531699874447	2.16600727034535
C	5.11775530108334	7.18213419805363	3.51249379785331
C	6.25165722300931	6.77822251871741	4.24348021907154
C	7.52441109334813	6.63694596577666	3.64329929677093
H	7.64953977174013	6.82995296911821	2.58802190668122
C	8.60755135244815	6.21308732995992	4.38134992946750
H	9.57076994342913	6.10191438284791	3.89659860121965
C	8.47350912659610	5.91683323603343	5.73579510571994
H	9.32968421210253	5.58187468340509	6.30901333079449
C	7.22754087025204	6.04778676203308	6.34354215977427
H	7.11331338823065	5.81557495492164	7.39633200050033
C	6.13246246371089	6.46732089107174	5.62033434515114
H	5.16777481655698	6.56542638866793	6.09986221302311
C	1.56559352119987	7.31693845415063	3.77122288992790
C	1.23410491596210	7.62890812358561	5.10552272729104
C	-0.05179894537570	7.51167555874759	5.59094610207311
C	-1.07414526748040	7.07358636381874	4.76085306213890
C	-0.78966263140877	6.75771986825533	3.44035243853695
C	0.49994460458091	6.87566856108804	2.96611905329398
C	2.90322232125751	7.39949702165211	3.28547363017983

Table A53. *XYZ* Coordinates for Optimized S_0 State of **7-F$_6$** in Units of Ångstrøm.
35

F	16.90994324769960	11.11734706237086	1.08389658076498
F	19.54427914502606	11.60514407122140	0.88930299570508
F	21.29186725025153	9.54261418828763	0.93388091882531
F	11.48785024404567	5.63985404043746	2.55948337379415
F	11.24955596881530	3.27554237219834	3.82910209231425
F	13.38867849884372	1.65909731535134	4.06515991198459
O	16.44147636536185	6.15922555610164	1.70467250081694
C	16.17245611024352	4.83674066196429	1.76272160221256
C	17.28334633987323	4.13971147160897	1.32378079904180
C	17.54137078751330	2.76687259003626	1.08463461577068
H	16.76870130521089	2.02354304528006	1.23589726932485
C	18.76977867319793	2.40363484678795	0.62588579488380
H	18.98673402323108	1.35976770240893	0.43115438214785
C	19.77629195758766	3.37421508376238	0.36272717259836
H	20.73721928263221	3.04042203078250	-0.00996407035356
C	19.54767081206951	4.70476899877758	0.53213676408397
H	20.31663572685281	5.41898340649089	0.27297470235709
C	18.28568840912726	5.12455617807355	1.02104267348265
C	17.70823949761182	6.35904474988948	1.27555770671305
C	18.17238255351294	7.72330568775796	1.18403293675188
C	19.54235039556805	7.99356610744353	1.09760084892841
H	20.28395989940140	7.21082165155795	1.14581404969204
C	19.98723580629454	9.29167165300745	1.00162423425738
C	19.10580711250630	10.35956660665380	0.98915072357910
C	17.74934620469482	10.08639314321144	1.08883232214318
C	17.27366065003701	8.79657423963782	1.18538487982018
H	16.20577175866763	8.63689939440341	1.25637719175608
C	14.88621312921758	4.43279069999225	2.28247734943051
C	13.77147197374314	5.26703768306088	2.16702558163856
H	13.83448593396063	6.22590567477221	1.67076930354819
C	12.55988359878413	4.86299345146411	2.67970011908947
C	12.41537602868621	3.64312364396395	3.32351472526520
C	13.52618320857521	2.82248462118809	3.43483717749615
C	14.74965375208689	3.19887579347151	2.92717594440747
H	15.59748091706859	2.54689791358206	3.08762285172778

Table A54. *XYZ* Coordinates for Optimized S_1 State of **7-F_6** in Units of Ångstrøm.
35

F	16.73477871943717	10.99572524142681	1.54114115278204
F	19.23774731629690	11.63012876974364	0.76992954606901
F	21.01380738709985	9.68384976575588	0.23151764872403
F	11.74046495927595	6.04119293053416	2.99652811007725
F	11.13298256589369	3.48499572112566	3.59446994818396
F	12.99633793335420	1.56309588372165	3.33992064551732
O	16.43098036767121	6.14275641647464	1.66941811496542
C	16.20444969851215	4.79967693762015	1.78236398908575
C	17.34463482728772	4.08564827852762	1.38156143980612
C	17.64137187482592	2.71615527753465	1.26617360643281
H	16.91483184091493	1.95045743013945	1.49218773393893
C	18.90907046019826	2.34859384271652	0.81517112458490
H	19.15244985456753	1.29689856950208	0.72224400266987
C	19.86281554633501	3.30258307639729	0.47580223014403
H	20.83541613117425	2.97964476109042	0.12406358373699
C	19.59317675697992	4.66809928449113	0.56923977458522
H	20.34953307031994	5.37813460779495	0.27193723514458
C	18.32595407752611	5.06975812639719	1.02762864339287
C	17.71609208405195	6.31813803730296	1.23361468123118
C	18.12969056406657	7.67158076239124	1.10926445316669
C	19.43573667409603	8.02044223691578	0.70999483015540
H	20.18624858339016	7.27637669994305	0.49553993640636
C	19.78533855428802	9.34245573612312	0.60331637612898
C	18.88003327053420	10.36351851575401	0.87994749118636
C	17.59316974407263	10.01705594769708	1.27656220979768
C	17.20935289934214	8.70535227289851	1.39508560137271
H	16.20027394931367	8.48249076042722	1.71156542121089
C	14.91249664381816	4.44097405667585	2.25274821056412
C	13.92965520931740	5.44338689450978	2.41051614451503
H	14.14196300456425	6.47587306649329	2.17122900961368
C	12.67595338182905	5.10860663650061	2.85580435949771
C	12.34370984530167	3.79474993240705	3.16733547632996
C	13.31897204529886	2.81171304208667	3.02230914738172
C	14.58102624677439	3.10976254577708	2.57510879126466
H	15.30324818027007	2.31076353410273	2.51210082233571

Table A55. *XYZ* Coordinates for Optimized T_1 State of **7-F$_6$** in Units of Ångstrøm.
35

F	16.72315206251601	11.02710110974429	1.20627345517214
F	19.28042827365957	11.62147620588540	0.57848118197388
F	21.09759794396880	9.64410601168612	0.35648853457612
F	11.69385556195188	5.96815628022996	3.01346669249102
F	11.13321850996677	3.39482685548518	3.62152770440006
F	13.04393830563289	1.51837660172835	3.40350386154021
O	16.43104208855020	6.16451479311213	1.75911058342581
C	16.17732253946676	4.81052182016876	1.82593177413983
C	17.33534386385060	4.09878679010143	1.37430585928550
C	17.58059120329790	2.76127242390414	1.10620714274987
H	16.81091472884618	2.00987416333815	1.21760848830389
C	18.84727915908039	2.38152495806801	0.64947306051085
H	19.04584337924035	1.33793510451525	0.43592049731722
C	19.83780837495990	3.32244154781668	0.45686437593146
H	20.81361523482248	3.01230569176695	0.10356504173149
C	19.59141051777586	4.68061548463776	0.68136228772515
H	20.37753285115218	5.39415823978436	0.48375065735695
C	18.33919942347103	5.07361848000970	1.12343862003506
C	17.73617909440897	6.35371443719952	1.35635094129069
C	18.15589701027224	7.68929269714931	1.18941752662818
C	19.49075316354898	8.02192851864835	0.87036960588281
H	20.26649001450521	7.27717571763262	0.78896841673761
C	19.84305371939053	9.33123783216050	0.66963462739142
C	18.91836905593673	10.36427475771908	0.78020752425189
C	17.60658198647613	10.03794113362555	1.10959065003935
C	17.21649962055730	8.73885470501387	1.31385278555284
H	16.18489616266493	8.53506933397607	1.56319859500292
C	14.90726587871509	4.43178336267641	2.30664395167101
C	13.90370226851253	5.41449587924983	2.46595147609810
H	14.09744580352002	6.44941735944586	2.22306801450774
C	12.65297854285451	5.05375093538562	2.89684509600174
C	12.34331516868396	3.73404795047523	3.20826573373502
C	13.34127727121539	2.77352750118114	3.07823066498071
C	14.59960625623352	3.09412998718365	2.63910407119144
H	15.33935922829419	2.30838092829473	2.59636199236998

Table A56. *XYZ* Coordinates for Optimized S_0 State of **7-F_{10}** in Units of Ångstrøm.
35

O	5.02865255773902	7.69283716393752	5.46581104446999
C	5.11018238568738	9.03701275112497	5.42236720941218
C	3.89685803126234	9.55005638970994	5.01597465842106
C	3.03303269539854	8.41834485751972	4.81059681498139
C	3.78892762204623	7.30098082263713	5.10884443866128
C	3.43505603998512	10.85996873333764	4.73485824776635
C	2.16550796503001	11.00864031456512	4.26991781894868
C	1.30685284618720	9.88790126636656	4.06877719713993
C	1.71443414035440	8.61631300553417	4.32954659202165
C	6.39281154590448	9.62092929542067	5.77398454319167
C	6.50353612074173	10.67813320439423	6.67620614959299
C	7.72972056146668	11.20575613343863	7.04213337398772
C	8.89161725325993	10.68088653323658	6.50029459683531
C	8.81608992076138	9.63716259382003	5.59137280481395
C	7.58183449522309	9.12508345560059	5.23622179401804
C	3.53312640444274	5.87255309659534	5.10189362016044
C	2.34125791820897	5.33513915926842	5.58955502087819
C	2.09417133233281	3.97402077037542	5.59654663981831
C	3.05156716068692	3.09882332138981	5.11128356641587
C	4.24871619238916	3.59626535510024	4.62132781137434
C	4.47612229187085	4.96074692581348	4.61764028317747
F	5.41769335787265	11.18755090342727	7.24335514858338
F	7.80022620416998	12.19060547248071	7.92436295649418
F	10.06666955668463	11.17449142116310	6.84751871215507
F	9.92182361657082	9.14901591939350	5.05318522700882
F	7.54875595870192	8.15540615226510	4.33497667734681
F	1.40943949992177	6.13081391888894	6.10063302842056
F	0.95747336409904	3.50248549762068	6.08504390060491
F	2.82333987928681	1.79773867141459	5.11524395394347
F	5.15918534469690	2.76438819143011	4.13970978065422
F	5.61942535636437	5.39215798982831	4.10742801788846
H	4.08098264934948	11.71668930251269	4.88158975225148
H	1.79119771707629	11.99911743731893	4.03899084024569
H	0.30504843448294	10.06163981988320	3.69356289121362
H	1.05117357974343	7.77627415318656	4.16954488710255

Table A57. *XYZ* Coordinates for Optimized S_1 State of **7-F_{10}** in Units of Ångstrøm.
35

O	5.07103785731072	7.66116198377539	5.45058639986314
C	5.12474962959440	9.02924083685869	5.44930762116443
C	3.87033917885593	9.55191957283861	5.10911315727434
C	3.01025898696053	8.42371646011637	4.90057898231274
C	3.79315677963192	7.28609356652889	5.13504940618176
C	3.39656676999983	10.85003329196030	4.86718261839175
C	2.08323668918155	11.01198186118274	4.43604022614870
C	1.24875539884532	9.91418436978125	4.22832379202580
C	1.69665088324205	8.61504719654838	4.44732941119956
C	6.39625777927021	9.60472624407415	5.75184148461865
C	6.52582813482439	10.83756788618978	6.42416526869302
C	7.75033805616654	11.38425660398937	6.73946154051909
C	8.91974095261612	10.71139341127726	6.40333146563855
C	8.83925405329848	9.48776359333837	5.75078884168542
C	7.60926072482793	8.95024358005229	5.43287408002484
C	3.54534968987149	5.88079813493396	5.08497995180969
C	2.29430208149347	5.32302241039931	5.42000628175544
C	2.04976911409194	3.96832196531622	5.36919347360240
C	3.05988225000407	3.09283356175891	4.98664743835167
C	4.31284350843278	3.59722831296637	4.66258232912559
C	4.54827858938621	4.95546891291503	4.71156306728215
F	5.44228231762562	11.47649919915373	6.84871589168859
F	7.82121397695621	12.53105840324595	7.39783746529303
F	10.09587822322441	11.22991094646223	6.70561048785812
F	9.95127911272552	8.85612744605272	5.40874893545323
F	7.59687881537355	7.81594485668926	4.75259064903569
F	1.32208306836529	6.10437415693725	5.87443136239252
F	0.86515848077953	3.48982339399790	5.71742437611031
F	2.83001521392833	1.79362978627490	4.93301065521779
F	5.26988097118885	2.76845191631600	4.27573687028386
F	5.74047255749414	5.38109905056375	4.32859159522571
H	4.03106629417238	11.71234028548913	5.01168217350574
H	1.70661696839802	12.01093276892687	4.25221357725184
H	0.23395564616764	10.07263298795680	3.88391677834782
H	1.03987124569460	7.77610104513181	4.26884234466693

Table A58. *XYZ* Coordinates for Optimized T_1 State of **7-F_{10}** in Units of Ångstrøm.
35

O	5.09872953651210	7.64972013331552	5.39965460262411
C	5.15220509310039	9.02732164556434	5.43063065436686
C	3.86490460780111	9.55582961239598	5.08715678887598
C	3.00170993758760	8.43760496546407	4.92375690889708
C	3.80017379942950	7.27336122450577	5.13991281393530
C	3.40954366893306	10.83222889112183	4.80856590729203
C	2.07635011581810	11.00155845860395	4.40775748934766
C	1.23452401162944	9.91844732448910	4.26908788153222
C	1.69129855242496	8.61648877241806	4.51428484468353
C	6.40756781864836	9.60344542952496	5.75821083687309
C	6.52693336856384	10.86561732523832	6.37720778131973
C	7.74361252102710	11.42283850115137	6.70611440195056
C	8.91841767909146	10.72917618063055	6.44672451342114
C	8.84892431521994	9.47566135040482	5.85425013361540
C	7.62788932895002	8.92901214573107	5.51990876502334
C	3.54415732885602	5.87444065745758	5.06729173646164
C	2.31702831407699	5.31325668248311	5.46606974156669
C	2.06792089280195	3.95833885593525	5.41459339335328
C	3.05017555190567	3.09025962899254	4.95920943022587
C	4.27799280070807	3.59986233501348	4.55897112738047
C	4.51674305805859	4.95791196753752	4.61355387282301
F	5.43533525993439	11.53311132302864	6.73761336890856
F	7.79588021983381	12.60298317745486	7.30561979736789
F	10.08873270289859	11.25254806532556	6.76498509706275
F	9.96503630025055	8.81801831233349	5.58128761372339
F	7.64147291577151	7.75562393454633	4.90856234047200
F	1.37159270590448	6.08923904846891	5.98465508757991
F	0.90794558110101	3.47609628815607	5.83440657028108
F	2.81776985529672	1.79113649957331	4.90781169843483
F	5.20481364347352	2.77802585629580	4.09130480751105
F	5.68157185559988	5.39141696833571	4.15970876004429
H	4.05880782893878	11.69170172503344	4.89089612777411
H	1.71143012170959	11.99979219701187	4.19805741908930
H	0.20879192461893	10.06858880873264	3.95436915753748
H	1.02652678352395	7.77526570772413	4.37810852864433

9. Crystal Pair Geometries for 1,3-Diphenylisobenzofuran and Derivatives

Table A59. *XYZ* Coordinates for Pair 1 in **7α** in Units of Ångstrøm

70

O	-0.001033000	0.689697000	0.019634000
C	-3.703155000	2.544871000	-0.542196000
C	0.714095000	-3.821589000	0.005454000
C	-4.847439000	1.913127000	-0.108501000
C	-1.424327000	-2.669486000	-0.020762000
C	-0.707927000	-3.821513000	-0.029401000
C	-2.484918000	1.894026000	-0.494462000
C	-4.774009000	0.631979000	0.396167000
C	1.427683000	-2.669823000	0.017312000
C	-3.559531000	-0.025929000	0.463585000
C	0.720947000	-1.427411000	0.004378000
C	-1.117792000	-0.103645000	0.028429000
C	-0.719087000	-1.426886000	0.013342000
C	-2.396339000	0.593209000	0.006600000
C	1.114816000	-0.103172000	0.002675000
C	4.767438000	0.628516000	-0.416504000
C	4.845859000	1.916014000	0.069520000
C	3.709275000	2.550644000	0.524329000
C	2.489129000	1.899184000	0.505649000
C	2.393984000	0.593345000	0.012976000
C	3.552101000	-0.030084000	-0.455515000
H	-3.750400000	3.413946000	-0.868463000
H	1.166356000	-4.634439000	0.020728000
H	-5.667442000	2.348557000	-0.155568000
H	-2.353510000	-2.687642000	-0.036803000
H	-1.159482000	-4.634518000	-0.058536000
H	-1.719185000	2.325101000	-0.797633000
H	-5.546374000	0.207048000	0.693096000
H	2.357895000	-2.686527000	0.034126000
H	-3.518546000	-0.886368000	0.815200000
H	5.535750000	0.200724000	-0.720141000
H	5.664364000	2.355951000	0.091303000
H	3.762770000	3.421539000	0.845121000
H	1.729283000	2.331439000	0.822518000
H	3.505389000	-0.894509000	-0.796029000
O	4.088966000	0.725698000	-3.789365000
C	7.642101000	0.005915000	-4.264515000
C	6.483985000	0.629345000	-3.796024000
C	6.579130000	1.935185000	-3.303351000
C	7.799276000	2.586645000	-3.284671000
C	8.935859000	1.952015000	-3.739479000
C	8.857439000	0.664516000	-4.225504000
C	5.204816000	-0.067172000	-3.806324000
C	1.693661000	0.629209000	-3.802400000
C	3.370913000	-1.390887000	-3.795658000
C	2.972208000	-0.067646000	-3.780571000
C	4.810948000	-1.391412000	-3.804622000

C	0.530469000	0.010070000	-3.345415000
C	5.517684000	-2.633823000	-3.791688000
C	-0.684009000	0.667980000	-3.412833000
C	1.605082000	1.930027000	-4.303462000
C	3.382073000	-3.785514000	-3.838402000
C	2.665673000	-2.633487000	-3.829762000
C	-0.757439000	1.949128000	-3.917501000
C	4.804095000	-3.785589000	-3.803545000
C	0.386845000	2.580872000	-4.351197000
H	7.595390000	-0.858510000	-4.605030000
H	5.819283000	2.367439000	-2.986481000
H	7.852771000	3.457540000	-2.963879000
H	9.754365000	2.391951000	-3.717697000
H	9.625750000	0.236724000	-4.529141000
H	0.571453000	-0.850368000	-2.993800000
H	6.447895000	-2.650527000	-3.774873000
H	-1.456374000	0.243049000	-3.115904000
H	2.370814000	2.361101000	-4.606634000
H	2.930517000	-4.598519000	-3.867536000
H	1.736489000	-2.651642000	-3.845803000
H	-1.577443000	2.384557000	-3.964568000
H	5.256356000	-4.598440000	-3.788271000
H	0.339599000	3.449947000	-4.677464000

Table A60. *XYZ* Coordinates for Pair 2 in **7α** in Units of Ångstrøm
70

O	0.001033000	-0.689697000	0.019634000
C	-3.552101000	0.030084000	-0.455515000
C	-2.393984000	-0.593345000	0.012976000
C	-2.489130000	-1.899184000	0.505650000
C	-3.709275000	-2.550644000	0.524328000
C	-4.845859000	-1.916014000	0.069521000
C	-4.767438000	-0.628516000	-0.416504000
C	-1.114816000	0.103172000	0.002675000
C	2.396338000	-0.593209000	0.006600000
C	0.719086000	1.426886000	0.013342000
C	1.117792000	0.103645000	0.028429000
C	-0.720947000	1.427411000	0.004378000
C	3.559531000	0.025929000	0.463584000
C	-1.427684000	2.669823000	0.017312000
C	4.774009000	-0.631979000	0.396167000
C	2.484918000	-1.894026000	-0.494462000
C	0.707926000	3.821513000	-0.029401000
C	1.424327000	2.669486000	-0.020762000
C	4.847438000	-1.913127000	-0.108500000
C	-0.714095000	3.821589000	0.005454000
C	3.703155000	-2.544871000	-0.542196000
H	-3.505390000	0.894509000	-0.796029000
H	-1.729282000	-2.331439000	0.822518000
H	-3.762770000	-3.421539000	0.845120000
H	-5.664364000	-2.355951000	0.091302000
H	-5.535750000	-0.200724000	-0.720140000
H	3.518547000	0.886368000	0.815199000
H	-2.357894000	2.686527000	0.034126000
H	5.546374000	-0.207048000	0.693096000
H	1.719185000	-2.325101000	-0.797634000
H	1.159482000	4.634518000	-0.058536000
H	2.353511000	2.687642000	-0.036803000
H	5.667442000	-2.348557000	-0.155568000
H	-1.166355000	4.634439000	0.020728000
H	3.750400000	-3.413946000	-0.868464000
O	-4.411866000	3.546823000	4.717553000
C	-5.131041000	2.789266000	1.213624000
C	-4.587493000	3.427739000	2.329999000
C	-4.115184000	4.736907000	2.188588000
C	-4.189269000	5.376923000	0.964498000
C	-4.717535000	4.727576000	-0.131272000
C	-5.184573000	3.436646000	-0.007178000
C	-4.500438000	2.743303000	3.612762000
C	-4.254037000	3.472912000	7.108493000
C	-4.347185000	1.437160000	5.452882000
C	-4.316370000	2.764199000	5.837821000
C	-4.458274000	1.422919000	4.017181000
C	-3.709853000	2.868865000	8.241708000
C	-4.483756000	0.174032000	3.322298000

C	-3.697169000	3.537627000	9.452057000
C	-4.759835000	4.770045000	7.220957000
C	-4.367961000	-0.957749000	5.465910000
C	-4.319420000	0.201042000	6.169697000
C	-4.207452000	4.814918000	9.549839000
C	-4.434068000	-0.970984000	4.045059000
C	-4.727184000	5.431952000	8.433719000
H	-5.459192000	1.922357000	1.292025000
H	-3.749314000	5.179113000	2.920169000
H	-3.881332000	6.250064000	0.880675000
H	-4.758032000	5.159916000	-0.953106000
H	-5.537887000	2.998940000	-0.748181000
H	-3.353909000	2.011208000	8.183447000
H	-4.532814000	0.148668000	2.393425000
H	-3.342192000	3.122662000	10.205101000
H	-5.120626000	5.191161000	6.474917000
H	-4.357299000	-1.766666000	5.925548000
H	-4.269335000	0.191547000	7.097797000
H	-4.200348000	5.257662000	10.367242000
H	-4.443228000	-1.787915000	3.600043000
H	-5.057484000	6.298528000	8.496349000

Table A61. *XYZ* Coordinates for Pair 1 in **7β** in Units of Ångstrøm

70

O	-0.002216000	0.687901000	-0.024248000
C	3.694786000	2.535832000	0.550944000
C	-3.710715000	2.539033000	-0.519114000
C	4.836954000	1.909044000	0.111652000
C	-0.697821000	-3.811113000	-0.000052000
C	4.767077000	0.640176000	-0.403323000
C	0.722372000	-3.805175000	0.033445000
C	-4.766599000	0.618047000	0.414692000
C	2.477988000	1.884548000	0.499673000
C	-4.844453000	1.903646000	-0.069387000
C	1.429766000	-2.652933000	0.021148000
C	-2.492727000	1.887588000	-0.503168000
C	-1.418342000	-2.664105000	-0.015711000
C	-0.716401000	-1.422779000	-0.003623000
C	3.553031000	-0.017970000	-0.473114000
C	2.390510000	0.597848000	-0.005502000
C	-3.549787000	-0.033699000	0.449871000
C	1.115699000	-0.100565000	-0.031094000
C	-2.395029000	0.587321000	-0.015288000
C	0.721393000	-1.421072000	-0.013903000
C	-1.115356000	-0.105686000	-0.006327000
H	3.742104000	3.403086000	0.884066000
H	-3.764301000	3.411761000	-0.835810000
H	5.656523000	2.345920000	0.163836000
H	-1.145997000	-4.625322000	-0.012152000
H	5.539207000	0.220741000	-0.707509000
H	1.177469000	-4.615438000	0.064156000
H	-5.533466000	0.188761000	0.718755000
H	1.711510000	2.312154000	0.806706000
H	-5.663326000	2.342393000	-0.092172000
H	2.359245000	-2.666307000	0.035528000
H	-1.733226000	2.319509000	-0.820283000
H	-2.347863000	-2.685839000	-0.034254000
H	3.510701000	-0.874287000	-0.833011000
H	-3.501270000	-0.899360000	0.788315000
O	-4.084117000	0.695501000	3.786052000
C	-0.387114000	2.543432000	4.361245000
C	-7.792616000	2.546634000	3.291185000
C	0.755054000	1.916644000	3.921952000
C	-4.779721000	-3.803514000	3.810248000
C	0.685178000	0.647777000	3.406977000
C	-3.359528000	-3.797576000	3.843746000
C	-8.848499000	0.625647000	4.224993000
C	-1.603911000	1.892148000	4.309973000
C	-8.926353000	1.911246000	3.740912000
C	-2.652134000	-2.645334000	3.831448000
C	-6.574628000	1.895188000	3.307131000
C	-5.500242000	-2.656506000	3.794589000
C	-4.798302000	-1.415180000	3.806677000

C	-0.528868000	-0.010370000	3.337186000
C	-1.691389000	0.605448000	3.804797000
C	-7.631687000	-0.026099000	4.260172000
C	-2.966200000	-0.092966000	3.779205000
C	-6.476930000	0.594922000	3.795011000
C	-3.360507000	-1.413473000	3.796397000
C	-5.197256000	-0.098086000	3.803973000
H	-0.339796000	3.410687000	4.694367000
H	-7.846201000	3.419362000	2.974490000
H	1.574623000	2.353521000	3.974136000
H	-5.227898000	-4.617722000	3.798148000
H	1.457307000	0.228341000	3.102790000
H	-2.904430000	-4.607839000	3.874456000
H	-9.615367000	0.196362000	4.529056000
H	-2.370389000	2.319754000	4.617006000
H	-9.745226000	2.349993000	3.718127000
H	-1.722655000	-2.658708000	3.845828000
H	-5.815126000	2.327110000	2.990017000
H	-6.429764000	-2.678240000	3.776046000
H	-0.571199000	-0.866687000	2.977289000
H	-7.583170000	-0.891760000	4.598615000

Table A62. *XYZ* Coordinates for Pair 2 in **7β** in Units of Ångstrøm
70

O	-0.002216000	0.687901000	-0.024248000
C	3.694786000	2.535832000	0.550944000
C	-3.710715000	2.539033000	-0.519114000
C	4.836954000	1.909044000	0.111652000
C	-0.697821000	-3.811113000	-0.000052000
C	4.767077000	0.640176000	-0.403323000
C	0.722372000	-3.805175000	0.033445000
C	-4.766599000	0.618047000	0.414692000
C	2.477988000	1.884548000	0.499673000
C	-4.844453000	1.903646000	-0.069387000
C	1.429766000	-2.652933000	0.021148000
C	-2.492727000	1.887588000	-0.503168000
C	-1.418342000	-2.664105000	-0.015711000
C	-0.716401000	-1.422779000	-0.003623000
C	3.553031000	-0.017970000	-0.473114000
C	2.390510000	0.597848000	-0.005502000
C	-3.549787000	-0.033699000	0.449871000
C	1.115699000	-0.100565000	-0.031094000
C	-2.395029000	0.587321000	-0.015288000
C	0.721393000	-1.421072000	-0.013903000
C	-1.115356000	-0.105686000	-0.006327000
H	3.742104000	3.403086000	0.884066000
H	-3.764301000	3.411761000	-0.835810000
H	5.656523000	2.345920000	0.163836000
H	-1.145997000	-4.625322000	-0.012152000
H	5.539207000	0.220741000	-0.707509000
H	1.177469000	-4.615438000	0.064156000
H	-5.533466000	0.188761000	0.718755000
H	1.711510000	2.312154000	0.806706000
H	-5.663326000	2.342393000	-0.092172000
H	2.359245000	-2.666307000	0.035528000
H	-1.733226000	2.319509000	-0.820283000
H	-2.347863000	-2.685839000	-0.034254000
H	3.510701000	-0.874287000	-0.833011000
H	-3.501270000	-0.899360000	0.788315000
O	4.431194000	-3.417361000	4.754093000
C	4.763466000	-5.235521000	8.495404000
C	4.205295000	-5.297561000	1.034098000
C	4.242360000	-4.604144000	9.600031000
C	4.472222000	1.076818000	4.028653000
C	3.724693000	-3.339617000	9.485578000
C	4.408008000	1.080900000	5.447796000
C	5.196272000	-3.377055000	0.030755000
C	4.791521000	-4.593021000	7.273192000
C	4.727547000	-4.666693000	-0.070705000
C	4.355016000	-0.066509000	6.161146000
C	4.132955000	-4.637652000	2.245467000
C	4.514044000	-0.075204000	3.317234000
C	4.486368000	-1.311549000	4.027476000

C	3.734037000	-2.690371000	8.264788000
C	4.284717000	-3.310711000	7.141722000
C	5.143198000	-2.716710000	1.242270000
C	4.342056000	-2.621293000	5.863054000
C	4.604004000	-3.333183000	2.366876000
C	4.377241000	-1.303438000	5.461138000
C	4.520169000	-2.631340000	3.638997000
H	5.098503000	-6.099952000	8.571894000
H	3.899046000	-6.172948000	0.965308000
H	4.241060000	-5.034976000	10.424446000
H	4.485373000	1.887813000	3.574716000
H	3.365247000	-2.917132000	10.231864000
H	4.401772000	1.894479000	5.897944000
H	5.549395000	-2.950827000	-0.716547000
H	5.153475000	-5.023615000	6.532800000
H	4.764153000	-5.111219000	-0.885952000
H	4.305346000	-0.046633000	7.089292000
H	3.767336000	-5.066663000	2.984543000
H	4.559323000	-0.060004000	2.388501000
H	3.372021000	-1.837041000	8.191514000
H	5.471540000	-1.848266000	1.307550000

Table A63. *XYZ* Coordinates for Pair 1 in **7-F$_{1a}$** in Units of Ångstrøm

70

symmetry c1

O	-0.294328200	-0.566039300	0.008946900
F	5.858159500	-1.635477600	0.038849800
C	4.662222100	-1.091169100	0.058318600
C	0.114674700	1.633889800	-0.001966600
C	-4.879619100	-2.503460500	-0.098142800
H	-5.626906700	-3.090335600	-0.128622800
C	-1.314004100	1.422825400	0.013404900
C	-2.672540500	-0.817578900	-0.001626500
C	-1.508305100	0.058307600	0.024914300
C	2.058831700	-0.118897400	0.009404500
C	3.123106300	0.659924700	-0.460637500
H	2.951045100	1.529299700	-0.804633300
C	0.633020200	2.963245500	0.001031800
H	1.570026400	3.119829400	0.006554700
C	0.697092300	0.382635800	-0.009048900
C	-2.200771300	2.548298800	0.002817100
H	-3.142024500	2.424225100	0.001056900
C	-1.665915500	3.788851000	-0.002515800
H	-2.245948900	4.542748200	-0.006397500
C	4.424465400	0.180784800	-0.433030000
H	5.142879500	0.718308400	-0.746307900
C	2.339345200	-1.403122600	0.508489500
H	1.629391300	-1.942721300	0.836843900
C	-0.245226300	3.999166000	-0.003811900
H	0.089892100	4.887539200	-0.008467400
C	-3.917147200	-0.383491800	0.460437800
H	-4.010440200	0.492753200	0.816067800
C	-2.564560700	-2.120320000	-0.500349300
H	-1.722185100	-2.431375200	-0.809951500
C	3.630109200	-1.889607600	0.526195900
H	3.809140200	-2.763556400	0.854218900
C	-3.660925800	-2.966377300	-0.554036100
H	-3.575145500	-3.849236500	-0.895989400
C	-5.020302700	-1.225810600	0.401757900
H	-5.868090700	-0.923898300	0.705051200
O	-4.285863000	-1.146790000	3.784899000
C	0.670686000	-1.671938000	3.834232000
H	1.557611000	-2.011313000	3.845494000
C	-3.876852000	1.053137000	3.773945000
F	-9.824255000	-4.050524000	3.714303000
C	-8.871162000	-3.084196000	3.677885000
C	-5.305531000	0.842079000	3.789333000
C	-6.664076000	-1.398321000	3.774352000
C	-5.499837000	-0.522438000	3.800867000
C	-1.932701000	-0.699657000	3.785327000
C	-0.868428000	0.079153000	3.315261000
H	-1.040489000	0.948523000	2.971253000
C	-3.358501000	2.382491000	3.776916000
H	-2.421494000	2.539072000	3.782428000

C	-3.294439000	-0.198119000	3.766878000
C	-6.192294000	1.967555000	3.778735000
H	-7.133548000	1.843485000	3.776986000
C	-5.657434000	3.208105000	3.773377000
H	-6.237464000	3.962005000	3.769488000
C	0.432929000	-0.399991000	3.342865000
H	1.151342000	0.137525000	3.029571000
C	-1.652188000	-1.983875000	4.284430000
H	-2.362141000	-2.523466000	4.612800000
C	-4.236744000	3.418415000	3.772064000
H	-3.901622000	4.306787000	3.767390000
C	-7.908677000	-0.964221000	4.236421000
H	-8.001963000	-0.087970000	4.592037000
C	-6.556106000	-2.701070000	3.275650000
H	-5.713735000	-3.012134000	2.966045000
C	-0.361426000	-2.470365000	4.302132000
H	-0.182395000	-3.344309000	4.630168000
C	-7.652475000	-3.547124000	3.221988000
H	-7.566708000	-4.429991000	2.880055000
C	-9.011836000	-1.806537000	4.177766000
H	-9.859620000	-1.504616000	4.481062000

Table A64. *XYZ* Coordinates for Pair 2 in **7-F_{1a}** in Units of Ångstrøm

70

O	0.285536000	0.559987800	-0.016776900
C	4.866160900	2.524836800	-0.070012300
H	5.613369300	3.110893200	-0.082902600
C	1.325780000	-1.421076800	0.002357000
F	-5.863303100	1.699467800	0.044949400
C	-4.667435200	1.057730400	0.084662200
C	-0.101524800	-1.641267100	-0.013273000
C	-2.060940800	0.098237200	-0.006266300
C	-0.689993100	-0.394985700	-0.029910700
C	2.665816600	0.827497900	-0.016417800
C	3.912222000	0.399372000	0.456184900
H	4.004232300	-0.480763600	0.803552400
C	2.213487600	-2.538159700	0.004224000
H	3.154958900	-2.411142800	-0.001055400
C	1.512827000	-0.053631800	0.004457000
C	-0.616496100	-2.978324400	0.001925400
H	-1.552425900	-3.137660100	0.003567400
C	0.260760700	-4.005647300	0.011779300
H	-0.070850300	-4.897163100	0.018749100
C	5.014135600	1.241235400	0.426271400
H	5.858980000	0.940945500	0.741322900
C	2.555069200	2.135416400	-0.520493300
H	1.717700200	2.440129100	-0.850625000
C	1.680214700	-3.787153500	0.013341400
H	2.262664600	-4.536968500	0.021252600
C	-3.121563400	-0.685673200	-0.466206400
H	-2.951734500	-1.551730300	-0.818463200
C	-2.342760600	1.376649200	0.487453100
H	-1.630008000	1.923690000	0.795559300
C	3.644689200	2.981217600	-0.540537100
H	3.557970200	3.867829700	-0.871944600
C	-3.640076000	1.861501800	0.538331500
H	-3.819033400	2.731617900	0.876896500
C	-4.424268300	-0.206368500	-0.410318300
H	-5.144902800	-0.746249400	-0.712141100
O	-3.444840000	-4.262075000	4.730562000
F	-2.792195000	-6.105478000	10.661297000
C	-2.992284000	-5.421447000	9.557221000
C	-3.714789000	-2.157738000	5.441889000
C	-3.455043000	-5.554092000	-0.077821000
H	-3.404936000	-6.028271000	-0.900277000
C	-3.822385000	-2.183182000	4.001860000
C	-3.602624000	-4.201089000	2.345051000
C	-3.654519000	-3.496773000	3.619638000
C	-3.307319000	-4.126653000	7.118039000
C	-2.864283000	-3.428168000	8.247650000
H	-2.664737000	-2.501396000	8.176756000
C	-3.864070000	-0.922493000	6.140289000
H	-3.811494000	-0.890419000	7.088306000

C	-3.478124000	-3.457375000	5.841676000
C	-4.049719000	-0.964918000	3.282616000
H	-4.111037000	-0.965175000	2.335201000
C	-4.176618000	0.182486000	3.984348000
H	-4.330862000	0.996249000	3.516573000
C	-2.710906000	-4.069152000	9.468096000
H	-2.417495000	-3.586715000	10.232529000
C	-3.590890000	-5.497658000	7.248198000
H	-3.898140000	-5.985536000	6.492823000
C	-4.083478000	0.206057000	5.417304000
H	-4.177642000	1.034014000	5.872446000
C	-4.227427000	-3.686886000	1.206544000
H	-4.711863000	-2.871164000	1.260405000
C	-2.914618000	-5.414515000	2.236595000
H	-2.492349000	-5.779925000	3.004950000
C	-3.427606000	-6.142953000	8.456497000
H	-3.610150000	-7.072644000	8.532587000
C	-2.834411000	-6.094157000	1.031454000
H	-2.363155000	-6.917497000	0.970144000
C	-4.143418000	-4.361224000	-0.005110000
H	-4.558619000	-4.003104000	-0.780507000

Table A65. *XYZ* Coordinates for Pair 1 in **7-F_{2a}** in Units of Ångstrøm

70

O	0.496426500	-0.512450000	-0.010319700
F	-5.309369200	0.962598600	-0.004872400
F	-3.509798300	-3.353451000	-0.094679600
C	1.700170500	0.133020300	-0.030961300
C	1.470672500	1.500501700	-0.009015600
C	-0.516315300	0.410511000	0.018915200
C	0.035251300	1.677670700	0.029338900
C	2.888242400	-0.710439300	-0.034623300
C	-1.861700900	-0.134394100	0.003126600
C	1.769085800	3.874462600	0.071058500
H	2.333972600	4.638052300	0.087347000
C	-3.340718200	-2.019327600	-0.046388000
C	2.801465100	-2.055057300	0.343992700
H	1.959034700	-2.432080100	0.569246500
C	-4.235316300	0.132325300	-0.013864600
C	-0.501936500	2.999641600	0.080956200
H	-1.441462200	3.137283800	0.106480100
C	2.327764800	2.636935400	0.027746900
H	3.271974600	2.531613800	0.021919300
C	4.135760900	-0.199759100	-0.403456200
H	4.205197400	0.704152700	-0.687402300
C	-2.055516300	-1.525044800	-0.021229500
H	-1.311485200	-2.115673800	-0.020433000
C	-4.469756800	-1.226272100	-0.041386400
H	-5.346900100	-1.590622600	-0.056129700
C	3.950000800	-2.839146400	0.390847800
H	3.888119200	-3.747543600	0.661778100
C	-2.989565500	0.698626600	0.004166900
H	-2.890340700	1.643333300	0.016648800
C	5.185293600	-2.308405700	0.046403900
H	5.967530100	-2.845479500	0.089170900
C	0.348012300	4.054764600	0.092866200
H	-0.007121800	4.935670500	0.116265300
C	5.266344400	-0.985146300	-0.361420800
H	6.105975300	-0.618916800	-0.613173900
O	-0.210573000	0.855550000	3.448680000
F	-6.016369000	2.330599000	3.454128000
F	-4.216798000	-1.985451000	3.364320000
C	0.993171000	1.501020000	3.428039000
C	0.763673000	2.868502000	3.449984000
C	-1.223315000	1.778511000	3.477915000
C	-0.671749000	3.045671000	3.488339000
C	2.181242000	0.657561000	3.424377000
C	-2.568701000	1.233606000	3.462127000
C	1.062086000	5.242463000	3.530058000
H	1.626973000	6.006052000	3.546347000
C	-4.047718000	-0.651328000	3.412612000
C	2.094465000	-0.687057000	3.802993000
H	1.252035000	-1.064080000	4.028246000

C	-4.942316000	1.500325000	3.445135000
C	-1.208937000	4.367642000	3.539956000
H	-2.148462000	4.505284000	3.565480000
C	1.620765000	4.004935000	3.486747000
H	2.564975000	3.899614000	3.480919000
C	3.428761000	1.168241000	3.055544000
H	3.498197000	2.072153000	2.771598000
C	-2.762516000	-0.157045000	3.437771000
H	-2.018485000	-0.747674000	3.438567000
C	-5.176757000	0.141728000	3.417614000
H	-6.053900000	-0.222623000	3.402870000
C	3.243001000	-1.471146000	3.849848000
H	3.181119000	-2.379544000	4.120778000
C	-3.696565000	2.066627000	3.463167000
H	-3.597341000	3.011333000	3.475649000
C	4.478294000	-0.940406000	3.505404000
H	5.260530000	-1.477480000	3.548171000
C	-0.358988000	5.422765000	3.551866000
H	-0.714122000	6.303670000	3.575265000
C	4.559344000	0.382854000	3.097579000
H	5.398975000	0.749083000	2.845826000

Table A66. *XYZ* Coordinates for Pair 1 in **7-F_{2b}** in Units of Ångstrøm

70

F	6.233201200	-2.090124300	-0.078096600
F	-6.237594200	-2.093309400	-0.096318500
C	4.905312100	-0.138500400	0.045470800
C	5.011592100	-1.529054200	-0.021161000
C	3.638452400	0.445980300	0.074948900
C	3.874551300	-2.342859800	-0.046889300
C	2.456141900	-0.337914200	0.049528900
C	2.614292700	-1.741127400	-0.011207000
C	1.122008400	0.290411100	0.114050100
C	0.719502000	1.641504700	0.010140000
C	-1.126375400	0.297714900	0.097437800
C	1.434137200	2.879142900	-0.086405700
C	-0.714528800	1.652498400	0.096970000
C	-2.463749600	-0.326211700	0.070546200
C	0.725475500	4.060575100	-0.153349000
C	-1.412921900	2.903830000	0.053236700
C	-3.649803300	0.456407900	0.075831900
C	-2.621214400	-1.731298200	0.014306800
C	-0.697586700	4.073816100	-0.088520200
C	-4.914424100	-0.128703600	0.009490800
C	-3.880990200	-2.334722100	-0.042697400
C	-5.018411400	-1.522658100	-0.047759200
O	0.002454100	-0.479745200	0.058777300
H	3.966092800	-3.422688100	-0.099984900
H	5.802844100	0.475724300	0.051697600
H	3.588218700	1.532591700	0.082693300
H	1.732684900	-2.373198800	-0.033040900
H	2.526630500	2.887367700	-0.073629300
H	1.249949000	5.013864400	-0.225038300
H	-2.494669600	2.939350000	0.153879000
H	-3.604413600	1.541223200	0.159718000
H	-1.736721800	-2.357872500	0.002942200
H	-1.214109500	5.035182300	-0.112445400
H	-5.809221700	0.484175700	-0.021221000
H	-3.980599300	-3.420534300	-0.079761000
F	4.155202000	-2.489124000	3.392903000
F	-8.315594000	-2.492310000	3.374681000
C	2.827312000	-0.537500000	3.516471000
C	2.933593000	-1.928054000	3.449838000
C	1.560452000	0.046980000	3.545949000
C	1.796551000	-2.741860000	3.424111000
C	0.378142000	-0.736914000	3.520529000
C	0.536293000	-2.140127000	3.459793000
C	-0.955992000	-0.108589000	3.585050000
C	-1.358498000	1.242505000	3.481140000
C	-3.204375000	-0.101285000	3.568438000
C	-0.643863000	2.480143000	3.384594000
C	-2.792529000	1.253498000	3.567970000
C	-4.541750000	-0.725212000	3.541546000

C	-1.352524000	3.661575000	3.317651000
C	-3.490922000	2.504830000	3.524237000
C	-5.727803000	0.057408000	3.546832000
C	-4.699215000	-2.130298000	3.485307000
C	-2.775587000	3.674816000	3.382480000
C	-6.992424000	-0.527704000	3.480491000
C	-5.958990000	-2.733722000	3.428303000
C	-7.096412000	-1.921658000	3.423241000
O	-2.075546000	-0.878745000	3.529777000
H	1.888093000	-3.821688000	3.371015000
H	3.724844000	0.076724000	3.522698000
H	1.510219000	1.133592000	3.553693000
H	-0.345315000	-2.772199000	3.437959000
H	0.448630000	2.488368000	3.397371000
H	-0.828051000	4.614864000	3.245962000
H	-4.572670000	2.540350000	3.624879000
H	-5.682414000	1.142223000	3.630718000
H	-3.814722000	-2.756873000	3.473942000
H	-3.292110000	4.636182000	3.358554000
H	-7.887222000	0.085176000	3.449779000
H	-6.058599000	-3.819534000	3.391239000

Table A67. *XYZ* Coordinates for Pair 1 in **7-F_{2c}** in Units of Ångstrøm

70

F	-3.607629200	-3.509560200	0.015966100
O	-0.005602200	-0.191070800	0.051523800
C	-3.611287600	-2.151000500	-0.016204600
C	-4.826109000	-1.498570500	-0.120498900
H	-5.643366400	-1.979954000	-0.186245000
F	3.633454700	-3.506146200	0.135879300
C	-4.802613300	-0.133925400	-0.123531000
H	-5.620304700	0.347279800	-0.167783400
C	-3.606433500	0.561914100	-0.064225000
H	-3.613303600	1.511810100	-0.092401700
C	-2.388502300	-0.117017600	0.037372600
C	-2.402912300	-1.504985900	0.047510300
H	-1.591740200	-1.997330700	0.096968600
C	-1.125599200	0.598195500	0.070909700
C	-0.731053900	1.925483500	0.079140900
C	-1.414788200	3.166998900	0.091235800
H	-2.363532600	3.188932300	0.134752800
C	-0.708480100	4.320239000	0.038147900
H	-1.170850700	5.149750100	0.024205200
C	0.716820300	4.308873700	0.004210300
H	1.186499200	5.134452600	-0.026507700
C	1.418048300	3.150675700	0.014803300
H	2.367468500	3.166826300	-0.000116400
C	0.728650600	1.915942400	0.047320400
C	1.122264700	0.591262400	0.024416900
C	2.371346300	-0.111405500	-0.040614900
C	2.412727300	-1.510718300	0.042322200
H	1.607594800	-2.012091800	0.107859800
C	3.618456500	-2.143830400	0.030289400
C	4.827187000	-1.491321200	-0.080894200
H	5.649214700	-1.966802500	-0.092570900
C	4.788187500	-0.117038600	-0.172657700
H	5.600597100	0.368892400	-0.245263400
C	3.581627700	0.567658300	-0.161328700
H	3.580234600	1.514635800	-0.235037200
F	-7.208629000	-1.214560000	-3.228034000
O	-3.606602000	2.103929000	-3.192476000
C	-7.212288000	0.144000000	-3.260205000
C	-8.427109000	0.796430000	-3.364499000
H	-9.244366000	0.315046000	-3.430245000
F	0.032455000	-1.211146000	-3.108121000
C	-8.403613000	2.161075000	-3.367531000
H	-9.221305000	2.642280000	-3.411783000
C	-7.207434000	2.856914000	-3.308225000
H	-7.214304000	3.806810000	-3.336402000
C	-5.989502000	2.177982000	-3.206627000
C	-6.003912000	0.790014000	-3.196490000
H	-5.192740000	0.297669000	-3.147031000
C	-4.726599000	2.893196000	-3.173090000

C	-4.332054000	4.220484000	-3.164859000
C	-5.015788000	5.461999000	-3.152764000
H	-5.964533000	5.483932000	-3.109247000
C	-4.309480000	6.615239000	-3.205852000
H	-4.771851000	7.444750000	-3.219795000
C	-2.884180000	6.603874000	-3.239790000
H	-2.414501000	7.429453000	-3.270508000
C	-2.182952000	5.445676000	-3.229197000
H	-1.233531000	5.461826000	-3.244116000
C	-2.872349000	4.210942000	-3.196680000
C	-2.478735000	2.886262000	-3.219583000
C	-1.229654000	2.183594000	-3.284615000
C	-1.188273000	0.784282000	-3.201678000
H	-1.993405000	0.282908000	-3.136140000
C	0.017456000	0.151170000	-3.213711000
C	1.226187000	0.803679000	-3.324894000
H	2.048215000	0.328197000	-3.336571000
C	1.187188000	2.177961000	-3.416658000
H	1.999597000	2.663892000	-3.489263000
C	-0.019372000	2.862658000	-3.405329000
H	-0.020765000	3.809636000	-3.479037000

Table A68. *XYZ* Coordinates for Pair 2 in **7-F_{2c}** in Units of Ångstrøm

70

F	-3.607629200	-3.509560200	0.015966100
O	-0.005602200	-0.191070800	0.051523800
C	-3.611287600	-2.151000500	-0.016204600
C	-4.826109000	-1.498570500	-0.120498900
H	-5.643366400	-1.979954000	-0.186245000
F	3.633454700	-3.506146200	0.135879300
C	-4.802613300	-0.133925400	-0.123531000
H	-5.620304700	0.347279800	-0.167783400
C	-3.606433500	0.561914100	-0.064225000
H	-3.613303600	1.511810100	-0.092401700
C	-2.388502300	-0.117017600	0.037372600
C	-2.402912300	-1.504985900	0.047510300
H	-1.591740200	-1.997330700	0.096968600
C	-1.125599200	0.598195500	0.070909700
C	-0.731053900	1.925483500	0.079140900
C	-1.414788200	3.166998900	0.091235800
H	-2.363532600	3.188932300	0.134752800
C	-0.708480100	4.320239000	0.038147900
H	-1.170850700	5.149750100	0.024205200
C	0.716820300	4.308873700	0.004210300
H	1.186499200	5.134452600	-0.026507700
C	1.418048300	3.150675700	0.014803300
H	2.367468500	3.166826300	-0.000116400
C	0.728650600	1.915942400	0.047320400
C	1.122264700	0.591262400	0.024416900
C	2.371346300	-0.111405500	-0.040614900
C	2.412727300	-1.510718300	0.042322200
H	1.607594800	-2.012091800	0.107859800
C	3.618456500	-2.143830400	0.030289400
C	4.827187000	-1.491321200	-0.080894200
H	5.649214700	-1.966802500	-0.092570900
C	4.788187500	-0.117038600	-0.172657700
H	5.600597100	0.368892400	-0.245263400
C	3.581627700	0.567658300	-0.161328700
H	3.580234600	1.514635800	-0.235037200
F	2.792029000	7.960934000	5.461442000
O	0.559232000	3.769598000	6.659587000
C	1.985374000	7.118927000	4.763542000
C	1.645121000	7.457816000	3.466731000
H	1.948781000	8.266604000	3.069725000
F	2.175309000	3.734668000	11.310033000
C	0.855970000	6.581256000	2.779928000
H	0.623852000	6.769275000	1.878315000
C	0.386544000	5.422129000	3.375430000
H	-0.181656000	4.838825000	2.885482000
C	0.739533000	5.099641000	4.689213000
C	1.546970000	5.982077000	5.393571000
H	1.790360000	5.802166000	6.294261000
C	0.231476000	3.903234000	5.335794000

C	-0.563547000	2.831240000	4.966750000
C	-1.200079000	2.431358000	3.765117000
H	-1.084024000	2.940241000	2.971354000
C	-1.975538000	1.322200000	3.755913000
H	-2.418180000	1.069610000	2.954455000
C	-2.136756000	0.527748000	4.928780000
H	-2.682434000	-0.249383000	4.891032000
C	-1.531402000	0.853036000	6.095395000
H	-1.646183000	0.304825000	6.862320000
C	-0.727477000	2.014760000	6.166053000
C	-0.023390000	2.639686000	7.177964000
C	0.204814000	2.400625000	8.574012000
C	1.072423000	3.220480000	9.310054000
H	1.493033000	3.966977000	8.898058000
C	1.307967000	2.934821000	10.620656000
C	0.723711000	1.884227000	11.294494000
H	0.906677000	1.719053000	12.211657000
C	-0.136916000	1.083433000	10.575714000
H	-0.555107000	0.346199000	11.003514000
C	-0.402599000	1.337251000	9.237913000
H	-1.006649000	0.776228000	8.766131000

Table A69. *XYZ* Coordinates for Pair 1 in **7-F_{3a}** in Units of Ångstrøm

70

O	-0.788507600	0.465840900	0.149216300
F	4.925403300	-1.381366000	0.223121600
C	0.154573300	-0.510561700	0.157070300
F	3.418754600	3.008120400	-0.263265200
F	5.448419200	1.242163100	-0.115546400
C	-4.015400000	3.081962900	-0.103250500
H	-3.863311800	4.012101400	-0.222175300
C	-2.030192600	-0.083338500	0.054551800
C	1.537207300	-0.079044900	0.128171300
C	-1.900584700	-1.460280400	-0.011512500
C	-0.930772900	-4.097684200	-0.211211900
H	-0.629661300	-4.994367000	-0.281801600
C	4.173875700	0.804732500	-0.021686100
C	-3.144325100	0.825335900	0.045177200
C	-5.540470700	1.230971700	0.153480000
H	-6.422940300	0.887017000	0.236557000
C	3.115539100	1.689013800	-0.082803900
C	-5.311556400	2.611405300	0.047573100
H	-6.041653700	3.219180400	0.079617800
C	-0.489387500	-1.740562900	0.055826800
C	-2.815688500	-2.540387300	-0.154180300
H	-3.753199600	-2.380490200	-0.180078200
C	-0.023370300	-3.084032600	-0.070000300
H	0.905779900	-3.273390200	-0.055599000
C	2.601428100	-0.971877500	0.208105300
H	2.438570800	-1.901132200	0.324137800
C	3.876222200	-0.503956200	0.119638900
C	-4.436852300	0.372128100	0.133069500
H	-4.587719000	-0.564425400	0.182631100
C	-2.947993600	2.207507300	-0.082191200
H	-2.063982900	2.548889900	-0.155454700
C	1.819723400	1.314379100	-0.022462100
H	1.118576800	1.954368600	-0.078335700
C	-2.325824600	-3.810610700	-0.253772000
H	-2.937102300	-4.531837200	-0.353969500
O	1.363547000	-0.745573000	3.586967000
F	-4.712577000	0.887653000	3.409209000
F	-3.489371000	-1.513431000	3.157643000
F	-3.209396000	3.134139000	3.614371000
C	-3.372877000	0.795088000	3.434963000
C	2.735438000	-0.708390000	3.568799000
C	2.050294000	2.831682000	3.361265000
H	1.276706000	3.384150000	3.335798000
C	-1.205085000	1.858918000	3.602176000
H	-0.697530000	2.652048000	3.727393000
C	-2.578055000	1.920760000	3.534013000
C	-1.377170000	-0.524435000	3.339934000
H	-0.973803000	-1.381997000	3.262682000
C	3.128280000	0.613949000	3.500609000

C	0.865730000	0.538948000	3.525649000
C	-2.718076000	-0.406486000	3.311251000
C	4.751428000	-2.118159000	3.893905000
H	5.226577000	-1.356752000	4.205388000
C	-0.568697000	0.633222000	3.488386000
C	3.281728000	3.379469000	3.282723000
H	3.361015000	4.323971000	3.210132000
C	3.421881000	-1.998119000	3.571286000
C	4.424852000	1.221159000	3.398842000
H	5.217901000	0.699337000	3.396135000
C	4.757684000	-4.430532000	3.319591000
H	5.227864000	-5.249236000	3.202153000
C	4.469917000	2.584268000	3.306335000
H	5.316128000	3.016298000	3.255498000
C	2.741062000	-3.156256000	3.140071000
H	1.818588000	-3.109857000	2.923304000
C	1.920962000	1.418986000	3.480416000
C	5.408180000	-3.319326000	3.776851000
H	6.327135000	-3.377578000	4.016281000
C	3.412968000	-4.353268000	3.032348000
H	2.944881000	-5.131843000	2.757563000

Table A70. *XYZ* Coordinates for Pair 2 in **7-F_{3a}** in Units of Ångstrøm

70

O	-0.788113000	-0.476236800	-0.019029500
F	4.927874900	1.396451600	-0.151657500
F	5.462484500	-1.239961900	0.049638200
F	3.438209500	-3.016695200	0.226756300
C	1.835492000	-1.301706600	0.084720900
H	1.138944600	-1.946689700	0.133492300
C	-1.887735800	1.483600200	0.016484700
C	3.138355500	-1.686343100	0.111004000
C	2.614999300	0.986679600	-0.089030800
H	2.447044500	1.919124700	-0.141612400
C	-3.156392000	-0.844328500	0.005242600
C	0.165086700	0.521765300	-0.028449600
C	-2.955570200	-2.163423400	-0.380335200
H	-2.091420400	-2.467444400	-0.629166600
C	-0.486526700	1.735215800	0.003465400
C	-2.359827000	3.813990100	0.009925500
H	-2.973031500	4.538467000	0.010004200
C	4.186249700	-0.826129800	0.022532400
C	3.877188700	0.520677800	-0.082378700
C	-5.302962800	-2.613226800	-0.078211200
H	-6.039811400	-3.209334000	-0.130129600
C	-4.433484300	-0.416247100	0.344122000
H	-4.577336300	0.490721200	0.591622500
C	-2.051946500	0.087374000	0.016401100
C	-0.972690500	4.083909900	-0.006309600
H	-0.681884200	4.987923200	0.004445200
C	-0.041809300	3.098448900	-0.036125900
H	0.883929100	3.306976300	-0.082149000
C	-4.052655000	-3.043715200	-0.398275400
H	-3.919528200	-3.954643400	-0.637173200
C	1.536204300	0.068299900	-0.015691800
C	-2.833169000	2.537147000	0.026094900
H	-3.767262200	2.360441900	0.042348000
C	-5.500901300	-1.296768400	0.323912200
H	-6.367517400	-1.004484000	0.583617900
F	-2.247337000	2.175266000	-3.288764000
O	2.632921000	1.389768000	-3.571163000
F	-3.473491000	-0.207051000	-3.349178000
C	2.099815000	0.114950000	-3.450094000
C	5.632603000	-0.648832000	-3.421751000
H	6.433443000	-0.144274000	-3.513646000
F	-1.983738000	-2.466581000	-3.507318000
C	4.506124000	-2.749732000	-3.138437000
H	4.574421000	-3.691208000	-3.020085000
C	0.667631000	0.036625000	-3.448887000
C	0.001685000	-1.218375000	-3.471345000
H	0.505187000	-2.024548000	-3.493754000
C	-0.110747000	1.197896000	-3.388980000
H	0.298341000	2.056063000	-3.380757000

C	4.383949000	0.001086000	-3.431258000
C	4.784918000	4.865881000	-4.553298000
H	4.351710000	5.608985000	-4.953589000
C	-2.142767000	-0.146931000	-3.381891000
C	-1.349890000	-1.258571000	-3.460609000
C	3.165887000	-0.786202000	-3.347627000
C	4.084175000	3.681340000	-4.342645000
H	3.175127000	3.621378000	-4.610105000
C	-1.458434000	1.072073000	-3.341475000
C	3.260241000	-2.195985000	-3.161137000
H	2.481186000	-2.729527000	-3.056451000
C	3.996660000	1.320258000	-3.565835000
C	5.685630000	-2.020333000	-3.278337000
H	6.526048000	-2.465964000	-3.274951000
C	4.711981000	2.563353000	-3.731833000
C	6.121249000	4.959930000	-4.178001000
H	6.607694000	5.760745000	-4.339879000
C	6.736900000	3.879952000	-3.567406000
H	7.645946000	3.942000000	-3.302851000
C	6.035443000	2.715739000	-3.341424000
H	6.472287000	1.993569000	-2.904128000

Table A71. *XYZ* Coordinates for Pair 3 in **7-F$_{3a}$** in Units of Ångstrøm

70

F	-3.455916900	2.978341300	0.506128900
O	0.789334000	0.464194000	-0.001551900
F	-4.882584400	-1.356402500	-0.538848600
F	-5.452077800	1.242251800	-0.020056900
C	3.162076300	0.836305900	-0.029405400
C	2.936442200	2.211444600	-0.080784600
H	2.044994200	2.536489900	-0.046575100
C	4.488515000	0.397880100	-0.055448400
H	4.682176800	-0.530133400	-0.001185500
C	-1.527543300	-0.058065800	-0.019238600
C	2.809765900	-2.575451700	0.154551000
H	3.746077400	-2.416170400	0.163139000
C	2.344801100	-3.832063000	0.208740600
H	2.958615800	-4.557557000	0.242235900
C	-4.176234100	0.786617700	-0.004814000
C	-3.859505300	-0.490157600	-0.255608600
C	0.028854500	-3.101928500	0.137165700
H	-0.903639700	-3.291155700	0.137340700
C	5.521944300	1.307942200	-0.158668800
H	6.418316000	0.995635000	-0.185233100
C	0.495346800	-1.753702300	0.055315800
C	0.931032800	-4.101806000	0.213649800
H	0.627566700	-4.999302000	0.273324200
C	-3.135026500	1.679843900	0.246213200
C	-1.835803700	1.270121100	0.244217500
H	-1.140130900	1.891819400	0.422815000
C	-0.164933800	-0.527480000	0.009635800
C	-2.587202500	-0.963892200	-0.289382700
H	-2.411835200	-1.875252600	-0.487376100
C	1.902391900	-1.471736200	0.086693100
C	3.968150700	3.103523700	-0.179702800
H	3.790880000	4.035957000	-0.217722100
C	5.274390000	2.645091000	-0.224087500
H	5.996383100	3.259402200	-0.300041400
C	2.054392000	-0.103858300	0.026530800
F	4.223594000	0.878778000	-3.326357000
O	-1.838370000	-0.697689000	-3.770824000
F	3.042454000	-1.524686000	-3.161746000
F	2.725572000	3.136169000	-3.463033000
C	0.102362000	0.636136000	-3.324280000
C	0.893905000	-0.505249000	-3.253718000
H	0.480832000	-1.359780000	-3.224621000
C	-2.397220000	1.400514000	-3.270974000
C	0.732689000	1.894944000	-3.401855000
H	0.221375000	2.692939000	-3.467797000
C	2.097582000	1.936471000	-3.379398000
C	2.864151000	0.800907000	-3.313234000
C	-1.334797000	0.533881000	-3.395506000
C	2.254847000	-0.413040000	-3.224763000

C	-2.490358000	2.791872000	-2.883765000
H	-1.707433000	3.286611000	-2.668501000
C	-4.839523000	1.322579000	-3.491247000
H	-5.639568000	0.853467000	-3.703525000
C	-5.174986000	-4.035838000	-5.366647000
H	-5.628778000	-4.777574000	-5.746612000
C	-4.892526000	2.644518000	-3.144040000
H	-5.731828000	3.088960000	-3.107899000
C	-3.814039000	-3.942404000	-5.500062000
H	-3.330204000	-4.621755000	-5.953139000
C	-3.703648000	3.368479000	-2.835939000
H	-3.770769000	4.282624000	-2.589281000
C	-3.147560000	-2.843289000	-4.966452000
H	-2.202001000	-2.781226000	-5.041773000
C	-3.867728000	-1.830842000	-4.319614000
C	-5.252855000	-1.974012000	-4.151093000
H	-5.748264000	-1.323014000	-3.669354000
C	-3.603488000	0.661603000	-3.531723000
C	-3.221059000	-0.626564000	-3.828214000
C	-5.891478000	-3.082593000	-4.696649000
H	-6.833455000	-3.178042000	-4.604633000

Table A72. *XYZ* Coordinates for Pair 4 in **7-F_{3a}** in Units of Ångstrøm

70

F	-5.465842300	1.229386700	0.025517700
O	0.761677200	0.477341400	0.057870600
F	-4.897434400	-1.368366600	-0.431774100
F	-3.438540400	2.989749600	0.409958400
C	2.027956100	-0.091412900	0.073557200
C	0.487318800	-1.734775600	0.068100900
C	1.904565500	-1.463355600	0.071797800
C	0.978454000	-4.093657800	0.072487500
H	0.691139900	-4.998621500	0.082850700
C	-0.171800500	-0.525254300	0.023269600
C	-4.172329200	0.801794100	0.024160000
C	2.928734300	2.194798000	-0.359753600
H	2.049622100	2.515832400	-0.520643800
C	2.384051800	-3.816142100	0.030931400
H	3.004598100	-4.534263700	-0.006208100
C	2.837045900	-2.543453000	0.043985400
H	3.770589500	-2.367878400	0.034961600
C	0.054719000	-3.120446500	0.096805000
H	-0.869729400	-3.336088000	0.132292500
C	3.128383000	0.871497300	-0.009443600
C	4.006624200	3.042510900	-0.475072400
H	3.859492100	3.943449700	-0.742768200
C	-3.863326200	-0.525041800	-0.206740000
C	-1.529757700	-0.067149300	0.026311800
C	4.430208100	0.440133900	0.307716600
H	4.572842600	-0.448530000	0.610490800
C	5.510606000	1.307708700	0.180990100
H	6.393079500	1.008229100	0.361189300
C	-2.580919500	-0.975173300	-0.213100900
H	-2.394649400	-1.892314100	-0.376662300
C	-1.832711600	1.265900500	0.212082600
H	-1.137877300	1.897695200	0.353570200
C	5.279238400	2.622874900	-0.213148600
H	6.007383000	3.226229200	-0.300831300
C	-3.131960600	1.673991700	0.193020800
F	2.444418000	-3.675197000	3.569133000
O	-2.961258000	-0.472015000	3.446619000
F	-0.117181000	-4.498896000	3.639413000
F	3.010887000	-1.020205000	3.465046000
C	-0.610771000	-0.905004000	3.551277000
C	1.711902000	-1.437775000	3.509152000
C	1.430488000	-2.763587000	3.562590000
C	-3.227707000	1.742475000	3.636579000
C	0.144665000	-3.169407000	3.573499000
C	-0.880431000	-2.283997000	3.585362000
H	-1.778570000	-2.594240000	3.616206000
C	-3.897389000	0.540205000	3.499246000
C	-5.276787000	0.146564000	3.380841000
C	0.710250000	-0.504278000	3.515622000

H	0.924559000	0.421660000	3.496538000
C	-1.817007000	1.438706000	3.704127000
C	-2.693958000	4.060282000	3.880282000
H	-2.966647000	4.970280000	3.929059000
C	-1.688318000	0.075560000	3.581198000
C	-7.953905000	-0.606010000	3.113383000
H	-8.864070000	-0.870349000	3.030979000
C	-3.636640000	3.098640000	3.713850000
H	-4.556163000	3.330876000	3.650826000
C	-0.867032000	2.495743000	3.902192000
H	0.061706000	2.313282000	3.975288000
C	-5.617052000	-1.142985000	2.960508000
H	-4.930994000	-1.766379000	2.758831000
C	-7.645332000	0.666798000	3.503293000
H	-8.335609000	1.291700000	3.689569000
C	-6.932693000	-1.516404000	2.835282000
H	-7.147921000	-2.397801000	2.558469000
C	-1.338188000	3.752932000	3.980530000
H	-0.719645000	4.460817000	4.109496000
C	-6.309632000	1.043178000	3.627655000
H	-6.100423000	1.932431000	3.886978000

Table A73. *XYZ* Coordinates for Pair 1 in **7-F_{3b}** in Units of Ångstrøm

70

O	-0.577312000	0.565270900	-0.105822900
F	2.542170000	-1.621085100	-1.378944000
F	1.275536100	2.036437100	1.332610700
F	5.717660000	1.584272700	-0.104416100
C	-1.534946400	-1.450083800	0.141436300
C	-0.108483000	-1.635075400	0.177373700
C	-1.783147000	-0.094969700	-0.047874400
C	-2.987017400	0.741275600	-0.162846400
C	-2.378053800	-2.597264700	0.328960500
H	-3.304279500	-2.515508800	0.308126500
C	1.808190400	0.150862900	0.000278700
C	0.438032300	-0.366946400	0.031622700
C	-1.786909200	-3.801430600	0.536685300
H	-2.327567900	-4.547132900	0.661236300
C	2.843059800	-0.487256500	-0.692423700
C	0.466865600	-2.921161800	0.431281500
H	1.386877400	-3.032909300	0.493682600
C	4.146037300	-0.043431500	-0.731527300
H	4.804602400	-0.513101600	-1.192143700
C	-0.373476700	-3.969692300	0.576486900
H	-0.020476100	-4.820967100	0.701699900
C	2.200464900	1.317314400	0.606421000
C	-4.239417700	0.197066200	-0.345286800
H	-4.330575700	-0.726226200	-0.408272900
C	3.496533800	1.830434600	0.611058700
H	3.713758400	2.619065100	1.055407200
C	-5.240427900	2.374614600	-0.362651800
H	-5.988722300	2.921879600	-0.437985200
C	-5.368037600	1.008299000	-0.433717200
H	-6.207093900	0.625660500	-0.539458400
C	4.428531800	1.107489600	-0.075441400
C	-2.862648200	2.096115600	-0.081219300
H	-2.021717300	2.472970000	0.039033000
C	-3.978496300	2.929468900	-0.176184700
H	-3.879626200	3.851524100	-0.113107800
O	-1.412312000	1.307271000	-3.811823000
F	1.707170000	-0.879085000	-5.084944000
F	0.440536000	2.778437000	-2.373389000
F	4.882660000	2.326273000	-3.810416000
C	-2.369946000	-0.708084000	-3.564564000
C	-0.943483000	-0.893075000	-3.528626000
C	-2.618147000	0.647030000	-3.753874000
C	-3.822017000	1.483276000	-3.868846000
C	-3.213054000	-1.855265000	-3.377039000
H	-4.139279000	-1.773509000	-3.397873000
C	0.973190000	0.892863000	-3.705721000
C	-0.396968000	0.375054000	-3.674377000
C	-2.621909000	-3.059431000	-3.169315000
H	-3.162568000	-3.805133000	-3.044764000

C	2.008060000	0.254743000	-4.398424000
C	-0.368134000	-2.179162000	-3.274718000
H	0.551877000	-2.290909000	-3.212317000
C	3.311037000	0.698568000	-4.437527000
H	3.969602000	0.228898000	-4.898144000
C	-1.208477000	-3.227692000	-3.129513000
H	-0.855476000	-4.078967000	-3.004300000
C	1.365465000	2.059314000	-3.099579000
C	-5.074418000	0.939066000	-4.051287000
H	-5.165576000	0.015774000	-4.114273000
C	2.661534000	2.572435000	-3.094941000
H	2.878758000	3.361065000	-2.650593000
C	-6.075428000	3.116615000	-4.068652000
H	-6.823722000	3.663880000	-4.143985000
C	-6.203038000	1.750299000	-4.139717000
H	-7.042094000	1.367660000	-4.245458000
C	3.593532000	1.849490000	-3.781441000
C	-3.697648000	2.838116000	-3.787219000
H	-2.856717000	3.214970000	-3.666967000
C	-4.813496000	3.671469000	-3.882185000
H	-4.714626000	4.593524000	-3.819108000

Table A74. *XYZ* Coordinates for Pair 1 in **7-F_4** in Units of Ångstrøm

70

F	5.938151500	-0.467583400	0.128330000
F	3.589557700	3.580466900	-0.041269400
F	-5.942909100	-0.453366800	0.141560200
F	-3.582307700	3.573716700	-0.070157100
O	0.000590800	0.232295000	-0.018017000
C	-1.122472100	-0.561482900	-0.016930700
C	-0.717270100	-1.882753800	-0.024539000
C	-1.415155300	-3.122187000	-0.047105900
H	-2.365029300	-3.138618400	-0.047802700
C	-0.707550100	-4.282247300	-0.067560400
H	-1.171659600	-5.110928400	-0.087392900
C	0.711240000	-4.279350200	-0.059778400
H	1.175536000	-5.108119200	-0.066345100
C	1.424633200	-3.120776200	-0.043504900
H	2.374794000	-3.137244500	-0.046686700
C	0.722282300	-1.882467900	-0.020358400
C	1.120047800	-0.552733500	-0.023743200
C	2.371487800	0.165713600	-0.018622600
C	3.595822200	-0.517008500	0.020735100
H	3.619467200	-1.466714100	0.021911800
C	4.764047200	0.212835900	0.057820100
C	4.808210000	1.583158800	0.043237400
H	5.628605400	2.061335500	0.073226500
C	3.589497200	2.224929000	-0.018087400
C	2.382675900	1.567225700	-0.047347800
H	1.568560000	2.055144200	-0.086580700
C	-2.378527300	0.156447500	-0.009698900
C	-3.602479400	-0.520471800	0.053983400
H	-3.628923500	-1.469393000	0.088162000
C	-4.761544200	0.210356300	0.065654000
C	-4.814832600	1.583762200	0.025611000
H	-5.635143200	2.062884700	0.036729600
C	-3.591215500	2.213869600	-0.031831700
C	-2.383454300	1.558083300	-0.048138000
H	-1.568328100	2.044664000	-0.085284800
F	5.820151000	0.974417000	-3.316670000
F	3.471558000	5.022467000	-3.486269000
F	-6.060909000	0.988633000	-3.303440000
F	-3.700308000	5.015717000	-3.515157000
O	-0.117409000	1.674295000	-3.463017000
C	-1.240472000	0.880517000	-3.461931000
C	-0.835270000	-0.440754000	-3.469539000
C	-1.533155000	-1.680187000	-3.492106000
H	-2.483029000	-1.696618000	-3.492803000
C	-0.825550000	-2.840247000	-3.512560000
H	-1.289660000	-3.668928000	-3.532393000
C	0.593240000	-2.837350000	-3.504778000
H	1.057536000	-3.666119000	-3.511345000
C	1.306633000	-1.678776000	-3.488505000

H	2.256794000	-1.695245000	-3.491687000
C	0.604282000	-0.440468000	-3.465358000
C	1.002048000	0.889266000	-3.468743000
C	2.253488000	1.607714000	-3.463623000
C	3.477822000	0.924991000	-3.424265000
H	3.501467000	-0.024714000	-3.423088000
C	4.646047000	1.654836000	-3.387180000
C	4.690210000	3.025159000	-3.401763000
H	5.510605000	3.503335000	-3.371773000
C	3.471497000	3.666929000	-3.463087000
C	2.264676000	3.009226000	-3.492348000
H	1.450560000	3.497144000	-3.531581000
C	-2.496527000	1.598448000	-3.454699000
C	-3.720479000	0.921528000	-3.391017000
H	-3.746923000	-0.027393000	-3.356838000
C	-4.879544000	1.652356000	-3.379346000
C	-4.932833000	3.025762000	-3.419389000
H	-5.753143000	3.504885000	-3.408270000
C	-3.709215000	3.655870000	-3.476832000
C	-2.501454000	3.000083000	-3.493138000
H	-1.686328000	3.486664000	-3.530285000

Table A75. *XYZ* Coordinates for Pair 1 in **7-F$_5$** in Units of Ångstrøm

70

O	-0.983965600	0.471174300	-0.064443200
F	0.878289000	1.959032700	1.209666500
C	-0.640323500	-1.712342600	0.304762300
F	3.418864700	2.775829000	1.083948200
C	-0.142604200	-3.016257100	0.587530700
H	0.791961700	-3.182730600	0.632212800
F	5.293225000	1.252122800	-0.169357700
C	-1.040387400	-4.018786400	0.793243900
H	-0.723940600	-4.892768400	0.985889000
F	4.593079300	-1.139167000	-1.241743700
C	-2.441907000	-3.785797700	0.725003000
H	-3.037120100	-4.512365500	0.866227600
F	2.046786900	-1.965739700	-1.171330900
C	-2.956457900	-2.554809700	0.462963200
H	-3.896042600	-2.421319100	0.424038600
C	-2.058714100	-1.466445200	0.247828200
C	-2.223214100	-0.112159500	0.019984200
C	-3.345152700	0.786477500	-0.181169000
C	-4.650545700	0.313332400	-0.310982600
H	-4.819544000	-0.618537800	-0.230141100
C	-5.698557400	1.172188300	-0.552849200
H	-6.579261900	0.826012700	-0.636927900
C	-5.484624600	2.530330200	-0.676442600
H	-6.211201300	3.116651900	-0.852980500
C	-4.197715500	3.028499300	-0.539824300
H	-4.040221400	3.962516700	-0.619905400
C	-3.141370000	2.171885200	-0.286385800
H	-2.266054400	2.526047300	-0.182828500
C	1.355305200	-0.043838800	0.025693500
C	1.765727000	1.176981000	0.572694700
C	3.067840400	1.607543700	0.520800700
C	4.021612700	0.829079700	-0.090006000
C	3.663824000	-0.375380700	-0.637038600
C	2.353669400	-0.795030800	-0.580241500
C	-0.027219400	-0.493950000	0.105521800
O	1.418517000	-0.868020000	3.237251000
F	-0.365205000	-2.697885000	4.117614000
C	1.126651000	1.090210000	4.287136000
F	-2.917354000	-3.464305000	3.926257000
C	0.665034000	2.237036000	4.993943000
H	-0.262046000	2.370989000	5.154201000
F	-4.858686000	-1.648882000	3.342175000
C	1.586428000	3.136825000	5.435318000
H	1.294357000	3.904755000	5.910807000
F	-4.209530000	0.964574000	3.015097000
C	2.976838000	2.952168000	5.198972000
H	3.588747000	3.606084000	5.515334000
F	-1.655487000	1.757459000	3.156635000
C	3.457549000	1.868475000	4.533183000

H	4.390417000	1.764162000	4.388230000
C	2.534546000	0.889971000	4.056321000
C	2.667150000	-0.325494000	3.409693000
C	3.761734000	-1.105145000	2.861287000
C	5.059867000	-0.600378000	2.791785000
H	5.244704000	0.262635000	3.144664000
C	6.078282000	-1.330461000	2.222323000
H	6.954641000	-0.965358000	2.187092000
C	5.840786000	-2.586088000	1.700241000
H	6.546318000	-3.080836000	1.299873000
C	4.561290000	-3.116547000	1.767154000
H	4.387967000	-3.981709000	1.413514000
C	3.535359000	-2.392279000	2.347487000
H	2.665667000	-2.770950000	2.398335000
C	-0.902476000	-0.432530000	3.648211000
C	-1.286762000	-1.767214000	3.818501000
C	-2.594051000	-2.175241000	3.728628000
C	-3.579953000	-1.256832000	3.457929000
C	-3.248350000	0.061723000	3.286290000
C	-1.932815000	0.457957000	3.376868000
C	0.487222000	-0.013629000	3.764911000

Table A76. *XYZ* Coordinates for Pair 2 in **7-F$_s$** in Units of Ångstrøm

70

O	-0.983966700	0.471169200	0.064443900
F	0.878289600	1.959036600	-1.209666900
C	-0.640324700	-1.712338000	-0.304762900
F	3.418875700	2.775831100	-1.083947200
C	-0.142605900	-3.016252800	-0.587531100
H	0.791959900	-3.182726700	-0.632212900
F	5.293224800	1.252124800	0.169358900
C	-1.040389600	-4.018781700	-0.793244500
H	-0.723943700	-4.892773700	-0.985887900
F	4.593077100	-1.139174500	1.241746400
C	-2.441909100	-3.785792400	-0.725004100
H	-3.037122400	-4.512359900	-0.866228800
F	2.046784700	-1.965747600	1.171322900
C	-2.956460100	-2.554814000	-0.462963100
H	-3.896044700	-2.421323000	-0.424038800
C	-2.058715300	-1.466440000	-0.247829300
C	-2.223214800	-0.112154200	-0.019985500
C	-3.345153700	0.786473500	0.181168800
C	-4.650546900	0.313329000	0.310982000
H	-4.819545600	-0.618541200	0.230140500
C	-5.698557700	1.172195100	0.552846700
H	-6.579262400	0.826020000	0.636925000
C	-5.484625300	2.530328700	0.676451500
H	-6.211191500	3.116648600	0.852979600
C	-4.197714900	3.028505500	0.539822100
H	-4.040221100	3.962512900	0.619904800
C	-3.141370400	2.171881100	0.286385600
H	-2.266053900	2.526052600	0.182827000
C	1.355304600	-0.043835000	-0.025693500
C	1.765727000	1.176984500	-0.572694700
C	3.067840000	1.607536800	-0.520798700
C	4.021612400	0.829082200	0.090006800
C	3.663833000	-0.375378500	0.637039800
C	2.353667600	-0.795037400	0.580243400
C	-0.027220900	-0.493955600	-0.105520800
O	-5.854522000	7.623020000	-5.051740000
F	-4.070785000	9.452890000	-4.171439000
C	-5.562640000	5.664799000	-4.001824000
F	-1.518638000	10.219306000	-4.362853000
C	-5.101012000	4.517986000	-3.295005000
H	-4.173919000	4.384034000	-3.134760000
F	0.422683000	8.403871000	-4.946936000
C	-6.022398000	3.618205000	-2.853598000
H	-5.730319000	2.850293000	-2.378102000
F	-0.226480000	5.790420000	-5.273958000
C	-7.412812000	3.802858000	-3.089924000
H	-8.024716000	3.148948000	-2.773540000
F	-2.780511000	4.997537000	-5.132372000
C	-7.893524000	4.886549000	-3.755725000

H	-8.826404000	4.990861000	-3.900664000
C	-6.970539000	5.865035000	-4.232619000
C	-7.103153000	7.080489000	-4.879266000
C	-8.197746000	7.860140000	-5.427668000
C	-9.495880000	7.355373000	-5.497140000
H	-9.680702000	6.492366000	-5.144242000
C	-10.514305000	8.085437000	-6.066596000
H	-11.390665000	7.720334000	-6.101805000
C	-10.276816000	9.341065000	-6.588695000
H	-10.982355000	9.835805000	-6.989070000
C	-8.997319000	9.871524000	-6.521823000
H	-8.824001000	10.736679000	-6.875482000
C	-7.971379000	9.147265000	-5.941496000
H	-7.101686000	9.525927000	-5.890667000
C	-3.533523000	7.187527000	-4.640811000
C	-3.149233000	8.522214000	-4.470551000
C	-1.841945000	8.930248000	-4.560455000
C	-0.856048000	8.011824000	-4.831153000
C	-1.187655000	6.693276000	-5.002764000
C	-2.503188000	6.297045000	-4.912157000
C	-4.923219000	6.768639000	-4.524082000

Table A77. *XYZ* Coordinates for Pair 1 in **7-F_6** in Units of Ångstrøm

70

F	-3.623567600	-3.366094200	-0.347539000
F	-5.956580000	-2.029963400	-0.240561100
F	-5.946451100	0.667968700	0.069654800
F	3.737066100	-3.251501800	0.739317100
F	5.949181400	-2.006949000	-0.174259700
F	5.842261300	0.611659700	-0.838057600
O	0.006586600	-0.039807200	0.177322200
C	1.115083500	0.763044100	0.185026800
C	0.710936100	2.085654800	0.164130300
C	1.416099100	3.327892100	0.174028300
H	2.364441800	3.347346900	0.226283100
C	0.700040300	4.482421300	0.107281900
H	1.158901000	5.314125600	0.110015500
C	-0.725231500	4.472168800	0.031910800
H	-1.189377600	5.299177300	-0.025430600
C	-1.438588000	3.316310300	0.040887500
H	-2.387491100	3.332140000	-0.001359200
C	-0.730725000	2.072367300	0.113905900
C	-1.115969200	0.740980700	0.127183900
C	-2.373158200	0.022800800	0.045411400
C	-3.593732800	0.710650000	0.100155800
H	-3.606170400	1.654517800	0.206706700
C	-4.770714300	0.010746100	-0.001205900
C	-4.796746400	-1.357541700	-0.149946900
C	-3.589896300	-2.027943100	-0.192671000
C	-2.385863000	-1.372157900	-0.100070200
H	-1.570551900	-1.858562900	-0.133632600
C	2.388287800	0.066654100	0.149726100
C	2.454980000	-1.285893600	0.500577500
H	1.679418500	-1.741077400	0.807307500
C	3.652185800	-1.948050600	0.397210800
C	4.798588000	-1.325366500	-0.057196900
C	4.724409600	0.006328000	-0.385497400
C	3.550198700	0.719796800	-0.290094300
H	3.526944400	1.641626300	-0.518633800
F	2.352471000	5.013472000	3.300475000
F	0.853093000	7.243053000	3.443537000
F	-1.847819000	7.035430000	3.636252000
F	2.709654000	-2.377870000	4.083932000
F	1.660832000	-4.628250000	3.029061000
F	-0.929947000	-4.671734000	2.257605000
O	-0.730010000	1.145495000	3.534466000
C	-1.452958000	-0.014508000	3.462815000
C	-2.798694000	0.298954000	3.401099000
C	-3.987913000	-0.489114000	3.328904000
H	-3.943031000	-1.437943000	3.342020000
C	-5.186100000	0.148692000	3.241247000
H	-5.983079000	-0.365551000	3.189559000
C	-5.272606000	1.573262000	3.223874000

H	-6.127089000	1.981925000	3.149605000
C	-4.170818000	2.362787000	3.311509000
H	-4.251312000	3.309335000	3.306882000
C	-2.884335000	1.738982000	3.409619000
C	-1.584799000	2.213260000	3.495912000
C	-0.953668000	3.518889000	3.495959000
C	-1.726911000	4.686167000	3.570067000
H	-2.672860000	4.629545000	3.636158000
C	-1.107591000	5.911448000	3.546539000
C	0.260399000	6.037203000	3.458216000
C	1.014807000	4.881895000	3.395906000
C	0.441708000	3.633039000	3.411507000
H	0.984945000	2.855038000	3.366168000
C	-0.668302000	-1.234501000	3.406365000
C	0.670351000	-1.223815000	3.812347000
H	1.057398000	-0.432965000	4.169452000
C	1.418311000	-2.367454000	3.689532000
C	0.896222000	-3.532988000	3.162830000
C	-0.423080000	-3.535762000	2.780562000
C	-1.220253000	-2.418201000	2.892283000

Table A78. *XYZ* Coordinates for Pair 2 in **7-F_6** in Units of Ångstrøm

70

F	-3.708728200	3.297454300	-0.588668400
F	-5.978587200	1.990609600	0.023829800
F	-5.917073400	-0.654681000	0.557788700
F	3.656651500	3.337130300	0.457183900
F	5.982263100	1.994847900	0.219447000
F	5.950774400	-0.671888100	-0.262893800
O	-0.008056600	0.050068800	-0.097317300
C	1.116710000	-0.734628300	-0.099926700
C	0.726401400	-2.064290900	-0.070517100
C	1.438915900	-3.298885100	-0.031975100
H	2.388757000	-3.311787400	-0.031464100
C	0.725383900	-4.461556200	0.003798800
H	1.192212700	-5.288425600	0.035391300
C	-0.696360200	-4.471511700	-0.004219800
H	-1.154394100	-5.303442100	0.016361800
C	-1.417170500	-3.317641900	-0.041293400
H	-2.366682400	-3.339421500	-0.059185900
C	-0.717199600	-2.074931900	-0.052914000
C	-1.117836400	-0.747718800	-0.065426400
C	-2.389867700	-0.047215300	-0.046359000
C	-3.573410900	-0.717424400	0.278291200
H	-3.555626700	-1.641197200	0.499686900
C	-4.762079400	-0.028297100	0.274773200
C	-4.814714800	1.324717500	-0.007367500
C	-3.641418000	1.974410400	-0.319782400
C	-2.433355700	1.321446300	-0.356390500
H	-1.639580600	1.788867600	-0.588435000
C	2.380097100	-0.024002500	-0.067163100
C	2.406030300	1.360510400	0.147638000
H	1.593828400	1.844834200	0.238271400
C	3.614135300	2.014872200	0.226687400
C	4.816537100	1.343825500	0.098378600
C	4.774838300	-0.016133600	-0.132095800
C	3.593670700	-0.709107900	-0.224653100
H	3.598001900	-1.643755400	-0.394406900
F	-1.133756000	8.154027000	-3.537522000
F	-0.062133000	10.429090000	-2.583074000
F	2.517919000	10.483552000	-1.791350000
F	-0.728129000	0.733223000	-3.203851000
F	0.798772000	-1.465238000	-3.523297000
F	3.489574000	-1.213828000	-3.727023000
O	2.316923000	4.638671000	-3.071696000
C	3.179277000	3.572681000	-3.101146000
C	4.467680000	4.042511000	-2.899933000
C	5.742313000	3.410480000	-2.803850000
H	5.825247000	2.468297000	-2.892047000
C	6.840452000	4.189827000	-2.582669000
H	7.692823000	3.776240000	-2.511611000
C	6.746058000	5.602723000	-2.454862000

H	7.536169000	6.108740000	-2.306545000
C	5.550812000	6.248022000	-2.540504000
H	5.503981000	7.193869000	-2.466027000
C	4.369923000	5.474547000	-2.744612000
C	3.023917000	5.788372000	-2.853885000
C	2.232707000	7.004291000	-2.785627000
C	2.779847000	8.189291000	-2.283867000
H	3.677254000	8.208433000	-1.972446000
C	2.008230000	9.325476000	-2.244721000
C	0.687876000	9.319557000	-2.656609000
C	0.159186000	8.144802000	-3.143197000
C	0.900138000	6.991119000	-3.227593000
H	0.516742000	6.196670000	-3.580103000
C	2.564034000	2.269512000	-3.260631000
C	1.171111000	2.133088000	-3.191044000
H	0.621702000	2.899114000	-3.073526000
C	0.603252000	0.883710000	-3.293737000
C	1.370429000	-0.253877000	-3.466570000
C	2.739297000	-0.101786000	-3.552680000
C	3.348759000	1.124701000	-3.461993000
H	4.293043000	1.197631000	-3.535547000

Table A79. *XYZ* Coordinates for Pair 1 in **7-F_{10}** in Units of Ångstrøm

70

O	-0.004598500	-0.087852000	-0.021776600
C	-1.116153800	0.673074500	0.198775100
C	-0.727900100	1.948266100	0.548086700
C	0.716091800	1.952918400	0.545884600
C	1.112969200	0.681400200	0.185156300
C	-1.443595900	3.147900600	0.867674400
C	-0.735851900	4.255715200	1.179179000
C	0.700104300	4.256687600	1.190432400
C	1.420445800	3.145451900	0.889751900
C	-2.394433900	0.001068400	0.005720400
C	-3.455548100	0.685312100	-0.538775900
C	-4.661876200	0.051127900	-0.720962300
C	-4.807096300	-1.267307900	-0.358651800
C	-3.745983600	-1.951551500	0.185834500
C	-2.539655400	-1.317367400	0.368021000
C	2.395499700	0.014859900	0.001583000
C	3.438263000	0.683010100	-0.595764900
C	4.648613700	0.053983200	-0.769011300
C	4.816188800	-1.243195900	-0.344897800
C	3.773411700	-1.911348000	0.252452100
C	2.563074800	-1.282319200	0.425696500
F	-3.313390300	1.975938900	-0.893435900
F	-5.700604100	0.720932800	-1.253967300
F	-5.987989800	-1.888123900	-0.536995500
F	-3.888140000	-3.242178500	0.540504500
F	-1.500918300	-1.987178400	0.901034600
F	3.274226600	1.952826900	-1.010936900
F	5.669389800	0.708041300	-1.353757900
F	6.001007700	-1.858960600	-0.514483600
F	3.937455900	-3.181170900	0.667622800
F	1.542284900	-1.936379300	1.010445100
H	-2.393205200	3.175228000	0.867956700
H	-1.187803000	5.060800100	1.402982000
H	1.172829200	5.050018800	1.413245900
H	2.369817100	3.176133800	0.905468100
O	-0.598132000	0.054604000	-2.716848000
C	0.120638000	-1.092783000	-2.890350000
C	1.362570000	-0.775045000	-3.395851000
C	1.390150000	0.660993000	-3.544752000
C	0.165334000	1.125082000	-3.110194000
C	2.514750000	-1.550135000	-3.749697000
C	3.598737000	-0.906548000	-4.235447000
C	3.621239000	0.520223000	-4.396485000
C	2.555301000	1.295731000	-4.070109000
C	-0.549892000	-2.326979000	-2.503067000
C	0.142616000	-3.301841000	-1.824324000
C	-0.490179000	-4.466584000	-1.458841000
C	-1.815488000	-4.656459000	-1.772090000
C	-2.508004000	-3.681591000	-2.450833000

C	-1.875209000	-2.516848000	-2.816316000
C	-0.460336000	2.436281000	-2.999965000
C	-1.806374000	2.578294000	-3.242089000
C	-2.396831000	3.815696000	-3.138068000
C	-1.641241000	4.911094000	-2.791914000
C	-0.295194000	4.769075000	-2.549791000
C	0.295254000	3.531679000	-2.653811000
F	1.439975000	-3.115978000	-1.517684000
F	0.187732000	-5.420888000	-0.794415000
F	-2.434938000	-5.796627000	-1.414315000
F	-3.805364000	-3.867454000	-2.757483000
F	-2.553111000	-1.562550000	-3.480742000
F	-2.546027000	1.505999000	-3.580939000
F	-3.714485000	3.954708000	-3.375081000
F	-2.219243000	6.122401000	-2.690078000
F	0.444460000	5.841370000	-2.210932000
F	1.612908000	3.392667000	-2.416798000
H	2.526958000	-2.495168000	-3.653462000
H	4.371522000	-1.399463000	-4.485106000
H	4.396998000	0.947220000	-4.740532000
H	2.599296000	2.237414000	-4.187578000

Table A80. *XYZ* Coordinates for Pair 2 in **7-F_{10}** in Units of Ångstrøm

70

O	-0.004599200	0.087858200	-0.021781200
C	-1.116162000	-0.673074700	0.198771900
C	-0.727892400	-1.948268200	0.548090400
C	0.716099500	-1.952920100	0.545887800
C	1.112974900	-0.681401700	0.185150100
C	-1.443601600	-3.147901200	0.867679800
C	-0.735851200	-4.255723700	1.179182800
C	0.700105100	-4.256695700	1.190435500
C	1.420446500	-3.145445700	0.889745000
C	-2.394428500	-0.001070800	0.005716000
C	-3.455541200	-0.685314400	-0.538770300
C	-4.661875700	-0.051122600	-0.720955200
C	-4.807097500	1.267312900	-0.358653800
C	-3.745983300	1.951556600	0.185842400
C	-2.539654900	1.317372700	0.368028100
C	2.395491200	-0.014859000	0.001578700
C	3.438268300	-0.683010400	-0.595772000
C	4.648606400	-0.053981000	-0.769006600
C	4.816181300	1.243197900	-0.344892500
C	3.773418000	1.911347400	0.252456200
C	2.563066100	1.282320000	0.425692800
F	-3.313384600	-1.975941200	-0.893441100
F	-5.700606800	-0.720941600	-1.253969500
F	-5.987985200	1.888120600	-0.536997400
F	-3.888141400	3.242183200	0.540503300
F	-1.500919200	1.987183700	0.901031700
F	3.274225700	-1.952833000	-1.010933500
F	5.669388800	-0.708032600	-1.353765200
F	6.000999800	1.858963000	-0.514478400
F	3.937452700	3.181164000	0.667618900
F	1.542291500	1.936377600	1.010450100
H	-2.393203000	-3.175222900	0.867961200
H	-1.187809400	-5.060801100	1.402976300
H	1.172838200	-5.050020800	1.413247200
H	2.369825200	-3.176135200	0.905469900
O	0.502078000	0.064294000	4.768154000
C	1.220837000	1.211682000	4.594656000
C	2.462769000	0.893942000	4.089156000
C	2.490352000	-0.542104000	3.940253000
C	1.265527000	-1.006183000	4.374810000
C	3.614951000	1.669029000	3.735313000
C	4.698942000	1.025431000	3.249554000
C	4.721443000	-0.401325000	3.088514000
C	3.655510000	-1.176838000	3.414896000
C	0.550309000	2.445879000	4.981940000
C	1.242825000	3.420744000	5.660674000
C	0.610026000	4.585482000	6.026169000
C	-0.715277000	4.775353000	5.712907000
C	-1.407793000	3.800488000	5.034172000

C	-0.775000000	2.635758000	4.668678000
C	0.639868000	-2.317383000	4.485033000
C	-0.706184000	-2.459390000	4.242910000
C	-1.296630000	-3.696793000	4.346926000
C	-0.541049000	-4.792185000	4.693081000
C	0.804995000	-4.650184000	4.935206000
C	1.395449000	-3.412775000	4.831188000
F	2.540177000	3.234871000	5.967327000
F	1.287938000	5.539784000	6.690597000
F	-1.334730000	5.915530000	6.070694000
F	-2.705151000	3.986369000	4.727520000
F	-1.452911000	1.681456000	4.004260000
F	-1.445835000	-1.387093000	3.904050000
F	-2.614293000	-3.835807000	4.109902000
F	-1.119056000	-6.003490000	4.794904000
F	1.544638000	-5.722473000	5.274056000
F	2.713103000	-3.273767000	5.068204000
H	3.627162000	2.614062000	3.831550000
H	5.471738000	1.518352000	2.999905000
H	5.497199000	-0.828338000	2.744467000
H	3.699501000	-2.118522000	3.297415000